

Science Synthesis Report: Atmospheric Impacts of Oil and Gas Development in Texas



Final Report to the Texas Commission on Environmental Quality

David D. Parrish
David.D.Parrish, LLC
Boulder, Colorado, 80304

Sue Kemball-Cook, John Grant and Greg Yarwood
Ramboll Environ US Corporation
Novato, California, 94945

30 June 2017



Disclaimer

The preparation of this work plan was financed through a contract from the State of Texas through the Texas Commission on Environmental Quality. The content, findings, opinions and conclusions are the work of the authors and do not necessarily represent findings, opinions or conclusions of the TCEQ.

Acknowledgements

A great many people and organizations contributed to this synthesis report. The primary contributors to the analyses underlying each Finding are indicated in each section. The institutions represented by Working Group Members are indicated by the logos on the front page.

This Report was submitted in fulfillment of TCEQ Work Order/PCR No. WO#582-16-63215-16, Contract # 582-15-50417, Tracking No. 2016-03. Work was completed as of 30 June 2017.

CONTENTS

GLOSSARY OF TERMS, SYMBOLS AND ACRONYMS	XV
ABSTRACT	1
EXECUTIVE SUMMARY.....	2
ES.1 Overview of Main Findings.....	2
ES.2 Findings Related to Study Questions.....	4
ES.2.1 Emissions.....	4
ES.2.2 Chemical Transformation.....	8
ES.2.3 Transport and Meteorology.....	12
1.0 INTRODUCTION	14
1.1 Recent Field Studies	14
1.2 Emissions	15
1.3 Chemical Transformation	21
1.4 Transport and Meteorology	23
1.5 References	24
2.0 SCIENCE QUESTIONS	28
2.1 Emissions	28
2.2 Chemical Transformations.....	28
2.3 Transport/Meteorology.....	29
3.0 SYNTHESIS OF RESULTS: EMISSIONS	30
3.1 Response to Question A	30
3.1.1 Working Group.....	30
3.1.2 Background	30
3.1.3 Findings	32
3.1.4 Summary and Recommendations for Further Analysis	40
3.1.5 References	41
3.2 Response to Question B	43
3.2.1 Working Group.....	43
3.2.2 Background	43
3.2.3 Findings	44
3.2.4 Summary and Recommendations for Further Analysis	54

3.2.5 References	55
3.3 Response to Question C	57
3.3.1 Working Group.....	57
3.3.2 Background	57
3.3.3 Findings	57
3.3.4 Summary and Recommendations for Further Analysis	64
3.3.5 References	65
3.4 Response to Question D	66
3.4.1 Working Group.....	66
3.4.2 Background	66
3.4.3 Findings	66
3.4.4 Summary and Recommendations for Further Analysis	73
3.4.5 References	73
3.5 Response to Question E.....	75
3.5.1 Working Group.....	75
3.5.2 Background	75
3.5.3 Findings	75
3.5.4 Summary and Recommendations for Further Analysis	84
3.5.5 References	84
4.0 SYNTHESIS OF RESULTS: CHEMICAL TRANSFORMATION	87
4.1 Response to Question F.....	87
4.1.1 Working Group.....	87
4.1.2 Background	87
4.1.3 Findings	88
4.1.4 Summary and Recommendations for Further Analysis	99
4.1.5 References	99
4.2 Response to Question G	102
4.2.1 Working Group.....	102
4.2.2 Background	102
4.2.3 Findings	102
4.2.4 Summary and Recommendations for Further Analysis	105
4.2.5 References	106
4.3 Response to Question H	107
4.3.1 Working Group.....	107
4.3.2 Background	107

4.3.3 Findings	108
4.3.4 Summary and Recommendations for Further Analysis	119
4.3.5 References	119
4.4 Response to Question I	121
4.4.1 Working Group.....	121
4.4.2 Background	121
4.4.3 Findings	122
4.4.4 Summary and Recommendations for Further Analysis	129
4.4.5 References	130
5.0 SYNTHESIS OF RESULTS: TRANSPORT AND METEOROLOGY.....	132
5.1 Response to Question J	132
5.1.1 Working Group.....	132
5.1.2 Background	132
5.1.3 Findings	133
5.1.4 Summary and Recommendations for Further Analysis	140
5.1.5 References	141
5.2 Response to Question K	142
5.2.1 Working Group.....	142
5.2.2 Findings	142
5.2.3 Summary and Recommendations for Further Analysis	146
5.2.4 References	146

APPENDICES

Appendix A: Correlation Analysis of Ambient Ozone Concentrations with Oil and Gas Development Activity

Appendix B: CAMx 2017 Ozone Source Apportionment Modeling

TABLES

Table 3-1. Nitrogen oxides (NOx) emissions, O&G activity, and emissions per surrogate for nonpoint compressor engines and heaters in Haynesville Shale counties and parishes at the border of Texas and Louisiana.	67
Table 3-2. 2014 NEI point source reporting for select states.	69

FIGURES

Figure 1-1. Trends in Texas state-wide well count (left) and O&G production (right). Data from Texas Railroad Commission.	14
--	----

Figure 1-2.	Upper panel: annual average price of West Texas Intermediate (WTI) Crude Oil (left axis, \$/Bbl, black) and the Henry Hub Natural Gas Spot Price (right axis, \$/MMBtu, red). Lower panel: Drilling permits for the Eagle Ford and Barnett Shale (Haynesville) plotted on left (right) axis. Haynesville permit data are for Texas wells only, and do not include wells in Louisiana. Data from Texas Railroad Commission	19
Figure 1-3.	Trends in Texas state-wide flaring and venting of natural gas. Data from Texas Railroad Commission.....	21
Figure 3-1.	NOx emissions in the Haynesville O&G production region from the TCEQ 2012 Model-Ready 4 km x 4 km Emission Inventory for June 29, 2012 at 7 am. (Upper panel) Point sources of NOx emissions are shown as circles with radii that indicate the magnitude of the NOx emissions in metric tons per day (tpd). Facilities with NOx emissions (during standard operations in 2012) of greater than 4 tpd are labelled. The color-coded grid represents low-level (i.e. non-point) emissions from urban areas, on-road mobile sources and rural areas with O&G production. Stars indicate the location of TCEQ monitors. (Lower panel) Color-coded grid showing low-level O&G production sources only.....	31
Figure 3-2.	Annual average production rate of dry shale gas from the Barnett, Haynesville and Eagle Ford Shales. Haynesville data includes production from Texas counties and Louisiana parishes. Data from the US Energy Information Administration (EIA).	32
Figure 3-3.	Annual average total liquid hydrocarbon (oil plus condensate) production from the major Texas shale formations. Production from the Eagle Ford (left axis) is much larger than for the other two formations, which are plotted against the right axis. Data from the Texas Railroad Commission.....	33
Figure 3-4.	Map of NOx emission estimates for the Haynesville O&G production region optimized by the Bayesian inverse modeling together with a flux ratio inversion technique. Total emissions are on the left, and the emissions from O&G activities alone are on the right. Units are $\mu\text{g m}^{-2}\text{s}^{-1}$	36
Figure 3-5.	Comparison of NOx emission estimates for the Haynesville O&G production region from the three top-down approaches discussed in the text with the bottom-up NEI 2011 inventory. The comparison is shown for all sources (left) and for the O&G sources only (right).	37
Figure 3-6.	Combustion plume excess NOx versus excess CO ₂ (a) for flares upwind of the monitoring site in Dimmit County, TX (b) during July and August 2015. The dashed line shows an ordinary linear regression forced through the origin, while the solid line is a bivariate regression with an	

intercept indistinguishable from zero. In (a) there are two data clusters: one below the regression lines, representing low combustion efficiency (higher VOC emissions), and one above representing high combustion efficiency (higher NOx emissions). The flare directly upwind of the field site (9 km to the SE) was detected on multiple days, and displayed both low and high combustion efficiencies.....	40
Figure 3-7. Shale play drilling and production statistics in the eight O&G basins investigated during the SONGNEX field campaign in 2015.....	44
Figure 3-8. Shale play drilling and production statistics in six O&G basins during NOAA field campaigns in 2011 - 2015. The Niobrara and the Denver-Julesburg refer to the same basin.....	45
Figure 3-9. Correlation of VOC and CH ₄ concentrations measured on four flights over two O&G basins. The slopes derived from linear regressions, with correlation coefficients, are annotated.	46
Figure 3-10. Comparison of VOC/CH ₄ molar enhancement ratios in fourteen O&G basins investigated during NOAA ground and airborne field campaigns.	46
Figure 3-11. Comparison of normalized VOC/CH ₄ enhancement ratios in fourteen O&G basins investigated during NOAA ground and airborne field campaigns.....	47
Figure 3-12. Map comparing of mole fractions of VOC to total VOC + CH ₄ in fourteen O&G basins investigated during NOAA ground and airborne field campaigns.....	48
Figure 3-13. Comparison of relative, median contributions of different VOC classes to OH radical reactivity in the HGB (in 2006) vs. the Floresville monitor (in 2013/14). The estimated oxygenated VOC contribution to the total at the latter site was ~10%, equivalent to approximate median mixing ratios of 0.6 ppb formaldehyde and 0.3 ppb acetaldehyde.....	49
Figure 3-14. Diurnal cycle of mean BTEX abundances measured at the Floresville site (dashed line) compared to the NMF-based source apportionment (colored swaths).	50
Figure 3-15. (right) Map of propane measurements made during the 10 June 2013 WP-3D flight over the Haynesville O&G Basin. Each data symbol is colored and sized according to the propane concentration, a marker for O&G emissions. (left) Summary of measured propane concentrations on the indicated upwind and downwind legs of the flight path.	51
Figure 3-16. (right) Map of propane as in Figure 3-15, with the flight track color-coded according to the continuous methane measurements. (left)	

Correlation between measured propane and methane concentrations with the square of the correlation coefficient annotated.	52
Figure 3-17. (right) Enlargement of a section of the map from Figure 3-16, with the location of natural gas processing plants indicated. Google Earth images of two of those plants are included. Wind barbs are included on the flight track.	53
Figure 3-18. Relationship between ethyne (acetylene) and benzene measured during the 10 June 2013 WP-3D flight over the Haynesville O&G Basin during the SENEX field campaign. Each data point is from analysis of a single whole air sample, and is colored and sized according to the propane concentration, a marker for O&G emissions.	54
Figure 3-19. Comparisons of the correlations between the concentrations of three alkanes with propane measured by the NOAA WP-3D aircraft (Haynesville, red symbols) and at the Karnack surface site (green symbols). Lines of the respective colors indicate the results of the linear regressions; the slopes with confidence limits and the correlation coefficients are annotated.	58
Figure 3-20. Enhancement ratios of nine VOCs relative to propane measured by the WP-3D aircraft and the Karnack, TX surface site in the Haynesville O&G Basin in 2013. The relative concentrations of four alkanes measured in samples of Haynesville raw natural gas (data from USGS Energy Geochemistry Database, accessed in November 2015) are included for comparison.	59
Figure 3-21. (left) Time series of concentrations of three VOC species measured in the Haynesville O&G Basin at the Karnack, TX surface monitoring site. The annual average number of active drilling rigs (from Baker-Hughes) and the natural gas production (from U.S. EIA) are included for comparison. The box and whisker symbols indicate mean, median, 25 th and 75 th percentiles, and minimum and maximum concentrations measured in each year. (right) Correlations of the annual mean VOC concentration with the annual mean number of active drilling rigs, with the correlation slopes and intercepts with confidence limits indicated, as well as the square of the correlation coefficients.	60
Figure 3-22. Time series of (top) annual average OMI NO ₂ data (1015 cm ⁻² on left, % on right) relative to the year 2005, and (bottom) U.S. Energy Information Administration (https://www.eia.gov/petroleum/drilling/) monthly statistics of production plus drilling activity in the Permian O&G basin.	62
Figure 3-23. Time series of (top) annual average OMI NO ₂ data (10 ¹⁵ cm ⁻² on left, % on right) relative to the year 2005, and (bottom) U.S. Energy Information Administration (https://www.eia.gov/petroleum/drilling/)	

monthly statistics of production plus drilling activity in the Eagle Ford O&G basin.....	63
Figure 3-24. Time series of (top) annual average OMI NO ₂ data (10^{15} cm^{-2} on left, % on right) relative to the year 2005, and (bottom) U.S. Energy Information Administration (https://www.eia.gov/petroleum/drilling/) monthly statistics of production plus drilling activity in the Bakken O&G basin.....	64
Figure 3-25. Median total OHR in three O&G basins based upon measurements made during the SONGNEX field campaign in 2015. The median total OHR is annotated, and the pie charts show how VOCs, CH ₄ , CO and NO ₂ each contribute to that reactivity.	71
Figure 3-26. OHR due to VOCs in the three O&G basins included in Figure 3-25. The median VOC OHR is indicated, and the pie charts show how four VOC families each contribute to that reactivity.....	72
Figure 3-27. OHR enhancements above nominal background OHR due to NMHCs in the three O&G basins included in Figure 3-25. The median NMHC OHR enhancement is indicated, and the pie charts show how CH ₄ and four NMHC families (alkanes, aromatics, cycloalkanes and alkenes) each contribute to that reactivity.....	73
Figure 3-28. Fractional contribution of top 5% of emitters in each of 18 reference studies (red) and 34 device-specific categories of data from single studies (orange). [Figure from <i>Brandt et al. 2016</i>].	76
Figure 3-29. Difference in near-surface ozone concentrations simulated with and without O&G emissions. Results are for 3 pm EDT averaged over June 2013.....	78
Figure 3-30. Difference in near-surface ozone concentrations simulated with and without O&G emissions in the Haynesville, Fayetteville and three other basins outside this region. The left map is calculated with the NEI-2011 inventory, and the right map is calculated with NOx emissions reduced to match the top-down evaluations discussed in the response to Question A of this report. Results are for 3 pm EDT averaged over June 2013.	79
Figure 3-31. In situ, airborne measurements upwind and downwind of the Haynesville O&G basin. Time series of particle volume in $\mu\text{m}^3 \text{ cm}^{-3}$ (approximately equal to 70% of PM _{2.5} in $\mu\text{g m}^{-3}$) are compared to those of methane and SO ₂ concentrations.	81
Figure 3-32. Soluble chloride concentrations observed during June 2011 at the TCEQ Eagle Mountain Lake measurement site [Figure from <i>Faxon, 2014</i>]......	83

Figure 4-1.	Time series of ozone design values (ODVs, solid lines) and median MDA8 ozone concentrations (dashed lines) for the May-September ozone season in the Bakken O&G basin in North Dakota. Ozone data are color-coded according to the site map that also shows the location of oil and natural gas wells. The history of oil production in the basin is indicated. The black lines indicate smooth fits to the respective data; root-mean-square deviations (RMSD) of the data from the fits are annotated.....	88
Figure 4-2.	Time series of ODVs (solid lines) and median MDA8 ozone concentrations (dashed lines) for the April-October ozone season in the Haynesville O&G basin. Figure is in the same format as Figure 4-1. The histories of drilling and gas production in the basin are indicated.....	89
Figure 4-3.	Time series of ODVs (solid lines) and median MDA8 ozone concentrations (dashed lines) for the April-October ozone season in the Barnett O&G basin. Figure is in the same format as Figure 4-1. The history of gas production in the basin is indicated.	89
Figure 4-4.	Time series of ODVs (solid lines) and median MDA8 ozone concentrations (dashed lines) for the April-October ozone season in the Eagle Ford O&G basin. Figure is in the same format as Figure 4-1. The Laredo data (red lines) are shown but not included in further analysis. The histories of drilling and oil production in the basin are indicated.....	90
Figure 4-5.	Time series of ODVs (solid lines) and median MDA8 ozone concentrations (dashed lines) for the April-October ozone season in the Austin-Killeen-Waco region. Figure is in the same format as Figure 4-1.....	90
Figure 4-6.	Time series of differences (i.e., the residuals) between the ODVs and median MDA8 ozone concentrations, and the respective smooth fits (black lines) in Figure 4-2 to Figure 4-5. The correlation coefficients between the oil basin residuals and those of the Austin-Killeen-Waco region are annotated.	91
Figure 4-7.	Contributions to projected 2017 ODVs at regulatory monitors in East Texas from O&G emissions in the Haynesville, Barnett and Eagle Ford Shales. RGV is the Rio Grande Valley and TLM is the Tyler-Longview-Marshall region of Northeast Texas.....	97
Figure 4-8.	May 1 – September 30 episode average contributions to daily maximum 8-hour average ozone from O&G NOx and VOC emissions at the Karnack and Calaveras Lake monitors	98
Figure 4-9.	PM _{2.5} formed from O&G emissions. Results are for 3 pm EDT averaged over June 2013.	103

- Figure 4-10. Comparison (left) of time series of PM concentrations to oil production in the Bakken O&G region in North Dakota, and map (right) of the region showing the location of oil/gas wells and urban areas in North Dakota. The PM data are three-month means (JFM, AMJ, JAS, and OND) of speciated and total PM concentrations measured at the two North Dakota IMPROVE sites, whose locations are given by the green triangles on the map.....104
- Figure 4-11. PM_{2.5} concentrations measured at twelve stations across Texas. Both the annual averages (lower curves) and the 98th percentiles of the 24-hr averages (upper curves) are plotted. Gray and black lines indicate the more urban areas: Houston (Houston East and Deer Park), Dallas (Hinton and Denton), San Antonio and El Paso. Green and blue lines indicate more rural and near-coastal sites, respectively. The site within the Haynesville O&G Basin (Karnack) is emphasized with heavier gold lines and points. Generally the highest concentrations are observed at the Houston East site (black lines). Two measures of O&G activity in the Haynesville O&G Basin are included for comparison.....105
- Figure 4-12. Flight tracks of NOAA P-3 aircraft during five field campaigns. 1-minute averages are shown for flight segments during daytime (5 AM-10 PM CDT) and altitudes within the boundary layer (maximum 1500 m above ground level). These flight segments are color coded according to NH₃ (top), HNO₃ (middle), and the product of these two concentrations (bottom). The data are sorted such that higher values are plotted on top of smaller values, so maximum observed values are highlighted and many of the smaller concentrations are hidden.....111
- Figure 4-13. Distributions of NH₃, HNO₃, and the product of these two concentrations for the measurements over four O&G basins in Texas. The boxes indicate the 25th and 75th percentiles along with the medians. The whiskers and circles encompass the 2nd to 98th and the 1st to 99th percentiles, respectively.....112
- Figure 4-14. Comparison of the measured NH₃ and HNO₃ concentration product with the theoretical dissociation constant for NH₄NO₃ as a function of temperature across the different seasons. Data are from Boulder, Wyoming, a rural region of active gas production. [Figure from *Li et al., 2014.*].....112
- Figure 4-15. Flight track of NOAA P-3 aircraft during over the Eagle Ford O&G basin on 7 April 2015. Symbols are 1-min averages color-coded according to measured ozone concentrations. The data shown are limited to the measurements within the boundary layer (altitude \leq 1 km AGL). The arrow indicates the approximate south-southeast wind direction.....113

- Figure 4-16. Observations of NO_x and NO_y mixing ratios in several western U.S. O&G basins measured from the NOAA WP-3D aircraft during the 2015 SONGNEX campaign. Dots denote mean concentrations. The box and whisker symbols indicate median, 25th-75th percentile ranges, and 5th-95th percentile ranges. In panels C and D, the observed mixing ratios are normalized to a 1000 m boundary layer to improve comparability between basins.115
- Figure 4-17. Calculated instantaneous ozone production rates along the P3 flight tracks in the Haynesville shale region during the SONGNEX mission on April 4, 2015 and April 25, 2015. Gas wells are denoted by the white to blue gradient dots, with the darker blue representing greater gas production as of 2014. Oil wells are denoted by white to magenta gradient dots, with darker magenta representing greater oil production as of 2014. Urban areas are outlined in dark gray. Wind barbs indicate the dominant wind direction and point in the direction of wind flow. Bowtie markers indicate locations of power plants.117
- Figure 4-18. Calculated instantaneous ozone production rates and observed NO_y along the P3 flight tracks in the Barnett shale region during the SONGNEX mission on April 4, 2015. Figures are in the same format as in Figure 4-17.....118
- Figure 4-19. Calculated instantaneous ozone production rates and observed NO_y along the P3 flight tracks in the Eagle Ford shale region during the SONGNEX mission on April 2, 2015. Figures are in the same format as in Figure 4-17.....119
- Figure 4-20. Diurnal variation of measured (gray dots are individual 10-minute average measurements) and modeled OH and HO₂ during SOAS. (a) OH measured by a traditional laser induced fluorescence technique is shown as squares and by a new chemical scavenger method is shown as circles. The latter is considered as the “true” ambient OH. Simulated OH from a photochemical box model with Master Chemical Mechanism (MCM) v3.3.1 is shown in pluses. (b) Measured and modeled HO₂ is shown as circles and pluses, respectively. The symbols are averages over all days of measurements for 1-hour periods of the diurnal cycle. [Figure from Mao *et al.*, 2016, modified from Feiner *et al.*, 2016].....123
- Figure 4-21. Correlation of soluble chloride and nitric acid concentrations observed during June 2011 at the TCEQ Eagle Mountain Lake measurement site [Faxon, 2014]. A 1:1 line is added for reference.125
- Figure 4-22. Correlation of HCl with HNO₃ colored by date for the entire CalNex 2010 Pasadena dataset.126

Figure 4-23. Diel average ozone observed (red line) compared to simulated with explicit (dotted black line) and lumped (dash-dot black line) VOC mechanisms.....	128
Figure 4-24. NO _x sensitivity of simulated maximum photochemical ozone mixing ratios for three VOC scenarios. Colors represent the VOC scenarios (black – observed VOCs, green – doubled O&G VOCs, blue – zero O&G VOCs). Solid lines are the updated MCM results, and the dotted lines are the CB6r3 results.....	129
Figure 5-1. Projected contributions to 2017 ODVs from O&G emissions within the East Texas shale regions. The magnitude of the contribution to ODVs at each East Texas regulatory ozone monitor is shown in Figure 4-5.....	133
Figure 5-2. Frequency distributions of the projected contributions to 2017 MDA8 ozone concentrations from O&G emissions within the East Texas shale regions, other emissions sources and boundary conditions (BCs) at four East Texas regulatory monitors. Upper left: Calaveras Lake monitor northwest of the Eagle Ford shale. Upper right: Karnack monitor within the Haynesville Shale. Lower left: Houston Aldine monitor. Lower right: Denton Airport South monitor in Dallas-Fort Worth within the Barnett Shale region.....	135
Figure 5-3. Frequency distributions of the projected contributions to 2017 MDA8 ozone concentrations from O&G emissions within the East Texas shale regions, other emissions sources and boundary conditions (BCs) at four East Texas regulatory monitors in the Houston-Galveston-Brazoria area. Upper left: Conroe Relocated monitor north of the Houston area. Upper right: Clinton monitor near the Houston Ship Channel. Lower left: Houston Westhollow monitor in the western part of the Houston urban area. Lower right: Manvel Croix in southern Houston.	138
Figure 5-4. Frequency distributions of the projected contributions to 2017 daily MDA8 ozone concentrations from O&G emissions within the East Texas shale regions, other emissions sources and boundary conditions (BCs) at four East Texas regulatory monitors in the Dallas-Fort Worth Area. Upper left: Eagle Mountain Lake monitor northwest of the DFW urban area in an O&G development area. Upper right: Grapevine Fairway monitor in the northern part of the DFW urban area. Lower left: Dallas Hinton monitor in the central DFW urban area. Lower right: Cleburne Airport south of the DFW urban area in an O&G development area.	140
Figure 5-5. Concentrations of gaseous NH ₃ , HNO ₃ and PM _{2.5} ammonium and nitrate measured at Boulder, Wyoming [after Li <i>et al.</i> 2014]. Note the complete depletion of NH ₃ in the wintertime coupled with residual	

nitric acid in the gas phase. The lack of available NH ₃ limits wintertime fine particle NH ₄ NO ₃ and haze formation at this location.....	143
Figure 5-6. The study domain for the Bakken Air Quality Study [Evanoski-Cole <i>et al.</i> , 2017]. Study measurement sites are indicated by stars; oil wells are indicated by pink dots.....	144
Figure 5-7. The PM _{2.5} concentrations at four Bakken area study sites as reported by Evanoski-Cole <i>et al.</i> [2017].	145

GLOSSARY OF TERMS, SYMBOLS AND ACRONYMS

AGL	Above ground level
AMCV	Air monitoring comparison value
APCA	Anthropogenic Precursor Culpability Assessment
BC	black carbon
BRAVO	Big Bend Regional Aerosol and Visibility Observational Study
BVOC	biogenic volatile organic compound
BTEX	benzene, toluene, ethyl benzene, xylenes
Btu	British thermal unit
CAMS	Continuous Air Monitoring Station
CAMx	Comprehensive Air Quality Model with Extensions
Carbonyl	a functional group composed of a carbon atom double-bonded to an oxygen
CB6r3	Carbon Bond 6 Revision 3 chemical mechanism
CBL	convective boundary layer
CCN	cloud condensation nuclei
CDT	Central Daylight Time
CFC(s)	chlorofluorocarbon(s)
CH ₄	methane
Cl ⁻	chloride ion
Cl ₂	molecular chlorine
CINO ₂	nitryl chloride
DJB	Denver-Julesburg Basin of Colorado
CO	carbon monoxide
CO ₂	carbon dioxide
COGCC	Colorado Oil and Gas Conservation Commission
DSMACC	Dynamically Simple Model for Atmospheric Chemical Complexity
EC	elemental carbon
EGU	electric generating unit
EPA	US Environmental Protection Agency
FINN	Fire Inventory from the National Center for Atmospheric Research
FRAPPÉ	Front Range Air Pollution and Photochemistry Experiment
GEOS	Goddard Earth Observing System
H ₂ O	water vapor
H ₂ SO ₄	sulfuric acid
HAPs	hazardous air pollutants
HARC	Houston Advanced Research Center
HCl	hydrochloric acid
HGB	Houston Galveston Bay
HNO ₃	nitric acid
HRVOCs	highly reactive volatile organic compounds
IMPROVE	Interagency Monitoring of Protected Visual Environments
IVOC	intermediate volatility organic compounds
LAC	light absorbing carbon

lbs	pounds
LDAR	leak detection and repair
MCM	Master Chemical Mechanism
MDA8	maximum daily 8-hour average
MEGAN	Model of Emissions of Gases and Aerosols from Nature
mmBtu	one million British thermal units
Mol	mole
NADP	National Atmospheric Deposition Program
NEAQS-ITCT	New England Air Quality Study - Intercontinental Transport and Chemical Transformation
N ₂ O	nitrous oxide
N ₂ O ₅	dinitrogen pentoxide
NAAQS	National Ambient Air Quality Standard
NASA	National Aeronautics and Space Administration
NCAR	National Center for Atmospheric Research
NCTCOG	North Central Texas Council of Governments
NEI	National Emission Inventory
NFR	Northern Front Range of Colorado
NH ₃	ammonia gas
NH ₄ ⁺	ammonium ion (also NH ₄)
NH ₄ NO ₃	particulate ammonium nitrate
NMF	non-negative matrix factorization
NO	nitric oxide
NO ₂	nitrogen dioxide
NOAA	National Oceanic and Atmospheric Administration
NOAA/CSD	NOAA Chemical Sciences Division
NOAA/GMD	NOAA Global Monitoring Division
NOMADSS	Nitrogen, Oxidants, Mercury and Aerosol Distributions, Sources and Sinks
NO _x	oxides of nitrogen, NO + NO ₂
NO _y	total reactive oxidized nitrogen, i.e., NO + NO ₂ + HONO + HNO ₃ + N ₂ O ₅ + ...
O ₃	ozone
O _x	total oxidant (often estimated as O ₃ + NO ₂)
OA	organic aerosol
OC	organic carbon
ODV	ozone design value
OH	hydroxyl radical
OHR	OH Reactivity
OPE	ozone production efficiency
PAN	peroxy acetyl nitrate
PBL	planetary boundary layer
PM	particulate matter
PM ₁	particulate matter smaller than 1 micron in aerodynamic diameter
PM _{2.5}	particulate matter less than 2.5 microns aerodynamic diameter
PMF	positive matrix factorization

POA	primary (directly emitted) organic aerosol
POM	particulate organic matter
ppb	parts-per-billion - mixing ratio unit based on mole ratio
ppm	parts-per-million - mixing ratio unit based on mole ratio
PPN	peroxy propionyl nitrate
RGV	Rio Grande Valley
RMSD	root mean square deviations
SEAC4RS	Studies of Emissions and Atmospheric Composition, Clouds and Climate Coupling by Regional Surveys
SENEX	Southeast Nexus (2013 NOAA field study)
S/L/T	State/Local/Tribal
SO ₂	sulfur dioxide
SO ₄ ⁼	sulfate ion (also, SO ₄)
SO _x	total oxidized sulfur, SO ₂ + SO ₄ ⁼
SOA	secondary (formed in the atmosphere, not directly emitted) organic aerosol
SOAS	Southern Oxidant & Aerosol Study
SONGNEX	Shale Oil and Natural Gas Nexus (2015 NOAA field study)
SVOC	Semivolatile organic compounds
TexAQS	Texas Air Quality Study
TLM	Tyler-Longview-Marshall area of Northeast Texas
tpd	metric tons per day
µg m ⁻³	micrograms per cubic meter
UGRB	Upper Green River Basin
UT/LS	upper troposphere/lower stratosphere
VIIRS	Visible Infrared Imaging Radiometer Suite
VOC(s)	volatile organic compound
WRF-Chem	Weather Research and Forecasting (WRF) model coupled with Chemistry

ABSTRACT

The past decade has seen expanded oil and natural gas (O&G) resource development in Texas. Advances in hydraulic fracturing and other drilling technologies led to intensive activity in areas with existing development as well as previously unexploited areas of the State. O&G development and production have the potential to affect air quality.

This report provides a scientific synthesis of recent study results pertaining to the air quality impacts of O&G development in Texas. This synthesis draws upon the results of aircraft and surface measurement campaigns, emission inventory development and modeling studies in order to reflect the latest and most rigorous scientific findings available. The Synthesis is intended to ensure that the results of recent field studies are made available in an accessible format to policy makers of the State of Texas as well as other interested parties. The approach was modeled on the Rapid Science Synthesis that was conducted as part of the Second Texas Air Quality Study (TexAQS II). This Synthesis is organized around 11 policy-relevant Science Questions formulated in consultation with the Texas Commission on Environmental Quality. Findings in response to each of these questions address three general areas:

1. Emissions,
2. Chemical transformation,
3. Transport and meteorology.

EXECUTIVE SUMMARY

This Synthesis is intended to address 11 policy-relevant Science Questions formulated in consultation with the Texas Commission on Environmental Quality (TCEQ). Answers to these questions are needed by TCEQ and other policy makers in Texas in order to formulate scientifically sound policies to simultaneously address concerns regarding air quality degradation and the increasing demand for energy as Texas' population grows.

This Report provides statements of Findings in response to each of the policy-relevant Science Questions. These Questions and Findings address three general areas:

1. Emissions,
2. Chemical transformation,
3. Transport and meteorology.

The Executive Summary organizes the main scientific Findings for use by TCEQ managers and other air-quality decision makers and stakeholders in Texas. It comprises a list of the 11 policy-relevant Science Questions and a series of Findings that have been developed in response to each of these questions. We emphasize that these Findings are based on analysis and interpretation of results that have so far emerged; additional analyses are continuing, and will yield important new information in the future.

Each section of this report is structured as a Response to address one of the Science Questions, including a numbered sequence of succinctly stated Findings in response to that question. Important references are given for publications upon which the Finding is based, and within some Findings is an acknowledgment of the individual(s) whose analyses and data contributed to that Finding, particularly if the analysis has not yet been published. A brief discussion of background and the evidence that supports each Finding is given.

As is common in scientific research, progress in addressing a given set of questions raises new questions suggesting additional analysis. Specific examples of additional analysis suggested by the Oil and Gas Synthesis results are collected in a concluding section.

The institutional affiliations of the scientists responsible for the field measurements and the analyses leading to these Findings are given in the Contributors section, which follows the discussion of the Science Questions and Findings.

ES.1 Overview of Main Findings

O&G activity results in direct emissions to the atmosphere of precursors of ozone and particulate matter (PM) such as volatile organic compounds (VOC) and nitrogen oxides ($\text{NO}_x = \text{NO} + \text{NO}_2$). O&G activity also produces emissions of air toxics (e.g., benzene and hydrogen sulfide [H_2S]).

Ozone is not emitted directly into the atmosphere, but is formed from photochemical reactions of precursor species in the presence of sunlight. The most important precursors of ground level ozone are NOx and VOC. In Texas O&G basins, VOC are generally readily available and the amount of ozone formed from O&G emissions is determined by the amount of available NOx (Findings F7, H5). Compared to other anthropogenic NOx emission sources, NOx emissions from O&G activities are not dominant, even in relatively rural O&G basins; however, O&G sources do provide emissions of NOx emissions in areas that would otherwise have very small emissions (Finding A6). Significant enhancements in local ozone production rates can occur near and/or downwind of local NOx sources (Finding H5).

Each O&G basin has its own characteristic VOC composition signature that depends upon the composition of extracted oil and natural gas and the technologies employed in that field (Finding B1). VOC measurements made in the vicinity of intensive O&G development show that light alkanes consistent with O&G production are present at concentrations well above those in most other U.S. areas; however, the relative contribution of O&G VOC emissions to ozone formation is variable and depends on the local influence of highly reactive biogenic VOCs (Findings F2, F3). The alkanes that comprise the bulk of O&G VOC emissions are relatively unreactive, as are their reaction products, and this limits their contribution to ozone formation (Finding F4). VOC emissions in the Haynesville O&G Basin correlate much more closely with drilling activity than with natural gas production (Finding C2).

The total hydroxyl radical reactivity (OHR) of measured VOCs varied markedly between Texas O&G basins. At a rural site adjacent to the Eagle Ford Shale the OHR was of similar magnitude to that found in the Houston/Galveston Bay (HGB) area during TexAQS 2006 (Finding B2a) while in the Permian Basin median OHR was more similar to measurements in the coastal offshore Gulf of Mexico during TexAQS 2006 (Finding D2).

There are uncertainties in current Texas O&G emission inventories. Emission measurements indicate that O&G methane and VOC emissions from high-emitting sources contribute a large fraction of O&G emissions; these emissions are incompletely captured by current bottom-up regulatory emission inventories, leading to underestimates (Finding E1). Uncertainty in NOx emissions from O&G activities limits our confidence in O&G ozone concentration enhancements predicted by photochemical modeling; generally, ozone impacts may be overestimated due to bottom-up emission inventory overestimates of O&G NOx emissions (Findings A5, E2).

Analysis of Texas ground level ozone monitoring data shows that decadal scale ozone changes in the Barnett, Eagle Ford and Haynesville Shale regions are not significantly correlated with O&G production or drilling activity. This lack of correlation indicates that O&G development does not have a major impact on ozone concentrations in Texas (<5 parts per billion [ppb] on ozone design values and median ozone season daily maximum 8-hour average (MDA8) ozone concentrations (Finding F1).

This finding is consistent with results of two different photochemical modeling studies of Texas O&G emission impacts. One study used the TCEQ's future year 2017 emission inventory and showed ozone contributions from O&G emissions to East Texas regulatory monitor design values were < 5 ppb (Finding F6). The other photochemical modeling study evaluated ozone impacts of O&G emissions using the 2011 National Emission Inventory and a second inventory in which the NEI NOx emission inventory over the Haynesville Shale was replaced with a top-down 2013 NOx emission inventory. O&G emission impacts on Texas ozone reached a maximum of 3.5 ppb using the 2011 NEI and 1.5 ppb using the top-down 2013 NOx top-down emission inventory as measured by 3 pm ozone values averaged over a one month (June) period.

Although O&G emissions can increase ozone in East Texas and can contribute to nonattainment of the National Ambient Air Quality Standard, their role is relatively minor and reductions in O&G emissions are unlikely to produce large declines in ozone design values at regulatory monitors in East Texas (Finding J1).

In Texas, concentrations of particulate matter less than 2.5 microns in aerodynamic diameter (PM_{2.5}) in urban areas, O&G basins and other rural areas are of similar magnitude and show similar decadal declines; there is no discernable indication that the O&G activities have affected total PM_{2.5} concentrations (Finding G3).

In the Haynesville and Eagle Ford O&G Basins, two different studies show that elevated ambient benzene concentrations are strongly associated with O&G sources, but do not exceed the TCEQ's health-based long-term air monitoring comparison value (AMCV) of 1.4 ppb for benzene (Finding B5). Benzene is a toxic chemical that is a carcinogen and the AMCV is used to assess risk to human health.

ES.2 Findings Related to Study Questions

ES.2.1 Emissions

Question A

What are the emissions of ozone and particulate matter (PM) precursors from O&G development in Texas?

The Response to Question A is focused on NOx emissions, while the Response to Question B discusses VOC emissions. Here, several methods for quantifying NOx emissions from O&G emissions are discussed and their results compared. With good confidence we find that NOx emissions from O&G activities do not dominate over other anthropogenic NOx emission sources, but efforts to accurately quantify O&G emissions are confounded by three issues: total O&G emissions from a basin change on relatively short time scales in response to basin development and economic forces; emissions from a particular sector of sources vary widely depending upon operating conditions of the particular source; and development is ongoing for the techniques providing both bottom-up activity based emissions estimates and top-down, observationally based emissions estimates. Preliminary comparisons indicate that NOx

emissions from O&G activities have been overestimated in earlier work, but there is relatively low confidence in this result. Further analysis should focus on the discrepancy between the inventories identified in Finding A5, to determine if it is solely due to the different basis years, or if it reflects significant errors in the inventories; if it is the latter, then further efforts to improve inventories may be justified.

Finding A1: Emissions from O&G activities can change rapidly and systematically on time scales of a year or less. In modeling or emissions comparisons, care must be taken to ensure that the selected emission inventory matches the year under study.

Finding A2: Public fuel use data provide a basis to estimate O&G emissions of nitrogen oxides (NOx).

Finding A3: Mass balance calculations based on aircraft data can estimate total NOx emissions from O&G basins.

Finding A4: Bayesian inverse modeling together with a flux ratio inversion technique can separately estimate total NOx emissions and O&G NOx emissions alone.

Finding A5: Three top-down and one bottom-up approaches are in reasonable agreement for the quantification of NOx emissions from the Haynesville O&G region in June 2013; the NOx emission estimates for the O&G sources in the U.S. Environmental Protection Agency's (EPA's) 2011 National Emission Inventory (NEI) are a factor of 2-3 higher.

Finding A6: Compared to other anthropogenic NOx emission sources, O&G activities are not dominant, even in relatively rural O&G basins; they do provide emissions of NOx in areas that would otherwise have very small emissions.

Finding A7: Measurements of NOx, VOCs, and CO₂ downwind of active flares in the Eagle Ford Shale confirmed that, on average, EPA's current AP-42 flare emission factors are accurate, although emissions can vary widely over short periods, producing at times either higher volatile organic compound (VOC) emissions (low combustion efficiency), or higher NOx emissions (high combustion efficiency).

Question B

How do the magnitude and composition of these emissions depend upon variables such as composition of extracted oil and natural gas and technologies employed? What are the important parameters controlling how these emissions vary over time and area?

The Response to Question B is focused on VOC emissions, while the Response to Question A discusses NOx emissions. The analysis given in this Response to Question B has only begun to scratch the surface of providing a definitive answer. Emissions of benzene, a toxic VOC, are of particular concern; the available measurements indicate that annual average benzene concentrations away from the immediate vicinity of sources are below the long-term AMCV, so that chronic exposure in these O&G basins is not expected to cause adverse health effects. The

limited available data provide no evidence for 1-hr average benzene concentrations exceeding the short-term AMCV in the Eagle Ford and Haynesville O&G basins. Future analysis of long-term VOC data sets could focus on the very highest observed VOC concentrations, and thereby provide better guidance regarding the frequency and/or the probability of 1-hr average benzene concentrations exceeding the short-term AMCV in Texas O&G fields. Ongoing mass balance analyses based on aircraft data promise to provide improved quantification of total VOC emissions from individual Texas O&G basins.

Finding B1: Each O&G basin has its own characteristic VOC composition signature that depends upon the composition of extracted oil and natural gas and the technologies employed in that field; NOAA field studies provide systematic (albeit limited) characterization of these signatures across U.S. O&G basins.

Finding B2a: At a rural site adjacent to the Eagle Ford Shale, in Floresville, Texas, the median total hydroxyl radical (OH) reactivity of measured VOCs during 2013-2014 was of similar magnitude to that found in the Houston/Galveston Bay (HGB) area during TexAQS 2006. However, the highest fraction of OH reactivity in the HGB area, which occurred in plumes of highly reactive volatile organic compounds (HRVOCs), was about an order of magnitude larger than the corresponding fraction in the Eagle Ford Shale.

Finding B2b: At a rural site adjacent to the Eagle Ford Shale, in Floresville, Texas, emissions from O&G activities (including both evaporative and combustion sources) substantially enhanced median concentrations of aromatic VOCs above those expected in rural regions without O&G activities. The combustion sources also enhanced alkene concentrations.

Finding B3: In the Haynesville O&G Basin, ambient propane concentration measurements are a useful tracer for O&G sources that provides information different from ambient methane concentrations.

Finding B4: In the Haynesville O&G Basin, elevated ambient benzene concentrations are strongly associated with O&G sources, but do not exceed the TCEQ's long-term air monitoring comparison value (AMCV), which is used to assess risk to human health.

Question C

How are these emissions divided between the various stages of fossil fuel extraction (exploration and production; product gathering and transmission; gas processing) and specific processes?

This Response to Question C provides only three example analyses that give preliminary indications of how O&G emissions are divided between the various stages of fossil fuel extraction and specific extraction processes. A comprehensive answer to this Science Question awaits results from additional analysis, some of which are currently being pursued by members of the Working Groups that provided this synthesis.

Finding C1: Ratios of concentrations of VOCs from a "snapshot" provided by a NOAA WP-3D aircraft flight over the Haynesville O&G basin are in reasonable accord (agreement within a factor of ≈ 2) with those from long-term canister measurements made at the Karnack, TX surface site located in that basin.

Finding C2: Long-term measurements at the Karnack, TX surface site indicate that VOC emissions in the Haynesville O&G Basin correlate much more closely with drilling activity than with natural gas production.

Finding C3: Increases of NO₂ concentrations over three U.S. O&G basins have been identified in satellite records; the time series of annual average concentrations correlate (at least qualitatively) with drilling activity and oil/natural gas production.

Question D

How do these emissions in Texas compare to other regions of the U.S.?

This Response to Question D discusses the difficulty of comparing emission inventories between states, and provides a single, observationally-based analysis example that gives a "snap shot" indication of how VOC OHR varies between three U.S. O&G basins, including the Permian Basin in Texas. Developing 1) observationally-based, quantitative descriptions of the air quality impacts and 2) accurate O&G emissions inventories for all U.S. O&G basins would provide a rich data set from which to seek correlations of the air quality impacts with the magnitude and composition of the O&G emissions. Neither of these developments has yet been completed.

Finding D1: Accurate comparison of regional bottom-up O&G criteria air pollutant emission inventories for different states is confounded by the use of inconsistent O&G emission inventory methodology.

Finding D2: The total rate of reactivity of hydroxyl radicals (OHR) has been calculated for three O&G basins. The results are similar in magnitude to those seen in the Gulf of Mexico, but the alkene contribution is much smaller and alkane contribution is larger. This difference suggests that ozone formation is less efficient in these O&G basins than in The Gulf of Mexico.

Question E

Are there gaps in our quantification of emissions that limit a full understanding of ozone and PM formation from these emissions?

The Findings in the Response to this Question identify several shortcomings in our understanding of the emissions from O&G activities. Estimating the magnitudes of the air quality impacts associated with these shortcomings will allow prioritization of future research efforts. It seems likely that improving our understanding of the impact of a small fraction of high-emitting VOC sources (Finding E1) and improving the accuracy of NOx emissions from O&G sources (Finding E2) are of greatest importance.

Finding E1: Bottom-up emission measurements indicate that O&G methane and VOC emissions from high-emitting sources contribute a large fraction of O&G emissions; these emissions are incompletely captured by bottom-up emission inventories, leading to underestimates.

Finding E2: Uncertainty in NOx emissions from O&G activities limits our confidence in ozone concentration enhancements predicted by photochemical modeling; generally they may be overestimated due to inventory overestimates of these NOx emissions.

Finding E3: Uncertainty regarding possible emissions of semivolatile organic compounds (SVOCs) and intermediate volatility organic compounds (IVOCs) limit our ability to accurately model secondary (formed in the atmosphere, not directly emitted) organic aerosol (SOA) formation in Texas O&G fields.

Finding E4: Preliminary analysis of measurements of particle volume downwind of O&G fields indicates that the associated emissions produce little particulate matter less than 2.5 microns aerodynamic diameter (PM_{2.5}), at least locally (i.e., on a time scale of a few hours).

Finding E5: Uncertainty remains in isoprene emission inventories; the latest comparisons of models and measurements indicate that on average the U.S. EPA's Biogenic Emission Inventory System Model (BEIS) was lower and the Model of Emissions of Gases and Aerosols from Nature (MEGAN) was higher than the measurements, with about a factor of 2 difference between the two inventories.

Finding E6: High concentrations of a gas-phase soluble chloride species (presumably hydrochloric acid, HCl) have been observed in the Barnett Shale region. The emission source(s) of the chlorine-containing precursor(s) to this species remain unidentified.

Finding E7: Environmental chamber experiments indicate that evaporation of flowback wastewater from hydraulic fracturing can result in formation of PM and ozone. Assessing the significance of air quality impacts from this source would require quantification of wastewater evaporating in O&G regions, which is currently lacking.

ES.2.2 Chemical Transformation

Question F

What are the contributions of emissions from O&G development to ambient ozone concentrations at regulatory monitors in Texas?

An observationally based analysis could discern no impact of O&G activity on ozone concentrations within or near Texas O&G basins. The smallest discernable impact is estimated as < 5 ppb, but could not be more quantitatively defined; it should be possible to develop a more sophisticated multivariate analysis that would provide a more rigorous limit for the smallest discernable impact. Photochemical modeling found that ozone contributions from O&G emissions to East Texas regulatory monitor design values were ≤ 5 ppb. Possible

overestimates of NOx emissions in the modeling (see Response to Question A) would cause an overestimate in the model estimated O&G emission impacts.

Finding F1: Decadal scale ozone changes in three Texas O&G basins can be quantitatively described as interannual variations about smooth, continuous declines; neither the variations nor the declines significantly correlate with O&G production or drilling activity. This lack of correlation indicates that O&G development does not have a major impact on ozone concentrations in Texas (<5 parts per billion [ppb] on ozone design values and median ozone season daily maximum 8-hour average (MDA8) ozone concentrations).

Finding F2: VOC measurements made in the vicinity of intensive O&G development show that light alkanes consistent with O&G production are present at concentrations well above those in most other U.S. areas, and can make up a large fraction of the observed total VOC mass and mixing ratio (e.g. ~80% in the Denver-Julesburg Basin).

Finding F3: Estimates of the relative contribution of O&G VOC emissions to the total OH reactivity are variable and depend on the local influence of highly reactive biogenic VOCs.

Finding F4: The relative contribution of O&G VOC emissions to photochemical ozone formation is smaller than their relative contribution to the total OH reactivity because of the relatively small radical propagation potential of alkanes (~20% in the Denver-Julesburg Basin).

Finding F5: In one O&G basin, analysis of observations indicates that the ozone production efficiency was 5.3 ± 3.6 ppb ozone formed per ppb NOx oxidized.

Finding F6: Photochemical modeling of a 2017 future year seasonal episode showed that projected ozone contributions from O&G emissions to East Texas regulatory monitor design values (ODVs) were 5 ppb or less.

Finding F7: The contribution to ozone at East Texas monitors from O&G NOx emissions is far larger than the contribution from O&G VOC emissions.

Question G

Are there significant differences in ozone (O_3) and PM formation mechanisms between the major oil and natural gas basins in Texas?

Modeling and observational analysis agree that O&G emissions are responsible for only very small PM_{2.5} enhancements in Texas O&G gas basins, at least in spring and summer. Modeling that incorporates our current understanding of PM formation mechanisms finds only very small PM_{2.5} enhancements from O&G emissions (Finding G1). Findings G2 and G3 examine long-term measurements of PM_{2.5} in North Dakota and Texas as well as PM_{2.5} speciation in North Dakota to evaluate the impact that increasing O&G emissions have had on various metrics of ambient PM_{2.5} concentrations. No discernible impact could be found in any of the analyses. More sophisticated analyses of these measurement records that consider in detail different metrics of ambient PM concentrations, as well as possible confounding factors such as the impacts of

long-term changes in other emission sources, could reveal more detailed information regarding O&G impacts on ambient PM_{2.5} concentrations. Although not discussed explicitly in the Responses to any of the Science Questions, all investigations of ozone formation from O&G emissions suggest that traditional photochemical mechanisms involving NOx and VOC precursors are adequate to account for the observed ozone enhancements.

Finding G1: Modeling utilizing current VOC emission inventories simulates very small summertime SOA concentrations from the oil/gas sector. These simulations may underestimate SOA formation by a factor of ~4 due to emission uncertainties, but even so the simulated O&G SOA contributions would be small.

Finding G2: In the Bakken O&G production region in North Dakota, that development has not discernably increased seasonal mean concentrations of any PM constituent.

Finding G3: In Texas, PM_{2.5} concentrations in urban areas and O&G basins are of similar magnitude and show similar decadal declines; there is no discernible indication that the O&G activities have affected total PM_{2.5} concentrations.

Question H

Are there important interactions between emissions from oil and natural gas development and emissions from other sources such as urban, point source and biogenic, including crops and animal husbandry?

Ambient concentrations of secondary PM result from a variety of mechanisms that convert several different precursors from two or more source sectors to PM components. Findings H1 and H2 review some surface and aircraft studies, respectively, that have identified generally small PM enhancements from the interactions of emissions from O&G emissions with other emission sectors. Findings H3, H4 and H5 present some preliminary results from analyses of data collected on flights of the NOAA WP-3D aircraft during 2013 and 2015; the focus here is on ozone production in air masses affected by VOC from O&G and NOx from urban or point source emissions. Some evidence for synergistic ozone production is identified, but no general conclusions can yet be drawn.

Finding H1: The impact of NOx emissions from O&G development on fine particle and haze formation can depend strongly on concentrations of other species, including sulfate and ammonia, as well as the relative importance of different pathways for total reactive oxidized nitrogen (NOy) formation.

Finding H2: Ammonium nitrate formation potential can be evaluated from aircraft measurements of gaseous ammonia (NH₃) and nitric acid (HNO₃); based on springtime data, this potential is small over four Texas O&G basins. However, at altitude or during colder times of year the NH₃ and HNO₃ product may exceed that required for particulate ammonium nitrate (NH₄NO₃) formation.

Finding H3: An April 2015 flight over the Eagle Ford Basin reveals the largest concentrations of ozone observed over the basin were in an urban plume transported through the area of O&G emissions.

Finding H4: Overall, daytime NOx and NOy mixing ratios in Texas O&G basins are moderate (NOx generally < 1 ppb), but meteorological conditions and non-O&G sources can lead to higher concentrations.

Finding H5: Due to the relatively high VOC availability, Texas O&G basins are NOx sensitive and significant enhancements in localized ozone production rates can occur near and/or downwind of local NOx sources.

Question I

Are there gaps in our understanding of chemical transformations that limit a full understanding of ozone and PM formation from O&G development emissions?

Ozone and PM are formed by chemical transformations of emissions to the atmosphere. These transformation mechanisms are complex, involving hundreds of chemical reactions and physical transformations. Our understanding of these processes is certainly incomplete, but we have not identified any gaps that imply major uncertainties in our understanding of the air quality impacts of emissions from O&G development. Recent research has narrowed some perceived gaps, including the magnitude of atmospheric OH concentrations (Finding I2) and the applicability of "lumped" chemical mechanisms to O&G emissions (Finding I7), yielding reduced uncertainty in our understanding.

Finding I1: In many oil and natural gas basins, isoprene plays a significant role in the atmospheric chemistry; models must include detailed isoprene oxidation mechanisms for accurate modeling of isoprene's role.

Finding I2: Observations collected during the Southeast Atmosphere Study (SAS) indicate that OH concentrations are accurately predicted by models, at least if they include detailed chemistry. Previous work has reported dramatically higher OH at low NOx concentrations than current chemistry predicts; these reports were due to measurement interferences rather than shortcomings in the model chemical mechanisms.

Finding I3: Fully defining the importance of SOA formation from VOC precursors emitted from O&G exploitation requires a better general characterization of SOA formation mechanisms from precursor VOCs.

Finding I4: High concentrations of a gas-phase soluble chloride species (presumably HCl) have been observed in the Barnett Shale region. The photochemical transformations that lead to the formation of this species, and any effect on photochemical ozone production, remain uncertain.

Finding I5: Chlorine radicals do play a significant but relatively minor role in tropospheric chemistry, likely in oil and natural gas basins as well as in urban areas; accurate photochemical modeling requires inclusion of Cl reactions in the chemical mechanism.

Finding I6: Photochemical ozone formation in the Denver-Julesburg O&G Basin in Colorado was modeled with both the "lumped" CB6r3 and the explicit Master Chemical Mechanism (MCM) chemical mechanisms. The total VOC OH reactivity and total ozone produced were very similar in the two calculations, and both show similar NOx dependence of the total ozone production.

ES.2.3 Transport and Meteorology

Question J

What is the impact on other regions of Texas from ozone, PM and their precursors transported from oil and natural gas development areas? How does the impact from O&G development compare to impacts from other sources, e.g., upwind cities, rural power plants, and biogenic emissions?

Photochemical modeling of O&G emissions finds modest impacts on ozone concentrations throughout Texas. These impacts decrease with distance from the O&G basin, and in urban areas are generally smaller than the impacts of emissions from other emission source sectors. The accuracy of these model results depends on the accuracy of the underlying emission inventories, which has been questioned. Comparisons of bottom-up and top-down NOx emission inventories in O&G regions indicate that bottom-up inventories overestimate NOx emissions, and that these overestimates may introduce bias into estimates of ozone impacts from O&G development so that the O&G ozone impacts found here may overestimate the actual ODV impacts. Future analysis aimed at resolving the emission inventory uncertainty could potentially improve the accuracy of the model results and would increase our confidence in them.

Finding J1: The ozone contribution at East Texas monitors from O&G emissions is greatest within the O&G development areas, but can extend outward beyond them. Although the contributions outside the development areas are relatively small, they can be large enough to affect ozone design values.

Finding J2: The magnitude of the O&G contribution relative to other emissions sources varies depending on each monitor's proximity to power plants, major roadways and heavily vegetated areas.

Finding J3: For all Houston-Galveston-Brazoria area monitors, the average and maximum contribution from East Texas shale O&G emissions to the MDA8 ozone was less than those of onroad mobile, natural, and electric generating unit (EGU) sources.

Finding J4: For all Dallas-Fort Worth area monitors, the average and maximum contributions from East Texas shale O&G emissions to the MDA8 ozone were less than those of onroad mobile source emissions.

Question K

What gaps remain to accurately attribute ozone and PM formation to emissions source sectors throughout the state?

We have identified no major gaps in our understanding of transport and meteorology that significantly impact our ability to accurately attribute ozone and PM formation to emissions source sectors throughout Texas, although better characterization of the distribution of NH₃ concentrations would improve our understanding of NH₄NO₃ formation from O&G NOx emissions.

Finding K1: Uncertainty regarding the spatial and temporal distribution of gas phase NH₃ concentrations limits our ability to predict O&G contributions of NH₄NO₃ to PM_{2.5} concentrations.

1.0 INTRODUCTION

The past decade has seen expanded oil and natural gas (O&G) resource development in Texas. Advances in hydraulic fracturing and other drilling technologies led to intensive activity in areas with existing development as well as previously unexploited areas of the State (Figure 1-1).

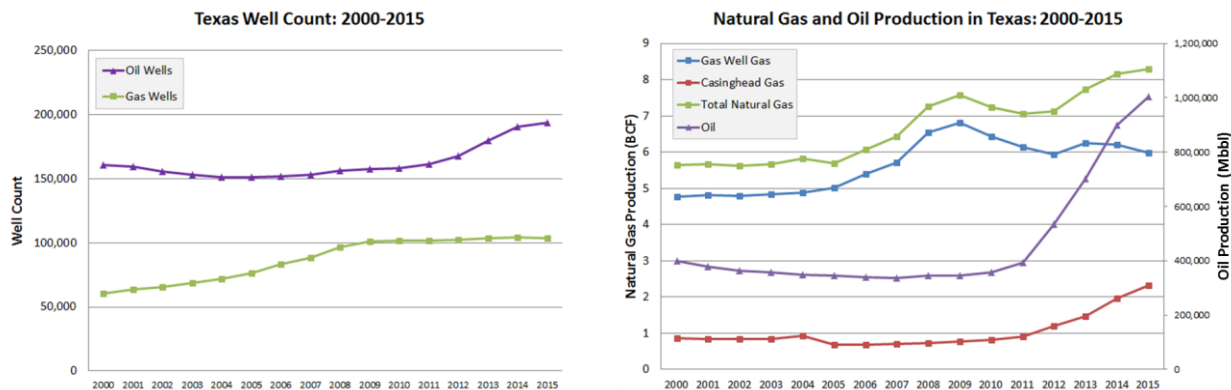


Figure 1-1. Trends in Texas state-wide well count (left) and O&G production (right). Data from Texas Railroad Commission¹.

Active areas include the Barnett Shale play near Fort Worth, the Eagle Ford play south of San Antonio, the Haynesville play in east Texas, as well as other formations (e.g., Granite Wash and Permian) throughout the State. O&G development and production activities have the potential to impact air quality. Direct emissions to the atmosphere associated with O&G activity include precursors of ozone and particulate matter (PM) (volatile organic compounds [VOC], nitrogen oxides [NOx]), and some air toxics (e.g., benzene and hydrogen sulfide [H₂S]).

1.1 Recent Field Studies

Several recent field studies investigated the atmospheric impacts of O&G emissions. A Dallas-Fort Worth (Barnett Shale) field campaign initiated in 2010 includes an augmented set of measurements in and around Eagle Mountain Lake in the summer of 2011 [Allen *et al.*, 2012]. The National Oceanic and Atmospheric Administration Chemical Sciences Division (NOAA/CSD) used the WP-3D aircraft to conduct the Southeast Nexus (SENEX) (Studying the Interactions Between Natural and Anthropogenic Emissions at the Nexus of Climate Change and Air Quality) field study during the summer of 2013. SENEX included two flights over the Haynesville formation [Peischl *et al.*, 2015]. The NOAA Global Monitoring Division (NOAA/GMD) [Yacovitch *et al.*, 2014] conducted flights over the Barnett Shale region in spring 2013. Allen *et al.* [2013] of the University of Texas directly measured emissions within O&G fields. The Houston Advanced Research Center (HARC) is working to analyze such emissions and has conducted modeling of air quality impacts in the Eagle Ford region [HARC, 2015]. Of particular interest is the work of Peischl *et al.* [2015], who found much lower rates of natural gas leakage from the

¹ <http://www.rrc.state.tx.us/oil-gas/research-and-statistics/production-data/historical-production-data/>

fields they studied compared to other earlier studies reported in the literature; notably, they studied the three basins (including the Haynesville play) that account for over half of the nation's shale gas production, while the earlier studies investigated basins with much smaller production. Thus, previous estimates of the national average loss rate may have been high.

Additional field studies that have investigated O&G emissions include the NOAA/CSD WP-3D aircraft-based SONGNEX (Shale Oil and Natural Gas Nexus - Studying the Atmospheric Effects of Changing Energy Use in the United States (U.S.) at the Nexus of Air Quality and Climate Change) during April-May 2015, and the FRAPPÉ (Front Range Air Pollution and Photochemistry Experiment) campaign in Colorado during July-August 2014. These campaigns have involved NOAA, the National Center for Atmospheric Research (NCAR), the National Aeronautics and Space Administration (NASA) and many other organizations and agencies, and the results have been and will continue to be presented in a wide range of journal publications and reports.

This synthesis draws upon the results from these and other relevant studies, in order to reflect the latest and most rigorous scientific findings available. A recent paper by *Allen* [2016] provides an excellent overview of the state of the science on O&G air impacts. Our aim is to build on that work, synthesizing results not available at the time that paper was written, and expanding the discussion of results most relevant for Texas.

1.2 Emissions

In this section, we provide an overview of emissions of precursors of ozone and PM as well as primary PM from O&G sources. Detailed descriptions of emissions from O&G sources may be found in *Moore et al.*, [2014] and *Armendariz* [2009] among many others. The life cycle of an O&G field can be divided into several phases [e.g. *Branosky*, 2012; *Moore et al.* 2014]: (1) preproduction; (2) production; (3) transmission, storage, and distribution; (4) end use; and (5) well production end-of-life. Here, we focus on exploration and production (upstream) O&G sources and describe emissions during the pre-production (well construction through completion) and production (post-completion) phases in the life of a well. Emissions in the transmission phase are composed mainly of methane [*Moore et al.*, 2014], which is not considered an ozone or PM precursor. While emissions of ozone and PM precursors occur in the use phase (e.g. NOx emissions from natural gas-fired power plants), that is not our focus in this study. The interested reader may find analysis of this topic in *Pacsi et al.* [2015].

The pre-production phase of an oil or gas well's life begins with clearing of the well pad site and construction of the well pad and any required roadways and/or pipelines. Next, the well is drilled and completed so that it is prepared for production. Well completion can include hydraulic fracturing ("fracking") of the rock surrounding the well bore to stimulate production. A section of the well bore is perforated, and hydraulic fracturing fluid, a mixture of water, proppant solids (sand or engineered materials) and chemical additives, is pumped down the well through the perforations into the rock. The water fractures the rock, releasing the gas. The proppant keeps the fractures open. Some of the fracturing fluid then flows back to the surface (frack flowback).

NOx emissions from the pre-production phase of the well's life come mainly from diesel engines powering the construction, drilling and fracking equipment. NOx is also emitted by heavy-duty diesel trucks transporting material and water to and from the well. If produced water and frack flowback are not sent to a pipeline or on-site surface impoundment, hundreds of heavy-duty truck trips are required to transport the water and fluid to a disposal site; emissions of NOx from heavy-duty truck traffic can be significant [e.g. NCTCOG² 2012; DenBleyker *et al.*, 2013].

VOC and hazardous air pollutants such as hydrogen sulfide (H_2S) arise during the pre-production phase from off-gassing as fluids and muds used to lubricate the drill bit return to the surface from the well bore [e.g. Macey *et al.*, 2014]. During well completion, water and other fluids used to fracture the well flow back to the surface; these liquids can contain dissolved VOCs and hazardous air pollutants (HAPs) such as benzene, ethylbenzene and n-hexane that are emitted to the air at the lower pressure of the surface [EPA, 2012]. H_2S can be emitted during drilling from frack fluid flowback or from produced water.

PM emissions from the pre-production phase come from diesel exhaust as well as direct emissions of fugitive dust from well pad construction and truck traffic on unpaved roads. VOCs are emitted from diesel exhaust, but the main sources are well completion venting, mud degassing, frack fluid flowback, and produced water. Relatively small amounts of SO_2 are emitted by diesel engines but are otherwise minimal provided the well is not accessing a formation containing significant amounts of H_2S . In this case, SO_2 can be emitted from well combustion processes, such as flaring.

Once a well is completed, it begins the production phase of its life. During the production phase, NOx is emitted by artificial lift (pumpjack) engines, compressor engines, heater treaters, process heaters, dehydrator glycol regenerator boilers and flares or combustors in dehydrators, tanks and pneumatic devices. Well workover equipment and truck traffic also produce NOx emissions and truck traffic emissions produce emissions of PM. The main sources of VOC emissions during the production phase are oil and condensate tanks, dehydrator flash vessels and regenerator vents, pneumatic devices and pumps, fugitives (leaks) and truck/rail liquid hydrocarbon loading operations, well re-completion, wellhead blowdowns, venting, produced water and evaporation ponds.

Emissions across a hydrocarbon-producing field vary in space, with many well site sources that are small individually, but large in the aggregate at basin scale. While individual wells share many of the same basic processes and emissions, when we consider O&G producing regions as a whole, the type and quantity of field-scale NOx and VOC emissions varies from field to field within Texas. Two important factors controlling the magnitudes of NOx and VOC emissions are the phase of development of the field as a whole and the composition of the hydrocarbons produced.

² North Central Texas Council of Governments

The quantity and composition of emitted VOCs and HAPs in the production phase is dependent on the composition of gas and liquids produced. Dry natural gas is composed almost entirely of methane and is the end product supplied to transmission pipelines and end users. At the well head, however, what is often produced is “wet gas”. Besides methane, wet gas contains other hydrocarbons including ethane and other light alkanes such as propane, butane and pentanes (natural gas liquids). The gas may also contain water vapor, CO₂, nitrogen and H₂S as well as other compounds. Natural gas is processed, either at well head or centralized processing sites, to remove these impurities as well as natural gas liquids so that the gas is sufficiently dry to enter transmission pipelines for delivery to end users. Wells with a larger amount of produced liquids have larger emissions of heavier VOCs and HAPs than wells that produce dry gas consisting nearly entirely of methane [e.g. Warneke *et al.*, 2014].

Within Texas, there is great variation from field to field in terms of the composition of produced hydrocarbons. For example, the Haynesville Shale has no oil production and little condensate production, while the Eagle Ford Shale wells range from deeper wells that produce mainly dry gas to shallower wells that produce mainly oil. There is far more liquid production from the Eagle Ford Shale than the Haynesville. The Barnett Shale region falls in between these other two Texas shales in terms of its ratio of liquid to gas production³.

The composition of the produced hydrocarbons also affects the reactivity of the emissions from the production phase. The reactivity is a measure of how likely emitted compounds are to participate in ozone formation. Dry gas, which is composed almost entirely of methane, has very low reactivity. Emissions from wells and processes producing wet gas and/or liquids have a higher concentration of VOCs [e.g. Warneke *et al.*, 2014] and therefore a higher reactivity. However, the reactivity of the VOCs emitted from O&G activities overall is relatively low. This is because VOC emissions from O&G activities are dominated by light alkanes, which have lower likelihood of participating in ozone formation compared to those of highly reactive biogenic species such as isoprene. However, O&G emissions can play an important role in determining the overall VOC reactivity in regions where the biogenic contribution is small [Gilman *et al.*, 2013; McDuffie *et al.*, 2016].

The intensity of NOx and VOC emissions and their relative amounts is influenced by the phase of production and the overall well count within a producing region. Production is driven by the price of O&G (Figure 1-2 upper panel). The price of natural gas, as measured by the annual average of the Henry Hub Spot Price⁴, exceeded 5\$/MMBtu from 2003 to 2008, reaching a peak of 8.9\$/MMBtu in 2008. The price dropped sharply in 2009 due to the global recession and an abundance of shale gas produced from formations across the U.S. The annual average price has remained below 5\$/MMBtu since 2009 as natural gas production and supply have remained strong. The price of crude oil, measured by the price of West Texas Intermediate Crude, rose from 2002 through 2008, then dropped sharply during the recession. From 2010-2013, oil

³ <http://www.rrc.state.tx.us/oil-gas/major-oil-gas-formations/>

⁴ <https://www.eia.gov/dnav/ng/hist/rngwhhdA.htm>

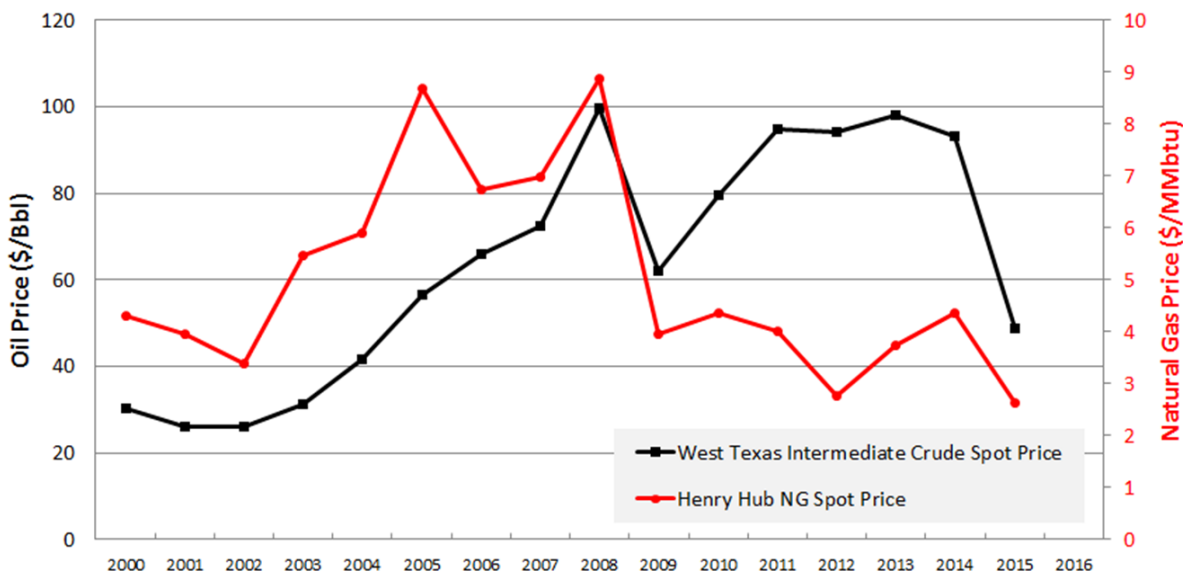
prices rose and economics favored production of oil over production of natural gas. The price of oil dropped sharply in 2015 due to strong global supply.

The lower panel of Figure 1-2 shows recent drilling activity in three East Texas shales. Drilling in the Barnett Shale increased as O&G prices rose between 2000 and 2008. Both natural gas and liquid hydrocarbons are produced in the Barnett. Drilling activity began in the Haynesville Shale in 2008. Haynesville wells were highly productive and overall production in the Haynesville (including production from Texas and Louisiana wells) surpassed that of the Barnett in 2010⁵.

The peak of drilling activity in the Haynesville occurred in 2010 and then dropped steadily as the price of natural gas fell. Haynesville wells produce mainly dry gas with little condensate, and as the price of natural gas remained low while oil prices climbed steadily during 2010-2015, drilling activity in the Haynesville dropped dramatically. Meanwhile, drilling in the Eagle Ford, which has much greater oil and condensate production, increased through 2014 and then fell dramatically as the price of oil declined sharply in 2015.

⁵ http://www.eia.gov/energyexplained/index.cfm?page=natural_gas_where

Oil and Natural Gas Prices: 2000-2015



Drilling Permits Issued in East Texas Shale Regions: 2000-2016

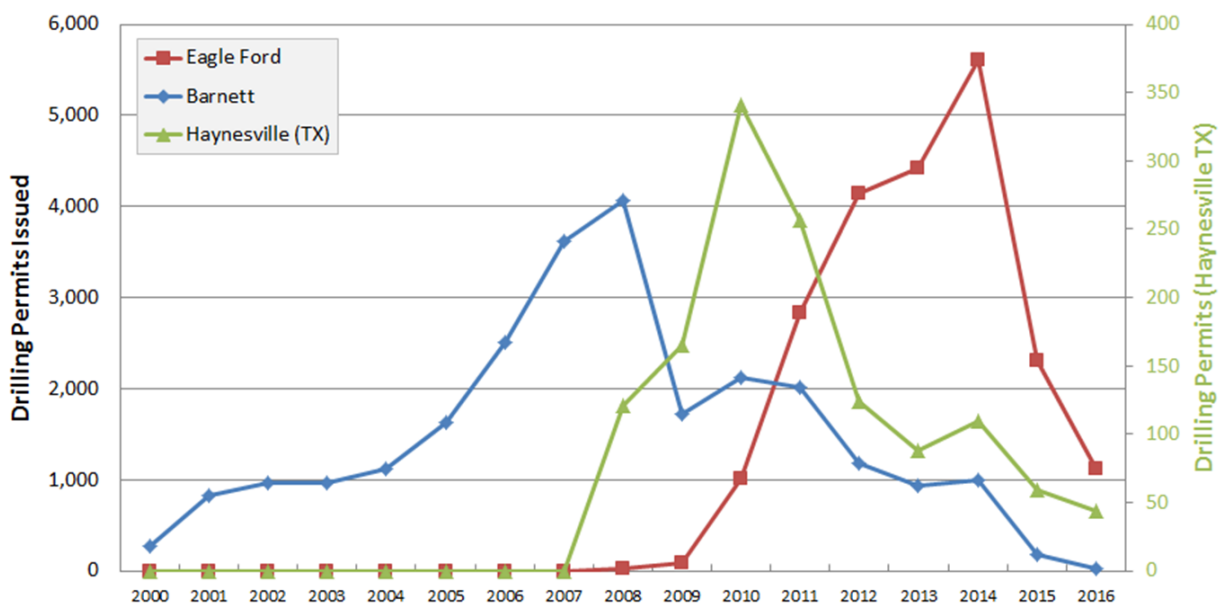


Figure 1-2. Upper panel: annual average price of West Texas Intermediate (WTI) Crude Oil (left axis, \$/Bbl, black) and the Henry Hub Natural Gas Spot Price (right axis, \$/MMBtu, red). Lower panel: Drilling permits for the Eagle Ford and Barnett Shale (Haynesville) plotted on left (right) axis. Haynesville permit data are for Texas wells only, and do not include wells in Louisiana. Data from Texas Railroad Commission⁶

⁶ <http://www.rrc.state.tx.us/oil-gas/research-and-statistics/production-data/historical-production-data/>

Field-wide emissions of NOx and VOC change over the life of the field. During the period of time when exploration is occurring and many wells in a field are in the pre-production phase, NOx emissions from drilling and fracking engines and truck traffic are important. Once a field is mature and the bulk of the wells are in the production phase, NOx emissions come mainly from artificial lift engines, compression and flaring. Peak field-wide NOx emissions typically occur while drilling and fracking activity are still intense and many wells have entered the production phase. Once drilling activity slows, NOx emissions remain relatively constant at a lower level. Field-wide VOC emissions are mainly driven by production emissions, which increase with the well count. For an individual well, maximum production typically occurs immediately after drilling and then productivity decreases with time as the reservoir is drained. As the pace of drilling slows when the field becomes fully developed, the field-wide VOC emissions begin to decline as production from wells decreases over time.

During the production phase, the relative amounts of emitted NOx and VOC are influenced by the hydrocarbon composition as well as emission controls. Natural gas can be produced in wells that mainly produce liquids; this associated gas is a by-product of the production of the liquids. A pipeline may not be available to transport the gas from the well to market, so the gas may be vented or flared at the wellsite. Flaring can also occur during maintenance of gas lines or compressors when gas pipeline capacity is exceeded and during gas plant service interruptions. When the gas is flared, a substantial fraction of VOC emissions is destroyed and NOx is produced as a result of high temperature combustion. Natural gas flaring has become quite prevalent in the Eagle Ford Shale, where associated gas is often produced along with the more valuable liquids and extensive pipeline infrastructure has not yet been developed. New Source Performance Standard (NSPS) OOOO promulgated by the EPA in 2012 required reduced emissions completions and control of many VOC-emitting wellsite processes for hydraulically fractured wells by January 2015. This increased the use of combustors or flares to reduce wellsite VOC emissions. Figure 1-3 shows a sharp increase in flaring and venting of natural gas coincident with the rapid development of the Eagle Ford as well as the promulgation of NSPS OOOO. Most of the flaring permit requests received by the Texas Railroad Commission are for flaring of associated gas from oil wells⁷. Increased incidence of flaring is important because of the emissions of NOx as well as the potential for uncombusted reactive hydrocarbons such as formaldehyde to be present in flare plumes. Emissions of NOx and VOC in the same plume may cause ozone formation downwind of the well site [Schade and Roest, 2016].

⁷ <http://www.rrc.state.tx.us/about-us/resource-center/faqs/oil-gas-faqs/faq-flaring-regulation/>

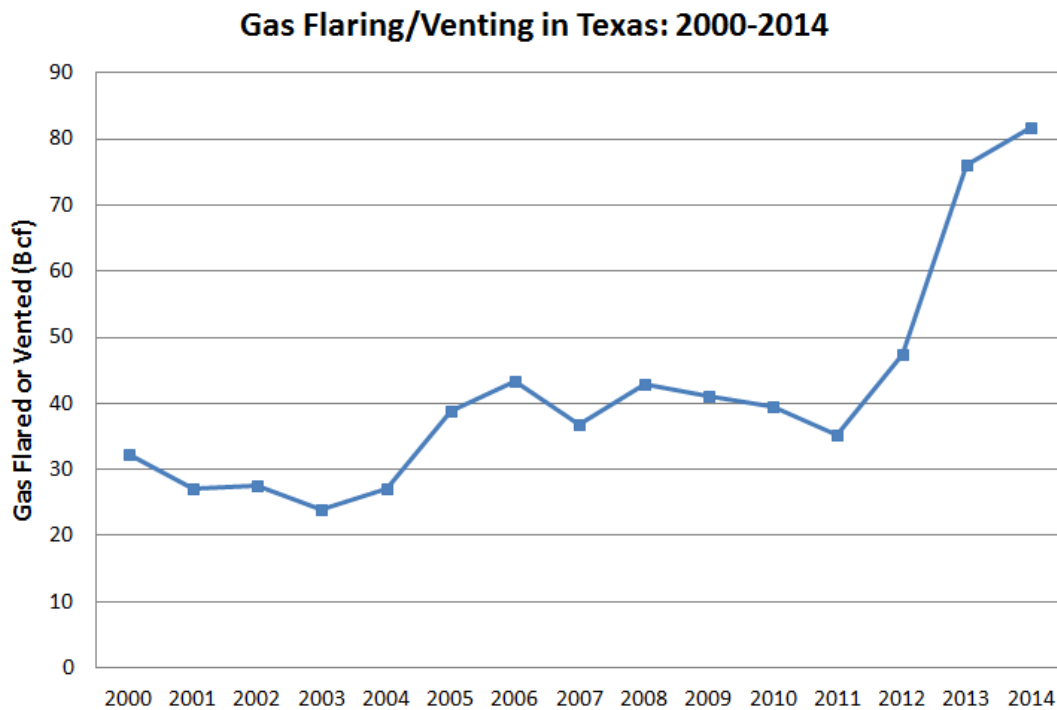


Figure 1-3. Trends in Texas state-wide flaring and venting of natural gas. Data from Texas Railroad Commission⁸.

As observed from space, NOx levels associated with O&G activity (e.g., flaring and combustion from O&G extraction machinery and transport vehicles) have recently increased over the Permian and Eagle Ford basins [Duncan *et al.*, 2016]. These basins had minimal NOx emissions and human activity prior to the onset of O&G extraction activity, so that the increase in NOx emissions can be directly linked to O&G sources. Night time satellite images show lights from drilling equipment, man camps and flares in the Eagle Ford Shale. The increase in night time lighting coincided with the location of enhanced NOx [Duncan *et al.*, 2016]. That the increased O&G activity in the Eagle Ford is visible from space indicates the scale of development and importance of evaluating the impact of O&G emissions on air quality in Texas.

1.3 Chemical Transformation

Ozone is not emitted directly into the atmosphere, but is formed from photochemical reactions of precursor species in the presence of sunlight. The most important precursors of ground level ozone are NOx and VOC. Emissions of these species from O&G sources have been shown to contribute to the formation of ozone under a wide range of ambient conditions.

In 2005, high ozone was measured in the Upper Green River Basin (UGRB) of Wyoming during winter. The phenomenon of winter high ozone under conditions with low sun angles and cold

⁸<http://www.rrc.state.tx.us/about-us/resource-center/faqs/oil-gas-faqs/faq-flaring-regulation/>

temperatures was novel, particularly because the UGRB is a rural area whose main source of ozone precursor emissions was O&G exploration and production. High ozone levels were recorded again in the UGRB in subsequent years as well as in the Uinta Basin region in rural eastern Utah, where extensive O&G production is also occurring. Field studies were carried out in the UGRB and in the Uinta Basin and the mechanisms for ozone formation under winter conditions were determined through analysis of ambient data [Schnell *et al.*, 2009; Oltmans *et al.*, 2014; Helmig *et al.*, 2014; Rappenglück *et al.*, 2014] as well as modeling studies [Carter and Seinfeld, 2012; Edwards *et al.*, 2013; 2014; Ahmadov *et al.*, 2015; Field *et al.*, 2015]. The conceptual model for winter ozone formation that arose from this work is that the following conditions are necessary: (1) shallow temperature inversion that limits vertical mixing; (2) highly reflective snow on ground that enhances sunlight available for ozone formation and facilitates development and maintenance of the temperature inversion; (3) few or no clouds; (4) stagnant and/or recirculating slow surface winds that limit dispersion of pollutants; (5) high precursor concentrations; and (6) high VOC/NOx emission ratio.

Winter ozone episodes occur in rural regions where (1) the only significant local sources of ozone precursors are O&G exploration and production activities and (2) transport of ozone and precursors is limited by stagnant winds and a strong temperature inversion. Summer ozone episode conditions are extremely different: summer ozone is typically associated with warm temperatures and abundant sunlight in urban areas where there is an abundance of ozone precursors from human activities other than O&G exploration and production [e.g. Trainer *et al.*, 2000; Ryerson *et al.*, 2003]. The high angle of the summer sun means there is sufficient sunlight available to drive the photochemical reactions that produce ozone. High summer temperatures enhance VOC emissions and speed the chemical reactions that produce ozone from its precursors, and light or stagnant winds typically limit dispersion. Under summer conditions, O&G emissions can increase ambient ozone concentrations, along with other sources of precursor emissions.

Several studies have performed regional and box modeling of summer episodes and determined that ozone production was positively influenced by emissions associated with O&G activity in the Haynesville region [Kemball-Cook *et al.*, 2010] and in the Eagle Ford region [Pacsi *et al.*, 2015] as well as across multiple western U.S. locations [Rodriguez *et al.*, 2009] and in the Colorado Front Range O&G production region [McDuffie *et al.*, 2016]. Rutter *et al.* [2015] found that VOC from O&G sources had sufficient OH reactivity to increase ozone concentrations in the Barnett Shale region. A remaining policy-relevant uncertainty is the magnitude of the ozone increases due to the O&G emissions, and how that magnitude varies spatially and temporally.

Recent work has suggested that O&G-associated NOx emissions can contribute disproportionately to summertime ozone production relative to VOC emissions. For example, O&G-associated VOC emissions only contribute 8% to ozone precursors in California's San Joaquin Valley [Gentner *et al.*, 2014] and less than 20% and 7%, respectively, to the ozone forming potential in the Barnett Basin near Fort Worth, Texas [Rutter *et al.*, 2015] and Pennsylvania's Marcellus Basin [Swarthout *et al.*, 2015]. Similarly, regional modeling of the Eagle Ford Basin in Texas showed that changes in regional summertime ozone concentrations

were not driven by O&G-associated VOCs but rather by emissions of NOx [Pacsi *et al.*, 2015]. The importance of the contribution to ozone formation from O&G-associated NOx and VOCs is affected by the magnitude and reactivity of regional biogenic VOC emissions. O&G VOC emissions are dominated by alkanes that have relatively low reactivity while the regional VOC emission inventories for the rural Haynesville and Eagle Ford Shale regions are dominated by highly reactive biogenic emissions (e.g. isoprene, monoterpenes) [e.g. Grant *et al.*, 2013]. The contribution of O&G emissions to ozone formation is therefore determined by the amount of O&G NOx emissions [Pacsi *et al.*, 2015]. The Barnett Shale region is far more urban than the Haynesville and Eagle Ford Shale areas and biogenic emissions are a smaller component of the Barnett Shale area VOC inventory. The background reactivity of the atmosphere is lower in the Barnett than in the Haynesville and Eagle Ford Shale regions, so that less ozone is formed from O&G emissions overall [Allen, 2016; Pacsi *et al.*, 2013].

1.4 Transport and Meteorology

In East Texas, the lack of major topographical features means that wind patterns are driven primarily by synoptic-scale meteorological influences. Episodes of high ground level ozone typically occur between March and October when the area is under the influence of a semi-permanent subtropical high-pressure system, vertical mixing of pollutants in the atmosphere is restricted, skies are clear to partly cloudy, temperatures are high, and winds are light [TCEQ, 2009; TCEQ, 2016]. These conditions, which are conducive to ozone formation, can also be produced by passage of a cold front or the presence of a stationary front. Most East Texas ozone episodes are associated with light near-surface winds from the north/east/south/southwest, with southerly directions appearing less frequently on days with highest ozone. Days during the ozone season with low ozone typically occur during periods of strong southerly winds that bring comparatively less polluted maritime air from the Gulf of Mexico northward into East Texas.

Berlin *et al.* [2013] define the regional background ozone to be “*the concentration that would be present if no ozone were produced from NOx and VOC precursors emitted locally on that day, or emitted on preceding days and recirculated locally by mesoscale circulations*”, and note that ozone measured at a particular location is the sum of the regional background transported into the area by the large-scale winds and ozone produced from local emissions of ozone precursors. In their analysis of ozone transport in Texas, Banta *et al.* [2005] described how ozone and precursors can be lofted above the boundary layer, transported far downwind overnight, and then mixed downward to affect a downwind surface location the next day. In this manner, ozone formed from O&G emissions, as well as other sources of ozone precursors, can contribute to the regional background ozone and can affect ozone in areas far downwind.

Kemball-Cook *et al.* [2010] used a photochemical model to evaluate potential changes in regional ozone due to projected increases in Haynesville Shale emissions. The modeling indicated that Haynesville emissions increases could cause ozone impacts extending well outside the immediate vicinity of the Haynesville Shale into other regions of Texas and Louisiana due to ozone transport by the modeled winds. Pacsi *et al.* [2015] used a

photochemical model to assess ozone impacts of O&G development in the Eagle Ford Shale. Under the weather conditions of their 2006 modeling episode, the San Antonio and Austin metropolitan areas were often downwind of the Eagle Ford Shale. Pacsi *et al.* [2015] calculated the ozone impact of Eagle Ford O&G emissions on these two areas, and found they varied from day to day during the month-long episode depending on the wind direction, with impacts on the daily maximum 8-hour average ozone that ranged from 0.1-2.5 ppb for San Antonio and 0.0-1.9 ppb for Austin.

These two studies indicate that ozone formed from emissions due to O&G development can affect Texas regions outside the exploration/production area and that evaluation of air quality impacts due to O&G development should include the surrounding region, especially areas that are downwind under wind conditions associated with high ozone events.

1.5 References

- Ahmadov, R., et al. (2015), *Understanding high wintertime ozone pollution events in an oil- and natural gas-producing region of the western US*, Atmos. Chem. Phys., 15(1), 411–429, doi:10.5194/acp-15-411-2015.
- Allen, D., E. McDonald-Buller, and G. McGaughey (2012), *State of the Science of Air Quality in Texas: Scientific Findings from the Air Quality Research Program (AQRP) and Recommendations for Future Research*, Final Report, Project Number 10-SSA, prepared for Air Quality Research Program.
- Allen, D., et al. (2013), *Measurements of methane emissions at natural gas production sites in the United States*, PNAS, 110 (44) 17768-17773, doi:10.1073/pnas.1304880110.
- Allen, D.T. (2016), *Emissions from oil and gas operations in the United States and their air quality implications*, J. Air & Waste Management Assoc., 66:6, 549-575, DOI: 10.1080/10962247.2016.1171263.
- Armendariz, A. (2009), *Emissions from Natural Gas Production in the Barnett Shale Area and Opportunities for Cost-Effective Improvements*. Prepared for Ramon Alvarez, Environmental Defense Fund. January. https://www.edf.org/sites/default/files/9235_Barnett_Shale_Report.pdf.
- Banta, R. M., C.J. Senff, J. Nielsen-Gammon, L.S. Darby, T.B. Ryerson, R.J. Alvarez, S.P. Sandberg, E.J. Williams, and M. Trainer (2005), *A Bad Air Day in Houston*, Bull. Am. Met. Soc., 86(5), 657-669.
- Berlin, S.R., A.O. Langford, M. Estes, M., M. Dong, and D.D. Parrish (2014), *Magnitude, decadal changes, and impact of regional background ozone transported into the greater Houston, Texas, Area*, Env. Sci. & Tech., 47, 13985–13992.
- Branosky, E.; Stevens, A.; Forbes, S. *Defining the Shale Gas Life Cycle: A Framework for Identifying and Mitigating Environmental Impacts*; World Resources Institute: Washington, DC, 2012.

- Carter, W. P. L., and J. H. Seinfeld (2012), *Winter ozone formation and VOC incremental reactivities in the Upper Green River Basin of Wyoming*, Atmos. Environ., 50, 255–266, doi:10.1016/j.atmosenv.2011.12.025.
- DenBleyker, A., Y. Alvarez, A. Bar-Ilan, S. Kemball-Cook and G. Yarwood (2013), *Haynesville Shale Mobile Sources Emission Inventory*. Report for the East Texas Council of Governments.
http://www.netac.org/UserFiles/file/NETAC/2013Reports/Updates/Haynesville_Mobile_EI_26Dec2013_Final.pdf.
- Duncan, B. N., L. N. Lamsal, A. M. Thompson, Y. Yoshida, Z. Lu, D. G. Streets, M. M. Hurwitz, and K. E. Pickering (2016), A space-based, high resolution view of notable changes in urban NO_x pollution around the world (2005–2014), J. Geophys. Res. Atmos., 121, 976–996, doi:10.1002/2015JD024121.
- Edwards, P. M., et al. (2013), *Ozone photochemistry in an oil and natural gas extraction region during winter: simulations of a snow-free season in the Uintah Basin, Utah*, Atmos. Chem. Phys., 13(17), 8955–8971, doi:10.5194/acp-13-8955-2013.
- Edwards, P. M., et al. (2014), *High winter ozone pollution from carbonyl photolysis in an oil and gas basin*, Nature, 514(7522), 351–354, doi:10.1038/nature13767.
- EPA (2012), *Overview of Final Amendments to Air Regulations for the Oil and Natural Gas Industry Fact Sheet*. April. https://www.epa.gov/sites/production/files/2016-09/documents/natural_gas_transmission_fact_sheet_2012.pdf
- Field, R. A., J. Soltis, M. C. McCarthy, S. Murphy, and D. C. Montague (2015), *Influence of oil and gas field operations on spatial and temporal distributions of atmospheric non-methane hydrocarbons and their effect on ozone formation in winter*, Atmos. Chem. Phys., 15(6), 3527–3542, doi:10.5194/acp-15-3527-2015.
- Gentner, D. R., et al. (2014), *Emissions of organic carbon and methane from petroleum and dairy operations in California's San Joaquin Valley*, Atmos. Chem. Phys., 14(10), 4955–4978, doi:10.5194/acp-14-4955-2014.
- Gilman, J. B., Lerner, B. M., Kuster, W. C., and de Gouw, J. A.: *Source Signature of Volatile Organic Compounds from Oil and Natural Gas Operations in Northeastern Colorado*, Environ. Sci. Technol., 47, 1297–1305, 2013.
- Grant, J., S. Kemball-Cook and G. Yarwood (2013) *Review of emissions for the East Texas Council of Governments Area*. Prepared for the East Texas Council of Governments, Kilgore, TX. December.
[http://www.netac.org/UserFiles/File/NETAC/2013Reports/Task%202.2%20ETCOG_EI_review_26Dec2013\(2.2\).pdf](http://www.netac.org/UserFiles/File/NETAC/2013Reports/Task%202.2%20ETCOG_EI_review_26Dec2013(2.2).pdf)
- Helmig, D., C. R. Thompson, J. Evans, P. Boylan, J. Hueber, and J. H. Park (2014), *Highly elevated atmospheric levels of volatile organic compounds in the Uintah Basin, Utah*, Environ. Sci. Technol., 48(9), 4707–4715, doi:10.1021/es405046r.

- Houston Advanced Research Center (2016) *Analyzing Methane Emissions from Upstream Oil and Gas Production Operations*,
http://www.harc.edu/work/Analyzing_Methane_Emissions_from_Upstream_Oil_and_Gas_Production_Operations.
- Kemball-Cook, S., A. Bar-Ilan, J. Grant, L. Parker, J. Jung, W. Santamaria, J. Mathews, and G. Yarwood (2010), *Ozone impacts of natural gas development in the Haynesville Shale*, Environ. Sci. Technol., 44(24), 9357–9363, doi:10.1021/es1021137.
- Macey, G. P., R. Breech, M. Chernaik, C. Cox, D. Larson, D. Thomas, and D.O. Carpenter (2014). *Air concentrations of volatile compounds near oil and gas production: a community-based exploratory study*. Environmental Health, 13, 82. <http://doi.org/10.1186/1476-069X-13-82>.
- McDuffie, E.E., P.M. Edwards, J.B. Gilman, B.M. Lerner, W.P. Dubé, M. Trainer, D.E. Wolfe, W.M. Angevine, J. deGouw, E.J. Williams, A.G. Tevlin, J. Murphy, E.V. Fischer, S. McKeen, T.B. Ryerson, J. Peischl, J.S. Holloway, K. Aikin, A.O. Langford, C.J. Senff, R.J. Alvarez II, S.R. Hall, K. Ullmann, K.O. Lantz, and S.S. Brown (2016), *Influence of oil and gas emissions on summertime ozone in the Colorado northern Front Range*, J. of Geophys. Res. Atmos., doi:10.1002/2016JD025265, 2016.
- Moore, C., B. Moore, G. Petron and R. Jackson (2014), *Air Impacts of Increased Natural Gas Acquisition, Processing, and Use: A Critical Review*. Environ. Sci. Technol., 2014, 48 (15), pp 8349–8359. DOI: 10.1021/es4053472.
- North Central Texas Council of Governments (2012), Development of oil and gas mobile source inventory in the Barnett Shale in the 12-County Dallas-Fort Worth Area. Report for the Texas Commission on Environmental Quality, Grant Number: 582-11-13174, https://www.tceq.texas.gov/assets/public/implementation/air/am/contracts/reports/mobile/5821113174FY1101-20120831-NCTCOG-BarnettShale_oil_gas_mobile_ei.pdf.
- Olaguer, E. P. (2016), *Atmospheric Impacts of the Oil and Gas Industry*. Academic Press.
- Oltmans, S., R. Schnell, B. Johnson, G. Petron, T. Mefford, and R. Neely (2014), *Anatomy of wintertime ozone associated with oil and natural gas extraction activity in Wyoming and Utah*, Elementa Sci. Anthropocene, 2, 000024, doi:10.12952/journal.elementa.000024.
- Pacsi, A. P., Y. Kimura, G. McGaughey, E. C. McDonald-Buller, and D. T. Allen (2015), *Regional ozone impacts of increased natural gas use in the Texas power sector and development in the Eagle Ford Shale*, Environ. Sci. Technol., 49(6), 3966–3973, doi:10.1021/es5055012.
- Peischl, J., T.B. Ryerson, K.C. Aikin, J.A. de Gouw, J.B. Gilman, J.S. Holloway, B.M. Lerner, R. Nadkarni, J.A. Neuman, J.B. Nowak, M. Trainer, C. Warneke, and D.D. Parrish (2015), *Quantifying atmospheric methane emissions from the Haynesville, Fayetteville, and northeastern Marcellus shale natural gas production regions*, J. Geophys. Res. - Atmos., 120, 2119–2139, doi:10.1002/2014JD022697.
- Rappenglück, B., et al. (2014), *Strong wintertime ozone events in the Upper Green River basin, Wyoming*, Atmos. Chem. Phys., 14(10), 4909–4934, doi:10.5194/acp-14-4909-2014.

- Rodriguez, M. A., M. G. Barna, and T. Moore (2009), *Regional impacts of oil and gas development on ozone formation in the Western United States*, J. Air Waste Manage., 59(9), 1111–1118, doi:10.3155/1047-3289.59.9.1111.
- Rutter, A. P., R. J. Griffin, B. K. Cevik, K. M. Shakya, L. Gong, S. Kim, J. H. Flynn, and B. L. Lefer (2015), Sources of air pollution in a region of oil and gas exploration downwind of a large city, *Atmos. Environ.*, 120, 89–99, doi:10.1016/j.atmosenv.2015.08.073.
- Ryerson, T. B., M. Trainer, W. M. Angevine, C.A. Brock, R.W. Dissly, F.C. Fehsenfeld, G.J. Frost, P.D. Goldan, J.S. Holloway, G. Hübner, R.O. Jakoubek, W.C. Kuster, J.A. Neuman, J. A., D.K. Nicks, D.D. Parrish, J.M. Roberts, D.T. Sueper, D. T., E.L. Atlas, S.G. Donnelly, F. Flocke, A. Fried, W.T. Potter, S. Schauffler, V. Stroud, A.J. Weinheimer, B.P. Wert, C. Wiedinmyer, R.J. Alvarez, R. M. Banta, L.S. Darby and C.J. Senff (2003) *Effect of petrochemical industrial emissions of reactive alkenes and NO_x on tropospheric ozone formation in Houston, Texas*, *J. Geophys. Res.*, 108, 4249, doi:10.1029/2002JD003070, 2003.
- Schade, G. and G. Roest (2016), *Analysis of non-methane hydrocarbon data from a monitoring station affected by oil and gas development in the Eagle Ford shale, Texas*, *Elem. Sci. Anth.*, 4, 000,096, doi:10.12952/journal.elementa.000096.
- Schnell, R. C., S. J. Oltmans, R. R. Neely, M. S. Endres, J. V. Molenar, and A. B. White (2009), *Rapid photochemical production of ozone at high concentrations in a rural site during winter*, *Nat. Geosci.*, 2(2), 120–122.
- Swarthout, R. F., R. S. Russo, Y. Zhou, B. M. Miller, B. Mitchell, E. Horsman, E. Lipsky, D. C. McCabe, E. Baum, and B. C. Sive (2015), *Impact of Marcellus Shale natural gas development in southwest Pennsylvania on volatile organic compound emissions and regional air quality*, *Environ. Sci. Technol.*, 49(5), 3175–3184, doi:10.1021/es504315f.
- TCEQ (2009) *Houston-Galveston-Brazoria Nonattainment Area Ozone Conceptual Model, Attachment 1 of Photochemical Modeling for the HGB Attainment Demonstration SIP Revision for the 1997 Eight-Hour Ozone Standard*, https://www.tceq.texas.gov/assets/public/implementation/air/sip/hgb/hgb_sip_2009/09017SIP_ado_Appendix_C.pdf.
- TCEQ (2016) DFW Conceptual Model, https://www.tceq.texas.gov/assets/public/implementation/air/sip/dfw/dfw_ad_sip_2016/DFW_AD_SIP_Appendix_D_2016ado.pdf.
- Trainer, M., D.D. Parrish, P.D. Goldan, J. Roberts, and F.C. Fehsenfeld (2000) *Review of observation-based analysis of the regional factors influencing ozone concentrations*, *Atmos. Environ.*, 34, 2045–2061.
- Warneke, C., F. Geiger, P. M. Edwards, W. Dube, G. Pétron, J. Kofler, A. Zahn et al. (2014) *Volatile organic compound emissions from the oil and natural gas industry in the Uintah Basin, Utah: oil and gas well pad emissions compared to ambient air composition*, *Atmos. Chem. Phys.*, 14, 10977–10988, doi:10.5194/acp-14-10977-2014.
- Yacovitch, T.I., et al. (2014), *Demonstration of an Ethane Spectrometer for Methane Source Identification*, *Environ. Sci. Technol.*, 48 (14), 8028–8034.

2.0 SCIENCE QUESTIONS

The following list of science questions was developed to guide this Report on the Atmospheric Impacts of Oil and Gas Development in Texas. The questions are intended to 1) address the issues of most importance to policy makers of the State of Texas, 2) be specific enough to provide a needed focus, and 3) be general enough to cover emerging scientific issues. These questions fall into three broad categories.

2.1 Emissions

- A. What are the emissions of ozone and PM precursors from O&G development in Texas?**
- B. How do the magnitude and composition of these emissions depend upon variables such as composition of extracted oil and natural gas and technologies employed? What are the important parameters controlling how these emissions vary over time and area?**
- C. How are these emissions divided between the various stages of fossil fuel extraction (exploration and production; product gathering and transmission; gas processing) and specific processes?**
- D. How do these emissions in Texas compare to other regions of the U.S.?**
- E. Are there gaps in our quantification of emissions that limit a full understanding of ozone and PM formation from these emissions?**

Air quality impacts of oil and gas development arise from emissions of precursors of O₃ and particulate matter (PM), specifically hydrocarbons (VOCs, primarily alkanes and aromatics) and oxides of nitrogen (NOx). A more thorough understanding of the atmospheric impact of these precursor emissions is desired.

2.2 Chemical Transformations

- F. What are the contributions of emissions from O&G development to ambient O₃ concentrations at regulatory monitors in Texas?**
- G. Are there significant differences in O₃ and PM formation mechanisms between the major oil and natural gas basins in Texas?**
- H. Are there important interactions between emissions from oil and natural gas development and emissions from other sources such as urban, point source and biogenic, including crops and animal husbandry?**
- I. Are there gaps in our understanding of chemical transformations that limit a full understanding of ozone and PM formation from O&G development emissions?**

Critical uncertainties remain in our understanding of how the primary emissions are transformed within the atmosphere.

2.3 Transport/Meteorology

- J. **What is the impact on other regions of Texas from ozone, PM and their precursors transported from oil and natural gas development areas? How does the impact from O&G development compare to impacts from other sources, e.g., upwind cities, rural power plants, and biogenic emissions?**
- K. **What gaps remain to accurately attribute ozone and PM formation to emissions source sectors throughout the state?**

3.0 SYNTHESIS OF RESULTS: EMISSIONS

3.1 Response to Question A

What are the emissions of ozone and PM precursors from O&G development in Texas?

3.1.1 Working Group

David Parrish - David.D.Parrish, LLC

Yuyan Cui - NOAA/ESRL/CSD

Sue Kemball-Cook - Ramboll Environ

Brian McDonald - NOAA/ESRL/CSD

Stuart McKeen - NOAA/ESRL/CSD

Jeff Peischl - NOAA/ESRL/CSD

Geoffrey Roest - Texas A&M University

Tom Ryerson - NOAA/ESRL/CSD

Gunnar Schade - Texas A&M University

3.1.2 Background

Precursors of ozone and PM emitted from the processes involved in O&G development include VOCs and NOx. In this Response to Question A, we focus on NOx emissions. The Response to Question B addresses VOC emissions.

A variety of methods for estimating NOx emissions from O&G basins are in various stages of development and application. The TCEQ 2012 Model-Ready Emission Inventory (see Figure 3-1 for example of these emissions) and the National Emission Inventory (NEI) use traditional activity data and emission factors to provide emission estimates; this approach will be generically referred to as “bottom-up”. In this Response, the NEI 2011 will be used as a basis for comparison with NOx emission estimates derived through other approaches. Research conducted in the Uinta Basin in northeastern Utah [Ahmadov *et al.*, 2015] indicated that the bottom-up emission inventory overestimated NOx emissions by a factor of ~4 in that basin. One important focus of this Synthesis is to investigate if this overestimate is confined to that particular basin, or if it is characteristic of O&G emissions in general.

Findings A2-A5 review and compare some NOx emission estimates from four alternative emission estimates for the Haynesville Shale region in northeastern Texas/northwestern Louisiana (Figure 3-1). These estimates include a bottom-up fuel based inventory and three top-down estimates: a total NOy mass balance determination from aircraft data, and two mesoscale Bayesian inversion techniques - the first for total NOx emissions and the second for O&G NOx emissions alone. The results from these alternative estimates are compared with those from the NEI 2011 inventory.

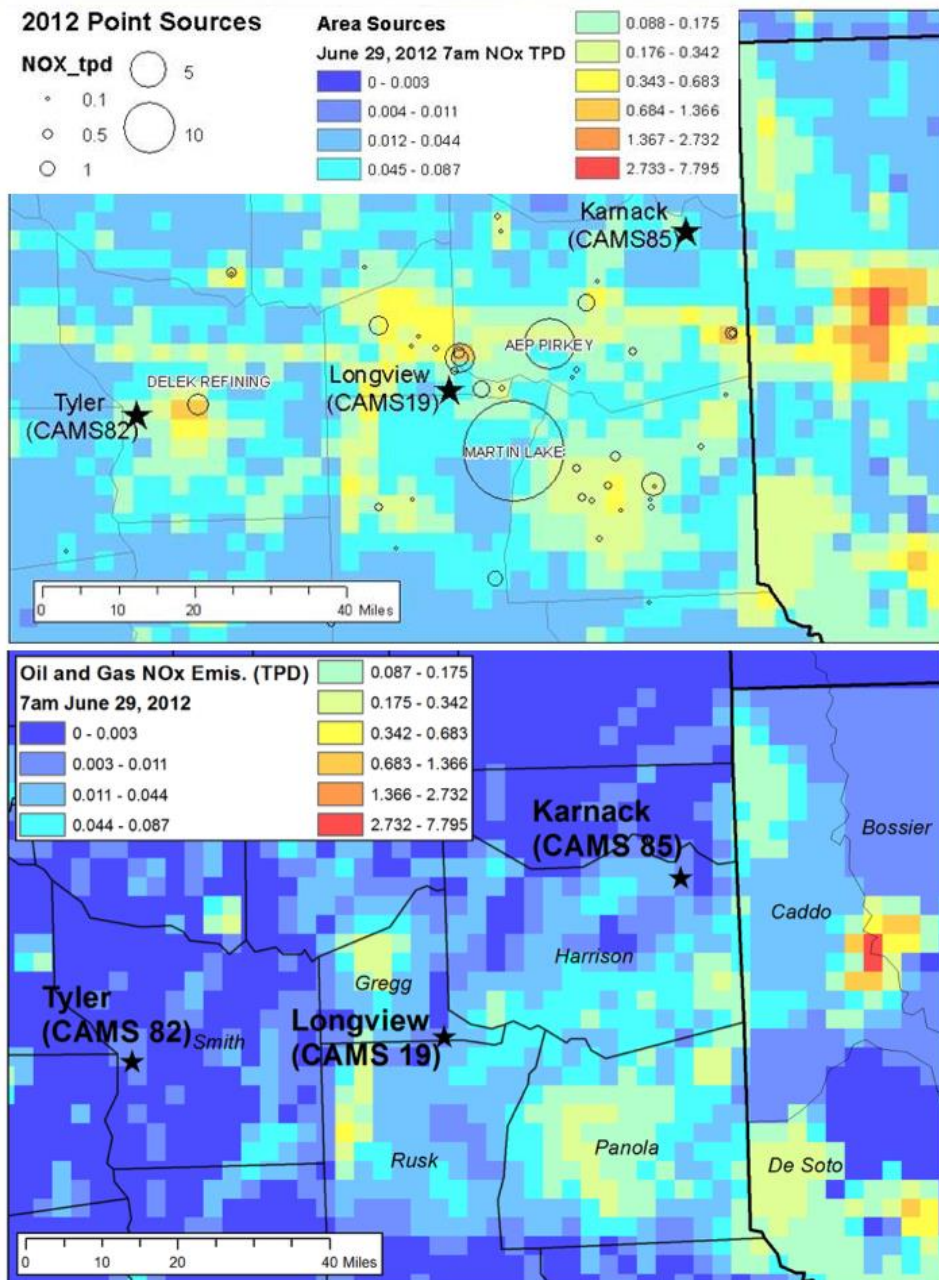


Figure 3-1. NOx emissions in the Haynesville O&G production region from the TCEQ 2012 Model-Ready 4 km x 4 km Emission Inventory for June 29, 2012 at 7 am. (Upper panel) Point sources of NOx emissions are shown as circles with radii that indicate the magnitude of the NOx emissions in metric tons per day (tpd). Facilities with NOx emissions (during standard operations in 2012) of greater than 4 tpd are labelled. The color-coded grid represents low-level (i.e. non-point) emissions from urban areas, on-road mobile sources and rural areas with O&G production. Stars indicate the location of TCEQ monitors. (Lower panel) Color-coded grid showing low-level O&G production sources only.

3.1.3 Findings

Finding A1: Emissions from O&G activities can change rapidly and systematically on time scales of a year or less. In modeling or emissions comparisons, care must be taken to ensure that the selected emission inventory matches the year under study.

Analysis: Sue Kemball-Cook-Ramboll Environ

O&G production can change rapidly in response to economic forces as well as the normal evolution of the field. Figure 3-2 shows the evolution of dry shale gas production in the Barnett, Haynesville and Eagle Ford Shales. All three regions have had periods of rapid increases in production when intensive drilling activity occurred and periods of declining production when drilling slowed. For example, Haynesville Shale gas production increased sharply following the onset of drilling in 2008. In 2011, low natural gas prices and a glut of shale gas resulted in a 25% decrease in Haynesville drilling activity relative to 2010 (Introduction Figure 1-2, lower panel). The reduced level of drilling caused Haynesville natural gas production to decline substantially in 2012. Production continued to decrease through 2015. Production trends for liquid hydrocarbons (sum of produced oil and condensate) also show large changes from year to year (Figure 3-3).

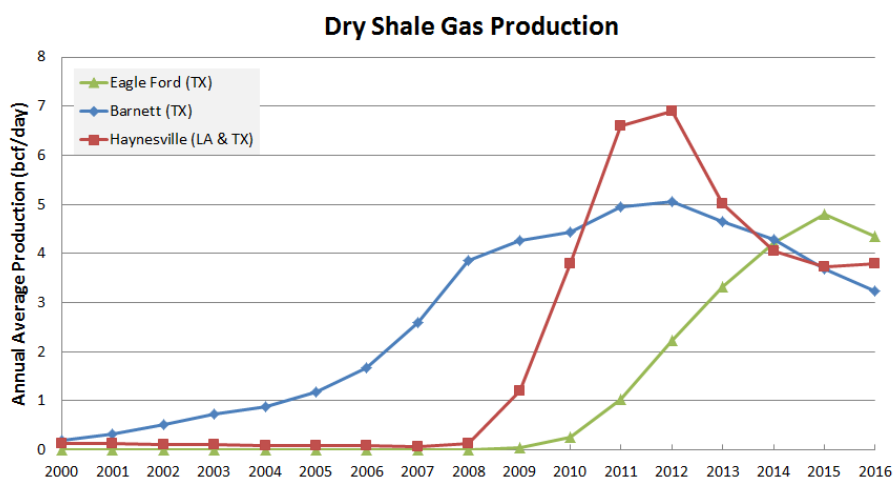


Figure 3-2. Annual average production rate of dry shale gas from the Barnett, Haynesville and Eagle Ford Shales. Haynesville data includes production from Texas counties and Louisiana parishes. Data from the US Energy Information Administration (EIA)⁹.

Bottom-up estimates of NOx and VOC emissions are proportional to the product of an emission factor and an activity metric. The activity metric for many pre-production phase emissions categories (e.g. drilling and completion) is the number of wells drilled. For production phase categories such as dehydrator or tank emissions, the activity metric is the quantity of gas or liquid hydrocarbon produced. During periods of rapid change in drilling activity and production,

⁹ http://www.eia.gov/energyexplained/index.cfm?page=natural_gas_where#shaledata

formation-wide bottom-up emissions estimates also change quickly. When modeling photochemistry in an O&G producing region, it is critical to use a bottom-up emission inventory developed for the year of interest. Comparisons of top-down emission estimates with bottom-up inventories must also be done using the same year.

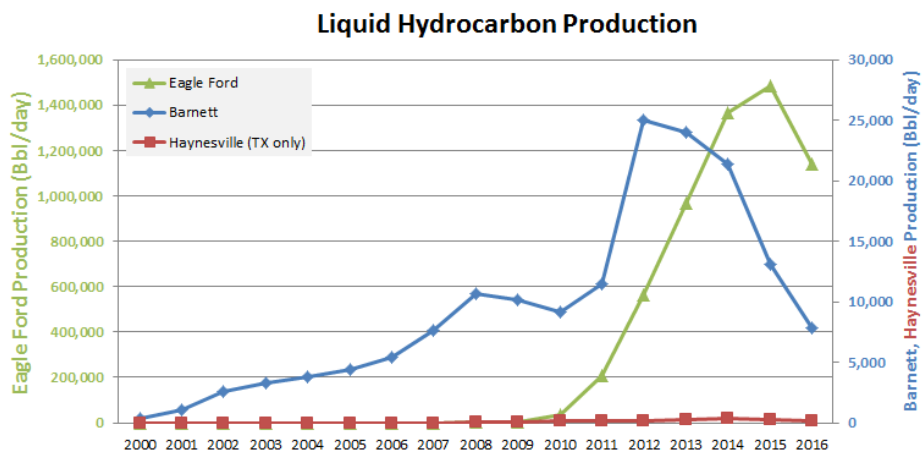


Figure 3-3. Annual average total liquid hydrocarbon (oil plus condensate) production from the major Texas shale formations. Production from the Eagle Ford (left axis) is much larger than for the other two formations, which are plotted against the right axis. Data from the Texas Railroad Commission¹⁰.

Finding A2: Public fuel use data provide a basis to estimate O&G emissions of NOx.

Analysis: Brian McDonald-CIRES/NOAA

Motor vehicle emissions have been effectively estimated using fuel sales as a measure of vehicle activity, and emission factors derived from a variety of ambient atmospheric measurements [e.g., *Harley et al.*, 2001 and references therein]. An analogous approach has been developed to estimate NOx emissions from O&G exploration and production activity. In this approach, the activity data are derived from the amount of fuel used in a given process, and the emission factors are the amount of the species emitted per unit of fuel burned in each process. Emissions from exploration activity (e.g., drilling, hydraulic fracturing) are estimated from off-road diesel fuel sales data, which are available from the U.S. Energy Information Administration (EIA). Emissions from production activity (e.g. dehydrators, heaters, compressors) are estimated from on-site natural gas fuel use, which is also available from the EIA. Emissions from larger point sources such as natural gas processing plants are estimated from the facility level CO₂ emissions reported by the U.S. EPA; these emissions are directly measured by Continuous Emission Monitoring Systems (CEMS). Combining the CO₂ emissions with NOx to CO₂ emission ratios reported by U.S. EPA's O&G tool, TCEQ [*Pring et al.*, 2010] and mobile van experiments [*Goetz et al.*, 2015] allows the NOx emissions to be derived. These

¹⁰ <http://www.rrc.state.tx.us/oil-gas/research-and-statistics/>

emissions can be spatially mapped onto the NEI 4 km x 4 km grid using drilling locations (exploration activity emissions), well locations (production emissions), and processing plant locations. This approach has been applied to the Uinta Basin in northeastern Utah to give a preliminary estimate of 4.9×10^3 tons NOx/day, which is in excellent agreement with 4.2×10^3 tons NOx/day estimated by Ahmadov *et al.* [2015], but is much lower than the 18.2×10^3 tons NOx/day given by the NEI 2011 v2 inventory.

A preliminary fuel-based NOx emission inventory has been completed for the Haynesville O&G region. Total NOx emissions from O&G activities are estimated to have been 1.3 (95% confidence limit range: 0.4 - 2.2) tons/hr in June 2013.

Finding A3: Mass balance calculations based on aircraft data can estimate total NOx emissions from O&G basins.

Analysis: Jeff Peischl-CIRES/NOAA

Aircraft measurements of ambient methane concentrations have been utilized to quantify the total emissions of methane from most of the major O&G basins in the U.S. through a mass balance of the fluxes of methane into and out of each basin [e.g., Peischl *et al.*, 2015; 2016 and references therein]. Exactly the same approach can quantify the total NOx emissions from those same basins by analyzing NOy measurements made on the same aircraft flights. Considerable effort is saved, since the wind fields and boundary layer heights have already been analyzed for the quantification of the methane emissions. A preliminary NOx emission estimate has been completed for the Haynesville O&G region using this method. Total NOx emissions from all sources (including O&G activities) are estimated to have been 7.6 ± 2.8 tons/hr in June 2013.

A related approach allows NOx emissions from the O&G activities to be separately estimated by multiplying the total methane emissions from these activities by the observed NOy to methane ratio. This approach gives an estimate of 1.4 metric tons/hr in June 2013 for the Haynesville region. The large difference between the total emissions, and the emissions due to the O&G activities alone emphasizes that the O&G activities are not the dominant NOx emission source even in the relatively rural Haynesville basin.

Finding A4: Bayesian inverse modeling together with a flux ratio inversion technique can separately estimate total NOx emissions and O&G NOx emissions alone.

Analysis: Yuyan Cui-CIRES/NOAA

Mesoscale inverse modeling based on aircraft measurements has been utilized to optimize spatially resolved methane (CH_4) and NOx emissions in the Haynesville O&G production region, and to provide a separate estimate for the spatially resolved O&G NOx emissions alone. At this time only preliminary results from analysis of data from the 10 June 2013 NOAA WP-3D flight over that region are available. Two Bayesian inversions optimized emissions from prior spatially resolved emission inventories. One, based on the NEI-2011 inventory, gave an

estimate for total NOx emissions, and the second, based on a bottom-up inventory for methane (provided by *Maasakkers et al.* [2016]), gave an estimate for total methane emissions. Meteorological variables play a significant role in the mesoscale inversion, so six different transport models were investigated to evaluate the uncertainty in the inversion estimates. Finally, a flux ratio inversion technique was utilized to derive NOx emission estimates from only the O&G sources; this approach used methane as a tracer species multiplied by the measured ratios of NOy to methane mixing ratios. This inversion was based on the methane emission inventory.

Within the uncertainties, the methane emission estimates for the Haynesville region within the red rectangle in Figure 3-4 from the inverse modeling (96 ± 19 metric tons/hr) are consistent with the mass balance estimate of methane emissions derived by *Peischl et al.* [2015] (80 ± 27 metric tons/hr). The inversion derived estimate is on average ~40% larger than the monthly mean for June of the prior (67 metric tons/hr), which was designed to be consistent with the 2016 US EPA Inventory of U.S. Greenhouse Gas Emissions and Sinks (GHGI) for 2012.

Figure 3-4 shows the Bayesian inversion results for total NOx emissions (left panel), and the flux ratio inversion for NOx emissions from O&G sources only (right panel). The Bayesian inversion estimated that the total NOx emissions from all sources in the region were 7.8 ± 1.6 metric tons/hr in June 2013, of which 2.5 metric tons/hr were from the O&G activity. These results are in excellent agreement with the mass balance results discussed in the previous finding. Ongoing work aims to provide quantitative uncertainty estimates for the NOx emissions from the Haynesville O&G activity.

Comparison of the two maps in Figure 3-4 shows some expected features, and some that are puzzling. As expected, the interstate highways (I-30 passing from northeast Texas into Arkansas, and I-20 passing west to east from Texas into Louisiana) are discernable in the total NOx emissions map, but do not appear in the O&G emissions only map. However, there are some grid cells where the estimated O&G emissions are larger than the total emissions; this physically unrealistic result arises from inconsistent spatial distributions of the O&G NOx and methane emissions between the NEI-2011 NOx emission inventory and the methane emissions in the GHG emission inventory. In the total NOx emissions map, the Martin Lake power plant is not as prominent as might be expected (see discussion in Finding A6); this results from the color scale selected for the map, where this large point source simply saturates the color in a single grid cell.

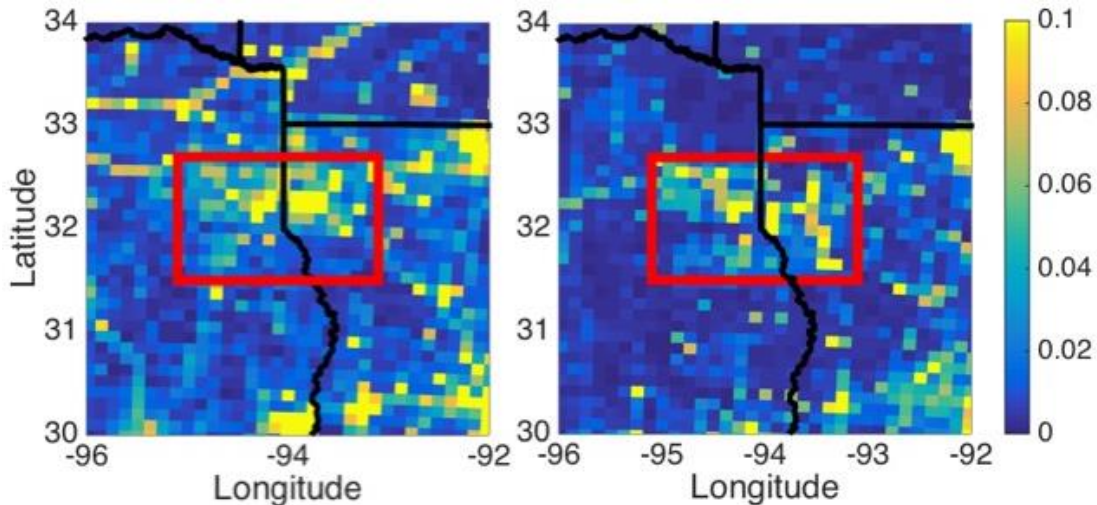


Figure 3-4. Map of NO_x emission estimates for the Haynesville O&G production region optimized by the Bayesian inverse modeling together with a flux ratio inversion technique. Total emissions are on the left, and the emissions from O&G activities alone are on the right. Units are $\mu\text{g m}^{-2} \text{s}^{-1}$.

Finding A5: Three top-down and one bottom-up approaches are in reasonable agreement for the quantification of NO_x emissions from the Haynesville O&G region in June 2013; the NO_x emission estimates for the O&G sources in the U.S. EPA's 2011 NEI are a factor of 2-3 higher.

Analysis: Yuyan Cui, Stuart McKeen, Brian McDonald, Jeff Peischl, Tom Ryerson-CIRES/NOAA

Findings A2-A4 introduce three top-down (the mass balance approach, Bayesian inversion, and a flux ratio inversion technique) and one bottom-up (fuel based approach) methods to quantify NO_x emissions from O&G exploration and development activities in any particular basin, at least when the required fuel use data are available and meteorological conditions are favorable. Preliminary results from each of the four approaches for the Haynesville O&G production are given in those Findings, and Figure 3-5 compares those three results with the emissions derived from the NEI 2011 bottom-up inventory. As noted in Finding A1, this comparison is not ideal since the four approaches discussed here are for 2013, and the NEI 2011 is optimized for two years earlier, but a newer NEI inventory is not available. The mass balance approach and the Bayesian inversion give results for total NO_x emissions, and the mass balance approach, the flux ratio inversion technique, and the fuel based method also give results for NO_x emissions from the O&G sources alone. The total emissions of the two top-down approaches are in excellent agreement with each other (7.8 ± 1.6 and 7.6 ± 2.8 metric tons/hr for Bayesian inversion and mass balance, respectively), but are significantly smaller than the bottom-up NEI 2011 inventory (12.1 metric tons/hr). The three estimates of the NO_x emissions from the O&G sources are in reasonable agreement (1.4, 2.5, and 1.3 metric tons/hr from mass balance approach, the flux ratio inversion technique, and the fuel based method, respectively), but are all a factor of 1.7 to 3.2 smaller than the corresponding emissions in the bottom-up inventory (4.2 metric tons/hr). If the total emissions from the NEI 2011 inventory

are adjusted downward (i.e., the Hybrid bar on the left in Figure 3-5) to correct for the overestimate (from the graph on the right) of the O&G emissions, better agreement is found with the total emissions from the inversion techniques and mass balance top-down approach.

The comparison discussed above and illustrated in Figure 3-5 must be considered preliminary, as the top-down estimates are still preliminary, and because the NEI 2011 inventory is not directly applicable to 2013. Figure 1-2 shows a steep decline in drilling in the Haynesville Shale between 2011 and 2013, along with a decline in gas production shown in Figure 3-2. Consistent with this change in O&G activity, area source oil and gas emissions estimates decreased from 2011 through 2014 in the Haynesville Basin; NOx emissions from the 10 county Haynesville Shale area were estimated to be 22,500 tons yr⁻¹ in 2011 and 19,000 tons yr⁻¹ in 2013 [Michael Ege, TCEQ, private communication] corresponding to a 16% lower emission rate. Comparing the 2013 top-down results to the 2014 NEI or to the TCEQ 2013 oil and gas emissions inventory would be preferred. The preceding paragraph discusses how changing O&G activity makes it difficult to directly compare top-down estimates from observations taken during a particular period with available bottom-up inventories. The evolution of the information that goes into developing bottom-up inventories also adds additional difficulty. For example, the EPA oil and gas estimation tool has recently been updated with new compressor engine factors (updated fraction of compressor engines per gas well; and updated compressor engine horsepower sizes). These updated factors result in a 49% decrease in NOx emissions estimates from wellhead compressor engines in the East Texas Basin where the Haynesville Shale is located compared to the previous factors. [Michael Ege, TCEQ, private communication]. Future work focused on more direct comparisons of top-down and bottom-up results may lead to further inventory improvement.

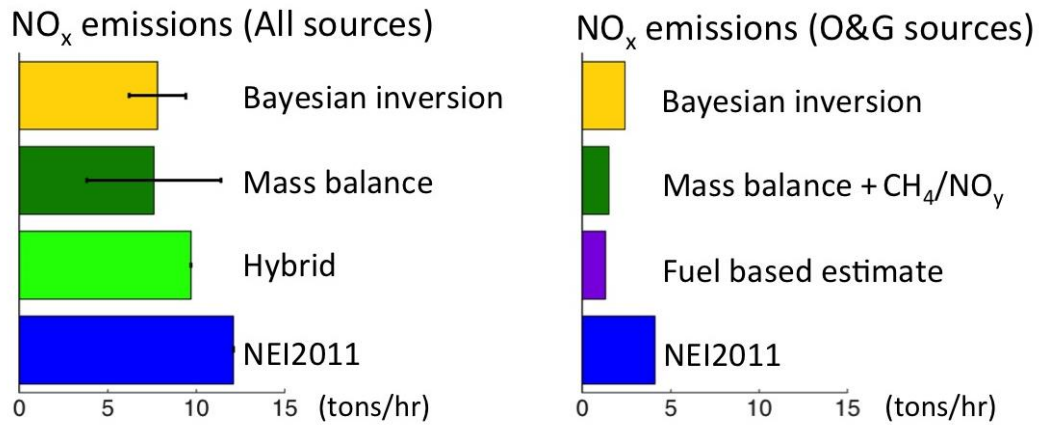


Figure 3-5. Comparison of NOx emission estimates for the Haynesville O&G production region from the three top-down approaches discussed in the text with the bottom-up NEI 2011 inventory. The comparison is shown for all sources (left) and for the O&G sources only (right).

Finding A6: Compared to other anthropogenic NOx emission sources, O&G activities are not dominant, even in relatively rural O&G basins; they do provide emissions of NOx in areas that would otherwise have very small emissions.

Analysis: Yuyan Cui, Stuart McKeen, Brian McDonald, Jeff Peischl, Tom Ryerson-CIRES/NOAA

The comparison in Figure 3-5 indicates that the emissions from O&G activities are a small fraction of the total in the Haynesville O&G basin. This is a relatively rural region, but the population on the Louisiana side (primarily Shreveport) is about 490,000 and on the Texas side (primarily Longview-Marshall) is about 370,000. The region is also crossed by I-49 and I-20 Interstate highways, and contains the Martin Lake power plant. This point source alone accounted for 1.6 metric tons/hr of NOx emissions on the day of the flight analyzed in the top-down mass balance and Bayesian inversion analyses discussed above; the emissions from this one source are approximately equal to all of the O&G NOx emissions estimated by the top-down approaches (see Finding A5). However, the impacts from a power plant point source (NOx emission plume) will be spatially and temporally different from an area source (O&G NOx emissions).

Finding A7: Measurements of NOx, VOCs, and CO₂ downwind of active flares in the Eagle Ford Shale confirmed that, on average, EPA's current AP-42 flare emission factors are accurate, although emissions can vary widely over short periods, producing at times either higher VOC emissions (low combustion efficiency), or higher NOx emissions (high combustion efficiency).

Analysis: Gunnar Schade, Geoffrey Roest-Texas A&M University

In 2015, a suite of VOCs, NOx, CO, ozone and CO₂ were measured in Dimmit County in the Eagle Ford Shale region, several miles downwind of new O&G exploration activity. During periods of favorable winds, numerous plumes from nearby flaring activity were detected, using the [NOx]/[O₃] ratio as an indicator of near-field combustion plume impacts. Figure 3-6 depicts the observed correlation between excess carbon dioxide and excess NOx in combustion plumes from flares active during the measurements as confirmed by using Visible Infrared Imaging Radiometer Suite (VIIRS) satellite data. The analysis showed that NOx emissions constituted $0.26 \pm 0.03 \times 10^{-3}$ (95% C.I. of bivariate slope analysis) mol per mol CO₂ produced in combustion. Assuming that (1) flare combustion consists of natural gas producing 117 lbs. CO₂ per million Btu (<http://www.eia.gov/tools/faqs/faq.cfm?id=73&t=11>), and (2) using EPA's emission factor of 0.068 lbs. NOx (as NO₂) per million Btu, the expected NOx/CO₂ emission ratio is 0.56×10^{-3} mol per mol CO₂. Thus, in this example, the observed [NOx]/[CO₂] ratio in various plumes was a factor of two smaller than what is currently assumed. In contrast, during another period the observed [NOx]/[CO₂] ratio was twice the expected value. Since the measurements were limited to one field location, we can conclude only that the currently used AP-42 emission factor for NOx agrees with observations within a factor of 2 for the limited observations available from the Eagle Ford.

A similar analysis was carried out for VOCs observed in the same combustion plumes. In this case, the observed [VOC]/[CO₂] ratio (considering only dominant C3-C7 hydrocarbons) was $3.1 \pm 0.7 \times 10^{-3}$ mol per mol CO₂. The respective expected value using EPA's emission factor of 0.14 lbs. of hydrocarbons (as methane) per million Btu is 3.3×10^{-3} mol per mol CO₂. Hence, similar to NOx, the Eagle Ford field measurements support the existing emission factor, albeit with a higher variability. Notably, neither the EPA emission factor, nor the field measurements included oxygenated species such as formaldehyde and acetaldehyde, which may be a significant component of flare VOC emissions [Knighton et al., 2012; Pikelnaya et al., 2013], and should be evaluated in future work.

Gvakharia et al. [2017] studied emissions of light alkanes and black carbon from flares in the Bakken region of North Dakota. They reach conclusions broadly consistent with the Eagle Ford study discussed above.

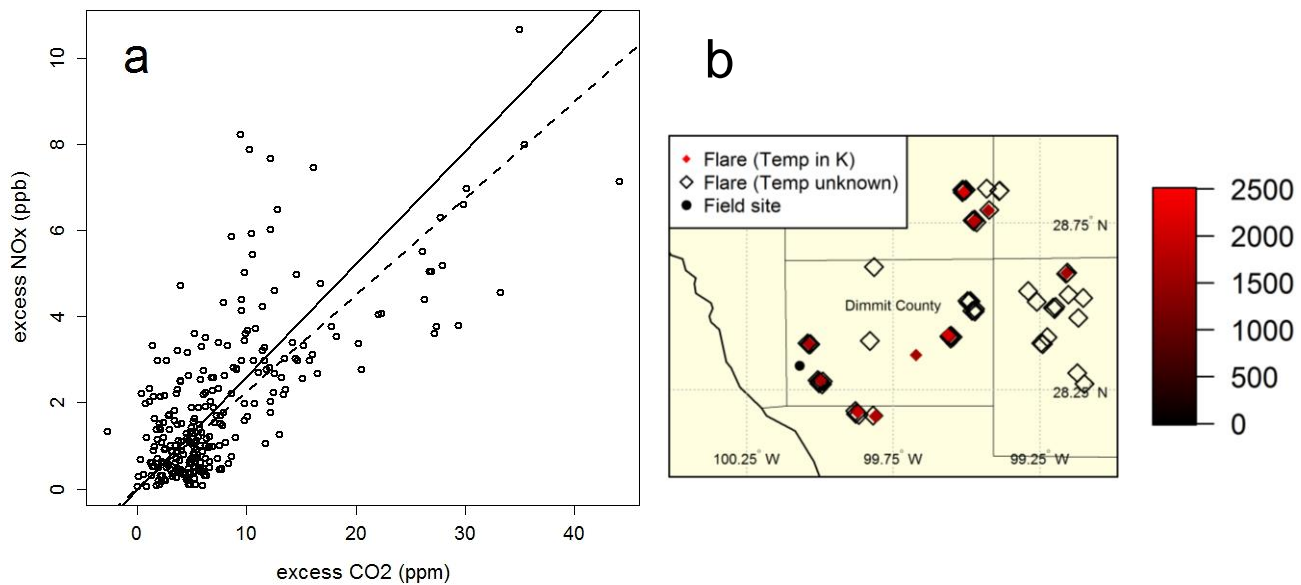


Figure 3-6. Combustion plume excess NOx versus excess CO₂ (a) for flares upwind of the monitoring site in Dimmit County, TX (b) during July and August 2015. The dashed line shows an ordinary linear regression forced through the origin, while the solid line is a bivariate regression with an intercept indistinguishable from zero. In (a) there are two data clusters: one below the regression lines, representing low combustion efficiency (higher VOC emissions), and one above representing high combustion efficiency (higher NOx emissions). The flare directly upwind of the field site (9 km to the SE) was detected on multiple days, and displayed both low and high combustion efficiencies.

3.1.4 Summary and Recommendations for Further Analysis

This Response to Question A is focused on NOx emissions, while the Response to Question B discusses VOC emissions. Here, several methods for quantifying NOx emissions from O&G emissions are discussed and their results compared. With good confidence we find that NOx emissions from O&G activities do not dominate over other anthropogenic NOx emission sources (Finding A6). Efforts to accurately quantify these emissions are confounded by three issues. First, total O&G emissions from a basin change on relatively short time scales (Finding A1) in response to basin development and economic forces. Second, emissions from a particular sector of sources vary widely depending upon operating conditions of the particular source (Findings A7 and E1). Third, development is ongoing for the techniques providing both bottom-up activity based emissions estimates (Findings A2 and A5) and top-down, observationally based emissions estimates (Findings A3, A4 and A5). Preliminary comparisons indicate that NOx emissions from O&G activities have been overestimated in earlier work (Finding A5), but there is relatively low confidence in this result. Further analysis should focus on the discrepancy between the inventories identified in Finding A5, to determine if it is solely due to the different basis years, or if it reflects significant errors in the inventories. If it is the latter, then efforts to improve inventories may be useful if it is judged that the uncertainty of

NOx emissions from O&G emissions justifies that effort. Mass balance calculations of total NOy emissions based on NOAA WP-3D aircraft data are in progress for all of the Texas O&G basins; it is hoped that comparison of these results with bottom up emission inventories will help to quantify this discrepancy.

3.1.5 References

- Ahmadov, R., et al. (2015), Understanding high wintertime ozone pollution events in an oil and natural gas producing region of the Western US, *Atmos. Chem. Phys.*, 15, 411-429, doi:10.5194/acp-15-411-2015.
- Goetz, J.D., et al. (2015), Atmospheric emission characterization of Marcellus shale natural gas development sites. *Environ. Sci. Technol.*, 49, 7012–7020.
- Gvakharia, A., E.A. Kort, A. Brandt, J. Peischl, T.B. Ryerson, J.P. Schwarz, M.L. Smith and C. Sweeney (2017), Methane, Black Carbon, and Ethane Emissions from Natural Gas Flares in the Bakken Shale, North Dakota, *Environ. Sci. Technol.*, 51 (9), 5317–5325, doi: 10.1021/acs.est.6b05183
- Harley, R. A., S. A. McKeen, J. Pearson, M. O. Rodgers, and W. A. Lonneman (2001), Analysis of motor vehicle emissions during the Nashville/Middle Tennessee Ozone Study, *J. Geophys. Res.*, 106(D4), 3559–3567, doi:10.1029/2000JD900677.
- Knighton, W.B., Herndon, S.C., Franklin, J.F., Wood, E.C., Wormhoudt, J., Brooks, W., Fortner, E.C., Allen, D.T., 2012. Direct measurement of volatile organic compound emissions from industrial flares using real-time online techniques: Proton Transfer Reaction Mass Spectrometry and Tunable Infrared Laser Differential Absorption Spectroscopy. *Industrial & Engineering Chemistry Research* 51, 12674-12684.
- Maasakkers, J. D., et al. (2016), Gridded National Inventory of U.S. Methane Emissions, *Environ. Sci. & Tech.*, 50 (23), 13123-13133 DOI: 10.1021/acs.est.6b02878
- Peischl, J., T.B. Ryerson, K.C. Aikin, J.A. de Gouw, J.B. Gilman, J.S. Holloway, B.M. Lerner, R. Nadkarni, J.A. Neuman, J.B. Nowak, M. Trainer, C. Warneke, and D.D. Parrish (2015), Quantifying atmospheric methane emissions from the Haynesville, Fayetteville, and northeastern Marcellus shale natural gas production regions, *J. Geophys. Res.*, doi:10.1002/2014JD022697.
- Peischl, J., A. Karion, C. Sweeney, E.A. Kort, M.L. Smith, A.R. Brandt, T. Yeskoo, K.C. Aikin, S.A. Conley, A. Gvakharia, M. Trainer, S. Wolter, and T.B. Ryerson (2016), Quantifying atmospheric methane emissions from oil and natural gas production in the Bakken shale region of North Dakota, *J. Geophys. Res.*, doi:10.1002/2015JD024631.
- Pikelnaya, O., Flynn, J.H., Tsai, C., Stutz, J., 2013. Imaging DOAS detection of primary formaldehyde and sulfur dioxide emissions from petrochemical flares. *J. Geophys. Res. - Atmos.*, 118, 8716-8728.
- Pring, M., D. Hudson, J. Renzaglia, B. Smith and S. Treimel (2010) Characterization of O&G production equipment and develop a methodology to estimate statewide emissions.

Prepared for Martha Maldonado, Texas Commission on Environmental Quality (TCEQ),
TCEQ Contract Number 582-7-84003-FY10-26.

3.2 Response to Question B

How do the magnitude and composition of these emissions depend upon variables such as composition of extracted oil and natural gas and technologies employed? What are the important parameters controlling how these emissions vary over time and area?

3.2.1 Working Group

David Parrish - David.D.Parrish, LLC

Jessica Gilman - NOAA/ESRL/CSD

Geoffrey Roest - Texas A&M University

Gunnar Schade - Texas A&M University

3.2.2 Background

Precursors of ozone and PM emitted from the processes involved in O&G development include VOCs and NOx. In this Response to Question B, we focus on VOC emissions. The Response to Question A addresses NOx emissions. In all of the results presented here, emissions of methane are not included when discussing the magnitude, reactivity and ozone formation potential of VOC emissions. Methane emissions have only minimal impacts on local ozone production [e.g., see Table 1 of *McDuffie et al.*, 2016].

Research conducted in the Uinta (also called Uintah) Basin in northeastern Utah [*Ahmador et al.*, 2015] indicates that the bottom-up emission inventory underestimated VOC emissions by a factor of ~2 in this basin. An important question is whether this underestimate is confined to this particular basin, or if it is characteristic of O&G emissions in general. At this point, to our knowledge, there is no analysis that provides a clear answer to this question. A difficulty in this regard is that any intensive field study provides only a "snap shot" of emissions at the particular time of the study. Longer-term, year-round data collected at surface sites provide essential complements to data from intensive field studies.

Over the 2011-2015 period, NOAA conducted five surface-based field studies (in the Denver-Julesburg Basin in 2011 and 2012 [*Gilman et al.*, 2013] and the Uintah Basin in winters 2012, 2013, 2014 [*Edwards et al.*, 2014]) and 23 research flights over O&G basins (5 during SENEX in 2013 [*Warneke et al.*, 2016] and 18 during SONGNEX in 2015). The research flights characterized VOC concentrations over O&G basins throughout the U.S. Findings B1, B3 and B4 are based on analyses of these data. The regions surveyed in these NOAA studies accounted for > 70% of U.S. shale gas production and > 83% of U.S. shale oil production in April 2015. Informative data sets are also being collected from VOC measurements spanning multiple years at sites within or near Texas O&G basins; Finding B2 is based on analyses of these longer-term data sets.

3.2.3 Findings

Finding B1: Each O&G basin has its own characteristic VOC composition signature that depends upon the composition of extracted oil and natural gas and the technologies employed in that field; NOAA field studies provide systematic (albeit limited) characterization of these signatures across U.S. O&G basins.

Analysis: Jessica Gilman-NOAA

Emissions from O&G activities change rapidly and systematically on time scales of a year or less (Finding A1). These changes are driven by changes in many variables associated with the progressive development of the field, and the economic climate of U.S. and world energy use. (See the Introduction for a complete discussion.) The NOAA ground and airborne field programs were conducted over the 2011-2015 period. Figure 3-7 and Figure 3-8 show some of the O&G activity metrics during the periods of the field studies. The drill rig count is an indicator of new well drilling activity.

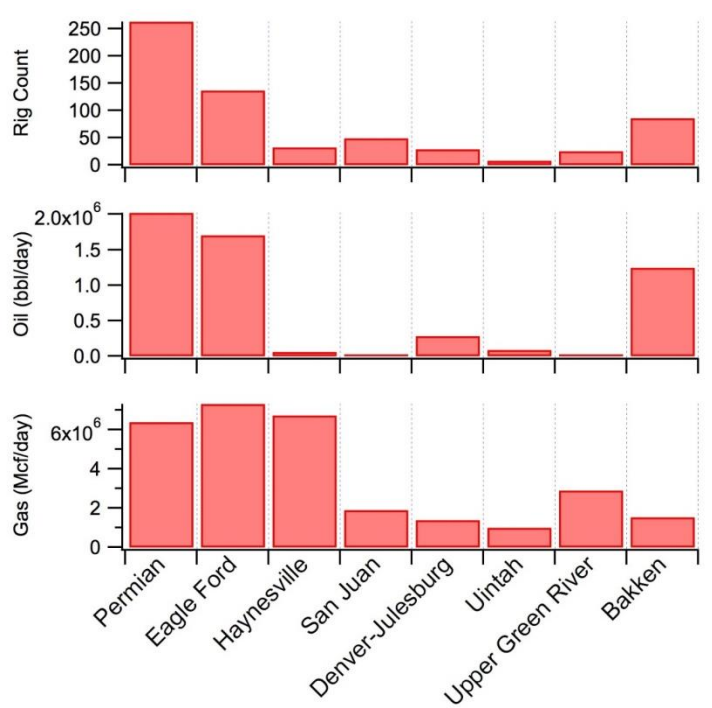


Figure 3-7. Shale play drilling and production statistics in the eight O&G basins investigated during the SONGNEX field campaign in 2015.

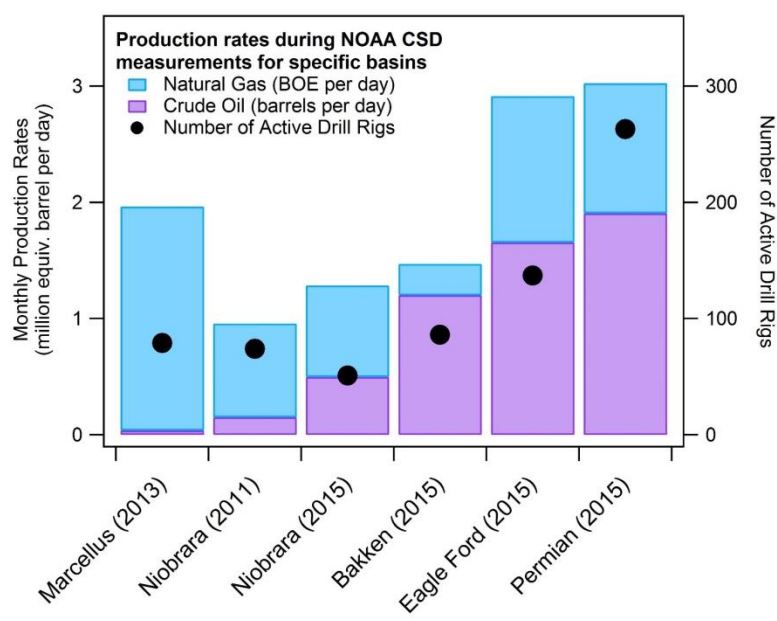


Figure 3-8. Shale play drilling and production statistics in six O&G basins during NOAA field campaigns in 2011 - 2015. The Niobrara and the Denver-Julesburg refer to the same basin.

Here we examine $[VOC]/[CH_4]$ enhancement ratios to characterize the unique VOC source signature for each O&G basin. Each ratio is calculated from the slope of the correlation of measured concentrations of a particular VOC with those of CH_4 . Figure 3-9 illustrates two example correlations, with the derived enhancement ratios (i.e., the slope of the linear regression) annotated in each graph. The enhancement ratios minimize the effects of air mass mixing and dilution on the original emission ratios; they give a robust measure of the relative rate of emissions of VOCs to CH_4 , at least for VOCs that are long-lived with respect to the time between emission and measurement. Figure 3-10 summarizes the results of the molar emission ratios of four alkanes relative to methane in fourteen U.S. O&G basins. Analogous results have been derived for a great many VOC species.

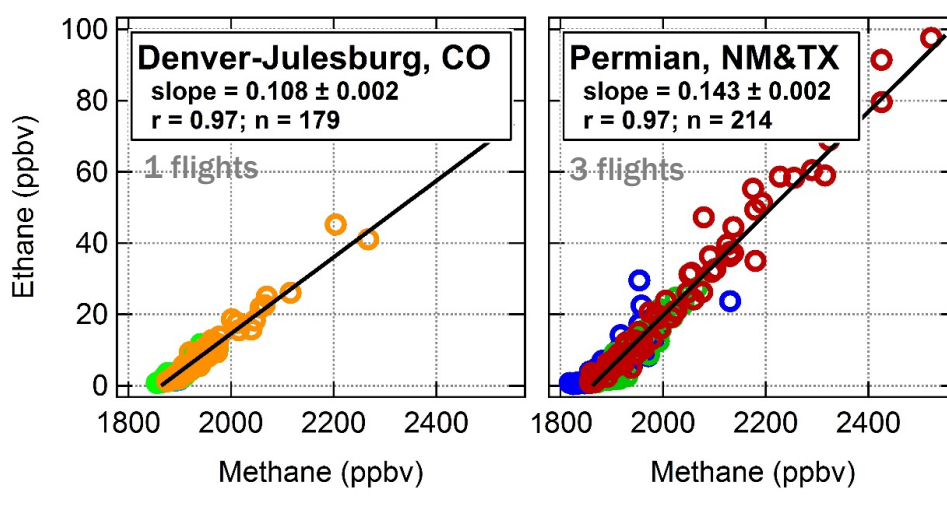


Figure 3-9. Correlation of VOC and CH₄ concentrations measured on four flights over two O&G basins. The slopes derived from linear regressions, with correlation coefficients, are annotated.

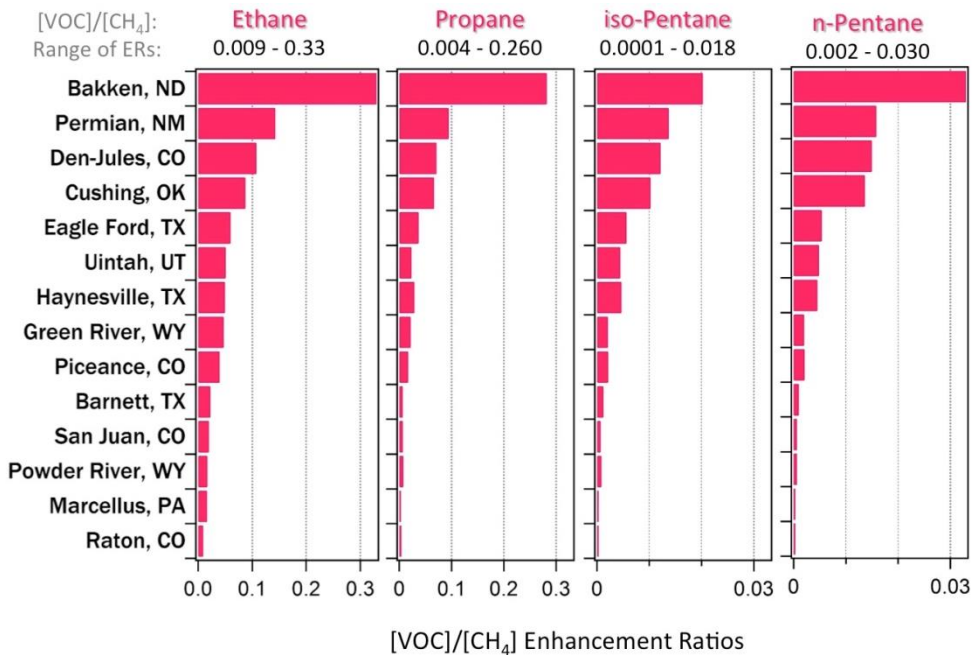


Figure 3-10. Comparison of VOC/CH₄ molar enhancement ratios in fourteen O&G basins investigated during NOAA ground and airborne field campaigns.

The source signature for each air basin is characterized by all of the derived emission ratios. Figure 3-11 summarizes the emission ratios for four families of VOCs emitted by O&G production activities. Here the emissions ratios are normalized by dividing by the maximum [VOC]/[CH₄] ratio measured in any basin for each of the VOC groups; for all four VOC families,

the Bakken Basin yielded this maximum ratio. The right-hand column in Figure 3-11 summarizes the VOC signatures observed in the different basins. In general the relative contributions from the heavier VOC families (C5+ alkanes, cycloalkanes, and aromatics) correlate with the contribution of the C2-C4 alkanes between basins, although there are some significant discrepancies from a perfect correlation.

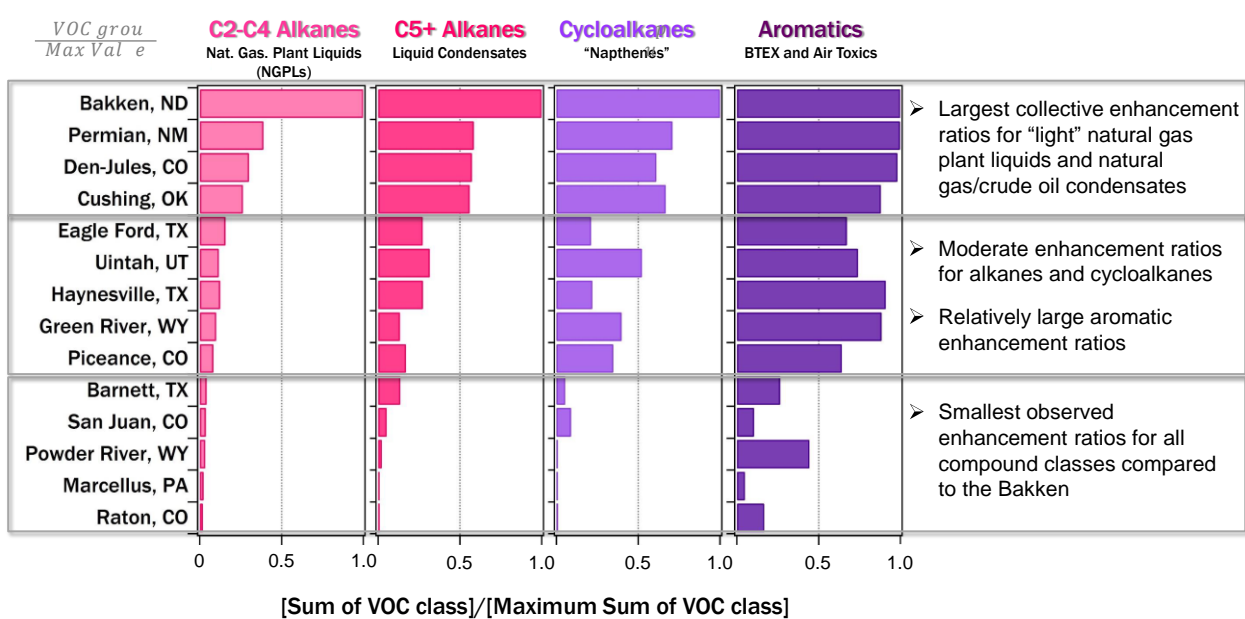


Figure 3-11. Comparison of normalized VOC/CH₄ enhancement ratios in fourteen O&G basins investigated during NOAA ground and airborne field campaigns.

The location of the fourteen basins are indicated in Figure 3-12 with symbols color and size coded according to the mole fraction of the total VOCs contributed by species heavier than CH₄. There is a wide range in these mole fractions: from 1.6% in the basin with the "driest" gas, to 46% in the basin with the "wettest" hydrocarbon mixture. There is no obvious correlation of this mole fraction with geographic location. Of the four Texas basins included in this analysis, the Permian represents the second "wettest" emissions of the fourteen basins, while the other three are near the mid-range.

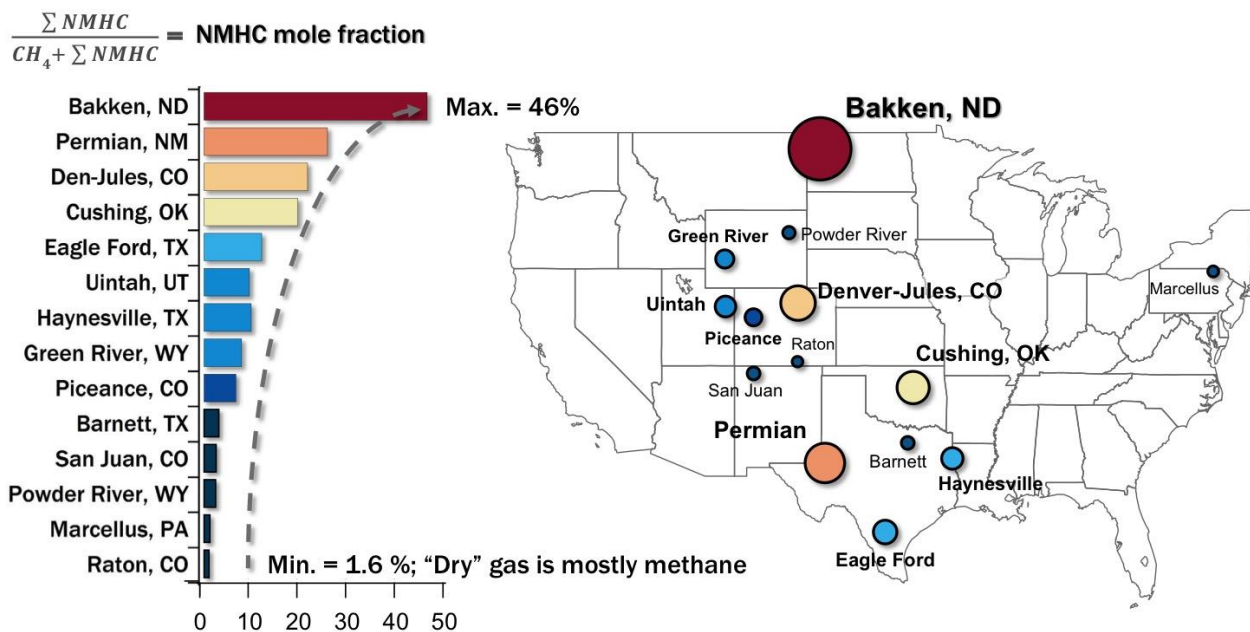


Figure 3-12. Map comparing of mole fractions of VOC to total VOC + CH₄ in fourteen O&G basins investigated during NOAA ground and airborne field campaigns.

Finding B2a: At a rural site adjacent to the Eagle Ford Shale, in Floresville, Texas, the median total OH reactivity of measured VOCs during 2013-2014 was of similar magnitude to that found in the Houston/Galveston Bay (HGB) area during TexAQS 2006. However, the highest fraction of OH reactivity in the HGB area, which occurred in plumes of HRVOCs, was about an order of magnitude larger than the corresponding fraction in the Eagle Ford Shale.

Finding B2b: At a rural site adjacent to the Eagle Ford Shale, in Floresville, Texas, emissions from O&G activities (including both evaporative and combustion sources) substantially enhanced median concentrations of aromatic VOCs above those expected in rural regions without O&G activities. The combustion sources also enhanced alkene concentrations.

Analysis: Gunnar W. Schade, Geoffrey Roest-Texas A&M University

Schade and Roest [2016] analyzed the first year (July 2013 to July 2014) of measurements from a monitoring site at the central north edge of the Eagle Ford Shale (TCEQ's Floresville Hospital Continuous Air Monitoring System (CAMS) station 1038). They discuss the abundances, diurnal variation and meteorological dependence of the dominant hydrocarbons, and compare them to other shale areas and the Houston Galveston Bay (HGB) area. They also carried out a factorial analysis to determine the dominant sources contributing to the observed VOC composition, and calculated the atmospheric OH radical reactivity (OHR - this quantity is discussed in more detail in the Responses to Questions D, F and I). Based upon median concentrations, the total OHR of the VOC mixtures were similar at HGB (2.1 s^{-1}) as derived from Table 1 in Gilman *et al.* [2009], and at the Eagle Ford Shale area (1.8 s^{-1} in summer). However, the relative contributions of

different classes of VOCs (Figure 3-13) differed markedly between the two sites. Although the OHR metric provides a simple assessment of the relative contribution of different VOCs to photochemical reactivity, they do not incorporate information about radical propagation or photochemical NO_x dependence, both of which are important for predicting the efficiency of ozone production. Additionally, the highest OHR (~95th percentile) in high concentration plumes of HRVOCs in HGB was about an order of magnitude larger than the same percentile in the Eagle Ford Shale; it is such plumes that form the highest ozone concentrations observed in HGB.

The factorial analysis consistently produced two dominant factors. The first factor dominated the variability, and based on the dominance of alkanes in its loadings composition, was assigned to O&G activity emissions. Alkenes and acetylene, with large contributions from NO_x and aromatic compounds, dominated the second factor, and was thus assigned to combustion emissions. The time dependence of these two derived parameters allowed a prediction of the NMHC concentrations at the monitoring site using i-butane and ethene as the predictors in a multi-linear model similar to *Gilman et al. [2013]*.

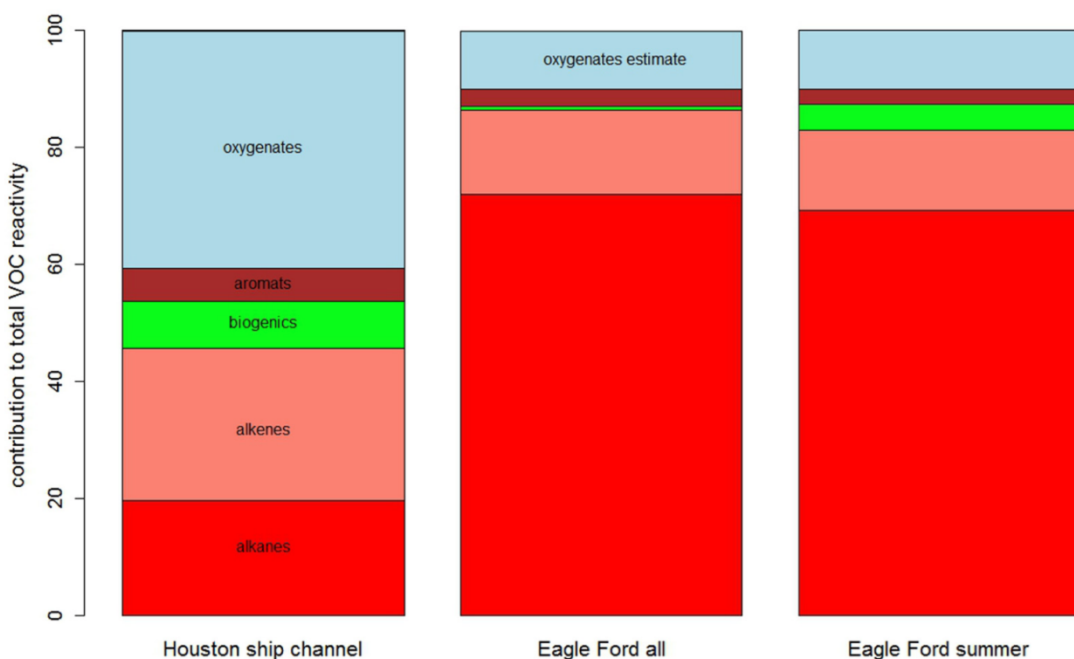


Figure 3-13. Comparison of relative, median contributions of different VOC classes to OH radical reactivity in the HGB (in 2006) vs. the Floresville monitor (in 2013/14). The estimated oxygenated VOC contribution to the total at the latter site was ~10%, equivalent to approximate median mixing ratios of 0.6 ppb formaldehyde and 0.3 ppb acetaldehyde.

Other factors in the factorial analysis indicated that emissions from flares play a significant role in determining the observed VOC and NO_x concentrations. A subsequent non-negative matrix factorization (NMF) revealed five consistent anthropogenic factors (and biogenic isoprene): an evaporative source, traffic, a second combustion source, an oil (as opposed to natural gas), and

a mixed source. These associations of factors with sources were chosen based on a comparison with another NMF analysis of 2015 VOC data acquired further south near the center of the Eagle Ford shale in Karnes City, TX, described in the next finding. The compositional breakdown of these factors provides the absolute contributions to mean benzene, toluene, ethylbenzene and xylene (BTEX) concentrations in Floresville (Figure 3-14).

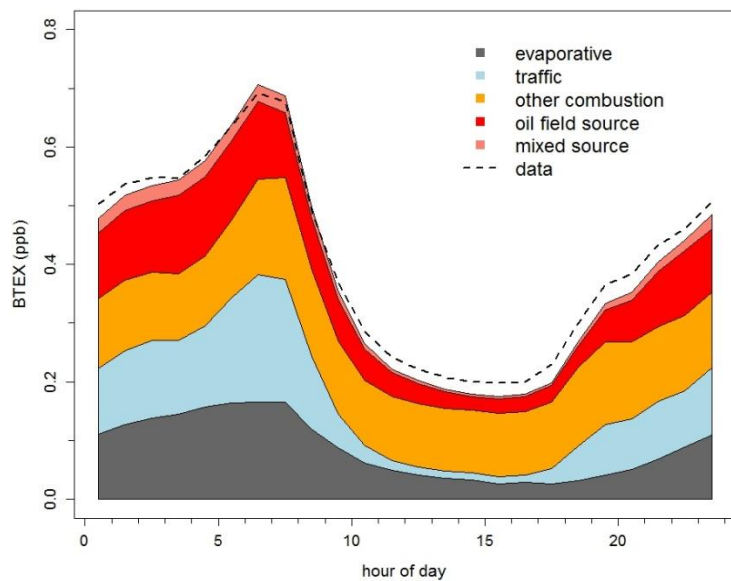


Figure 3-14. Diurnal cycle of mean BTEX abundances measured at the Floresville site (dashed line) compared to the NMF-based source apportionment (colored swaths).

Finding B3: In the Haynesville O&G Basin, ambient propane concentration measurements are a useful tracer for O&G sources that provides information different from ambient methane concentrations.

Analysis: Jessica Gilman-NOAA

Characteristic VOC composition signatures for the various O&G basins are discussed in Finding B1. Figure 3-10 shows that propane is a light NMHC that is enhanced in the emissions in these basins; it constitutes approximately 3% of the O&G VOC emissions in the Haynesville Basin. Figure 3-15 shows the 10 June 2013 flight track of the WP-3D aircraft over the Haynesville Basin, with color and size coded symbols indicating the magnitude of the measured propane concentrations and the location of each measurement. The box and whisker plots indicate the degree to which propane concentrations are elevated during the transport of boundary layer air over the Haynesville Basin by the prevailing south-southwest winds. There are modest (~1 ppb) elevations of mean and median concentrations, with a maximum enhancement of ~6 ppb. Figure 3-16 shows a similar plot with propane concentration measurements indicated by the open symbols, and the continuous methane concentration measurements indicated by the color-coding of the flight track. Generally propane and methane are both enhanced by O&G

emissions, but the relatively poor correlation ($r^2 = 0.33$) indicates that there are significant differences in the emissions sources of methane and propane.

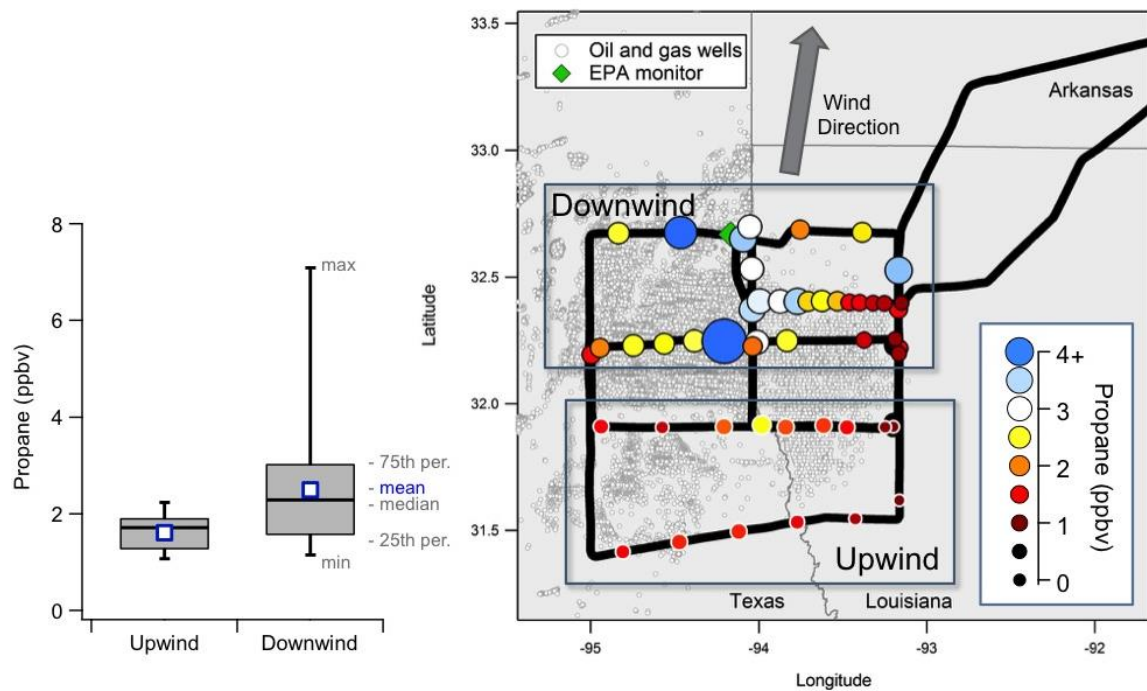


Figure 3-15. (right) Map of propane measurements made during the 10 June 2013 WP-3D flight over the Haynesville O&G Basin. Each data symbol is colored and sized according to the propane concentration, a marker for O&G emissions. **(left)** Summary of measured propane concentrations on the indicated upwind and downwind legs of the flight path.

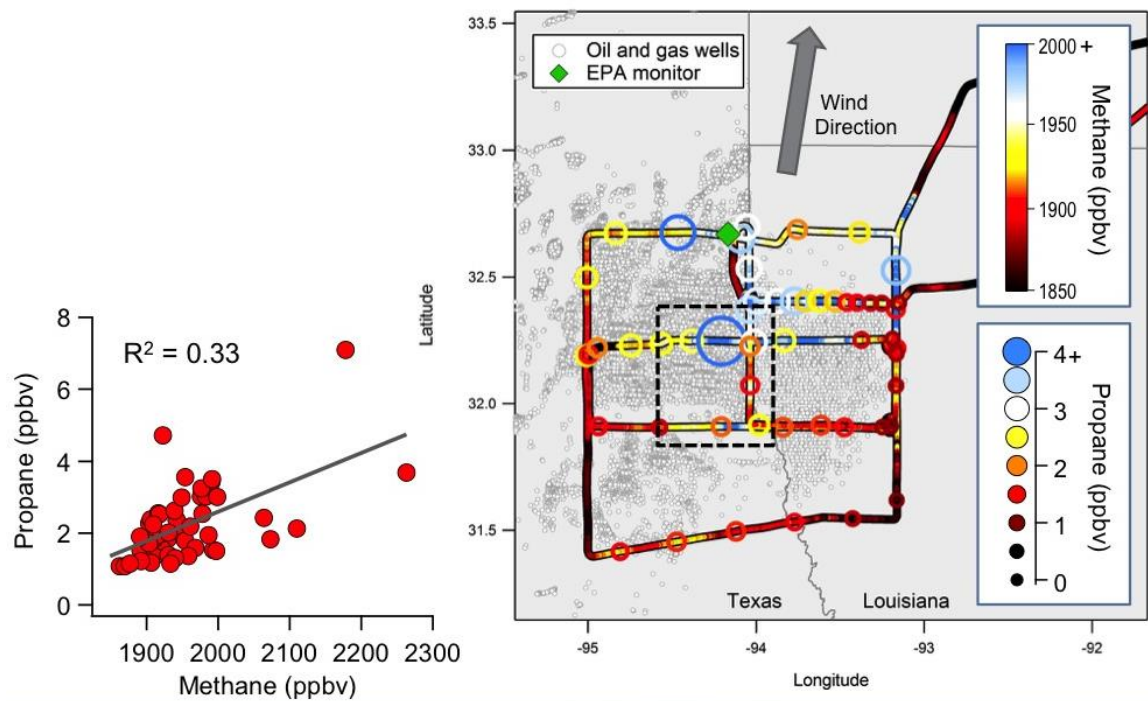


Figure 3-16. (right) Map of propane as in Figure 3-15, with the flight track color-coded according to the continuous methane measurements. (left) Correlation between measured propane and methane concentrations with the square of the correlation coefficient annotated.

Figure 3-17 shows one reason for the poor propane-methane correlation. The locations of two natural gas processing plants are indicated in relation to the flight track of the NOAA WP-3D aircraft. The plume from these two plants was intercepted on two flight segments (nearest to the plants on the east-west segment, and further downwind on the north-south segment). Both methane and propane were enhanced in these plume intercepts, but the propane enhancement was relatively larger than that of methane. Airborne sampling of VOC plumes in O&G fields offers the potential for detailed characterization of the sources of VOC emissions.

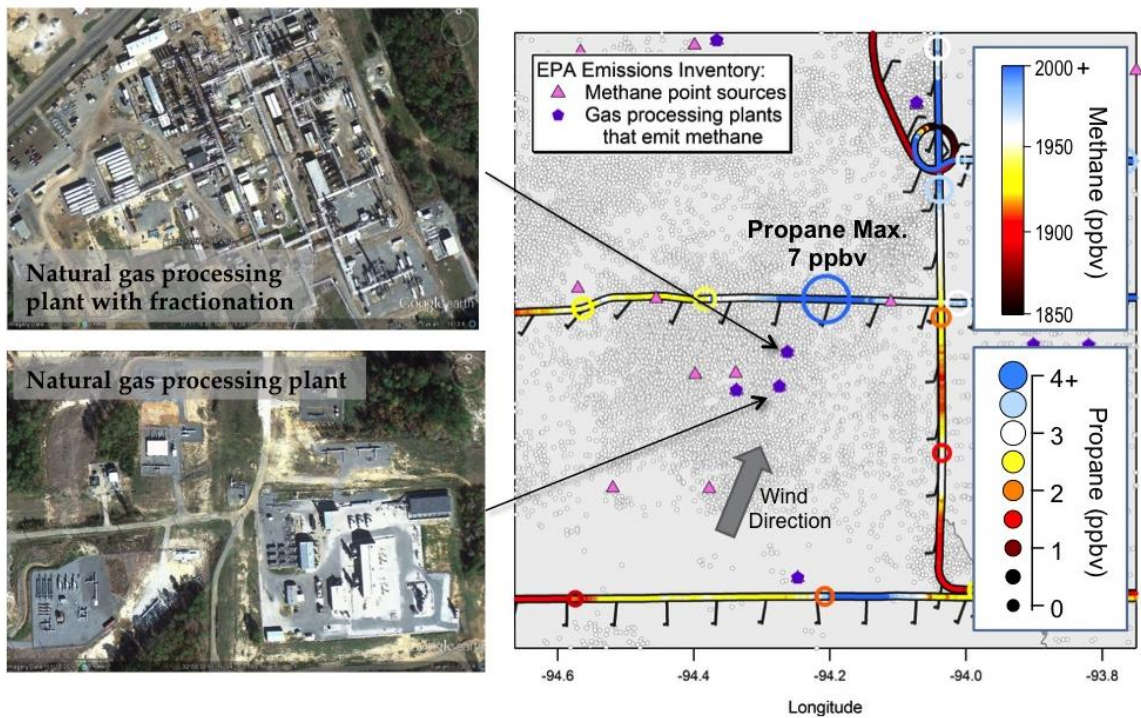


Figure 3-17. (right) Enlargement of a section of the map from Figure 3-16, with the location of natural gas processing plants indicated. Google Earth images of two of those plants are included. Wind bars are included on the flight track.

Finding B4: In the Haynesville O&G Basin, elevated ambient benzene concentrations are strongly associated with O&G sources, but do not exceed the TCEQ's long-term air monitoring comparison value (AMCV), which is used to assess risk to human health.

Analysis: Jessica Gilman-NOAA

Benzene is a toxic VOC species that is of particular concern due to its negative health impacts. It is released from a wide variety of sources: combustion sources that are predominately found in urban areas (e.g., on-road and off-road vehicle fleets), industrial sources (e.g., refineries and petrochemical plants), and O&G activity. During the WP-3D flight over the Haynesville Basin discussed in Finding B3, benzene and acetylene concentrations were measured in the same whole air samples that provided the propane measurements. Figure 3-18 shows the correlation between benzene and acetylene. This correlation is useful because acetylene is emitted predominately by the combustion sources that also emit benzene at an approximately constant ratio [e.g., Fortin *et al.*, 2005]. The "urban signature" line included in Figure 3-18 indicates this ratio, and the points that are well approximated by this line represent air parcels with benzene concentrations predominately from combustion sources. However over the Haynesville Basin the largest benzene concentrations are observed in air parcels with relatively low acetylene concentrations. The larger enhancements in benzene concentrations therefore are dominated by O&G emissions, a conclusion confirmed by the relatively large propane concentrations that

accompany the highest benzene concentrations, as indicated by the color and size of the symbols in Figure 3-18. To provide context for Figure 3-18, the TCEQ's health-based long-term air monitoring comparison value (AMCV) for benzene is 1.4 ppb and the short-term AMCV is 180 ppb. The long-term and short-term AMCVs are ambient concentrations below which no adverse health effects are expected for continuous and 1-hour inhalation exposures, respectively. Aircraft whole air sample measurements of benzene shown in Figure 3-18 and ground-level ambient BTEX concentrations in Figure 3-14 are much lower than the long-term AMCV of 1.4 ppb.

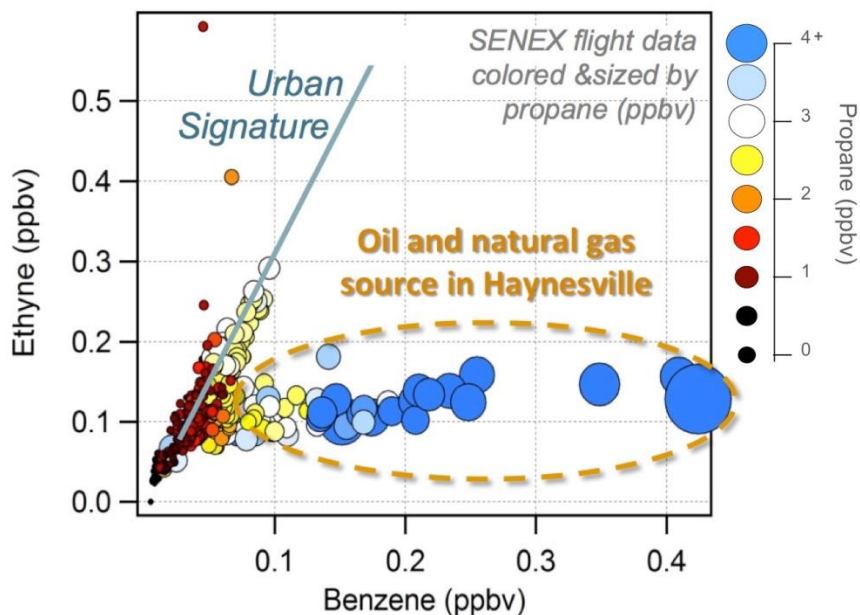


Figure 3-18. Relationship between ethyne (acetylene) and benzene measured during the 10 June 2013 WP-3D flight over the Haynesville O&G Basin during the SENEX field campaign. Each data point is from analysis of a single whole air sample, and is colored and sized according to the propane concentration, a marker for O&G emissions.

3.2.4 Summary and Recommendations for Further Analysis

This Response to Question B is focused on VOC emissions, while the Response to Question A discusses NOx emissions. The analysis given in this Response to Question B has only begun to scratch the surface of providing a definitive description of how the magnitude and composition of VOC emissions from O&G activities depend upon variables such as composition of extracted oil and natural gas and technologies employed, and the important parameters controlling how these emissions vary over time and area.

From a health perspective, emissions of benzene, a toxic VOC, are of particular concern. The analyses supporting Findings B2, B4 and C2 report ambient benzene concentrations in Texas O&G fields. These analyses indicate that annual average benzene concentrations away from the immediate vicinity of sources are below the long-term AMCV, so that chronic exposure in these O&G basins is not expected to cause adverse health effects. This result is consistent with

TCEQ monitoring of long-term ambient benzene concentrations in the Barnett Shale [Ethridge *et al.*, 2015], which found no exceedances of the long-term AMCV for benzene, consistent with grouping the Barnett into the shale areas with low aromatics contributions (Figure 3-11).

The analyses supporting Findings B2, B4 and C2 cannot address the short term AMCV, since very rare events that were not investigated during these studies may result in larger ambient concentrations than are reflected in the figures. Ethridge *et al.* [2015] reviewed TCEQ's extensive, multi-year HAP monitoring efforts in the Barnett Shale and reported a single exceedance of the short -term AMCV for benzene out of 1,299 samples taken in locations accessible to the public (i.e. outside restricted access areas of O&G operations such as a well pad or gas plant). The applicability of the Barnett results to the Eagle Ford and Haynesville basins is not explicitly known, but Figure 3-11 does indicate that emissions of aromatic VOCs relative to methane are higher in these two basins than in the Barnett Shale region. Future analysis of long-term VOC data sets collected in the Eagle Ford and Haynesville O&G basins could focus on the very highest observed VOC concentrations, and thereby may provide guidance regarding the frequency and/or the probability of 1-hr average benzene concentrations exceeding the short-term AMCV in these two basins.

Finding B2 discusses analyses of VOC measurements at a monitoring site adjacent to the Eagle Ford Shale region. These analyses indicate that emissions from natural gas flaring in that region are important not only to the reactivity of the VOC emissions, but also to the magnitude of the NO_x emissions in this region. More complete characterization of the emissions from the relatively low temperature flares found in O&G regions is important because the ozone formation potential of emissions in these regions depends strongly on both the magnitude of the emissions, especially the NO_x emissions, and the reactivity of the VOC emissions. Finding B1 discusses VOC composition signatures that characterize each of the O&G basins, and Findings B3 and B4 give some example analyses that use these characterizations to investigate VOC emission sources. A wide range of such analyses can be envisioned; productive future research findings could follow from careful consideration of important policy-relevant questions that could be addressed by such analyses.

Additional analyses currently underway will provide a more complete answer to this Science Question, but results are not yet available. Mass balance calculations based on aircraft data have estimated total emissions from O&G basins for NOx (see Finding A3) and for methane [e.g., Peischl *et al.*, 2015; 2016 and references therein]. The same approach can quantify the total VOC emissions by combining the methane results with measured ambient ratios of VOC to methane concentrations [Jessica Gilman, NOAA].

3.2.5 References

- Ahmadov, R., et al. (2015), Understanding high wintertime ozone pollution events in an oil and natural gas producing region of the Western US, *Atmos. Chem. Phys.*, 15, 411-429, doi:10.5194/acp-15-411-2015.
- Edwards, P.M., et al. (2014) High winter ozone pollution from carbonyl photolysis in an oil and gas basin, *Nature*, 514, 351-354, doi:10.1038/nature13767.

- Ethridge, S., T. Bredfeldt, K. Sheedy, S. Shirley, G. Lopez, and M. Honeycutt (2015), The Barnett Shale: From problem formulation to risk management, *Journal of Unconventional Oil and Gas Resources*, 11 (2015) 95–110, <http://dx.doi.org/10.1016/j.juogr.2015.06.001>.
- Fortin, T.J., B.J. Howard, D.D. Parrish, P.D. Goldan, W.C. Kuster, E.L. Atlas, and R.A. Harley (2005), Temporal changes in U.S. benzene emissions inferred from atmospheric measurements, *Environ. Sci. Technol.*, 39, 1403-1408.
- Gilman, J. B., et al. (2009), Measurements of volatile organic compounds during the 2006 TexAQS/GoMACCS campaign: Industrial influences, regional characteristics, and diurnal dependencies of the OH reactivity, *J. Geophys. Res.*, 114, D00F06, doi:10.1029/2008JD011525.
- Gilman, J.B., B.M. Lerner, W.C. Kuster, and J.A. de Gouw (2013), Source signature of volatile organic compounds from oil and natural gas operations in northeastern Colorado, *Environ. Sci. Tech.*, 47(3), 1297-1305, doi:10.1021/es304119a.
- McDuffie, E. E., et al. (2016), Influence of oil and gas emissions on summertime ozone in the Colorado Northern Front Range, *J. Geophys. Res.-Atmos.*, 121(14), 8712-8729, doi:10.1002/2016jd025265.
- Peischl, J., T.B. Ryerson, K.C. Aikin, J.A. de Gouw, J.B. Gilman, J.S. Holloway, B.M. Lerner, R. Nadkarni, J.A. Neuman, J.B. Nowak, M. Trainer, C. Warneke, and D.D. Parrish (2015), Quantifying atmospheric methane emissions from the Haynesville, Fayetteville, and northeastern Marcellus shale natural gas production regions, *J. Geophys. Res.*, doi:10.1002/2014JD022697.
- Peischl, J., A. Karion, C. Sweeney, E.A. Kort, M.L. Smith, A.R. Brandt, T. Yeskoo, K.C. Aikin, S.A. Conley, A. Gvakharia, M. Trainer, S. Wolter, and T.B. Ryerson (2016), Quantifying atmospheric methane emissions from oil and natural gas production in the Bakken shale region of North Dakota, *J. Geophys. Res.*, doi:10.1002/2015JD024631.
- Schade, G.W., and G. Roest (2016), Analysis of non-methane hydrocarbon data from a monitoring station affected by O&G development in the Eagle Ford shale, Texas, *Elementa Sci. Anth.* 4: 000029, doi:10.12952/journal.elementa.000096.
- Warneke, C., et al. (2016) Instrumentation and Measurement Strategy for the NOAA SENEX Aircraft Campaign as Part of the Southeast Atmosphere Study 2013, *Atmospheric Measurement Techniques*, 9, 3063-3093, doi:10.5194/amt-9-3063-2016.

3.3 Response to Question C

How are these emissions divided between the various stages of fossil fuel extraction (exploration and production; product gathering and transmission; gas processing) and specific processes?

3.3.1 Working Group

David Parrish - David. D. Parrish, LLC

Bryan Duncan - NASA

Jessica Gilman - NOAA/ESRL/CSD

Lok Lamsal - NASA

3.3.2 Background

Each of the many different processes involved in fossil fuel extraction has its own characteristic emissions of VOC and NOx. Examination of how ambient concentrations of these species vary as the activity of any of the different processes increase or decrease may provide methods to quantify various characteristics of the associated emissions. Findings C1 and C2 discuss the correlation of long-term variations of VOC concentrations in the Haynesville Basin with drilling activity, and Finding C3 examines long-term variations of NOx concentrations as measured by satellite over three O&G basins.

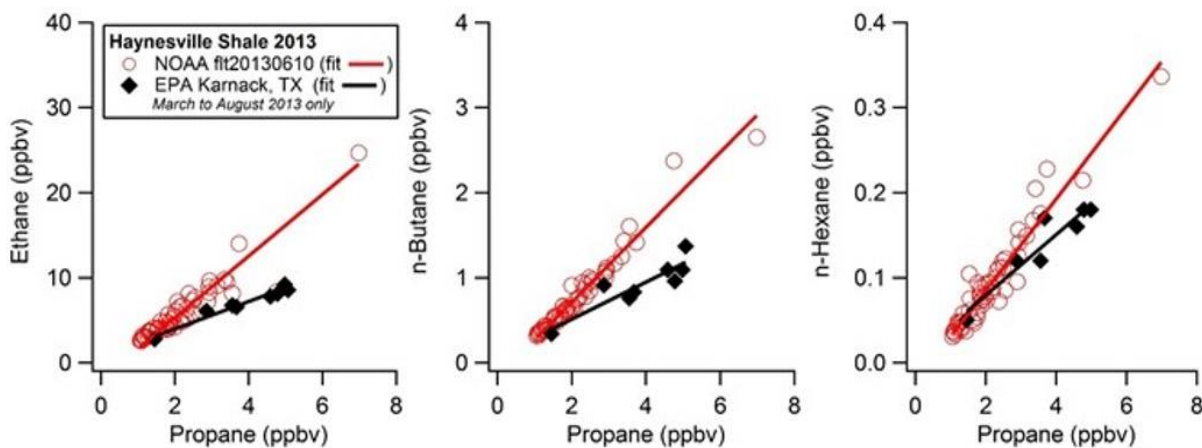
3.3.3 Findings

Finding C1: Ratios of concentrations of VOCs from a "snapshot" provided by a NOAA WP-3D aircraft flight over the Haynesville O&G basin are in reasonable accord (agreement within factor of ≈ 2) with those from long-term canister measurements made at the Karnack, TX surface site located in that basin.

Analysis: Jessica Gilman-NOAA

Flights across O&G basins by the NOAA WP-3D aircraft provide very detailed information regarding the ambient chemical concentrations of a wide variety of species, including primary emissions and the intermediates and products formed during the photochemical processing of those emissions. However, the flights are performed on time scales of a few hours or less, during daytime. There is a concern that such "snapshots" provide a distorted picture of the longer-term chemical environment of the O&G basins. Here we present a comparison of the relative concentrations of VOCs determined on a single flight over the Haynesville O&G Basin on 10 June 2013 and the March to August 2013 measurements at the Karnack, TX (CAMS 85) surface site located in that basin (indicated by a green diamond in the map in Figure 3-15). It should be noted that both the aircraft and the surface measurements are based on whole air samples collected in canisters and analyzed later after shipment to home laboratories.

The method selected to compare the VOC concentration signatures between the airborne and surface measurements is illustrated in Figure 3-19. Enhancement ratios are calculated for each VOC species relative to propane from orthogonal distance linear regression slopes; agreement between these enhancement ratios is expected if each platform accurately characterizes the VOC concentration signature in the Haynesville Basin. Consideration of enhancement ratios minimizes the effects of air mass mixing and dilution. Systematic differences between the derived slopes are larger than their confidence limits, but the agreement is within a factor of ≈ 2 . The excellent correlations (r is 0.90 to 0.98) indicate that there is little variability in the ambient enhancement ratios, and that the disagreement between the data sets may arise from calibration differences.



Haynesville Shale	EPA Karnack, TX*		NOAA fit20130610	
	<i>*March to August 2013 only</i>		<i>Strongest ONG source signature</i>	
<u>Enhancement Ratios</u>	<u>Slope</u> <i>ODR2</i>	<u>Fit Coeff.</u> <i>r</i>	<u>Slope</u> <i>ODR2</i>	<u>Fit Coeff.</u> <i>r</i>
[Ethane]/[Propane]	1.61 ± 0.14	0.98	3.6 ± 0.2	0.93
[n-Butane]/[Propane]	0.22 ± 0.04	0.90	0.441 ± 0.013	0.98
[n-Hexane]/[Propane]	0.0356 ± 0.006	0.94	0.0539 ± 0.0023	0.96
	<i>Ground measurements</i>		<i>Airborne measurements</i>	

Figure 3-19. Comparisons of the correlations between the concentrations of three alkanes with propane measured by the NOAA WP-3D aircraft (Haynesville, red symbols) and at the Karnack surface site (green symbols). Lines of the respective colors indicate the results of the linear regressions; the slopes with confidence limits and the correlation coefficients are annotated.

Figure 3-20 compares the enhancement ratios for 7 alkanes and 2 aromatics measured at the surface and from aircraft. All derived ratios agree within a factor of ≈ 2 , and the ambient enhancement ratios of the alkanes agree with those measured in samples of Haynesville raw natural gas, suggesting that emissions of unprocessed natural gas is the dominant source of these alkanes to the atmosphere over the Haynesville Basin. These comparisons indicate that the enhancement ratios derived from either data set can be used to investigate the identity and relative importance of emission sources.

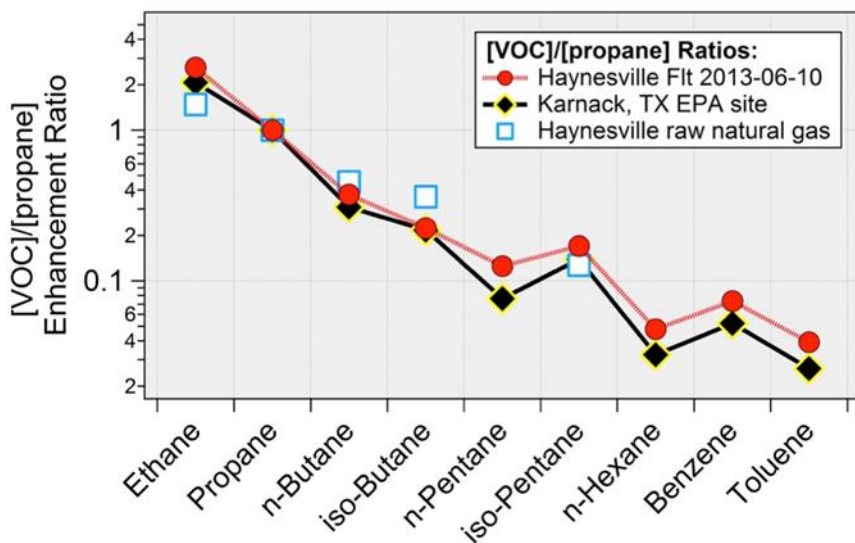


Figure 3-20. Enhancement ratios of nine VOCs relative to propane measured by the WP-3D aircraft and the Karnack, TX surface site in the Haynesville O&G Basin in 2013. The relative concentrations of four alkanes measured in samples of Haynesville raw natural gas (data from USGS Energy Geochemistry Database, accessed in November 2015) are included for comparison.

Finding C2: Long-term measurements at the Karnack, TX surface site indicate that VOC emissions in the Haynesville O&G Basin correlate much more closely with drilling activity than with natural gas production.

Analysis: Jessica Gilman-NOAA

The VOC concentration data set collected at the Karnack, TX surface site provides the basis for quantifying changes in VOC emissions in the Haynesville O&G Basin. Figure 3-21 illustrates an analysis of 3 NMHCs: propane, benzene and ethyne (acetylene). The primary emission sources for these three species are expected to be natural gas production in the Haynesville Basin for propane, regional vehicular traffic for ethyne, and both of these sources for benzene. The time series in Figure 3-21 provide confirmation of these expectations, and a clear indication of how the VOC emissions depend upon the various stages of fossil fuel extraction. Perhaps surprisingly, none of the time series of the VOC emissions (as reflected by the ambient concentrations) correlate with the total natural gas production in the basin; instead annual

average propane and benzene correlate well ($r^2 = 0.97$ and 0.87 , respectively) with the annual average number of drilling rigs active in the basin. Average ethyne concentrations remained nearly constant over the 8-year period, with only a weak ($r^2 = 0.17$) correlation with drilling activity; this weak correlation may result from a correlation of vehicle traffic supporting the drilling activity. This analysis demonstrates that the active drilling of natural gas wells plays a dominant role in VOC emissions, at least in the Haynesville Basin. However, the situation in this basin may be particularly simple in that dry natural gas production dominates here (as well as in the Barnett Basin). In basins with significant production of natural gas liquids, condensate and/or oil (e.g., the Eagle Ford Basin), there are additional sources, such as venting of storage tanks and flares, that likely complicate the VOC source dependence.

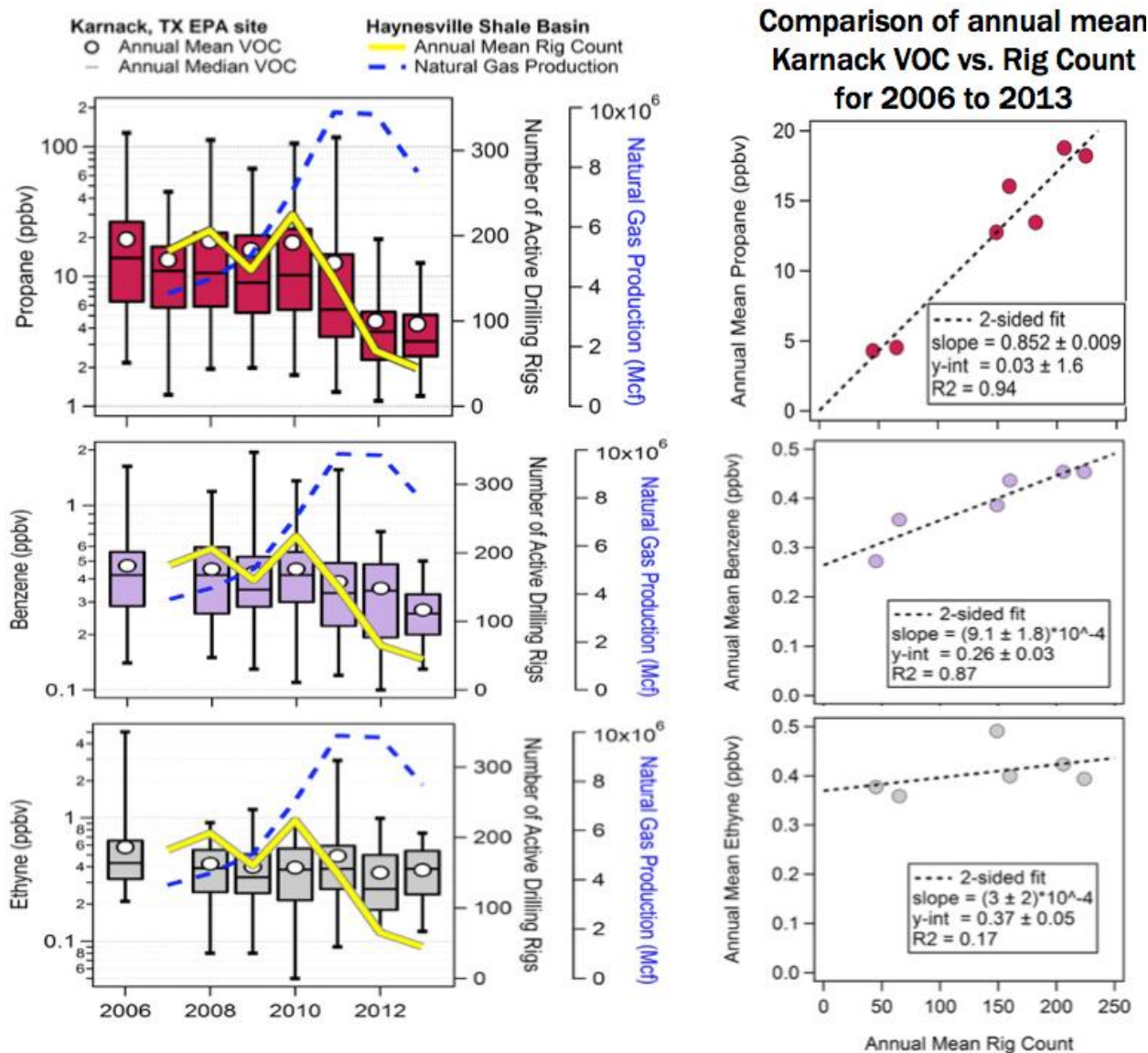


Figure 3-21. (left) Time series of concentrations of three VOC species measured in the Haynesville O&G Basin at the Karnack, TX surface monitoring site. The annual average

number of active drilling rigs (from Baker-Hughes) and the natural gas production (from U.S. EIA) are included for comparison. The box and whisker symbols indicate mean, median, 25th and 75th percentiles, and minimum and maximum concentrations measured in each year. (right) Correlations of the annual mean VOC concentration with the annual mean number of active drilling rigs, with the correlation slopes and intercepts with confidence limits indicated, as well as the square of the correlation coefficients.

Finding C3: Increases of NO₂ concentrations over three U.S. O&G basins have been identified in satellite records; the time series of annual average concentrations correlate (at least qualitatively) with drilling activity and oil/natural gas production.

Analysis: Bryan Duncan, Lok Lamsal-NOAA

Duncan et al. [2016] discuss spatially resolved (0.1° latitude x 0.1° longitude) changes in global NO₂ concentrations over the 2005-2014 period measured by the satellite-borne Ozone Monitoring Instrument (OMI). NO₂ concentrations generally decreased over the U.S.; the only significant exceptions identified, namely spatial NO₂ increases, were over three rural O&G basins - the Permian and the Eagle Ford in Texas, and the Bakken in North Dakota. Such increases could not be identified over other U.S. O&G basins, but those basins (e.g., the Barnett) have urban populations or major point sources with decreasing NOx emissions large enough to obscure possible increases from O&G development. Figure 3-22 through Figure 3-24 compare the satellite observed increasing trends in NO₂ concentrations in these three basins with their trends of drilling activity and O&G production. The correlations identify O&G production activities as a significant NOx emission source, and may provide the basis for quantifying the NOx emissions and/or providing information regarding the specific O&G production sector that dominates these NOx emissions.

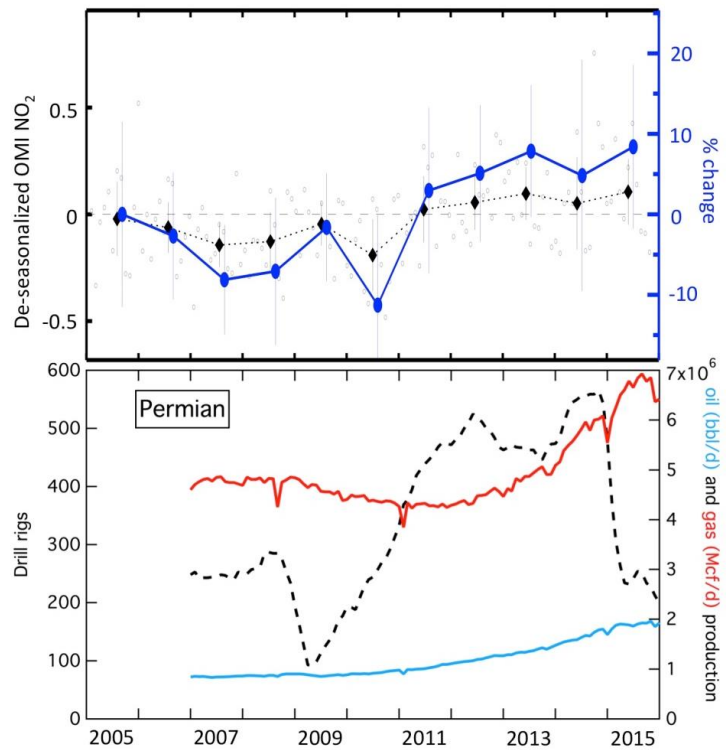


Figure 3-22. Time series of (top) annual average OMI NO₂ data (1015 cm⁻² on left, % on right) relative to the year 2005, and (bottom) U.S. Energy Information Administration (<https://www.eia.gov/petroleum/drilling/>) monthly statistics of production plus drilling activity in the Permian O&G basin.

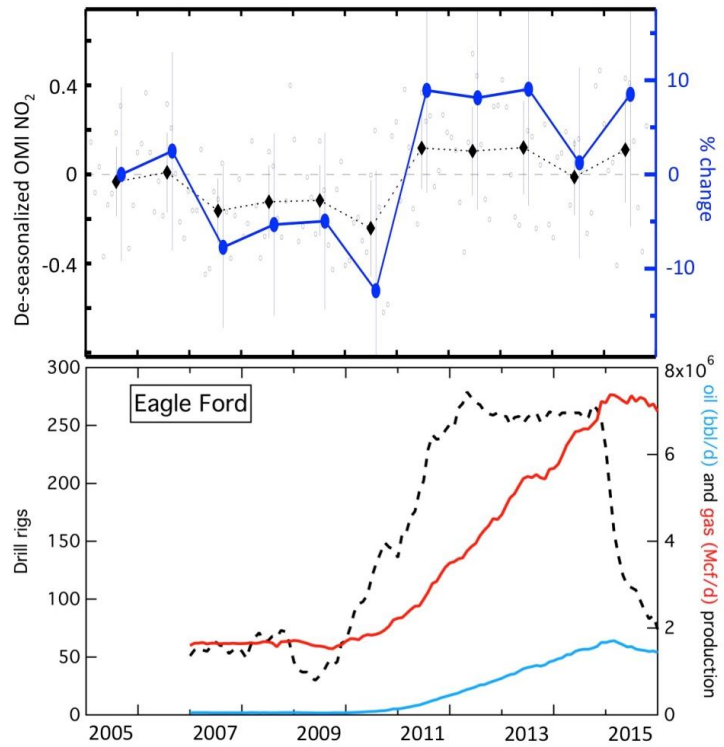


Figure 3-23. Time series of (top) annual average OMI NO₂ data (10^{15} cm^{-2} on left, % on right) relative to the year 2005, and (bottom) U.S. Energy Information Administration (<https://www.eia.gov/petroleum/drilling/>) monthly statistics of production plus drilling activity in the Eagle Ford O&G basin.

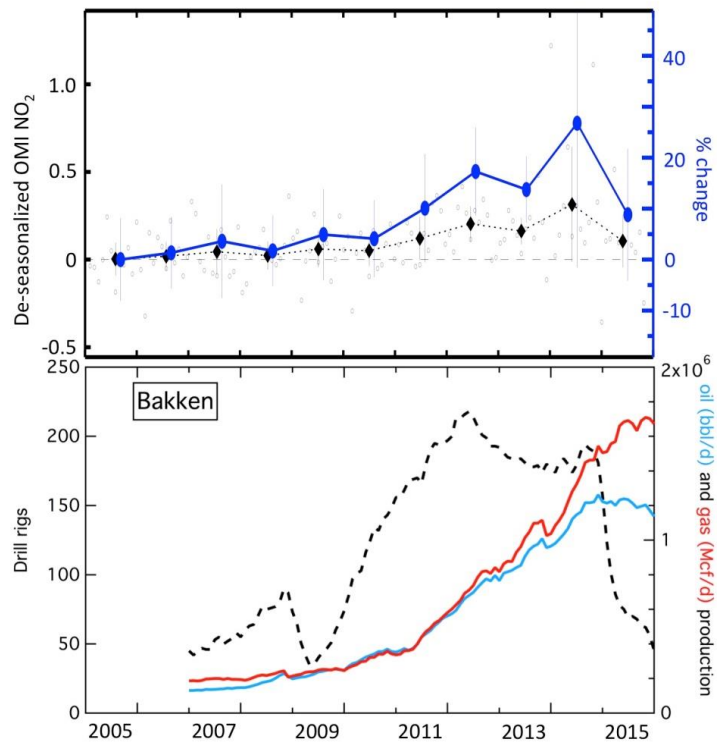


Figure 3-24. Time series of (top) annual average OMI NO₂ data (10^{15} cm^{-2} on left, % on right) relative to the year 2005, and (bottom) U.S. Energy Information Administration (<https://www.eia.gov/petroleum/drilling/>) monthly statistics of production plus drilling activity in the Bakken O&G basin.

3.3.4 Summary and Recommendations for Further Analysis

This Response to Question C provide only three sample analyses that give preliminary indications of how O&G emissions are divided between the various stages of fossil fuel extraction and specific extraction processes. A comprehensive answer to this Science Question awaits much additional analysis. One can envision many avenues for examination of co-variation of emissions with metrics that quantify the activities of different oil and gas production processes; perhaps the biggest challenge is to prioritize these avenues to maximize the policy-relevant information obtained. In particular it may be useful to conduct a quantitative correlation analysis of the satellite NO₂ measurements with the metrics of drilling and oil and gas production. Surveys by an instrumented van of individual well pads and O&G processing facilities in O&G basins in Utah and Colorado have collected much detailed information regarding VOC emissions as a function of well development phase (e.g., "fracking", flowback, liquid unloading, production); analysis of these data are underway [Jessica Gilman, NOAA]. Similar observational surveys could provide equivalent information for Texas O&G basins in order to evaluate regional differences.

3.3.5 References

Duncan, B.N., L.N. Lamsal, A.M. Thompson, Y. Yoshida, Z. Lu, D.G. Streets, M.M. Hurwitz, and K. E. Pickering (2016), A space-based, high-resolution view of notable changes in urban NO_x pollution around the world (2005–2014), *J. Geophys. Res. Atmos.*, 121, doi:10.1002/2015JD024121.

3.4 Response to Question D

How do these emissions in Texas compare to other regions of the U.S.?

3.4.1 Working Group

Sue Kemball-Cook - Ramboll Environ

Amnon Bar-Ilan - Ramboll Environ

Jessica Gilman - NOAA/ESRL/CSD

John Grant - Ramboll Environ

3.4.2 Background

For a full understanding of the air quality impacts of O&G emissions, it would be very helpful to compare the air quality impacts between all of the U.S. O&G basins. Such a comparison would provide a rich data set from which to seek correlations of the impacts with the magnitude and composition of the O&G emissions. However, it is not yet possible to conduct this effort because at present neither the air quality impacts nor the O&G emissions are accurately quantified. Finding D1 discusses the difficulty of comparing emission estimates based upon emission inventories. Finding D2 presents an observation-based comparison of one measure of the potential impacts of O&G VOC emissions on photochemical ozone formation.

3.4.3 Findings

Finding D1: Accurate comparison of regional bottom-up O&G criteria air pollutant emission inventories for different states is confounded by the use of inconsistent O&G emission inventory methodology.

Analysis: John Grant, Amnon Bar-Ilan-Ramboll Environ

State and federal agencies develop regional O&G criteria air pollutant emission inventories for use in air quality planning. Comparison of region- or state-level emission inventories could potentially provide information on topics such as the effect of region-specific control programs on emissions, the effect of region-specific O&G development histories on emissions, and differences in emissions by O&G formation¹¹. However, comparisons of regional O&G inventories are often confounded by differences in emission inventory development methodology. Here we analyze the 2014 National Emission Inventory (NEI) in order to illustrate some of these methodology differences.

The U.S. Environmental Protection Agency (EPA) compiles a comprehensive national criteria air pollutant emission inventory for anthropogenic sources in the triennial NEI. We focus our

¹¹ Typical oil and gas production phase equipment configuration, vent and flash gas composition, typical drill rig and hydraulic fracturing equipment configuration are examples of emission inventory input factors that are expected to vary by oil and gas formation.

discussion on the 2014 NEI (version 1)¹² since it is the most recent compilation of national O&G criteria air pollutant emissions and incorporates the results of several state and regional emission inventory efforts. Nonpoint O&G emissions in the 2014 NEI are based on a combination of O&G emissions submitted to the EPA by state, local, and tribal (S/L/T) agencies; for area/source category combinations which are not submitted to EPA by S/L/T agencies, emissions are based on the O&G Tool¹³ [EPA, 2016].

To illustrate differences in regional nonpoint O&G emission inventory estimates, Table 3-1 compares emissions for select source categories in Texas and Louisiana border counties that are within the Haynesville Shale formation. There are substantial differences in by-source-category emissions per surrogate¹⁴ between the Texas counties and Louisiana parishes for compressor engines and heaters.

Table 3-1. Nitrogen oxides (NOx) emissions, O&G activity, and emissions per surrogate for nonpoint compressor engines and heaters in Haynesville Shale counties and parishes at the border of Texas and Louisiana.

Parameter	Caddo Parish, LA	De Soto Parish, LA	Harrison County, TX	Panola County, TX
Wellhead Compressor Engines				
2014 NEI (v1) NOx Emissions (tpy ¹)	1,073	2,287	2,458	6,156
Percent of Nonpoint O&G Emissions	25%	42%	89%	90%
2014 Gas Production (MMCF/yr ²)	178,843	629,226	139,732	358,458
NOx Emission Rate (lb/MMCF³)	12.0	7.3	35.2	34.3
Lateral Compressor Engines				
2014 NEI (v1) NOx Emissions (tpy)	702	1,496	-	-
Percent of Nonpoint O&G Emissions	16%	28%	0%	0%
2014 Gas Production (MMCF/yr)	178,843	629,226	139,732	358,458
NOx Emission Rate (lb/MMCF)	7.8	4.8	-	-
Wellhead + Lateral Compressor Engines				
2014 NEI (v1) NOx Emissions (tpy)	1,775	3,783	2,458	6,156
Percent of Nonpoint O&G Emissions	41%	70%	89%	90%
2014 Gas Production (MMCF/yr)	178,843	629,226	139,732	358,458
NOx Emission Rate (lb/MMCF)	19.8	12.0	35.2	34.3
Heaters				
2014 NEI (v1) NOx Emissions (tpy)	332	89	0.1	0.1
Percent of Nonpoint O&G Emissions	8%	2%	0.005%	0.002%
2014 Well Count (no. of active wells)	10,695	2,849	2,834	5,504
NOx Emission Rate (lb/well⁴)	62	63	0.10	0.04

¹ tons per year

² million cubic-feet per year

³ pounds per million cubic-feet

⁴ pounds per well

¹² <https://www.epa.gov/air-emissions-inventories/2014-national-emissions-inventory-nei-data>

¹³ The O&G Tool is a database which estimates U.S. nonpoint source O&G emissions by county and source category based on county-level O&G production, well count, and drilling activity combined with county-level, source category specific input factors (e.g. device counts and bleed rates for the pneumatic controller source category).

¹⁴ A surrogate is the O&G activity statistic (e.g. active well count, gas production) most closely related to emissions from a given source category (e.g. the surrogate for heaters is well count, the surrogate for drill rigs is spuds).

Emissions from wellhead and lateral compressor engines are estimated in the 2014 NEI (version 1) by the O&G Tool for Louisiana; Louisiana O&G Tool compressor engine inputs (i.e. engine prevalence, engine average horsepower, engine load factor, and the fraction of engines that are rich burn and lean burn) are based on [*ENVIRON and Eastern Research Group, 2012*] and emission factors are based on EPA AP-42 guidance¹⁵. [*ENVIRON and Eastern Research Group, 2012*] compressor engine inputs are based on industry surveys. Quality ratings for compressor engine inputs assigned in [*ENVIRON and Eastern Research Group, 2012*] were either “low” (inputs based on regional/national default values or industry averages) or “medium” (inputs based on limited survey data). Compressor engine emission inventory inputs for Texas are based on data derived from two sources. The fraction of emissions by compressor engine configuration (i.e. rich burn versus lean burn and horsepower range) and emission factors by engine configuration were taken from the 2011 Barnett Shale Area Special Inventory¹⁶. Data on compressor engine energy required per unit of gas production was taken from the [*HARC, 2005*] study. The 2011 Barnett Shale Area Special Inventory was based on survey data received from operators in the Barnett Shale Area; participation in the survey effort was required by the TCEQ, so the Barnett Shale data set is highly detailed. *HARC, [2005]* estimated compression energy required per unit of gas production based on field surveys conducted circa-2005 of 66 compressor engines located in Texas.

As described above, the methodology for determining compressor engine activity differs for Louisiana and Texas. For Louisiana, wellhead and lateral compressor engine activity is based on the number of wellhead and lateral compressor engines per well combined with representative engine characteristics. Texas compressor engine activity is based on region-specific horsepower-hours per unit of gas production combined with the distribution of compressor engine activity by engine configuration.

Similar to compressor engines, emissions from heaters in Louisiana are estimated in the 2014 NEI (version 1) by the O&G Tool; Louisiana O&G Tool inputs for heaters (i.e. heater size, number of heaters per well, average annual hours of operation, and average fuel heat content) are based on [*ENVIRON and Eastern Research Group, 2012*]¹⁷ and emission factors are based on EPA AP-42 guidance¹⁵. [*ENVIRON and Eastern Research Group, 2012*] heater inputs are based on *Bar-Ilan et al. [2008]*, which developed calendar year 2002 emission inventory improvements based on limited operator surveys. Texas heater emission inventory inputs (i.e. heater size, number of heaters per well with liquids production, average annual hours of operation, and average fuel heat content) are based on a Texas-specific emission inventory study [*Eastern Research Group, 2013*], which developed heater inputs based on operator surveys.

As described above, the methodology for determining heater activity differs for Louisiana and Texas. For Louisiana, heater activity is based on an average estimate of the number of heaters

¹⁵ <https://www.epa.gov/air-emissions-factors-and-quantification/ap-42-compilation-air-emission-factors>

¹⁶ <https://www.tceq.texas.gov/airquality/barnettshale/bshale-data>

¹⁷ The number of heaters per well is the only input not derived from ENVIRON and Eastern Research Group (2012); this input is based on EPA Subpart W data.

per well combined with heater size, average annual hours of operation, and average fuel heat content. Texas heater activity is based on an average estimate of the number of heaters per well with liquids production (wells without liquids production are assumed not to include a heater) combined with heater size, average annual hours of operation, and average fuel heat content.

The substantial differences in emissions per surrogate for these nonpoint source categories could be an artifact of different emission inventory input assumptions/methodology and/or could result from real operational differences for O&G sources in Texas and Louisiana for these counties and parishes.

Point source O&G emissions are typically developed based on facility-level reporting. For the NEI, S/L/T agencies report facility-level point source emissions for facilities that are classified as Title V facilities; some S/L/T agencies also report emissions at facilities that are not classified as Title V but meet a state-defined emission threshold. O&G facility reporting thresholds for select states are listed in Table 3-2 below [Grant and Bar-Ilan, 2017].

Table 3-2. 2014 NEI point source reporting for select states.

State	Title V Sources	Minor Sources	Minor Sources Threshold(s)
Arkansas	✓	-	
Louisiana	✓	✓	Attainment Areas: 15 tpy VOC ³ Nonattainment Areas: 10 tpy VOC, 25 tpy NOx
New Mexico	✓	-	
Oklahoma	✓	✓	40 tpy actual or 100 tpy potential of any criteria air pollutant, 10 tpy potential emissions of any hazardous air pollutant, or 25 tpy potential emissions of total hazardous air pollutants ²
Texas ¹	✓	✓	Actual: 10/100 tpy (VOC), 25/100 tpy (NOx) Potential: 25-100 tpy (VOC), 25-100 tpy (NOx)

¹ Reporting thresholds in Texas vary by county depending on ozone attainment status

² A facility would also be included if it is required to obtain a construction permit to allow the installation of any emission unit that is subject to an emission limit, equipment standard, or work practice standard required by any New Source Performance Standard (NSPS) or National Emission Standard for Hazardous Air Pollutants (NESHAP)

³ volatile organic compounds

Depending on S/L/T agency specific point source emissions reporting, point source O&G emissions from facilities that are not classified as Title V may be missing from the NEI O&G inventory. It is unclear whether emissions from omitted facilities would be captured as nonpoint sources.

Reliable comparisons of regional criteria air pollutant emission inventories cannot be developed at this time as a result of (1) inconsistent nonpoint emission inventory development inputs and/or methodology by region and (2) inconsistent characterization of point source facility O&G emissions.

Finding D2: The total rate of reactivity of hydroxyl radicals (OHR) has been calculated for three O&G basins. The results are similar in magnitude to those seen in the Gulf of Mexico, but the alkene contribution is much smaller and alkane contribution is larger. This difference suggests that ozone formation is less efficient in these O&G basins than in The Gulf of Mexico.

Analysis: Jessica Gilman-NOAA

As discussed in Findings F3 and F4, the total rate of reactivity of hydroxyl radicals (OH) - OHR - provides one (albeit incomplete - see Finding F4) measure of the potential rate of photochemical ozone production [e.g., *Gilman et al.*, 2009]. Figure 3-25 shows median OHR for three O&G basins that contain only very limited urban development. The pie charts in this figure show how the total OHR in each basin is divided between contributions from VOCs, CH₄ plus CO and NOx, two other species emitted by anthropogenic activities. The total OHR is similar in these basins (~ 1 to 2 s^{-1}). For comparison *Gilman et al.* [2009] show that average total OHR varied from a low of $\sim 1 \text{ s}^{-1}$ in the central Gulf of Mexico, to $\sim 10 \text{ s}^{-1}$ in the HGB area. It should be appreciated that Figure 3-26 was derived from a very limited number of aircraft flights over each basin: one over Raton, two over the Bakken and three over the Permian. Since median OHR values are dependent on ambient conditions (i.e., wind speed, boundary layer evolution), these values may be unrepresentative of the general photochemical environment in these basins. However, the comparison of the relative contributions of the different species to the total OHR will be much less affected.

In the O&G Basins included in Figure 3-25, three of the OH reactant categories make significant contributions, while NO₂ contributes only 3 to 6% of total OHR. The primary difference between the three basins is due to the differing contributions from VOCs. This difference is even greater than indicated by the differing percent OHR contribution (32 - 65%), since the larger fractional VOC contribution is seen in the basins with the larger median OHR. Figure 3-26 shows that the median OHR due to VOCs varies by a factor of ~ 5 (0.29 to 1.5 s^{-1}).

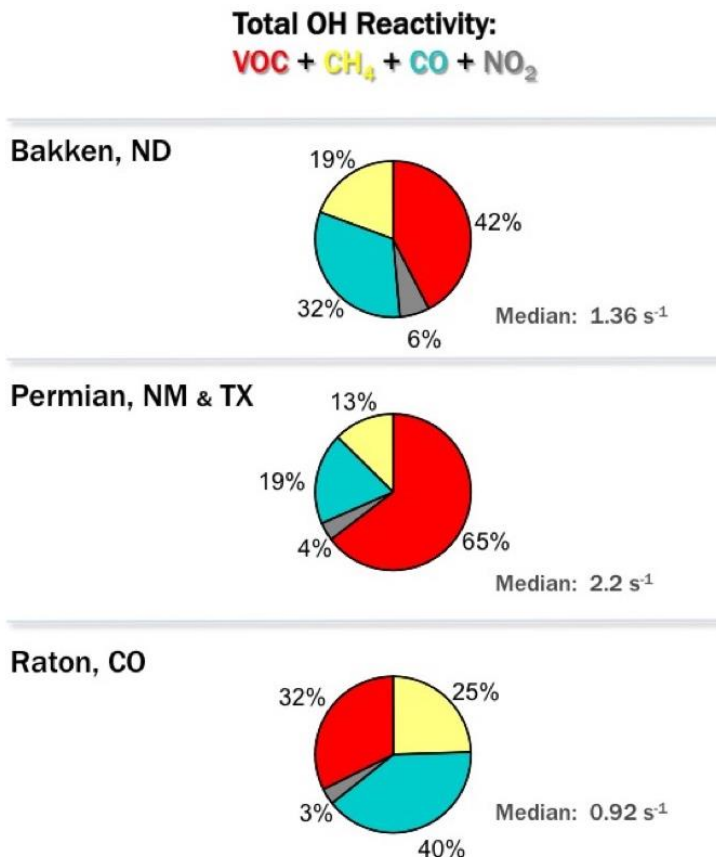


Figure 3-25. Median total OHR in three O&G basins based upon measurements made during the SONGNEX field campaign in 2015. The median total OHR is annotated, and the pie charts show how VOCs, CH₄, CO and NO₂ each contribute to that reactivity.

The median contributions of four families of VOC species to OHR are quantified in Figure 3-26. In all basins, oxygenated VOCs (OVOCs) account for the majority of median OHR. Formaldehyde, which accounts for the majority of the OVOC contribution, is formed during the oxidation of many VOC species, including CH₄, as well as CO. Hence this OVOC contribution to OHR does not reflect solely O&G emissions. In all basins, the contributions from biogenic VOCs are small ($\leq 4\%$ of VOC total), which contrasts with some other Texas O&G basins where BVOCs make much larger OHR contributions (see Finding F3).

It is informative to compare the pie charts in Figure 3-26 with Figure 6 of Gilman *et al.* [2009], which shows similar plots calculated for contrasting regions near Houston TX. The Raton Basin results are generally similar, both in magnitude and partitioning between VOC families, to measurements in the central Gulf of Mexico, except that in the Raton Basin the contribution from alkenes is much smaller and that from alkanes is much larger. The Bakken and Permian Basins are more similar in magnitude and VOC family partitioning with measurements in the coastal offshore Gulf of Mexico, again with the contributions from alkenes much smaller and from alkanes much larger. The bottom line here is that the ambient VOC concentrations in these three O&G basins give total OHR similar to that seen in the Gulf of Mexico. However, in

the O&G basins, the alkene contribution is much smaller and alkane contribution is larger. This difference is important, because ozone formation is much less efficient in the oxidation of alkanes compared to other VOCs (see Finding F4).

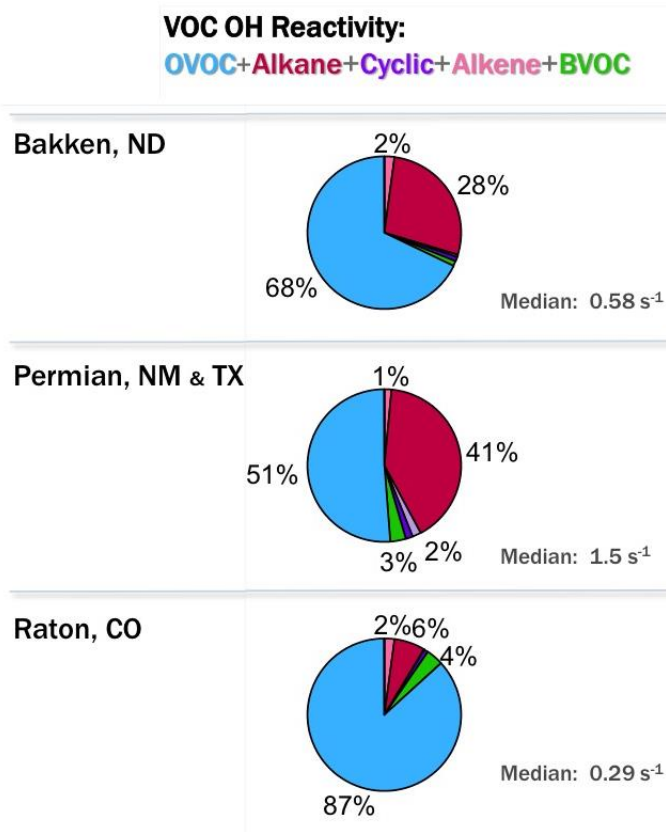


Figure 3-26. OHR due to VOCs in the three O&G basins included in Figure 3-25. The median VOC OHR is indicated, and the pie charts show how four VOC families each contribute to that reactivity.

Figure 3-27 compares the median contributions of CH_4 and four NMHC families to the enhancement in OHR (i.e., OHR above that due to nominal, observed background concentrations of CH_4 and the NMHCs). The totals of these enhancements vary over a factor of ~ 50 (0.02 to 0.98 s^{-1}), and this variation correlates with the characteristic VOC concentration signatures discussed in Finding B1. Of the fourteen basins included in Figure 3-10 and Figure 3-11, the Bakken and the Permian Basins produce the "wettest" hydrocarbon mixture, and the Raton Basin produces the "driest" (i.e., low NMHC emissions relative to methane). Alkanes dominate the NMHC contribution to OHR in all basins, with CH_4 , aromatics, cycloalkanes and alkenes making only small contributions; the apparently larger contributions from these groups in the Raton Basin is due to the very small total OHR contribution from the NMHCs in that basin, which allows NMHCs from sources other than O&G to make relatively larger contributions to OHR.

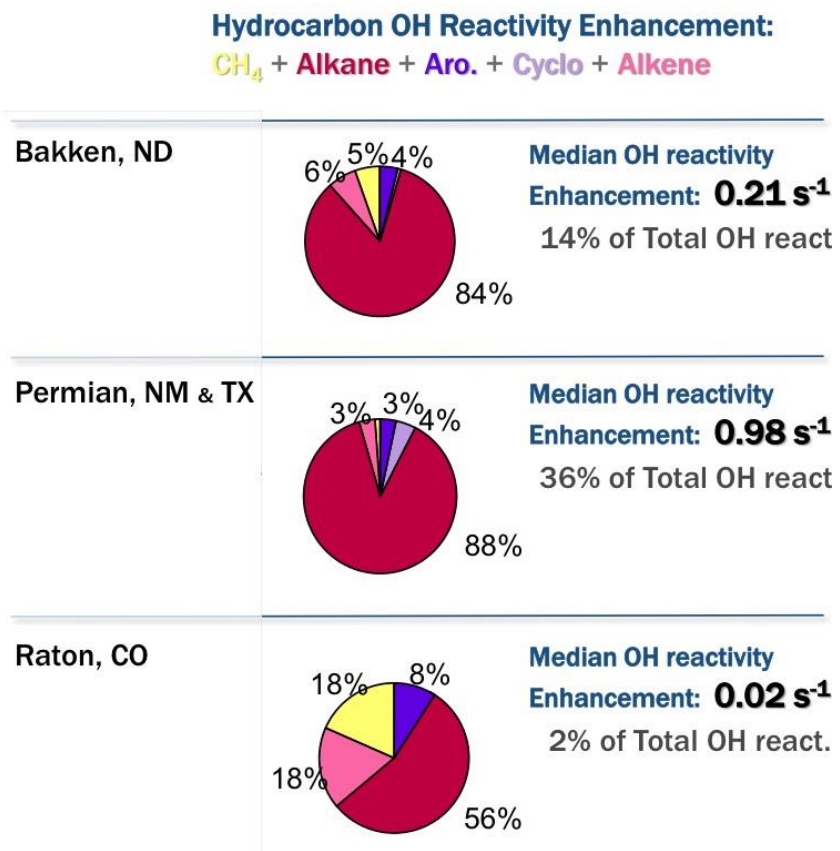


Figure 3-27. OHR enhancements above nominal background OHR due to NMHCs in the three O&G basins included in Figure 3-25. The median NMHC OHR enhancement is indicated, and the pie charts show how CH_4 and four NMHC families (alkanes, aromatics, cycloalkanes and alkenes) each contribute to that reactivity.

3.4.4 Summary and Recommendations for Further Analysis

This Response to Question D discusses the difficulty of comparing emission inventories between states, and provides a single, observationally-based analysis example that gives a "snap shot" indication of how VOC OHR varies between 3 three U.S. O&G basins, including the Permian Basin in Texas. Developing 1) observationally-based, quantitative descriptions of the air quality impacts and 2) accurate O&G emissions inventories for all U.S. O&G basins would provide a rich data set from which to seek correlations of the air quality impacts with the magnitude and composition of the O&G emissions. Neither of these developments has yet been completed.

3.4.5 References

Bar-Ilan et al. (2008), "Final Report: Recommendations for Improvements to the CENRAP States' O&G Emissions Inventories". Prepared for the Central States Regional Air Partnership. November 2008. https://www.wrapair.org//forums/ogwg/documents/2008-11_CENRAP_O&G_Report_11-13.pdf

- Environmental Protection Agency (2016), "2014 National Emissions Inventory, version 1 Technical Support Document". U.S. Environmental Protection Agency Office of Air Quality Planning and Standards Air Quality Assessment Division Emissions Inventory and Analysis Group. December 2016. https://www.epa.gov/sites/production/files/2016-12/documents/nei2014v1_tsdf.pdf
- Eastern Research Group (2013), "Upstream Oil and Gas Heaters and Boilers Final Report". Prepared for the Texas Commission on Environmental Quality. August 2013. https://www.tceq.texas.gov/assets/public/implementation/air/am/contracts/reports/ei/5821199776FY1317-20130831-erg-upstream_oil_gas_heaters_boilers.pdf
- ENVIRON and Eastern Research Group (2012), "2011 Oil and Gas Emission Inventory Enhancement Project for CenSARA States". Prepared for the Central States Air Resources Agencies (CenSARA). December 2012. <http://www.censara.org/filedepot?fid=14>
- Gilman, J. B., et al. (2009), Measurements of volatile organic compounds during the 2006 TexAQS/GoMACCS campaign: Industrial influences, regional characteristics, and diurnal dependencies of the OH reactivity, *J. Geophys. Res.*, 114, D00F06, doi:10.1029/2008JD011525.
- Grant and Bar-Ilan (2017), "Memorandum: Analysis of the National Oil and Gas Emission Inventory". Ramboll Environ. February 2017. https://www.wrapair2.org/pdf/NatOG_Anlys_Memo_06Feb2017post.pdf
- Houston Advanced Research Center (2005), "Natural Gas Compressor Engine Survey and Engine NOx Emissions at Gas Production Facilities". Prepared by Eastern Research Group, Inc. August 2005. <http://dept.ceer.utexas.edu/ceer/GHG/files/ConfCallSupp/H40T121FinalReport.pdf>.

3.5 Response to Question E

Are there gaps in our quantification of emissions that limit a full understanding of ozone and PM formation from these emissions?

3.5.1 Working Group

Sue Kemball-Cook - Ramboll Environ

Ravan Ahmadov - NOAA/ESRL/GSD

David Allen - University of Texas, Austin

Chuck Brock - NOAA/ESRL/CSD

Lea Hildebrandt Ruiz - University of Texas, Austin

John Grant - Ramboll Environ

Stu McKeen - NOAA/ESRL/GSD

Carsten Warneke - NOAA/ESRL/GSD

3.5.2 Background

The Responses to the preceding four Science Questions have summarized some recent advances in our understanding of emissions from O&G activities, with a particular focus on O&G fields in Texas. Here we identify some remaining uncertainties that could potentially be reduced through further research. In general, we have found that the impacts of O&G activities on ambient ozone and PM_{2.5} concentrations are small (see Findings A8, F1 and G2) and the uncertainties in quantifying these emissions constrain our ability to quantify upper limits for the magnitudes of these impacts.

3.5.3 Findings

Finding E1: Bottom-up emission measurements indicate that O&G methane and VOC emissions from high-emitting sources contribute a large fraction of O&G emissions; these emissions are incompletely captured by bottom-up emission inventories, leading to underestimates.

Analysis: John Grant-Ramboll Environ

Bottom-up inventories estimate emissions at the source or facility level over a defined time period and geographical area based on the product of emission factors (e.g. emissions per device) and activity factors (e.g. number of devices). In contrast, top-down studies estimate emissions from multiple sources at an entire facility or from multiple facilities across a region. Brandt *et al.* [2014] summarize results from recent top-down studies that indicate higher methane emissions than are estimated in bottom-up emission inventories, with top-down studies indicating excess methane emissions that are 1.25 to 1.75 times U.S. Environmental Protection Agency (EPA) bottom-up greenhouse gas emission inventory estimates. A major

challenge is to determine which sources (O&G or otherwise) are missing from or underrepresented in the bottom-up inventory.

Analyses of bottom-up O&G hydrocarbon emissions measurements collected in 18 studies across the U.S. (including six studies in Texas) show that a small percentage of O&G sites contribute a large fraction of hydrocarbon emissions [Brandt *et al.*, 2016]. Based on the results of 18 bottom-up measurement studies (Figure 3-28), the largest 5% of emission sources contributed a median of 57% of total methane emissions. In the Barnett Shale region of Texas, 2% of O&G facilities were estimated to be responsible for 50% of O&G methane emissions and 10% of facilities were responsible for 90% of methane emissions [Zavala-Araiza *et al.*, 2015]. Bottom-up O&G emission inventories typically do not include adequate representation of emissions from high emitters because (1) there is insufficient data on high emitter emissions factors and high emitter prevalence to accurately estimate high emitter emissions in bottom-up inventories and (2) bottom-up measurements cannot always identify which process is the cause of high emissions. Since VOC and methane are emitted together from fugitive and vent sources at O&G sites, VOC emissions are also likely under predicted in bottom-up emission inventories; Roest and Schade [2016] reach a similar conclusion.

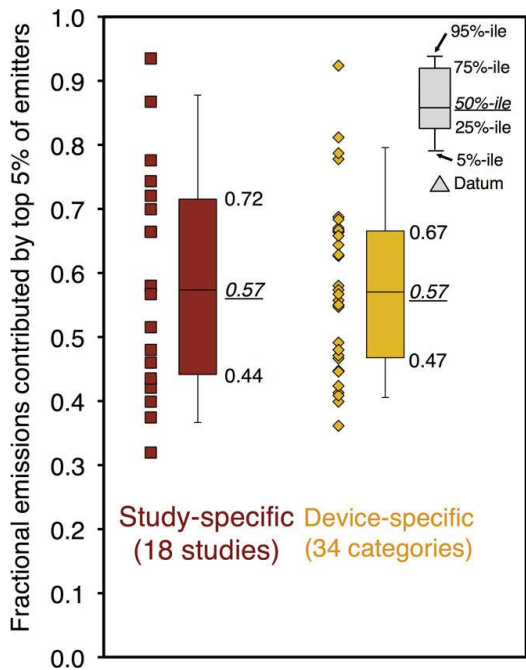


Figure 3-28. Fractional contribution of top 5% of emitters in each of 18 reference studies (red) and 34 device-specific categories of data from single studies (orange). [Figure from Brandt *et al.* 2016].

High emitters have been determined to result from persistent or episodic abnormal process conditions rather than routine operations in both O&G production and processing [Zavala-Araiza *et al.*, 2017] and flares [Schade and Roest, 2016]. Results of helicopter-based infrared

surveys of more than 8,000 O&G well pads across several O&G areas in the U.S. (including the Barnett Shale and Eagle Ford Shale in Texas) showed that 4% of all surveyed O&G well pads were high emitters with over 92% of high emitters due to tank vents and hatches and the remaining high emitters due to dehydrators, separators, trucks unloading oil from tanks, and unlit or malfunctioning flares [Lyon *et al.*, 2016].

Several studies [Brandt *et al.*, 2016; Lyon *et al.*, 2016; and Mitchell *et al.*, 2015] suggest that leak detection and repair (LDAR) surveys of O&G sites could reduce high emitter emissions. Zavala-Araiza *et al.* [2017] suggest frequent or, if possible, continuous monitoring to detect high emitter emissions. Allen [2014] suggests that control programs to reduce high emitter emissions may be developed based on smart sensing devices, aircraft, satellite, or ground-based monitoring. Additional research is needed to characterize the process conditions and other factors associated with high emitters and to develop and test high emitter control strategies.

Finding E2: Uncertainty in NO_x emissions from O&G activities limits our confidence in ozone concentration enhancements predicted by photochemical modeling; generally they may be overestimated due to inventory overestimates of these NO_x emissions.

Analysis: Ravan Ahmadov, Stu McKeen-NOAA

Ahmadov *et al.* [2015] investigated wintertime ozone formation in the Uinta Basin in Utah. They showed that the EPA NEI-2011 (version 1) emission inventory overestimated the Uinta Basin O&G NO_x emissions by a factor of 4 and underestimated VOC emissions by a factor of more than 2. These conclusions were based upon top-down comparisons of observations with the modeled precursor emissions. Model runs based on the NEI-2011 inventory did not show significant ozone production; however, when the inventory was modified to match the top-down determinations, the model well reproduced the observed ozone concentrations which exceeded 130 ppb (see their Figure 3).

It has not been definitively established that similar overestimates of NO_x emissions are present in bottom-up inventories for O&G basins other than the Uinta; however **Finding A5** of this Synthesis Report suggests that an important overestimate is present in the NEI 2011 inventory for the NO_x O&G emissions in the Haynesville Basin. To investigate this issue, the Weather Research and Forecasting (WRF) coupled with Chemistry (WRF-Chem) model with the EPA NEI-2011 inventory was utilized to simulate surface ozone concentrations in two calculations: one with and one without the O&G emissions throughout the U.S. Figure 3-29 shows the difference in the resulting afternoon ozone concentrations in Texas and the surrounding states. The maximum difference (≥ 5 ppb) in the south-central U.S. is seen over the Haynesville O&G basin.

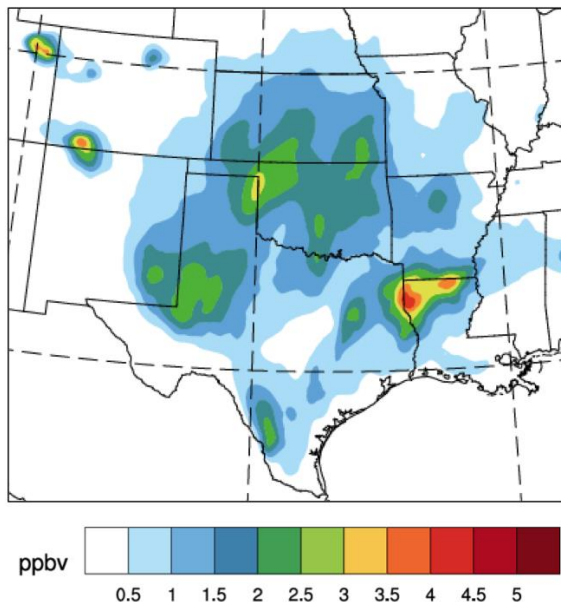


Figure 3-29. Difference in near-surface ozone concentrations simulated with and without O&G emissions. Results are for 3 pm EDT averaged over June 2013.

Figure 3-30 shows the results of a similar WRF-Chem simulation with and without the O&G emissions in five O&G basins only, including the Haynesville and Fayetteville basins in the region shown. The graph on the left, which is based on the NEI-2011 inventory, shows that the maximum difference (3 to 3.5 ppb) in the south-central U.S. is again seen over the Haynesville O&G basin. The graph on the right shows the result when the O&G emissions of NOx are reduced to be consistent with emissions quantified by the top-down techniques discussed in the Response to Question A of this report. The maximum difference over the Haynesville O&G is now much smaller (1 to 1.5 ppb) than found in either simulation based on the NEI 2011 emissions. No definitive conclusion can be drawn from these comparisons, but it is apparent that the small differences seen with the modeling based on the smaller top-down NOx emissions are more consistent with the investigation of long-term ozone trends over O&G basins in Texas, which are described in the Response to Question F of this report. Modeling of East Texas O&G ozone impacts done for this study (see Response to Question F) is based on bottom-up emission inventories for 2017. Ozone formation over most of East Texas is NOx-limited, and overestimates in the bottom-up O&G NOx emissions may cause the modeling to overstate the ozone impact of O&G emissions.

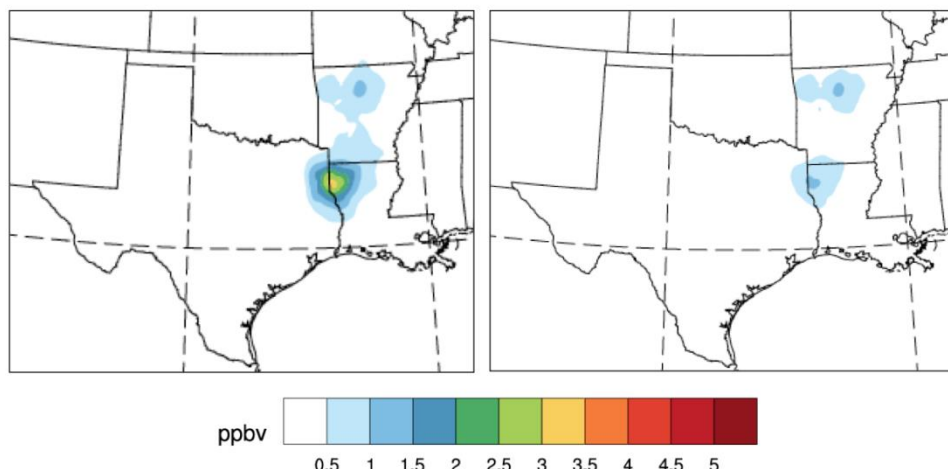


Figure 3-30. Difference in near-surface ozone concentrations simulated with and without O&G emissions in the Haynesville, Fayetteville and three other basins outside this region. The left map is calculated with the NEI-2011 inventory, and the right map is calculated with NO_x emissions reduced to match the top-down evaluations discussed in the response to Question A of this report. Results are for 3 pm EDT averaged over June 2013.

Finding E3: Uncertainty regarding possible emissions of SVOCs and IVOCs limit our ability to accurately model SOA formation in Texas O&G fields.

Analysis: Ravan Ahmadov, Stu McKeen-NOAA

During the Deepwater Horizon oil spill, semi-volatile compounds (SVOCs) and intermediate-volatility compounds (IVOCs) were identified as the predominant precursors of SOA formed downwind of the spill [de Gouw *et al.*, 2011]. Mining of Canadian oil sands releases these same classes of species, and they are directly responsible for the majority of the large concentrations of SOA PM mass observed to form downwind of those operations [Liggio *et al.*, 2016].

Significant concentrations of organic PM were observed in the Uinta O&G Basin in Utah during the winter of 2013 during the time periods that ozone concentrations exceeding 130 ppb were observed. This correlation with photochemical production of ozone indicates that this PM is predominately of secondary origin. WRF-Chem modeling that included mechanisms for organic aerosol formation has been conducted to investigate these observations. Simulations that included only the observed VOC species could explain less than half of the observed organic PM concentrations. It has been speculated that SVOCs and IVOCs can possibly account for this difference.

The emissions of SVOCs and IVOCs from O&G operations in Texas have not (to our knowledge) been investigated. The Deepwater Horizon oil spill and the Canadian oil sands represent petroleum sources very different from those encountered in Texas, and the emissions of IVOCs and SVOCs will certainly depend strongly on the composition of the O&G produced as well as the physical setting in which emissions are released. The photochemical production of organic

PM in the Uinta Basin may be more relevant to Texas. The composition of the emissions of gas-phase organics (VOCs, IVOCs, SVOCs) from storage tanks and other sources is not well known, and this lack of knowledge may impact our ability to accurately model SOA formation in Texas O&G fields.

Finding E4: Preliminary analysis of measurements of particle volume downwind of O&G fields indicates that the associated emissions produce little PM_{2.5}, at least locally (i.e., on a time scale of a few hours).

Analysis: Charles Brock-NOAA

Airborne, in situ measurements were made aboard the NOAA WP-3D aircraft on flight legs upwind and downwind of the Haynesville O&G basin during the May–July 2013 Southeastern Nexus of Air Quality and Climate (SENEX) mission. The instrumentation measured particle volume [Brock *et al.*, 2016] as well as a wide variety of gas phase species. Figure 3-31 compares the particle volume measurements with those of methane, a tracer of the O&G emissions, and SO₂, a tracer for the emissions from the Martin Lake electrical generation plant, which is located in the Haynesville region. The methane concentrations are clearly enhanced in the downwind leg; Peischl *et al.* [2015] analyzed these data to derive their top-down estimate of the total methane emissions from this O&G basin. However, there is no clear correlation of the particle volume enhancements with the methane concentration enhancements, and generally the particle volume is similar on the upwind and downwind flight legs. The only clear increase in particle volume is in the Martin Lake power plant plume, which is clearly identified by the large SO₂ enhancement during the downwind leg. The time required to transport an air parcel between the locations of the upwind and downwind flight legs is calculated as 5.5 hours (from measured wind speeds) and 5 hours (from HYSPLIT trajectory calculations); thus, over these time scales the emissions from the O&G activity in the Haynesville Basin do not enhance PM_{2.5} concentrations by a discernible amount.

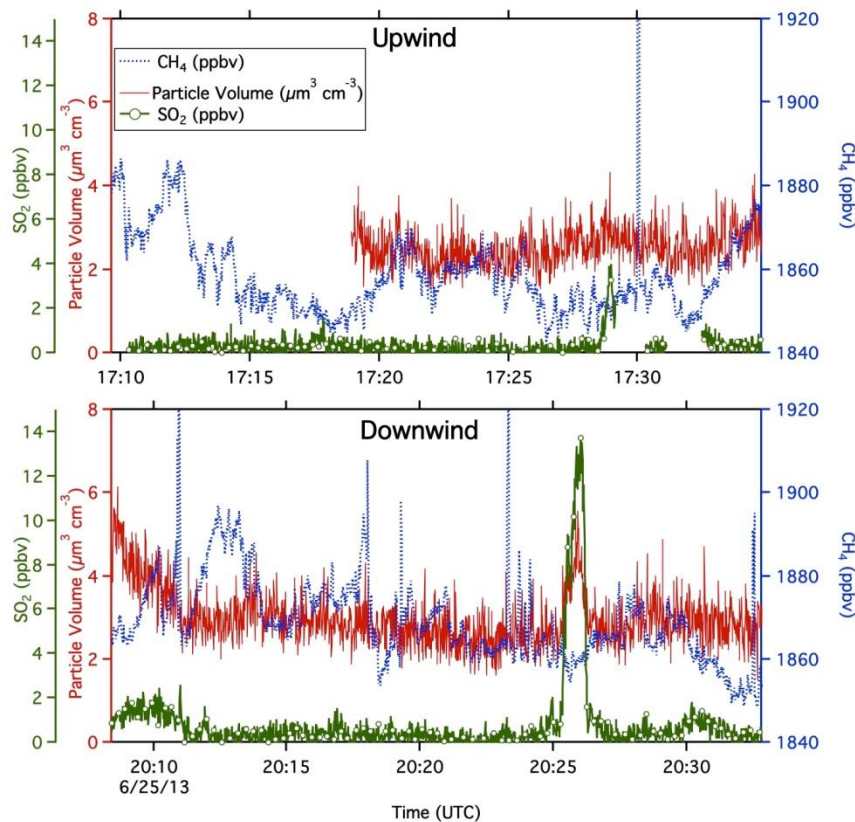


Figure 3-31. In situ, airborne measurements upwind and downwind of the Haynesville O&G basin. Time series of particle volume in $\mu\text{m}^3 \text{cm}^{-3}$ (approximately equal to 70% of $\text{PM}_{2.5}$ in $\mu\text{g m}^{-3}$) are compared to those of methane and SO_2 concentrations.

Finding E5: Uncertainty remains in isoprene emission inventories; the latest comparisons of models and measurements indicate that on average BEIS was lower and MEGAN was higher than the measurements, with about a factor of 2 difference between the two inventories.

Analysis: C. Warneke-NOAA

Biogenic VOCs can contribute significantly to, or even dominate, the VOC reactivity in some air basins [e.g. in the Barnett Shale region, Rutter *et al.*, 2015]. Previous studies suggest that isoprene emissions based on the Model of Emissions of Gases and Aerosols from Nature (MEGAN) [Guenther *et al.*, 2012] can be twice those based on the Biogenic Emission Inventory System (BEIS) [Bash *et al.*, 2015] over the Eastern US [e.g., Warneke *et al.*, 2010]. During the Southeast Atmosphere Study (SAS), isoprene emissions were measured onboard two aircraft using different techniques. The two methods of estimating isoprene emissions agreed within their uncertainties. Isoprene emissions were estimated along the flight tracks using different versions of the BEIS and MEGAN models (BEIS3.12, BEIS3.13, MEGAN2.0, MEGAN2.1, and MEGAN_v2015) with meteorological data measured on the aircraft as input. The measurements and model estimates were compared and showed that on average, BEIS was lower than the measurements and MEGAN was higher than the measurements. MEGAN2.1

predicted isoprene emissions in the Southeast US were again about twice as high as those from BEIS [Mao *et al.*, 2016].

Landcover characteristics including Leaf Area Index (LAI) and tree species composition data are critical driving variables for MEGAN isoprene and monoterpene emission factors. The isoprene and monoterpene emission factors were estimated using the airborne flux measurements. It was found that the isoprene emission factors agreed well with MEGAN2.1 for landscapes dominated by high isoprene emitting species, but landscapes that had the high isoprene emitters in the understory showed emissions lower than expected by the model. The isoprene emission factor was linearly correlated with the high isoprene emitter plant species fraction in the landscape data set. This shows the need for models to include canopy vertical heterogeneity of the isoprene-emitting fraction [Yu *et al.*, submitted].

Isoprene mixing ratios were modeled with 1) WRF-Chem using BEIS and with 2) the Comprehensive Air Quality Model with Extensions (CAMx; [Ramboll Environ, 2017]) using MEGAN and the results were consistent with the measurement-inventory comparison: WRF-Chem was biased low and CAMx biased high. [Warneke *et al.*, in preparation].

Wang *et al.* [2017] simulated ambient isoprene concentrations with the Community Multi-scale Air Quality Model (CMAQ; Appel *et al.*, [2017]) using biogenic emissions estimated by MEGAN and several different gridded isoprene emission factor (EF) fields. They found unbiased agreement between model and ambient measurements at most non-urban monitors using isoprene emission estimation from the MEGAN-BEIS361, one of the EF fields.

Finding E6: High concentrations of a gas-phase soluble chloride species (presumably HCl) have been observed in the Barnett Shale region. The emission source(s) of the chlorine containing precursor(s) to this species remain unidentified.

Analysis: C.B. Faxon and David Allen-U. Texas at Austin

During the Dallas-Fort Worth (Barnett Shale) field campaign [Griffin *et al.*, 2011] measurements at the TCEQ Eagle Mountain Lake site revealed large concentrations (as high as ~2 ppb) of a soluble gas phase chloride species (Figure 3-32). This species is believed to be hydrochloric acid (HCl). The species' diurnal cycle and its relationships to other measured species indicate that the HCl is a product of photochemical transformations in the atmosphere (see further discussion in Finding I4). Faxon [2014] present detailed investigations of emissions of chlorine containing species that could act as HCl precursors, but none were identified that could account for such large ambient HCl concentrations. This work considered both gaseous and particulate phase precursors associated both with the Barnett Shale O&G exploitation activities and the nearby Dallas-Fort Worth urban area. Importantly, particle measurements were limited to the sub-micron size range. Understanding the HCl precursor emissions is potentially important, since the photochemical processes expected to be involved in forming HCl are also involved in forming ozone. The discussion of Finding I4 does indicate that these emissions are not solely associated with O&G development, and instead may be common to urban areas, such as the Dallas-Fort Worth area.

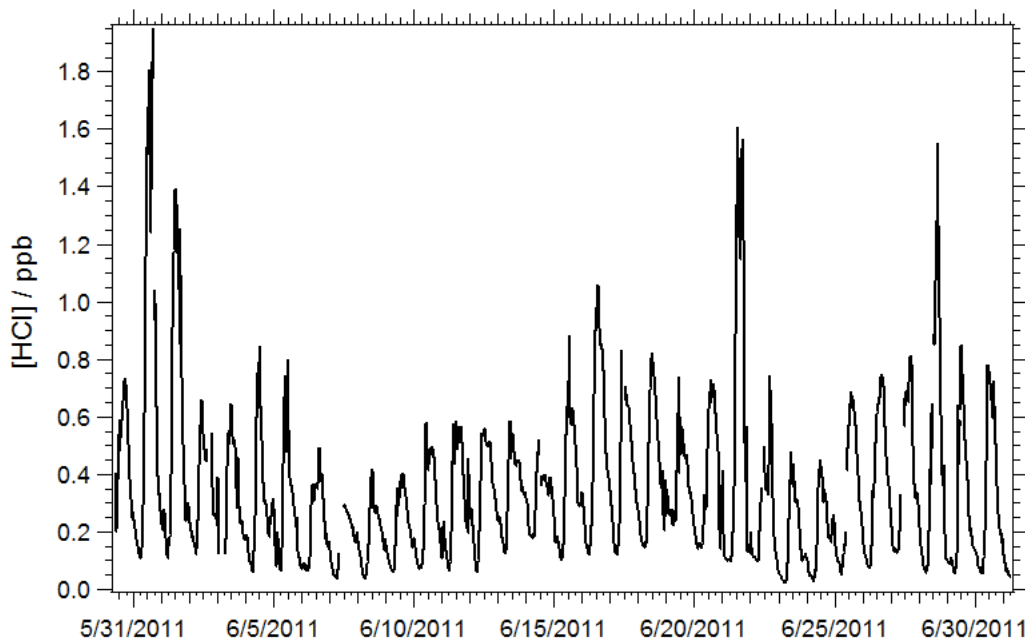


Figure 3-32. Soluble chloride concentrations observed during June 2011 at the TCEQ Eagle Mountain Lake measurement site [Figure from Faxon, 2014].

Finding E7: Environmental chamber experiments indicate that evaporation of flowback wastewater from hydraulic fracturing can result in formation of PM and ozone. Assessing the significance of air-quality impacts from this source would require quantification of wastewater evaporating in O&G regions, which is currently lacking.

Analysis: J.K. Bean and L. Hildebrandt Ruiz-U. Texas at Austin

Experiments conducted at the University of Texas at Austin quantified emissions from samples of hydraulic fracturing flowback wastewater collected in the Permian Basin, and investigated the photochemical processing of these emissions leading to the formation of particulate matter and ozone [Bean, 2016]. The amount of total volatile carbon (TVC, hydrocarbons evaporating at room temperature) averaged 29 milligrams per liter (mg/L) and the TVC evaporation rate averaged 1360 mg C/L·m⁻²·min. After photochemical oxidation under high NO_x conditions, the amount of organic particulate matter formed per milliliter of wastewater evaporated averaged 24 micrograms (μ g); the amount of ammonium nitrate formed averaged 260 μ g. A simple scaling analysis suggests that in the state of Texas, the estimated potential formation of PM from evaporated flowback wastewater is similar to the estimated PM emissions from oil rigs, emphasizing the need to further understand these emissions and their atmospheric processing. In an experiment at moderate NO_x conditions (approximately 1:1 VOC:NO_x) ozone production was observed, which was in line with amounts predicted by the SAPRC model for the photo-oxidation of decane using the Carbon Bond 6 chemical mechanism [revision 2, CB6r2, Yarwood et al., 2010].

It is not yet possible to assess the potential of flowback wastewater to influence air quality. Additional measurements would be required to quantify the extent of evaporation, which is difficult to estimate for complex and uncharacterized mixtures such as flowback wastewater. Ventilated storage tanks further complicate estimates of evaporation. Knowledge of the wastewater composition and tank parameters and condition are needed to correctly estimate evaporation from flowback wastewater, and the resulting formation of ozone and particulate matter.

3.5.4 Summary and Recommendations for Further Analysis

The Findings in the Response to this Question identify several shortcomings in our understanding of the emissions from O&G activities. Estimating the magnitudes of the air quality impacts associated with these shortcomings will allow prioritization of future research efforts. It seems likely that improving our understanding of the impact of a small fraction of high-emitting VOC sources (Finding E1) and improving the accuracy of NOx emissions from O&G sources (Finding E2) are of greatest importance. .

Findings E6, I4 and I5 discuss large measured concentrations of HCl at the TCEQ Eagle Mountain Lake site during the Dallas-Fort Worth (Barnett Shale) field campaign. The emission sources that provide the initial chlorine containing species have not been identified; one possible source that was not considered by *Faxon* [2014] is super-micron particulates containing chloride. The chemical transformations responsible for forming the HCl and the effect of those transformations on ozone formation are also not understood. For example, if HCl results from acid displacement from reaction of HNO₃ or H₂SO₄ with soil-derived particles or sea-salt, there would be little impact on ozone concentrations, but if the HCl is formed from the reaction of chlorine atoms with VOCs, then a significant impact on the ozone budget would be expected. A clear understanding of these issues would strengthen our understanding of the atmospheric transformation processes, both in O&G basins and in urban areas.

3.5.5 References

- Allen (2014), Review: Methane emissions from natural gas production and use: reconciling bottom-up and top-down measurements, Current Opinion in Chemical Engineering 2014, 5, 78–83. <http://dx.doi.org/10.1016/j.coche.2014.05.004>
- Ahmadov, R., et al. (2015), Understanding high wintertime ozone pollution events in an oil- and natural gas-producing region of the western US, Atmos. Chem. Phys., 15(1), 411–429, doi:10.5194/acp-15-411-2015.
- Appel, W., et al. (2017). Description and evaluation of the Community Multiscale Air Quality (CMAQ) modeling system version 5.1. Geoscientific Model Development, 10:1703-1732.
- Bash, J., K. Baker, M. Beaver, (2015). Evaluation of Improved Land Use and Canopy Representation in BEIS v3.61 with biogenic VOC measurements in California, Geoscientific Model Development Discussions, 8, 8117-8154. DOI: 10.5194/gmdd-8-8117-2015.

- Bean, JK (2016) Interactions of Nitric Oxide, Organic Compounds, and Particulate Matter and their Effects on Air Quality, Ph.D. Thesis, The University of Texas at Austin, 2016.
<https://repositories.lib.utexas.edu/bitstream/handle/2152/41603/BEAN-DISSERTATION-2016.pdf?sequence=1&isAllowed=y>
- Brandt, A.R., et al. (2014), Methane Leaks from North American Natural Gas Systems, *Science*, 343, 733-735.
- Brandt, A.R., et al. (2016), Methane Leaks from Natural Gas Systems Follow Extreme Distributions, *Environmental Science & Technology*, 2016, 50, 12512-12520, doi: 10.1021/acs.est.6b04303.
- Brock, C.A., et al. (2016), Aerosol optical properties in the southeastern United States in summer - Part 1: Hygroscopic growth, *Atmospheric Chemistry and Physics*, doi:10.5194/acp-16-4987-2016.
- de Gouw, J.A., et al., (2011), Organic aerosol formation downwind from the Deepwater Horizon Oil Spill, *Science*, 331, 1295-1299, doi:10.1126/science.1200320.
- Faxon, C.B. (2014), Urban atmospheric chlorine chemistry: mechanism development, evaluation and implications, PhD thesis, U. Texas - Austin, <http://hdl.handle.net/2152/25225>.
- Griffin, R., Dibb, J., Lefer, B., & Steiner, A. (2011). Final Report: Surface Measurements and One-Dimensional Modeling Related to Ozone Formation in the Suburban Dallas-Fort Worth Area (pp.1–45), AQRP, U. Texas - Austin, [http://aqrp.ceer.utexas.edu/projectinfo/10-024/10-024 Final Report.pdf](http://aqrp.ceer.utexas.edu/projectinfo/10-024/10-024%20Final%20Report.pdf).
- Guenther A., X. Jiang, C. Heald, T. Sakulyanontvittaya, T. Duhl, L. Emmons, X. Wang, (2012). The Model of Emissions of Gases and Aerosols from Nature version 2.1 (MEGAN2.1): an extended and updated framework for modeling biogenic emissions, *Geoscientific Model Development*, 5, 1471-1492, doi:10.5194/gmd-5-1471-2012.
- Lyon, D.R., et al. (2016), Aerial Surveys of Elevated Hydrocarbon Emissions from Oil and Gas Production Sites, *Environmental Science & Technology*, 2016, 50, 4877-4886, doi: 10.1021/acs.est.6b00705.
- Mao, J., et al. (2016) Southeast Atmosphere Studies: learning from model-observation syntheses, *Atmos. Chem. Phys. Discuss.*, doi:10.5194/acp-2016-1063.
- Mitchell, A.L., et al. (2015), Measurements of Methane Emissions from Natural Gas Gathering Facilities and Processing Plants: Measurement Results, *Environmental Science & Technology*, 2015, 49, 3219-3227, doi: 10.1021/es5052809.
- Peischl, J., et al. (2015), Quantifying atmospheric methane emissions from the Haynesville, Fayetteville, and northeastern Marcellus shale gas production regions, *J. Geophys. Res. Atmos.*, 120, 2119–2139, doi:10.1002/2014JD022697.
- Roest, G., and G. Schade (2016), Quantifying alkane emissions in the Eagle Ford Shale using boundary layer enhancement, *Atmos. Chem. Phys. Discuss.*, doi:10.5194/acp-2016-861.

- Rutter, A.P., R.J. Griffin, B.K. Cevik, K.M. Shakya, L. Gong, S. Kim, J.H. Flynn, and B.L. Lefer (2015), Sources of air pollution in a region of oil and gas exploration downwind of a large city, *Atmos. Environ.*, 120, 89–99, doi:10.1016/j.atmosenv.2015.08.073.
- Schade, G. W., and G. Roest (2016), Analysis of non-methane hydrocarbon data from a monitoring station affected by oil and gas development in the Eagle Ford shale, Texas, *Elem. Sci. Anth.*, 4, 000,096, doi:10.12952/journal.elementa.000096.
- Wang, P., G. Schade, M. Estes, Q. Ying (2017) Improved MEGAN predictions of biogenic isoprene in the contiguous United States. *Atmos. Environ.*, 148, 337-351, doi:10.1016/j.atmosenv.2016.11.006
- Warneke, C., et al. (2010), Biogenic emission measurement and inventories determination of biogenic emissions in the eastern United States and Texas and comparison with biogenic emission inventories, *J. Geophys. Res.-Atmos.*, 115, 10.1029/2009jd012445.
- Yu, H., et al. (2017), Airborne measurements of isoprene and monoterpane emissions from southeastern U.S. forests, *Sci. Total Environ.*, 595, 149-158, doi.org/10.1016/j.scitotenv.2017.03.262.
- Zavala-Araiza, D., et al. (2015), Reconciling divergent estimates of oil and gas methane emissions, *Proceedings of the National Academy of Sciences*, 112, 51, 15597-15602, doi: www.pnas.org/cgi/doi/10.1073/pnas.1522126112.
- Yarwood G, Jung J, Whitten GZ, et al. (2010) Updates to the Carbon Bond Mechanism for Version 6 (CB6). In: 9th Annual CMAS Conference. Chapel Hill, NC, pp 11–14.
- Zavala-Araiza, D., et al. (2017), Super-emitters in natural gas infrastructure are caused by abnormal process conditions, *Nature Communications*, 8, 14012, doi: 10.1038/ncomms14012.

4.0 SYNTHESIS OF RESULTS: CHEMICAL TRANSFORMATION

4.1 Response to Question F

What are the contributions of emissions from O&G development to ambient O₃ concentrations at regulatory monitors in Texas?

4.1.1 Working Group

Sue Kemball-Cook - Ramboll Environ

David Parrish - David.D.Parrish, LLC

Erin McDuffie - NOAA/ESRL/CSD

4.1.2 Background

Multiple peer-reviewed studies have characterized and quantified NOx and VOC emissions from O&G basins across the US, including multiple basins in eastern Texas [e.g., *Rutter et al.*, 2015; *Schade and Roest*, 2016]. There have been relatively few studies, however, that address the influence of these emissions on local and regional ozone production [*Kemball-Cook et al.*, 2010; *Pacsi et al.*, 2013; 2015; *Rutter et al.*, 2015; *Ahmadi and John*, 2015; *Evans and Helmig*, 2017; *Roohani et al.*, 2017]. Due to the complicated nature of ozone production, multiple metrics (observation- and model-based) have been developed to assess and quantify the influence of various precursor emission sources on ozone formation. In this Response, the contribution of O&G emissions to ozone formation has been addressed through analysis of ambient measurements and multiple modeling techniques.

Statistical analysis of long-term ozone observations from Texas state monitors provides the basis for Finding F1. Comparison of long-term trends at monitors located near O&G fields, to those near urban emissions, can possibly help elucidate an influence from recent increases in O&G activities. Findings F2-F5 are based on an analysis by *McDuffie et al.* [2016] that used multiple metrics to assess and quantify the influence of O&G VOC emissions on ozone production in the Denver-Julesburg Basin of Colorado (DJB). This region is an appropriate case-study for understanding the photochemical environment in Texas, as there are many pertinent similarities between the DJB and O&G basins throughout Texas. First, O&G activity in the Wattenberg Field of the greater DJB has increased dramatically over the last few years [*Colorado Oil and Gas Conservation Commission (COGCC)*, 2016]; similar increases have been observed in the Eagle Ford, Barnett, and Haynesville fields (see Figure 1-2 of the Introduction). Second, the proximity of the Wattenberg field to the city of Denver is similar to that of the Barnett, Eagle Ford, and Haynesville fields to the cities of Dallas-Fort Worth, San Antonio, and Longview, TX/Shreveport, LA, respectively. All four regions have large urban populations with ~3 million in the Denver metropolitan area, over 6 million in Dallas-Fort Worth, 1.5 million in San Antonio, and 0.9 million in the Longview-Shreveport region [*U.S. Census Bureau*]. Findings F6 and F7 are supported by CAMx photochemical grid modeling with source apportionment, conducted by Ramboll Environ, to assess the contributions of O&G and other emissions sources to ozone concentrations throughout East Texas.

4.1.3 Findings

Finding F1: Decadal scale ozone changes in three Texas O&G basins can be quantitatively described as interannual variations about smooth, continuous declines; neither the variations nor the declines significantly correlate with O&G production or drilling activity. This lack of correlation indicates that O&G development does not have a major impact on ozone concentrations in Texas (<5 ppb on design values and median ozone season MDA8 concentrations).

Analysis: David Parrish-David.D.Parrish, LLC

Figure 4-1 to Figure 4-4 compare the recent history of ambient ozone concentrations to the history of O&G production activity in four O&G basins, one in North Dakota and three in Texas. Figure 4-5 shows a similar analysis for the Austin-Killeen-Waco region, an area with much less O&G development activity. Maps showing the location of the ozone monitoring sites in relation to the basin's well locations are included. In all four of the O&G basins there is little indication of gradients across the regions, except that more urban sites (blue symbols) in the Barnett and Eagle Ford basins have somewhat higher concentrations than the other, more rural sites. Ozone concentrations are not noticeably higher where active wells are concentrated.

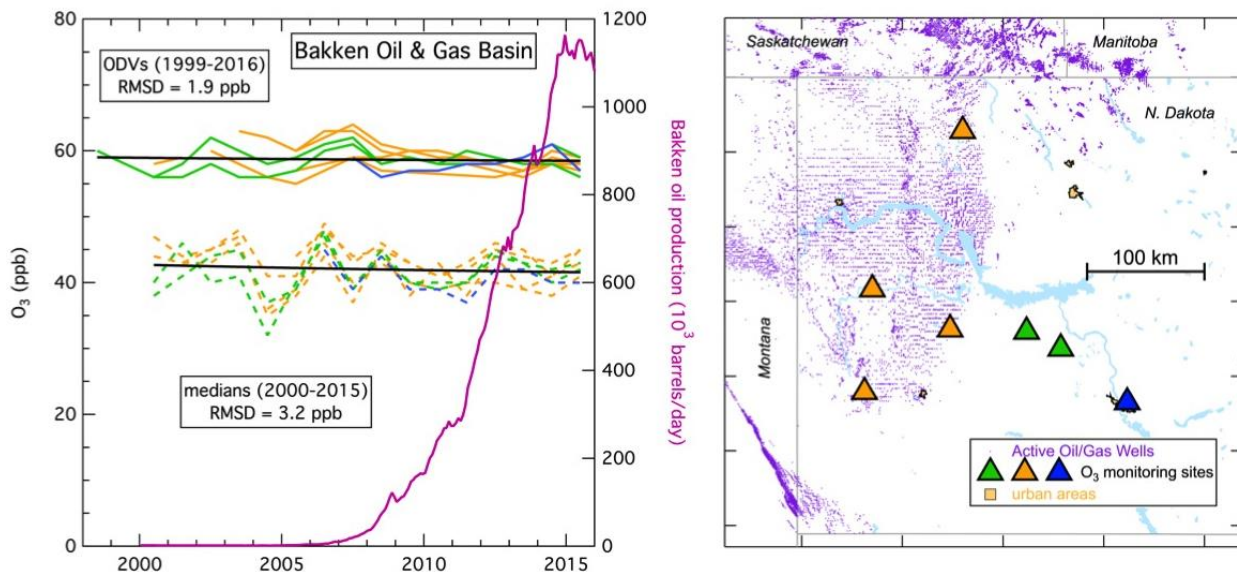


Figure 4-1. Time series of ozone design values (ODVs, solid lines) and median MDA8 ozone concentrations (dashed lines) for the May-September ozone season in the Bakken O&G basin in North Dakota. Ozone data are color-coded according to the site map that also shows the location of oil and natural gas wells. The history of oil production in the basin is indicated. The black lines indicate smooth fits to the respective data; root-mean-square deviations (RMSD) of the data from the fits are annotated.

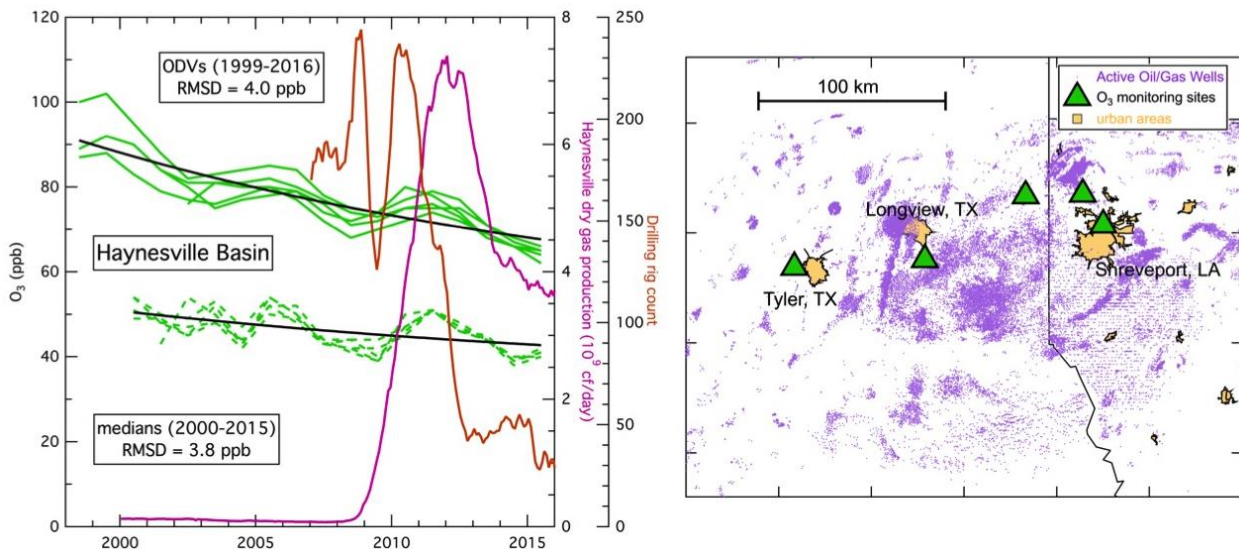


Figure 4-2. Time series of ODVs (solid lines) and median MDA8 ozone concentrations (dashed lines) for the April-October ozone season in the Haynesville O&G basin. Figure is in the same format as Figure 4-1. The histories of drilling and gas production in the basin are indicated.

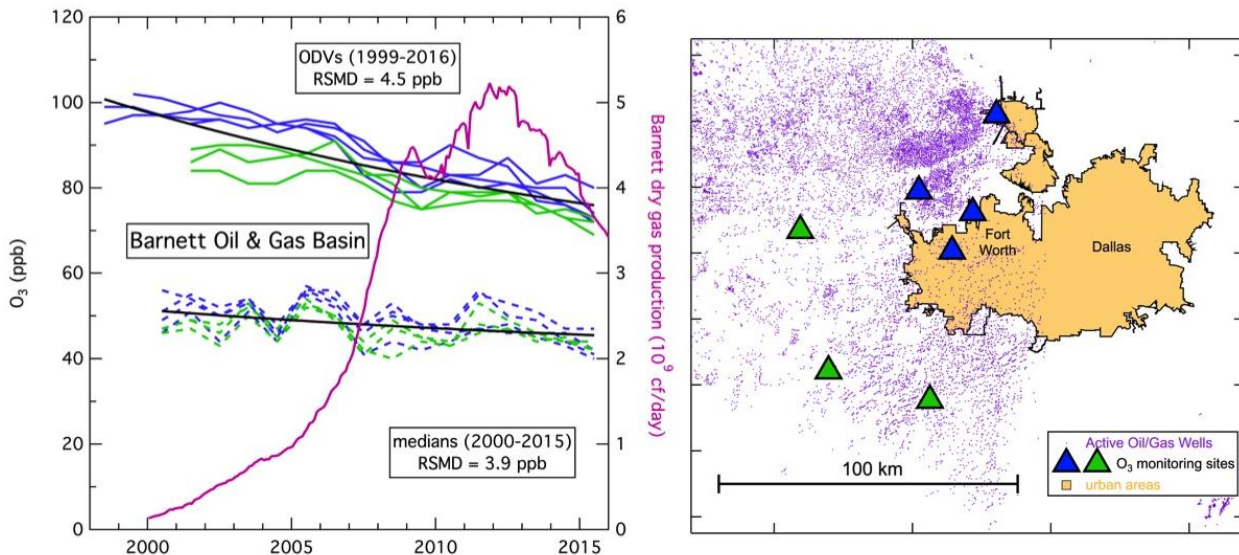


Figure 4-3. Time series of ODVs (solid lines) and median MDA8 ozone concentrations (dashed lines) for the April-October ozone season in the Barnett O&G basin. Figure is in the same format as Figure 4-1. The history of gas production in the basin is indicated.

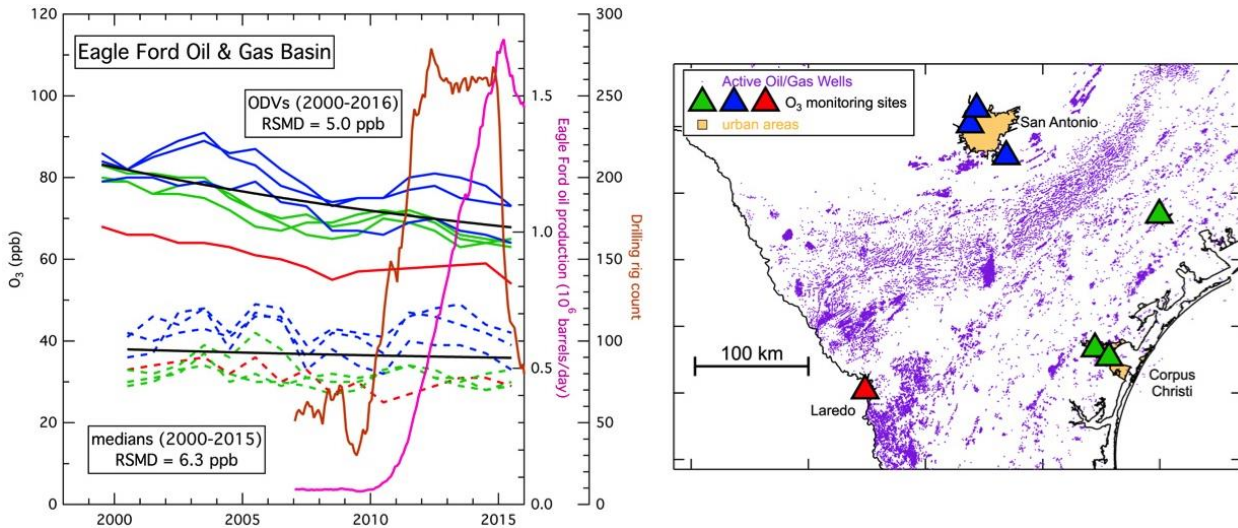


Figure 4-4. Time series of ODVs (solid lines) and median MDA8 ozone concentrations (dashed lines) for the April-October ozone season in the Eagle Ford O&G basin. Figure is in the same format as Figure 4-1. The Laredo data (red lines) are shown but not included in further analysis. The histories of drilling and oil production in the basin are indicated.

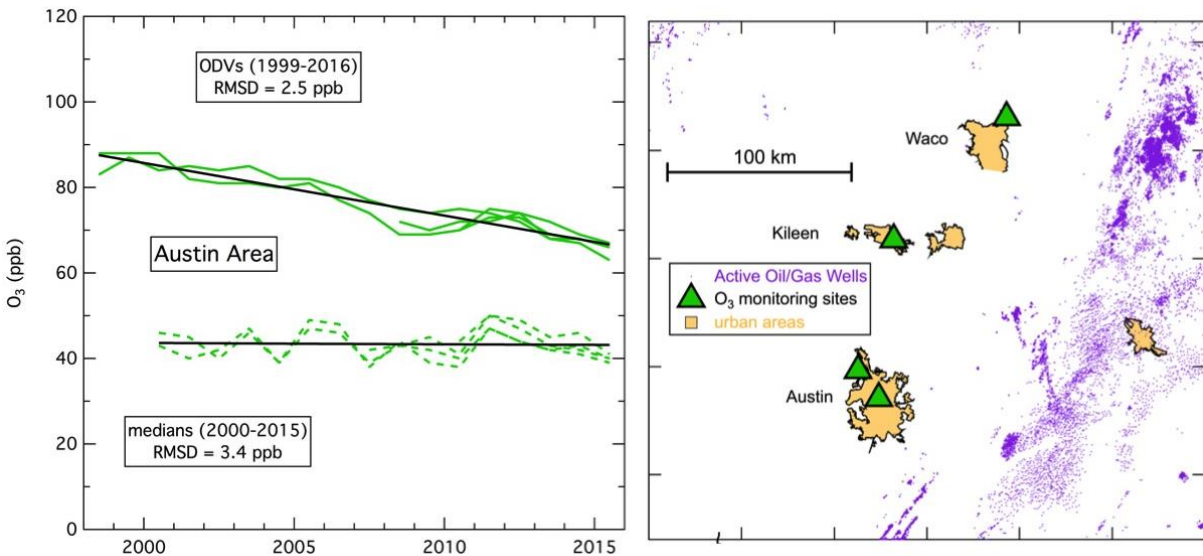


Figure 4-5. Time series of ODVs (solid lines) and median MDA8 ozone concentrations (dashed lines) for the April-October ozone season in the Austin-Killeen-Waco region. Figure is in the same format as Figure 4-1.

Ozone concentrations in each of the four O&G basins show no discernible temporal response to the O&G development, which in all cases changed dramatically over the fifteen-plus years of measurements. There is no indication that the long-term ozone decreases (in the Texas basins)

or the near constant concentrations (in the Bakken) were significantly perturbed by the increase in O&G activities.

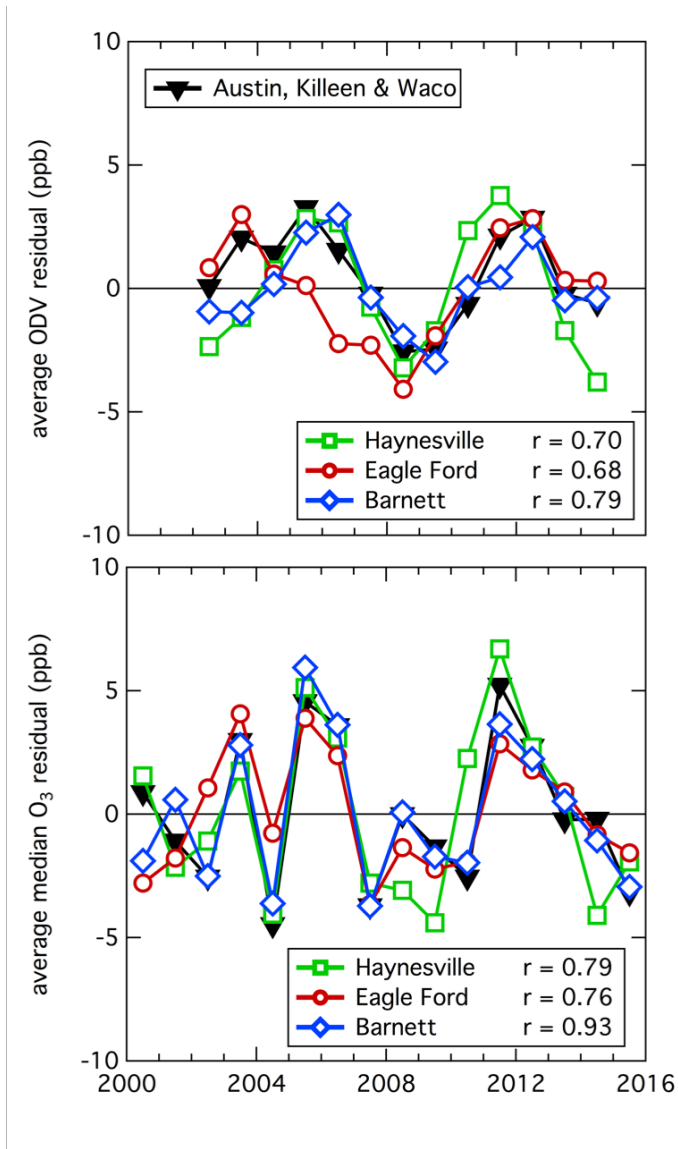


Figure 4-6. Time series of differences (i.e., the residuals) between the ODVs and median MDA8 ozone concentrations, and the respective smooth fits (black lines) in Figure 4-2 to Figure 4-5. The correlation coefficients between the oil basin residuals and those of the Austin-Killeen-Waco region are annotated.

Appendix A of this report describes a statistical analysis of the correlations of the interannual variations of the measured ozone concentrations about the long-term trends between the four Texas regions, and with statistics quantifying O&G activity in the respective basins. It is this correlation analysis that leads to the conclusions given above. The time series in Figure 4-6 shows the correlations between the interannual variability, as quantified by residuals about the

smooth fits, from the four different Texas regions. The high correlations ($r = 0.68$ to 0.93) between the residuals from the O&G basins and the Austin-Killeen-Waco region clearly indicate that the interannual variability arises from meteorologically-driven variability in the state wide background ozone concentrations. This indication is supported by a GEOS-Chem model simulation (Yuxuan Wang, University of Houston, private communication) for the eastern U.S. with emissions in the state of Texas set to zero. This simulation well-reproduces the residuals in the Barnett, San Antonio and Fort Worth region ($r = 0.67$ to 0.88) without any influence from Texas emissions.

It has not been possible for us to put quantitative confidence limits on this analysis, but the correlations plots included in Appendix A suggest that we could clearly discern an impact of 5 ppb on either the ODVs or the median MDA8 ozone concentrations in these three Texas O&G basins.

Finding F2: VOC measurements made in the vicinity of intensive O&G development show that light alkanes consistent with O&G production are present at concentrations well above those in most other U.S. areas, and can make up a large fraction of the observed total VOC mass and mixing ratio (e.g. ~80% in the Denver-Julesburg Basin).

Analysis: Erin McDuffie-CIRES/NOAA

Ozone photochemistry is highly non-linear and net regional production depends on the amount of NOx emissions relative to VOCs, as well as the specific types of VOCs emitted from each regional sector. Some VOCs are efficiently oxidized by the OH radical, initiating the ozone formation process (see Finding F3), while others lead to the oxidation and loss of NOx over ozone formation. Characterizing the contribution of O&G emissions to ambient VOCs can help identify the potential influence of O&G activity on local and regional ozone production.

Gilman et al. [2013] quantified the fractional contribution of O&G activity to ambient VOCs observed at a location within the greater Denver-Julesburg Basin, using a multivariate analysis to determine whether particular VOCs varied more closely with urban (i.e. acetylene) or O&G tracers (i.e. propane). When these results were applied to observations made during summer 2012 at the same location, *McDuffie et al. [2016]* determined that 82% of the measured non-methane VOC carbon mass was from C2-C9 alkanes. Of these compounds, light (C2-C4) alkanes were the most abundant and ~80% of their carbon mass could be attributed to regional O&G activity.

Rutter et al. [2015] analyzed ambient VOC measurements made in June 2011 at the Eagle Mountain Lake monitoring site in Texas. This site is influenced by the Dallas-Fort Worth urban plume as well as O&G activity from the Barnett Shale region. *Rutter et al. [2015]* performed source apportionment on the VOC measurements using Positive Matrix Factorization (PMF) [Norris et al., 2008] and found one PMF factor associated with natural gas production and one with fugitive emissions. Relative to five other emission source factors, the natural gas PMF factor, which contained most of the light alkanes such as ethane and propane, had the largest contribution to both mean and maximum VOC mixing ratios. Ethane was the most abundant

observed non-methane VOC with an average mixing ratio of 5.5 ppb and peak mixing ratio that exceeded 40 ppb during the study period.

Schade and Roest [2016] performed a factor analysis of VOC and NOx observations from July 2013 to July 2014 at the TCEQ Floresville monitoring site located southeast of San Antonio on the northwestern edge of the Eagle Ford Shale area. The factor most closely associated with O&G exploration and production contributed about half of the total VOC variability in the data set over the one year-long study. A second factor may also have had significant contributions from O&G activity; together these two factors accounted for 80% of the data set variability in VOC observations. Measured ethane mixing ratios occasionally exceeded 100 ppb during periods when the monitor was downwind of the Eagle Ford Shale. The median concentration of the Eagle Ford ethane measurements was 9 ppb and exceeded the range of mean concentrations (0.56-8.7 ppb) measured in 28 U.S. urban areas during the early 2000s [*Baker et al., 2008*].

These three studies are consistent in showing that VOC emissions from O&G activities can make a substantial contribution to the total measured mass of VOCs at monitoring sites downwind of the development area. To further assess the importance of these emissions to ozone production, their reactivity and oxidation mechanisms must be evaluated, and also the availability of NOx must be considered.

Finding F3: Estimates of the relative contribution of O&G VOC emissions to the total OH reactivity are variable and depend on the local influence of highly reactive biogenic VOCs.

Analysis: Erin McDuffie-CIRES/NOAA

The VOC OH reactivity (OHR) [e.g., *Gilman et al., 2009*] is a measure of the kinetic oxidation of VOCs by the OH radical, which is often the rate limiting step in photochemical ozone production. This metric has been used to highlight the potential contribution of O&G VOCs to summertime ozone production in multiple U.S. basins [e.g. *Gilman et al., 2013; Swarthout et al., 2015*]. VOC measurements from the summers of 2011 and 2012 show that the total non-methane VOC OHR ranged from $1\text{-}5 \text{ s}^{-1}$ in the Barnett [*Rutter et al., 2015*], compared to an average of $2.4 \pm 0.9 \text{ s}^{-1}$ in the DJB of Colorado [*McDuffie et al., 2016*]. *Schade and Roest [2016]* found that total non-methane VOC OHR during 2013-2014 at the Floresville site in the Eagle Ford ranged from $1\text{-}2 \text{ s}^{-1}$ depending on season and wind direction.

Though the total VOC OHR in these three regions was similar, the fractional contribution of various emission sources was not. *McDuffie et al. [2016]* found a ~50% contribution from O&G activity to average OHR in the DJB. *Schade and Roest [2016]* estimated a ~70% contribution from alkanes downwind of the Eagle Ford Shale area. In contrast, *Rutter et al. [2015]* determined that VOCs associated with natural gas and fugitive emissions from O&G production in the Barnett Shale region only contributed 13% to OHR over the course of a summertime three-week study.

A large difference between these three regions is the abundance of biogenic VOCs (e.g. Isoprene), which have a faster OH-oxidation rate constant than those emitted from O&G activity [Atkinson, 2000]. The fractional contribution of biogenic VOCs and their oxidation products was 70% in the Barnett [Rutter *et al.*, 2015], while contributions from primary biogenic VOCs only averaged 8% in the DJB in 2012 [McDuffie *et al.*, 2016] and less than 10% in the Eagle Ford [Schade and Roest, 2016]. This difference in the biogenic contribution is indicative of the higher density and availability of biogenic sources in north Texas. Though the DJB is adjacent to the Rocky Mountains, it is not influenced by mountain vegetation during the day due to easterly, upslope winds [Toth and Johnson, 1985]. Like the DJB, the Floresville monitoring site in the Eagle Ford is not heavily affected by biogenics, but other regions of the Eagle Ford are more densely vegetated and show a dominant biogenic influence on the OHR [Sullivan *et al.*, 2014]. Due to similarities in vegetation cover, a similar biogenic contribution may be expected in the Barnett and Haynesville regions.

Additional differences in fractional VOC-class contributions to OHR may be explained by differences in the proximity of each site to urban VOC emission sources.

Finding F4: The relative contribution of O&G VOC emissions to photochemical ozone formation is smaller than their relative contribution to the total OH reactivity because of the relatively small radical propagation potential of alkanes (~20% in the Denver-Julesburg Basin).

Analysis: Erin McDuffie-CIRES/NOAA

Although the carbon mass and OHR metrics provide simple assessments of the relative contribution of different VOCs to photochemical reactivity, they do not incorporate information about radical propagation or photochemical NOx dependence, both of which are important for predicting the efficiency of ozone production. For example, McDuffie *et al.* [2016] used a photochemical box model, constrained to observations, to determine that the average contribution of O&G non-methane VOCs to photochemical ozone production in the DJB was only ~20% (or 3 ppb), despite a 50% contribution of the same VOCs to the OHR and 80% contribution to the ambient observed carbon mass. In conclusion, analysis of carbon mass and VOC OHR can be useful metrics for comparing regions with similar emission sources, but cannot quantify the contribution of those sources to photochemical ozone production.

Finding F5: In one O&G basin, analysis of observations indicates that the ozone production efficiency was 5.3 ± 3.6 ppb ozone formed per ppb NOx oxidized.

Analysis: Erin McDuffie-CIRES/NOAA

The ozone production efficiency (OPE) [i.e. Trainer *et al.*, 1993] is defined as the number of O₃ molecules produced, or number of NOx interconversion cycles completed, by each NOx molecule before it is lost through termination reactions (e.g., formation of nitric acid (HNO₃) or organic nitrates). Observationally, OPE is estimated from the slope of odd oxygen (O_x = NO₂ + O₃) plotted against NOz (NOz = NOy – NOx, where NOy is total oxidized reactive nitrogen). OPE

analyses have been used frequently to characterize urban and rural regions across the U.S. as summarized in Table 1 of *Griffin et al.* [2004]. The principle utility of the OPE metric is that it's an observable quantity that should differentiate between air parcels of different VOC composition and NOx mixing ratios, for example, those influenced by O&G versus urban emissions. When derived from field observations however, the OPE metric provides an upper limit as it is affected by artifacts such as depositional NOy loss [i.e. *Neuman et al.*, 2009; *Trainer et al.*, 1993]

To our knowledge *McDuffie et al.* [2016] are the first to derive an OPE from observations in an O&G basin. They report an average OPE of 5.3 ± 3.6 ppb O₃ produced per ppb NOx [*McDuffie et al.*, 2016] for the most precise subset of their determinations during summer 2014 in the DJB. Based on observed wind-directions at this measurement site and its location relative to nearby O&G wells and Denver, the OPE of air primarily influenced by O&G emissions could not be statistically differentiated from the OPE of more urban-influenced air. This is most likely due to mixing of air influenced by both emission sources prior to reaching the measurement location.

The OPE is beneficial as it can compare the ozone production efficiency of various emission sources. Similar to Colorado, however, many of the Texas monitoring locations may be mixed and the contribution from nearby urban and O&G sources may not be distinguishable. In addition, there are many uncertainties in observationally-derived OPEs that limit their ability to be quantitative.

Finding F6: Photochemical modeling of a 2017 future year seasonal episode showed that projected ozone contributions from O&G emissions to East Texas regulatory ODVs were 5 ppb or less.

Analysis: Sue Kemball-Cook -Ramboll Environ

Ramboll Environ used the CAMx¹⁸ photochemical grid model to assess the contributions of O&G sources and other emissions sources to ozone concentrations throughout East Texas [*Johnson et al.*, 2017]. See Appendix B for an overview of the modeling methods. The modeling used the TCEQ's 2012/2017 seasonal modeling platform¹⁹ and was performed with the CAMx model's Anthropogenic Precursor Culpability Assessment (APCA) source apportionment capability. The APCA tool uses multiple tracer species to track the fate of NOx and VOC emissions and the ozone formation caused by these emissions within a simulation. The ozone reaction tracers allow ozone formation from multiple "source groupings" to be tracked simultaneously. A source grouping can be defined in terms of geographical area and/or emission category. Here, we focus on the contribution of East Texas shale O&G emissions to ODVs in a future year emissions scenario for the year 2017. Figure 4-7 shows the contribution to projected 2017 ODVs from East Texas shale region O&G sources.

¹⁸ Comprehensive Air Quality Model with Extensions; Ramboll Environ, 2016, (www.camx.com).

¹⁹ <https://www.tceq.texas.gov/airquality/airmod/data/tx2012>

The largest total O&G contributions to 2017 ODVs at regulatory monitors occurred at Northeast Texas monitors within or near the Haynesville Shale region (Karnack, 4.9 ppb; Longview, 3.7 ppb) and near San Antonio in the Eagle Ford Shale region (Calaveras Lake, 2.8 ppb).

The total contribution to 2017 ODVs from O&G emissions in the East Texas shale regions exceeded 2 ppb only at monitors in the San Antonio area and in Northeast Texas. At East Texas monitors with 2017 ODVs projected to exceed the National Ambient Air Quality Standard of 70 ppb, the sum of O&G contributions from the three East Texas Shale regions was 2 ppb or less. This suggests that while O&G emissions can contribute to nonattainment of the NAAQS, their role is relatively minor and reductions in O&G emissions are unlikely to produce large declines in ODVs at regulatory monitors in East Texas.

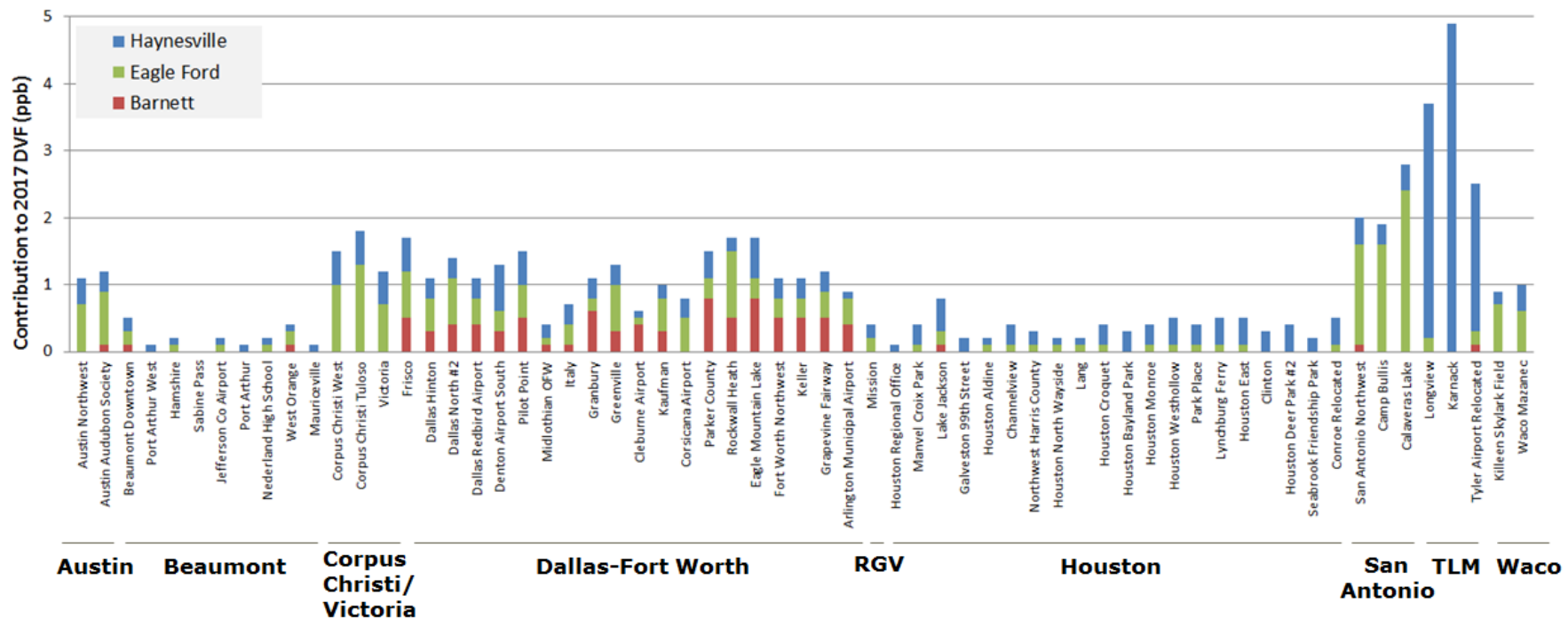


Figure 4-7. Contributions to projected 2017 ODVs at regulatory monitors in East Texas from O&G emissions in the Haynesville, Barnett and Eagle Ford Shales. RGV is the Rio Grande Valley and TLM is the Tyler-Longview-Marshall region of Northeast Texas.

Finding F7: The contribution to ozone at East Texas monitors from O&G NOx emissions is far larger than the contribution from O&G VOC emissions.

Analysis: Sue Kemball-Cook -Ramboll Environ

The CAMx APCA source apportionment tool was used to evaluate the relative magnitude of ozone contributions from O&G NOx and VOC emissions in the 2017 seasonal modeling episode described in Finding F6. The APCA tool estimates the fractions of ozone arriving at a receptor that were formed en-route under VOC- or NOx-limited conditions. This information suggests whether ozone concentrations at the receptor may be more responsive to reductions in VOC or NOx precursor emissions. The relative contributions of O&G NOx and VOC emissions to ozone at all East Texas regulatory monitors were evaluated in the 2017 modeling.

For all East Texas monitors, the ozone contribution from O&G NOx emissions far exceeded that of O&G VOC emissions. The monitor with the largest ozone contribution from O&G VOC was the Calaveras Lake monitor that lies between the Eagle Ford Shale and the San Antonio metropolitan area (Figure 4-8). For this monitor, the NOx emission contribution was far larger than the VOC emission contribution. Also shown in Figure 4-8 are the NOx and VOC emission contributions to ozone at the Karnack monitor, which is located within the Haynesville Shale and had the largest O&G ozone contribution of any monitor in East Texas (Figure 4-7). Results for these two monitors are typical of results at other East Texas regulatory monitors. Controls on O&G NOx emissions are therefore expected to be more effective in reducing the ozone contribution from O&G sources than will controls on O&G VOC sources.

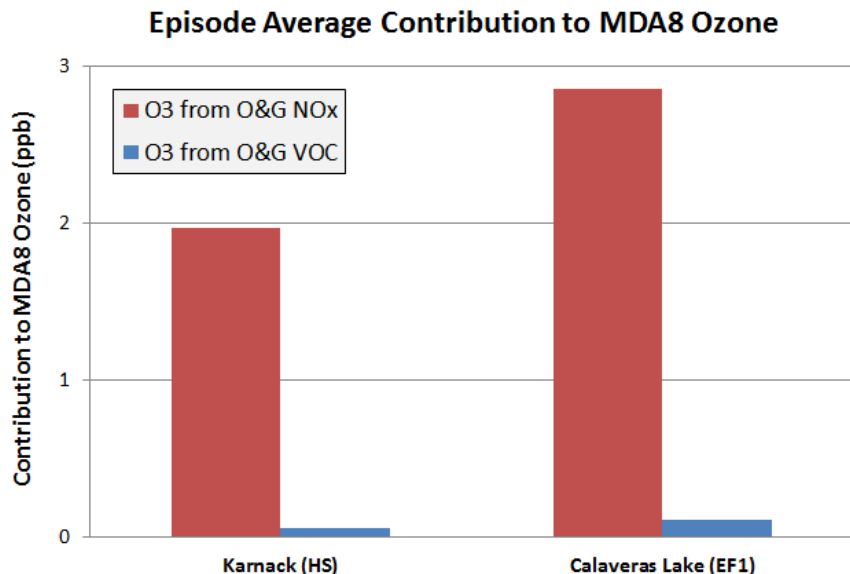


Figure 4-8. May 1 – September 30 episode average contributions to daily maximum 8-hour average ozone from O&G NOx and VOC emissions at the Karnack and Calaveras Lake monitors

This finding is consistent with the regional modeling study of *Pacsi et al.* [2015], who determined that changes in ozone in the Eagle Ford region due to changes in O&G emissions were driven by NOx emissions rather than VOC emissions. *Pacsi et al.* [2015] attributed this to the relatively low reactivity of the O&G VOC emissions in comparison to the highly reactive biogenic emissions present in the region.

McDuffie et al. [2016] used a box model, constrained to observations, to investigate the sensitivity of ozone in the DJB to changes in NOx and VOC mixing ratios. They found that average, locally produced ozone was more sensitive to reductions in O&G-associated VOC emissions than to O&G-associated NOx emissions, which were estimated based on the 2011-National Emissions Inventory. Relative to Texas, the greater importance of O&G VOC emissions in the DJB reflects the stronger influence of highly reactive biogenic emissions in Texas (discussed in Finding F3). With a less reactive mix of VOCs in the DJB, O&G VOC emissions assume a greater importance in ozone formation.

4.1.4 Summary and Recommendations for Further Analysis

Finding F1 discusses an analysis of the correlation between observed ambient ozone concentrations and the history of O&G production activity in four O&G basins. That relatively simple analysis could discern no impact of O&G activity on the observed ozone concentrations. The smallest discernable impact is < 5 ppb, but could not be more quantitatively defined; it should be possible to develop a more sophisticated multivariate analysis that would provide a more rigorous limit for the smallest discernable impact.

Comparisons of bottom-up and top-down NOx emission inventories in O&G regions indicate that bottom-up inventories overestimate NOx emissions ([*Ahmadov et al.*, 2015]; Finding A5) and that these overestimates may introduce bias into estimates of ozone impacts from O&G development (Finding E2). Because the analysis presented here is based on bottom-up emission inventories and ozone formation is NOx-limited in the CAMx Photochemical Model (Finding F7), the ODV impacts shown here may overestimate the actual ODV impacts. Future work aimed at refining the estimates of NOx emissions in O&G inventories may reduce these uncertainties.

4.1.5 References

- Ahmadi, M., and K. John (2015), Statistical evaluation of the impact of shale gas activities on ozone pollution in North Texas, *Science of The Total Environment*, 536, 457-467.
- Ahmadov, R., et al. (2015), Understanding high wintertime ozone pollution events in an oil- and natural gas-producing region of the western US, *Atmos. Chem. Phys.*, 15(1), 411–429, doi:10.5194/acp-15-411-2015.
- Atkinson, R. (2000), Atmospheric chemistry of VOCs and NOx, *Atmos. Environ.*, 34(12–14), 2063-2101, doi:[http://dx.doi.org/10.1016/S1352-2310\(99\)00460-4](http://dx.doi.org/10.1016/S1352-2310(99)00460-4).
- Baker, A. K., A. J. Beyersdorf, L. A. Doezena, A. Katzenstein, S. Meinardi, I. Simpson, D. R. Blake, and F. S. Rowland (2008), Measurements of nonmethanehydrocarbons in 28 United States cities, *Atmos. Environ.*, 42, 170–182, doi:10.1016/j.atmosenv.2007.09.007.

- Colorado Oil and Gas Conservation Commision (COGCC) (2016), County level production available in the "DataBase" section. [Available at <http://cogcc.state.co.us/>].
- Evans, J.M., and D. Helmig (2017), Investigation of the influence of transport from oil and natural gas regions on elevated ozone levels in the northern Colorado front range. *Journal of the Air & Waste Management Association*, 67, 196-211.
- Gilman, J. B., et al. (2009), Measurements of volatile organic compounds during the 2006 TexAQS/GoMACCS campaign: Industrial influences, regional characteristics, and diurnal dependencies of the OH reactivity, *J. Geophys. Res.*, 114, D00F06, doi:10.1029/2008JD011525.
- Gilman, J. B., B. M. Lerner, W. C. Kuster, and J. A. de Gouw (2013), Source signature of volatile organic compounds from oil and natural gas operations in northeastern Colorado, *Environmental science & technology*, 47(3), 1297-1305, doi:10.1021/es304119a.
- Griffin, R. J., C. A. Johnson, R. W. Talbot, H. Mao, R. S. Russo, Y. Zhou, and B. C. Sive (2004), Quantification of ozone formation metrics at Thompson Farm during the New England Air Quality Study (NEAQS) 2002, *Journal of Geophysical Research: Atmospheres*, 109(D24), D24302, doi:10.1029/2004JD005344.
- Johnson, J., Z. Liu, A. Wentland, S. Kemball-Cook and G. Yarwood (2017). Photochemical modeling of 2012 and 2017 for the Heart of Texas Council of Governments. Report in preparation.
- Kemball-Cook, S., A. Bar-Ilan, J. Grant, L. Parker, J. Jung, W. Santamaria, J. Mathews, and G. Yarwood (2010), Ozone Impacts of Natural Gas Development in the Haynesville Shale, *Environmental science & technology*, 44(24), 9357-9363, doi:10.1021/es1021137.
- McDuffie, E. E., et al. (2016), Influence of oil and gas emissions on summertime ozone in the Colorado Northern Front Range, *Journal of Geophysical Research: Atmospheres*, 121(14), 8712-8729, doi:10.1002/2016jd025265.
- Norris, G., Vedantham, R., Wade, K., Brown, S., Prouty, J., Foley, C. (2008), EPA Positive Matrix Factorization (PMF) 3.0 Fundamentals & User Guide. US Environmental Protection Agency, Office of Research and Development, Washington, DC.
- Neuman, J. A., et al. (2009), Relationship between photochemical ozone production and NO_x oxidation in Houston, Texas, *Journal of Geophysical Research: Atmospheres*, 114(D7), D00F08, doi:10.1029/2008JD011688.
- Pacsi, A. P., N. S. Alhajeri, D. Zavala-Araiza, M. D. Webster, and D. T. Allen (2013), Regional Air Quality Impacts of Increased Natural Gas Production and Use in Texas, *Environmental science & technology*, 47(7), 3521-3527, doi:10.1021/es3044714.
- Pacsi, A. P., Y. Kimura, G. McGaughey, E. C. McDonald-Buller, and D. T. Allen (2015), Regional Ozone Impacts of Increased Natural Gas Use in the Texas Power Sector and Development in the Eagle Ford Shale, *Environmental science & technology*, 49(6), 3966-3973, doi:10.1021/es5055012.

- Roohani, Y.H., Roy, A.A., Heo, J., Robinson, A.L., Adams, P.J. (2017), Impact of natural gas development in the Marcellus and Utica shales on regional ozone and fine particulate matter levels, *Atmospheric Environment*, 155, 11-20.
- Rutter, A. P., R. J. Griffin, B. K. Cevik, K. M. Shakya, L. Gong, S. Kim, J. H. Flynn, and B. L. Lefer (2015), Sources of air pollution in a region of oil and gas exploration downwind of a large city, *Atmospheric Environment*, 120, 89-99, doi:<http://dx.doi.org/10.1016/j.atmosenv.2015.08.073>.
- Schade, G. W., and G. Roest (2016), Analysis of non-methane hydrocarbon data from a monitoring station affected by oil and gas development in the Eagle Ford shale, Texas, *Elem. Sci. Anth.*, 4, 000,096, doi:10.12952/journal.elementa.000096.
- Sullivan D. (2014), Eagle Ford shale mobile monitoring study. University of Texas at Austin: 66. GAD Number 582-13-30089-FY14-01.
https://www.tceq.texas.gov//assets/public/implementation/air/am/contracts/reports/oth/5821330089FY1401-20140801-uta-Eagle_Ford_Shale_Mobile_Monitoring.pdf.
- Swarthout, R. F., R. S. Russo, Y. Zhou, B. M. Miller, B. Mitchell, E. Horsman, E. Lipsky, D. C. McCabe, E. Baum, and B. C. Sive (2015), Impact of Marcellus Shale Natural Gas Development in Southwest Pennsylvania on Volatile Organic Compound Emissions and Regional Air Quality, *Environmental science & technology*, 49(5), 3175-3184, doi:10.1021/es504315f.
- Toth, J. J., and R. H. Johnson (1985), Summer Surface Flow Characteristics over Northeast Colorado, *Monthly Weather Review*, 113(9), 1458-1469, doi:10.1175/1520-0493(1985)113<1458:SSFCON>2.0.CO;2.
- Trainer, M., et al. (1993), Correlation of ozone with NO_y in photochemically aged air, *Journal of Geophysical Research*, 98(D2), 2917, doi:10.1029/92jd01910.
- U.S. Census Bureau Population Change for Metropolitan and Micropolitan Statistical Areas in the United States and Puerto Rico : 2000 to 2010 [Available at: <https://www.census.gov/population/www/cen2010/cph-t/CPH-T-5.pdf>].

4.2 Response to Question G

Are there significant differences in O₃ and PM formation mechanisms between the major oil and natural gas basins in Texas?

4.2.1 Working Group

David Parrish - David.D.Parrish, LLC

Ravan Ahmadov - NOAA/ESRL/GSD

Jeffrey Collett - Colorado State University

Stuart McKeen - NOAA/ESRL/CSD

4.2.2 Background

The Background material in the Responses to Questions F, H and J discuss aspects of ozone formation throughout the State, and the Response to Question H, I, J and K discuss various aspects of PM formation, including the interactions of anthropogenic and biogenic emissions in PM formation. In this response, we give an overview of modeling of secondary organic aerosol from O&G emissions (Finding G1) and an overview of ambient PM_{2.5} concentrations (Findings G2 and G3).

4.2.3 Findings

Finding G1: Modeling utilizing current VOC emission inventories simulates very small summertime secondary organic aerosol (SOA) concentrations from the oil/gas sector. These simulations may underestimate SOA formation by a factor of ~4 due to emission uncertainties, but even so the simulated O&G SOA contributions would be small.

Analysis: Ravan Ahmadov, Stu McKeen-NOAA

The WRF-Chem model with the EPA NEI-2011 inventory was utilized to simulate surface organic aerosol concentrations over the U.S. in two calculations: one with and one without the O&G emissions throughout the U.S. Figure 4-9 shows the difference in the resulting afternoon PM_{2.5} concentrations in Texas and other southern and eastern states. The maximum difference ($\leq 0.8 \mu\text{g m}^{-3}$) is seen over the Haynesville O&G basin, with the highest concentrations over Louisiana. These simulated enhancements, which are predominately SOA, must be considered lower limits because 1) there are indications that the NEI-2011 underestimated emissions of aromatic VOCs (see Finding E1) and 2) the inventory does not include IVOC emissions, which can enhance SOA formation (see Finding E2). If the inventory were adjusted to account for these issues, the SOA enhancements could be a factor of ~4 larger.

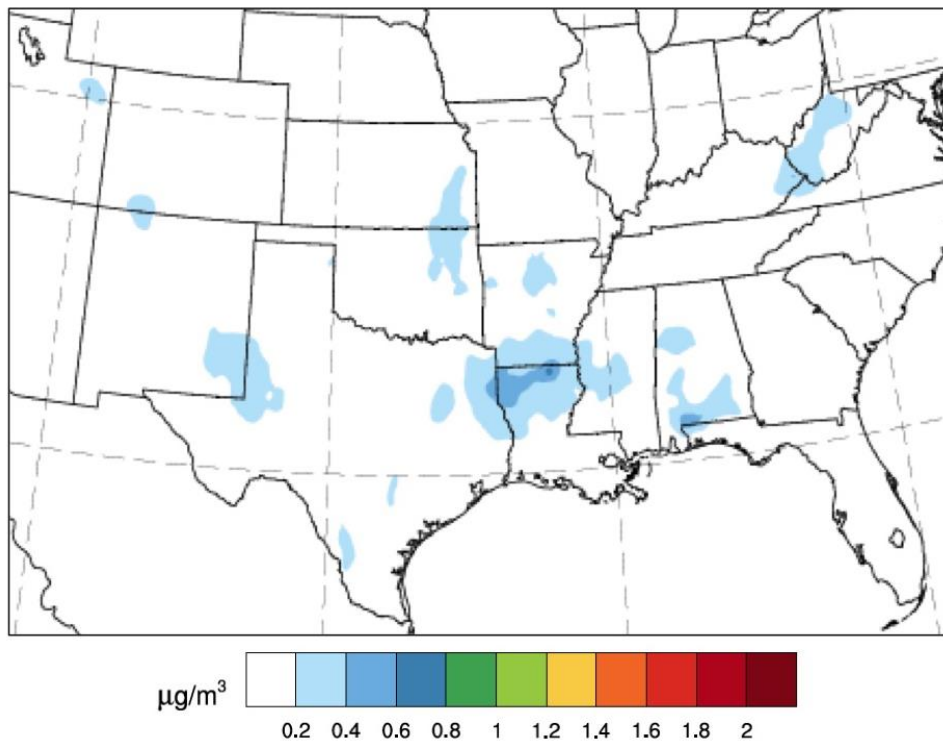


Figure 4-9. PM_{2.5} formed from O&G emissions. Results are for 3 pm EDT averaged over June 2013.

Finding G2: In the Bakken O&G production region in North Dakota, that development has not discernably increased seasonal mean concentrations of any PM constituent.

Analysis: Dan Murphy-NOAA

Based upon data from the Interagency Monitoring of Protected Visual Environments (IMPROVE) program, *Hand et al. [2012]* identified increasing trends in wintertime particulate sulfate and nitrate ion concentrations in the Great Plains of the United States over the 2000 to 2010 period; they suggested that O&G development was a possible cause. Figure 4-10 presents a more detailed examination of possible influences of O&G development on PM_{2.5} component concentrations measured at the two IMPROVE sites located within the Bakken O&G production region in North Dakota. This region has experienced very rapid development of O&G activities during the 2000 to 2014 period covered by the IMPROVE data. Figure 4-10 shows time series of three-month mean PM concentrations. Comparison of the concentrations before 2008, when oil production began its rapid increase, with more recent data shows no discernible differences. Further, there is no statistically significant trend of total PM or any PM component in any season.

Three additional points should be noted. First, *Prenni et al. [2016]* identified some significant changes in NO₂ and light absorbing carbon (LAC also called black carbon) concentrations, and *Evanoski-Cole et al. [2017]* discuss impacts from O&G development on regional, wintertime fine

particle concentrations dominated by inorganic species. Evidently the influence of these phenomena is not large enough to discernably raise the overall 3-month average PM_{2.5} concentrations in any season. Second, other anthropogenic emissions of NOx to the Bakken region (e.g., the mobile fleet and electrical generation plants) have been decreasing over this time period, so any PM enhancement from O&G sources may be obscured by decreased enhancement from other sources. While PM nitrate concentrations have decreased across most of the U.S. from 2000–2015, changes in the Bakken region are generally flat. Finally, the seasonal average PM_{2.5} concentrations in this region are all much lower than the NAAQS for annual average concentrations (12 µg m⁻³). Evidently, relative to the annual average NAAQS, O&G development has not significantly increased the ambient PM_{2.5} concentrations in the Bakken region.

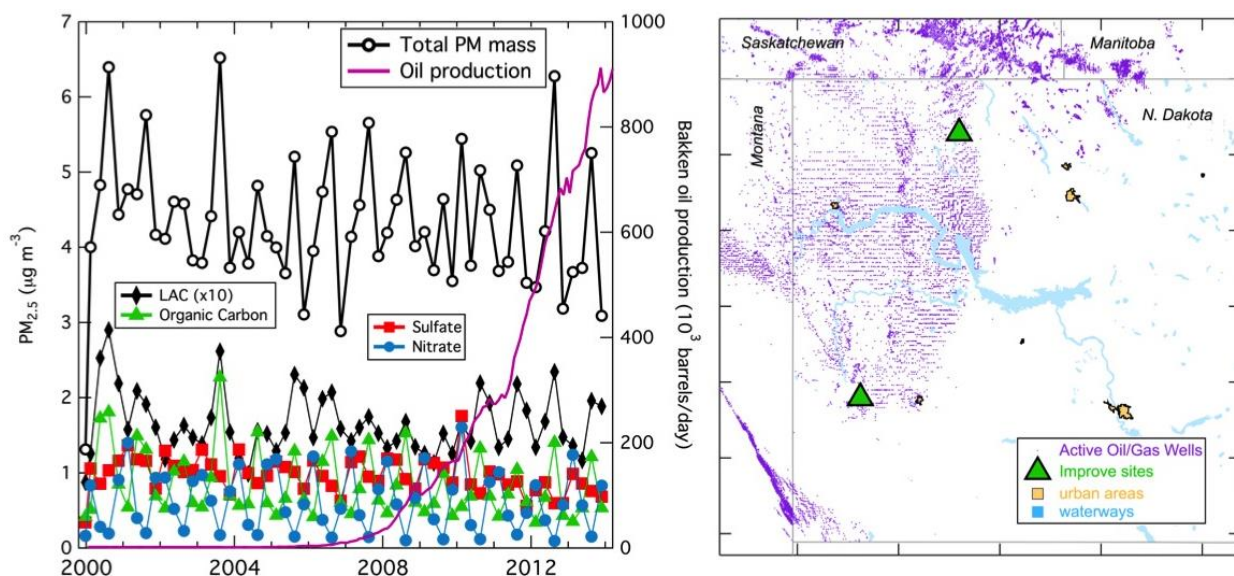


Figure 4-10. Comparison (left) of time series of PM concentrations to oil production in the Bakken O&G region in North Dakota, and map (right) of the region showing the location of oil/gas wells and urban areas in North Dakota. The PM data are three-month means (JFM, AMJ, JAS, and OND) of speciated and total PM concentrations measured at the two North Dakota IMPROVE sites, whose locations are given by the green triangles on the map.

Finding G3: In Texas PM_{2.5} concentrations in urban areas and O&G basins are of similar magnitude and show similar decadal declines; there is no discernible indication that the O&G activities have affected total PM_{2.5} concentrations.

Analysis: David Parrish-David. D. Parrish, LLC

PM_{2.5} concentration measurements have been made over the past 17 years (Figure 4-11) at urban and rural sites throughout Texas. These sites have varying proximity to O&G activity, with one located within the Haynesville O&G Basin (the Karnack site, whose results are

highlighted in the figure). The observed concentrations are similar at all sites, both in magnitude and in long-term changes. The long-term changes in drilling and gas production in the Haynesville O&G basin (both plotted in Figure 4-11) have not been accompanied by any discernable correlated change in the PM_{2.5} concentrations at the Karnack site, relative to the other urban and rural sites. Assigning confidence limits to the maximum possible PM_{2.5} enhancement from O&G activities is difficult, but it is expected that a systematic increase of 3 $\mu\text{g m}^{-3}$ in the annual average PM_{2.5} concentration at the Karnack site should be evident.

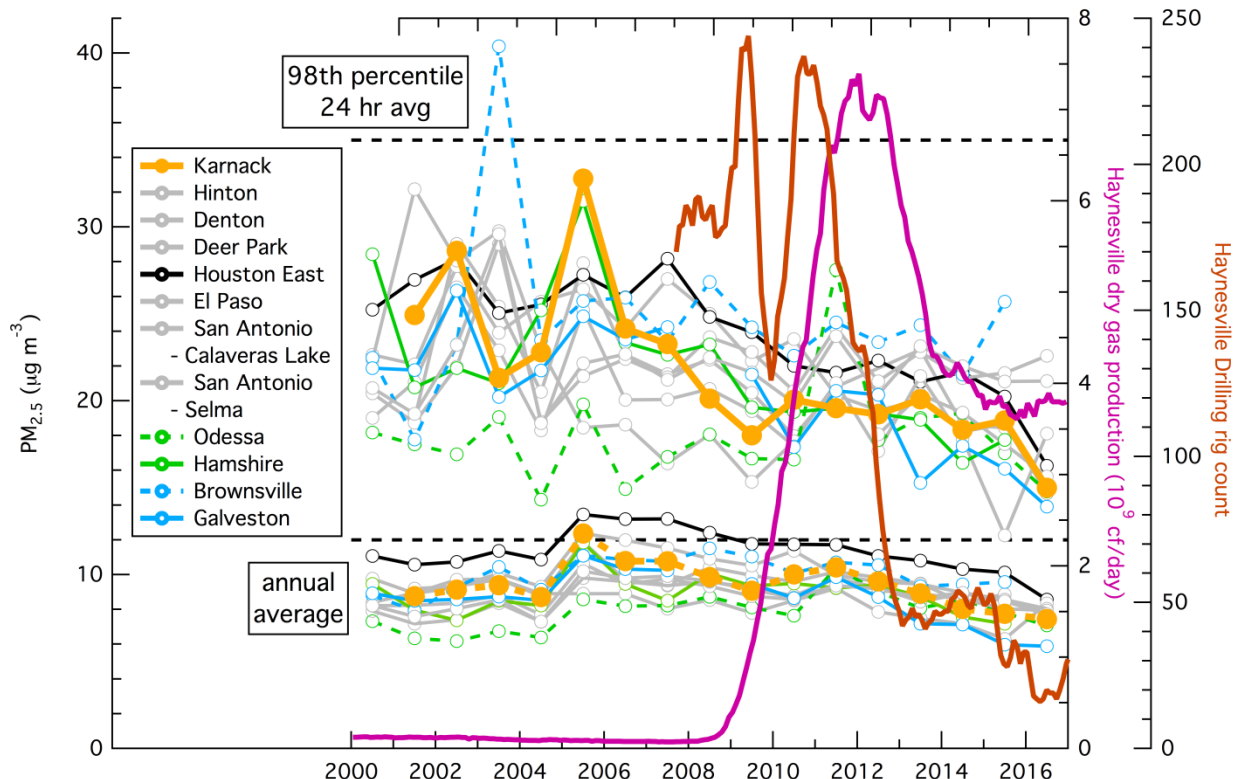


Figure 4-11. PM_{2.5} concentrations measured at twelve stations across Texas. Both the annual averages (lower curves) and the 98th percentiles of the 24-hr averages (upper curves) are plotted. Gray and black lines indicate the more urban areas: Houston (Houston East and Deer Park), Dallas (Hinton and Denton), San Antonio and El Paso. Green and blue lines indicate more rural and near-coastal sites, respectively. The site within the Haynesville O&G Basin (Karnack) is emphasized with heavier gold lines and points. Generally the highest concentrations are observed at the Houston East site (black lines). Two measures of O&G activity in the Haynesville O&G Basin are included for comparison.

4.2.4 Summary and Recommendations for Further Analysis

Modeling and observational analysis agree that O&G emissions are responsible for only very small PM_{2.5} enhancements in Texas O&G gas basins, at least in spring and summer. Modeling that incorporates our current understanding of PM formation mechanisms finds only very small PM_{2.5} enhancements from O&G emissions (Finding G1). Findings G2 and G3 examine long-term

measurements of PM_{2.5} in North Dakota and Texas as well as PM_{2.5} speciation in North Dakota to evaluate the impact that increasing O&G emissions have had on various metrics of ambient PM_{2.5} concentrations. No discernible impact could be found in any of the analyses. More sophisticated analyses of these measurement records that consider in detail different metrics of ambient PM concentrations, as well as possible confounding factors such as the impacts of long-term changes in other emission sources, could reveal more detailed information regarding O&G impacts on ambient PM_{2.5} concentrations. Although not discussed explicitly in the Responses to any of the Science Questions, all investigations of ozone formation from O&G emissions suggest that traditional photochemical mechanisms involving NOx and VOC precursors are adequate to account for the observed ozone enhancements.

4.2.5 References

- Evanoski-Cole, A.R., Gebhart, K.A., Sive, B.C., Zhou, Y., Capps, S.L., Day, D.E., Prenni, A.J., Schurman, M.I., Sullivan, A.P., Li, Y., Hand, J.L., Schichtel, B.A., and Collett, Jr., J.L. (2017) Composition and sources of winter haze in the Bakken oil and gas extraction region. *Atmos. Environ.* 156, 77-87, doi:10.1016/j.atmosenv.2017.02.019.
- Hand, J.L., K.A. Gebhart, B.A. Schichtel, and W.C. Malm, (2012), Increasing trends in wintertime particulate sulfate and nitrate ion concentrations in the Great Plains of the United States (2000–2010), *Atmos. Environ.*, 55, 107–110, doi:10.1016/j.atmosenv.2012.03.050.
- Prenni, A.J., et al. (2016), Oil and gas impacts on air quality in federal lands in the Bakken region: an overview of the Bakken Air Quality Study and first results, *Atmos. Chem. Phys.*, 16, 1401-1416, doi:10.5194/acp-16-1401-2016.

4.3 Response to Question H

Are there important interactions between emissions from oil and natural gas development and emissions from other sources such as urban, point source and biogenic, including crops and animal husbandry?

4.3.1 Working Group

Sue Kemball-Cook - Ramboll Environ

Jeffrey Collett - Colorado State University

Scott Eilerman - NOAA/ESRL/CSD

Erin McDuffie - NOAA/ESRL/CSD

Andy Neuman - NOAA/ESRL/CSD

Chelsea Thompson - NOAA/ESRL/CSD

4.3.2 Background

New or expanded O&G operations bring the associated emissions into environments with preexisting, natural and anthropogenic sources of ozone and PM precursors. An important issue is the degree to which VOC and NOx emitted from O&G activity will combine and react with other local emission sources. In Texas, ozone formation due to O&G production activities is strongly influenced by NOx emissions from O&G sources reacting with natural sources of VOCs [Pacsi *et al.*, 2015; Rutter *et al.*, 2015]. These natural VOC sources vary widely over the diverse ecosystems of Texas. Therefore, within Texas, there are different levels of concern about emissions from O&G operations. Here we discuss three specific examples of the interaction of O&G emissions with biogenic and other anthropogenic emissions. Findings H1 and H2 address ammonium nitrate (NH_4NO_3) particle formation that can occur when nitric acid (HNO_3) formed from O&G NOx emissions reacts with ammonia (NH_3) from biogenic sources (primarily agriculture and animal husbandry). Finding H3 investigates one example of the interaction of O&G emissions with urban emissions: the urban emissions from Laredo TX transported over the Eagle Ford Basin.

During two field campaigns (SENEX in 2013 and SONGNEX in 2015) the NOAA WP-3D aircraft conducted multiple flights over Texas O&G basins. Flights typically flew upwind, over, and downwind of these basins, and included two flights over the Permian, two over the Eagle Ford, one over the Haynesville, and one flight over both the Barnett Shale and Haynesville Basins. The aircraft was outfitted with a full suite of instrumentation for measurement of a wide range of emitted species and their photochemical products and intermediates. This data set provides a resource for observationally based analysis and for comparison with photochemical grid modeling. Analysis of these data is still in its early stages, with few publications of final results. The three examples presented here serve to provide an indication of analyses that can be conducted with these data.

4.3.3 Findings

Finding H1: The impact of NOx emissions from O&G development on fine particle and haze formation can depend strongly on concentrations of other species, including sulfate and ammonia, as well as the relative importance of different pathways for NOy formation.

Analysis: Jeffery Collette—Colorado State University

Reaction between gaseous HNO_3 and gaseous NH_3 can lead to formation of semivolatile NH_4NO_3 particles. The position of the equilibrium between the precursor gases and the particulate product depends strongly on environmental conditions. Several factors are key to determining the ultimate impact of the formation of fine particle NH_4NO_3 . Particle formation is favored when temperatures are low and humidities are high. Other important factors include the rate and yield of NOx conversion to HNO_3 , which depends on oxidant availability as well as the VOC/NOx ratio, and the availability of ambient NH_3 . Agriculture, including use of nitrogen-based fertilizers and animal feeding operations, is believed to dominate U.S. ammonia emissions. A tendency for co-location of O&G production with agricultural production in some regions may favor interactions of these emissions to yield NH_4NO_3 particles. The Response to Question K of this report discusses these issues in more detail.

Studies of O&G impacts on fine particle formation in the Jonah-Pinedale region of western Wyoming [Li *et al.*, 2014] and in the Bakken O&G basin of North Dakota [Evanoski-Cole *et al.*, 2017] reveal that the availability of ambient NH_3 is critical to controlling the amount of NH_4NO_3 formed, especially during the heart of winter. In the Li *et al.* [2014] study in Wyoming, wintertime formation of NH_4NO_3 consumed essentially all of the available gas phase NH_3 , limiting the ultimate amount of haze formation. The situation is a bit more complex in the Bakken [Evanoski-Cole *et al.*, 2017], where both NH_3 and HNO_3 exert some control on NH_4NO_3 formation, with NH_3 availability the more limiting factor during the coldest period of the winter.

Prior studies of the chemistry of the ammonia-nitrate-sulfate system in rural Texas (e.g., the Big Bend Regional Aerosol and Visibility Observational (BRAVO) Study in Big Bend National Park [Lee *et al.*, 2004]) found the aerosol to usually be acidic, but this study did not look at wintertime conditions when ammonium nitrate formation is more likely to be important and sulfate may be less abundant. Sulfate concentrations have also decreased significantly since 2000 across Texas [Hand *et al.*, 2012], presumably leaving relatively larger amounts of ammonia to participate in NH_4NO_3 formation. Of course NH_3 concentrations in Texas are expected to be highly variable across the state. With U.S. NH_3 emissions tied primarily to agricultural activity, including animal feeding operations, regions of the state with greater agricultural and animal husbandry activity are likely to have more NH_3 available to react with HNO_3 produced from atmospheric oxidation of O&G (and other) NO_x emissions to form NH_4NO_3 particles. The AMon network, for example, finds gas phase NH_3 concentrations in the Texas panhandle that commonly exceed 4 $\mu\text{g m}^{-3}$ [<http://nadp.sws.uiuc.edu/AMoN/AMoNFactSheet.pdf>], substantially higher than measured in the BRAVO campaign in Big Bend National Park.

Even in the absence of NH₃, however, HNO₃ can enter the particle phase through reactions with soil dust or sea salt particles. The resulting coarse nitrate is supermicron but a significant portion does fall within the PM_{2.5} mode. *Lee et al.* [2004] observed the formation of significant sodium and calcium nitrate between 1 and 2.5 µm during the Big Bend National Park BRAVO campaign.

Finding H2: Ammonium nitrate formation potential can be evaluated from aircraft measurements of NH₃ and HNO₃; based on springtime data, this potential is small over four Texas O&G basins. However, at altitude or during colder times of year the NH₃ and HNO₃ product may exceed that required for NH₄NO₃ formation.

Analysis: Scott Eilerman and Andy Newman-NOAA

To assess the potential for NH₄NO₃ formation over Texas O&G basins relative to other regions in the U.S., Figure 4-12 examines concentrations of NH₃ and HNO₃ from several NOAA aircraft field campaigns in the last 15 years (SONGNEX 2015, SENEX 2013, CalNex 2010, TexAQS 2006, and NEAQS-ITCT²⁰ 2004).

Ammonia concentrations are greatest in regions with large livestock concentrations (California and northeastern Colorado) while HNO₃ concentrations are highest downwind of urban centers (including Houston). Note that moderately high NH₃ concentrations (10-20 ppbv) were observed over the Bakken O&G basin on one flight when the winds were from the southeast; those winds carried the emissions plume from the Great Plains Synfuels Plant in Beulah, ND, which is the largest point source of NH₃ in the EPA's 2011 National Emissions Inventory. On a second flight over the same region, the winds were from the northwest, and NH₃ concentrations were much lower (0-5 ppbv).

The potential for NH₄NO₃ formation is proportional to the concentration product of NH₃ and HNO₃, and also depends on ambient temperature and relative humidity. At 20 °C ambient temperature, the dissociation constant for solid NH₄NO₃ formation is approximately 10 ppb² (e.g., see Nowak *et al.*, 2012). Below this concentration product, NH₄NO₃ formation is not favored. To illustrate the potential formation regardless of ambient conditions, the concentration product is included in Figure 4-12 and Figure 4-13. Based on these springtime measurements over Texas O&G basins, the NH₃ and HNO₃ mixing ratios were generally insufficient to promote NH₄NO₃ formation. No large NH₃ sources were measured over Texas O&G basins, where NH₃ mixing ratios averaged 2.2 ± 1.3 ppb over the Permian basin, 3.5 ± 1.0 ppb over the Eagle Ford, 1.7 ± 1.1 ppb over the Barnett, and 1.2 ± 1.7 ppb over the Haynesville. Similarly, HNO₃ levels over the O&G regions were small compared to urban regions, averaging 0.74 ± 0.42 ppb over Permian, 0.64 ± 0.42 ppb over Eagle Ford, 1.10 ± 0.69 ppb over Barnett, and 0.59 ± 0.42 ppb over Haynesville. Compared to other O&G basins, the potential for NH₄NO₃ formation over Texas is less than basins that also contain extensive agricultural activity (e.g. the Denver-Julesburg basin).

²⁰ New England Air Quality Study - Intercontinental Transport and Chemical Transformation

Despite these conclusions based on springtime measurements, at altitude or during colder times of year the NH_3 and HNO_3 concentration product may exceed that required for NH_4NO_3 formation because the dissociation constant for NH_4NO_3 is a strong function of temperature. It is approximately 10 ppb² at 20 °C but drops to ~0.03 ppb² at 0 °C. Figure 4-14 shows results from a Wyoming O&G field for all seasons of the year. The NH_3 and HNO_3 concentration product decreased in winter, but the dissociation constant decreased even more, so that NH_4NO_3 formation was favored to occur in that season. A full understanding of NH_4NO_3 formation in Texas would require characterization of the seasonal and spatial distribution of NH_3 concentrations, which are expected to be generally smaller in winter; the Response to Question K has further discussion of these issues.

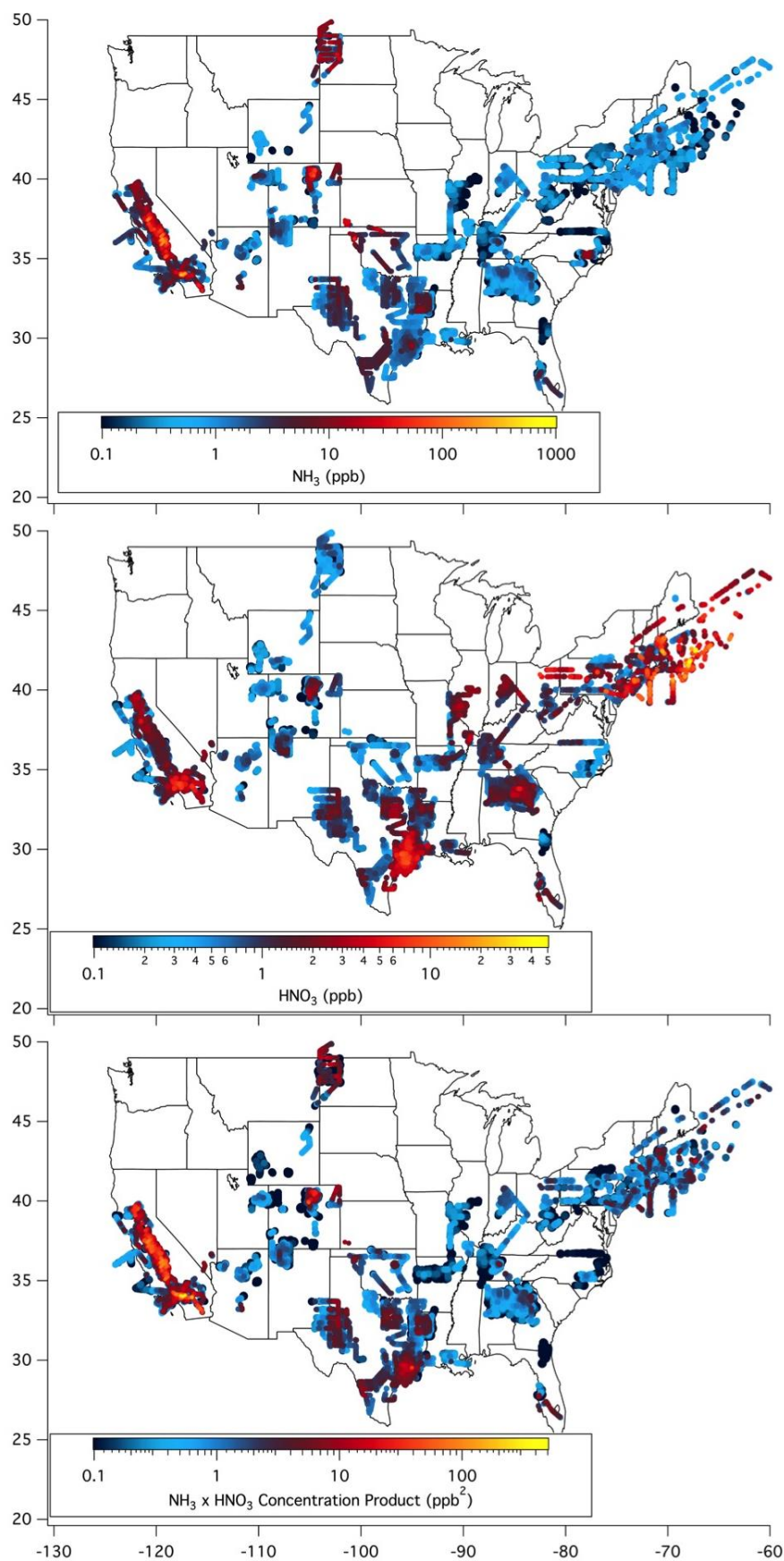


Figure 4-12. Flight tracks of NOAA P-3 aircraft during five field campaigns. 1-minute averages are shown for flight segments during daytime (5 AM-10 PM CDT) and altitudes within the boundary layer (maximum 1500 m above ground level). These flight segments are color coded according to NH_3 (top), HNO_3 (middle), and the product of these two concentrations (bottom). The data are sorted such that higher values are plotted on top of smaller values, so maximum observed values are highlighted and many of the smaller concentrations are hidden.

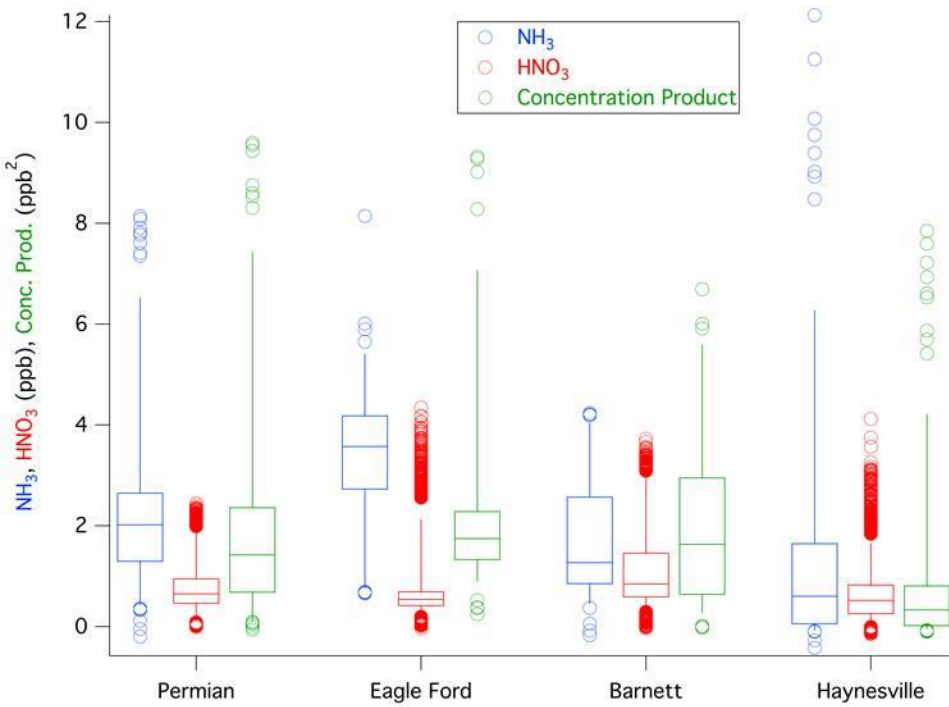


Figure 4-13. Distributions of NH_3 , HNO_3 , and the product of these two concentrations for the measurements over four O&G basins in Texas. The boxes indicate the 25th and 75th percentiles along with the medians. The whiskers and circles encompass the 2nd to 98th and the 1st to 99th percentiles, respectively.

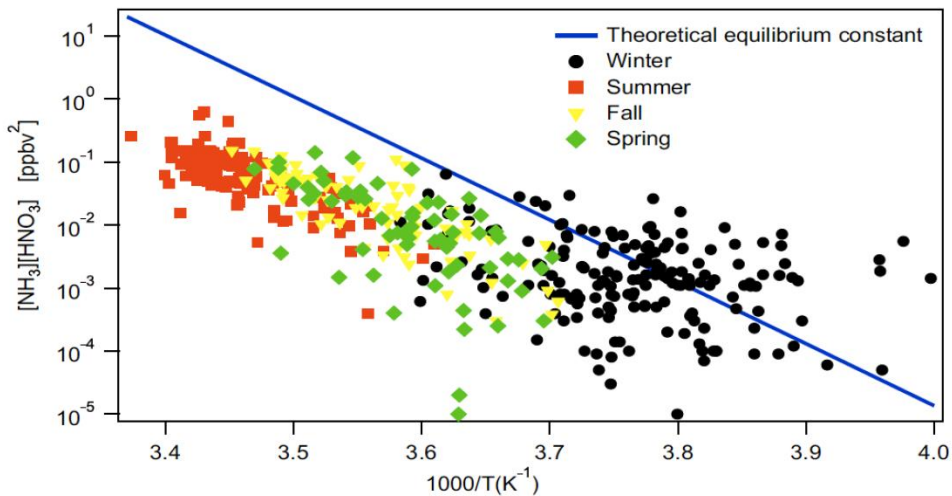


Figure 4-14. Comparison of the measured NH_3 and HNO_3 concentration product with the theoretical dissociation constant for NH_4NO_3 as a function of temperature across the different seasons. Data are from Boulder, Wyoming, a rural region of active gas production. [Figure from Li *et al.*, 2014.]

Finding H3: An April 2015 flight over the Eagle Ford Basin reveals the largest concentrations of ozone observed over the basin were in an urban plume transported through the area of O&G emissions.

Analysis: Chelsea Thompson-NOAA

Figure 4-15 shows the ambient ozone concentrations measured in the boundary layer over the Eagle Ford O&G basin on 7 April 2015. The highest concentrations were observed in a plume transported downwind from Laredo. The upwind ozone concentrations entering the city were 39 ppb, and measured ozone reached a maximum concentration of 54 ppb approximately 160 km downwind. Smaller ozone enhancements (≤ 6 ppb) were observed over the O&G basin not impacted by the Laredo plume. These results suggest an interaction of the urban emissions with the O&G emissions that enhanced ozone formation within the urban plume, but we have no means to quantify the degree to which ozone production in the Laredo plume was enhanced by comingling with O&G emissions. This April flight was conducted during a period of low urban photochemical ozone production due to the early spring season and the steady south-southeast flow; the maximum MDA8 ozone reported at any monitor in the area shown in Figure 4-15 was 42 ppb at Camp Bullis, located downwind of San Antonio on this day. These results provide an example of ozone formation occurring in an urban plume transported over an O&G region, but the influence of the O&G emissions on this formation has not yet been determined. A full understanding of the ozone production in this environment requires detailed modeling of this episode.

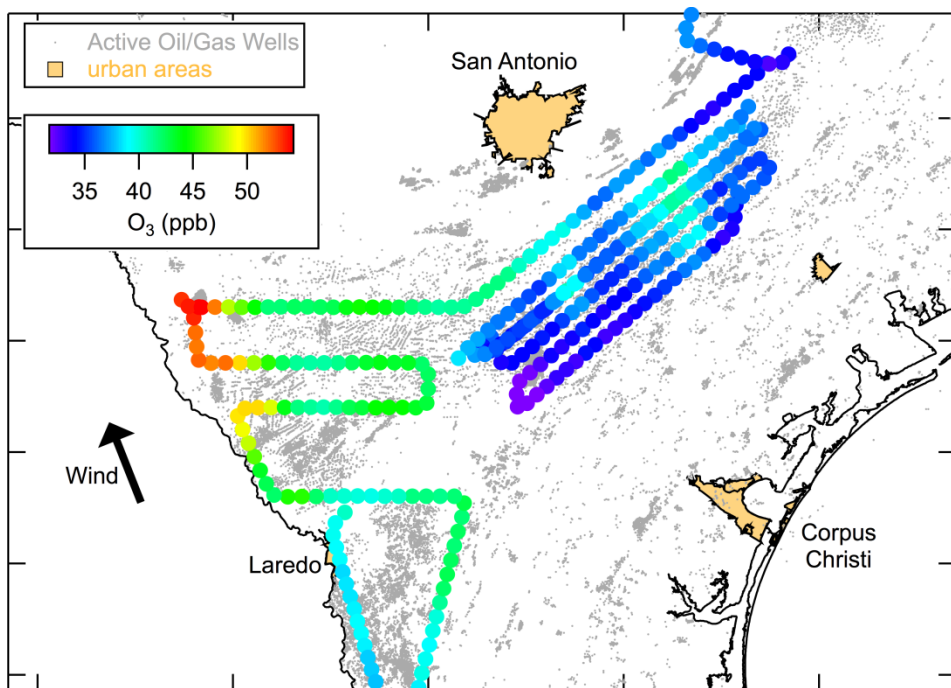


Figure 4-15. Flight track of NOAA P-3 aircraft during over the Eagle Ford O&G basin on 7 April 2015. Symbols are 1-min averages color-coded according to measured ozone

concentrations. The data shown are limited to the measurements within the boundary layer (altitude \leq 1 km AGL). The arrow indicates the approximate south-southeast wind direction.

Finding H4: Overall, daytime NO_x and NO_y mixing ratios in Texas O&G basins are moderate (NO_x generally $<$ 1 ppb), but meteorological conditions and non-O&G sources can lead to higher concentrations.

Analysis: Chelsea Thompson-NOAA

Aircraft-based observations of NO_x and NO_y from O&G basins in the western U.S. made during the 2015 NOAA SONGNEX campaign (Figure 4-16) reveal that basin-wide mixing ratios of these compounds are generally moderate relative to urban areas, and that some of the Texas O&G basins experience relatively lower NO_x and NO_y mixing ratios than comparable basins in other states. Of the basins sampled, those in close proximity to urban centers (e.g., the Denver-Julesburg near Denver and the Barnett near Dallas-Fort Worth) and those containing large power plants (e.g., San Juan and Uintah) experience greater mean NO_x values, and greater variability in NO_x due to the presence of these large localized sources.

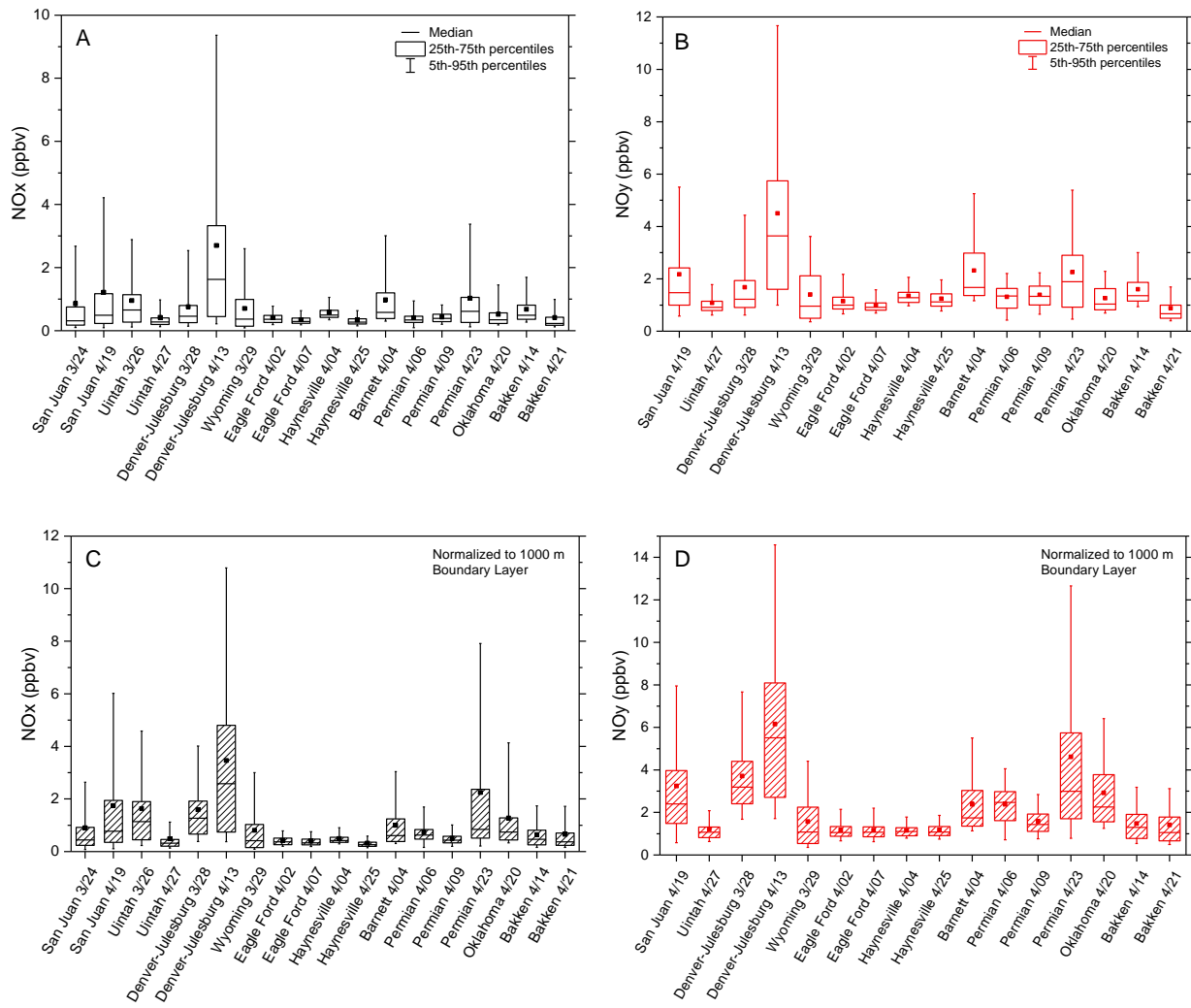


Figure 4-16. Observations of NOx and NOy mixing ratios in several western U.S. O&G basins measured from the NOAA WP-3D aircraft during the 2015 SONGNEX campaign. Dots denote mean concentrations. The box and whisker symbols indicate median, 25th-75th percentile ranges, and 5th-95th percentile ranges. In panels C and D, the observed mixing ratios are normalized to a 1000 m boundary layer to improve comparability between basins.

Observed mixing ratios of NOx and NOy are a function of both emissions and meteorology. A shallow boundary layer and stagnant conditions can lead to greatly enhanced mixing ratios even if emissions are low. The reverse is also true: high boundary layers and high winds give lower mixing ratios even with high emissions. As a result, the differences in the observations between basins shown in Figure 4-16 A and Figure 4-16 B are not necessarily indicative of significantly different emissions between these basins. In Figure 4-16 C and Figure 4-16 D the observed NOx and NOy mixing ratios are normalized to a 1000 m boundary layer height to improve the comparability between the basins; however meteorological differences still influence the comparison. For example, the higher mixing ratios observed in the Permian on 4/23 relative to 4/06 and 4/09 are primarily due to overnight and morning stagnant conditions

that allowed emissions to accumulate in the basin. However, the production of ozone depends on the mixing ratio, not the emission rate, of NOx (and VOCs), thus the observed mixing ratios are informative for air quality.

Finding H5: Due to the relatively high VOC availability, Texas O&G basins are NOx sensitive and significant enhancements in localized ozone production rates can occur near and/or downwind of local NOx sources.

Analysis: Chelsea Thompson-NOAA

Ozone production depends non-linearly on the availability of NOx and VOCs. At high NOx mixing ratios, chemical destruction of ozone can dominate production via NO + O₃ titration, leading to a net ozone loss. At very low NOx mixing ratios, RO₂ and HO₂ self-reactions will dominate over reaction with NO, leading to little or no net ozone production. The efficiency of ozone production maximizes at moderate levels of NOx, when NOx can cycle multiple times between NO and NO₂, each time producing O₃ before terminating to HNO₃. The net change in ozone in an air parcel is a balance between production (denoted as $P(O_3)$), loss (chemical destruction and surface deposition), and transport of ozone into or out of the air parcel. Both chemical destruction (through photolysis or reaction with HO_x) and surface deposition loss rates for ozone are relatively slow, resulting in an ozone lifetime of up to several days within the continental boundary layer. The instantaneous ozone production rate, $P(O_3)$, can be estimated from the rate of NO₂ photolysis via Equation 1.

$$P(O_3) = J_{NO_2}[NO_2] - k_{(NO+O_3)}[NO][O_3] \quad (1)$$

The second term in this equation corrects for the reaction of NO + O₃, which produces NO₂ at the expense of O₃, thus resulting in a null cycle with respect to O₃. $P(O_3)$ is an informative metric for determining the extent to which O₃ can be produced at given NO_x and VOCs concentrations in an air parcel. However, this metric gives a snapshot in time for a sampled air parcel; it does indicate the amount of ozone produced at a location during an entire day.

As noted in Finding F3, VOC composition is an important factor in controlling ozone production. The VOCs that primarily compose natural gas emissions are relatively unreactive, but at high mixing ratios, they can represent a significant source of ozone production. VOCs that are characteristic of urban emissions are generally more reactive, as are biogenic VOCs emitted from trees and foliage. The Haynesville Shale in East Texas is a region of high biogenic VOC emissions. The SONGNEX mission performed flights in the Haynesville on April 4, prior to the start of growing season, and again on April 25 after the growing season was underway. VOC measurements found four times greater mixing ratios of α- and β-pinene on 4/25 compared to 4/04. The calculated OH reactivity averaged 0.74 s⁻¹ and 2.6 s⁻¹ on 4/04 and 4/25, respectively. The calculated instantaneous $P(O_3)$ values along the flight tracks on 4/04 and 4/25 are presented in Figure 4-17. Despite the much greater VOC reactivity on 4/25, $P(O_3)$ calculations revealed an overall greater ozone production rate on 4/04, which is a result of the greater NOx mixing ratios on that day (Figure 4-16). These observations support the conclusion that O₃

production in this region is driven by NOx emissions, consistent with the modeling results presented in Finding F7 and in the study by *Pasci et al.* [2015].

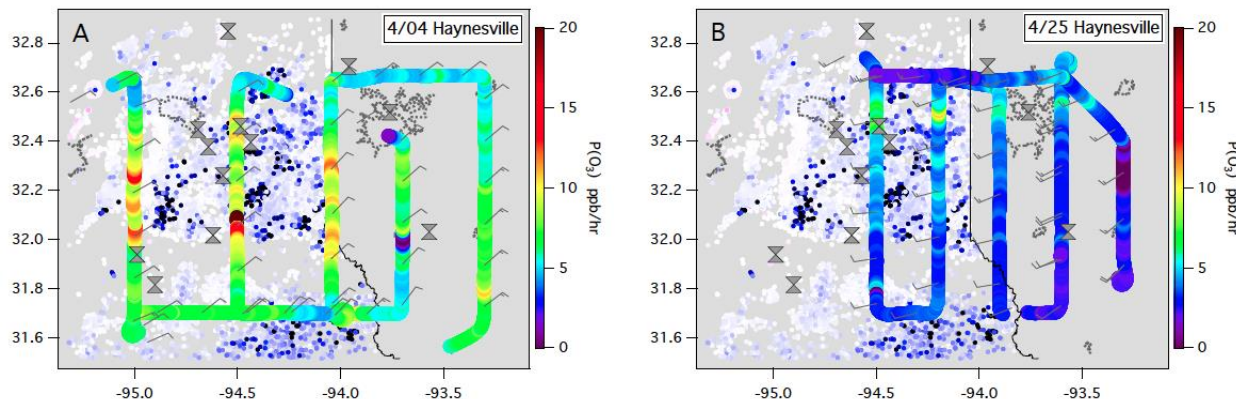


Figure 4-17. Calculated instantaneous ozone production rates along the P3 flight tracks in the Haynesville shale region during the SONGNEX mission on April 4, 2015 and April 25, 2015. Gas wells are denoted by the white to blue gradient dots, with the darker blue representing greater gas production as of 2014. Oil wells are denoted by white to magenta gradient dots, with darker magenta representing greater oil production as of 2014. Urban areas are outlined in dark gray. Wind barbs indicate the dominant wind direction and point in the direction of wind flow. Bowtie markers indicate locations of power plants.

A characteristic of the $P(O_3)$ presented in Figure 4-17 is high spatial heterogeneity. Averaged over the entire basin, $P(O_3)$ is approximately 7 ppb/hr, however, localized enhancements up to 15 ppb/hr are apparent near to and downwind of localized NOx point sources. Some of these are power plants, but processing facilities or other industrial complexes are also NOx point sources. One location of greatly diminished $P(O_3)$ is also seen immediately downwind of a power plant on 4/04 as a result of greater O₃ titration from higher NO emissions. The high spatial heterogeneity of O₃ production with enhancements in proximity to NOx sources lends further support to the NOx-sensitivity of this basin, and illustrates the air quality consequences associated with co-locating large NOx emitters with VOC-emitting sources.

The high spatial heterogeneity in the Haynesville can be contrasted with the Barnett, shown in Figure 4-18, which on April 4, was located immediately downwind of the Dallas urban plume. In this case, the city of Dallas served as essentially one large NOx source, leading to a region of high ozone production downwind of the city. The flight track color-coded by NOy in Figure 4-18 B illustrates this large area source. The greatest O₃ production rate determined for the Barnett was located in the region of greatest gas production; however, the Dallas urban plume contributed more reactive VOCs to this region. Further work is needed to determine the relative contribution of O&G VOCs and urban VOCs in this region.

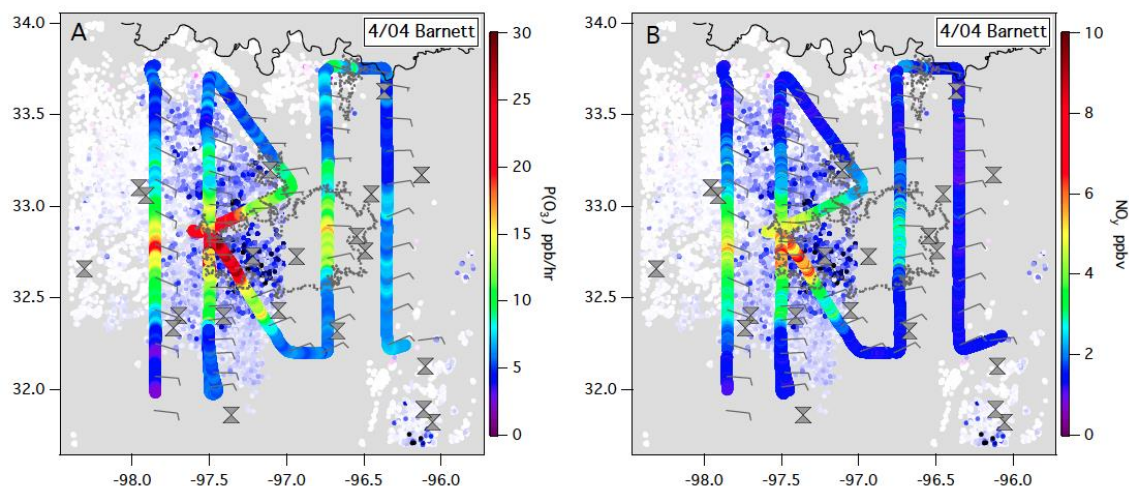


Figure 4-18. Calculated instantaneous ozone production rates and observed NO_y along the P3 flight tracks in the Barnett shale region during the SONGNEX mission on April 4, 2015. Figures are in the same format as in Figure 4-17.

Finally, the Eagle Ford Shale region is shown in Figure 4-19. This region is characterized by a greater density of oil-producing wells in the eastern portion of the formation and greater density of gas-producing wells in the western section. Oil-producing wells generally emit less NO_x and fugitive VOC emissions than gas-producing wells. This difference is apparent in the flight track color-coded by NO_y in Figure 4-19 B, which indicates generally low nitrogen oxides across the eastern portion of the region with localized enhancements downwind of point sources. In contrast, the western part of the Eagle Ford has more enhanced nitrogen oxides, spread over a large portion of this region. This western part of the Eagle Ford also had the greatest ethane emissions observed on this day, consistent with the high natural gas production. $P(O_3)$ calculations confirm the more enhanced ozone production rates in the western portion of the field. Further contributing to the enhanced (and more widespread) ozone production on this day are the urban emissions from the city of Laredo, which add both NO_x and highly reactive VOCs to this region. Again, further research is needed to apportion the contribution of O&G and urban emissions to ozone production here. These observations near Dallas and Laredo highlight the challenges associated with co-located O&G and urban emissions.

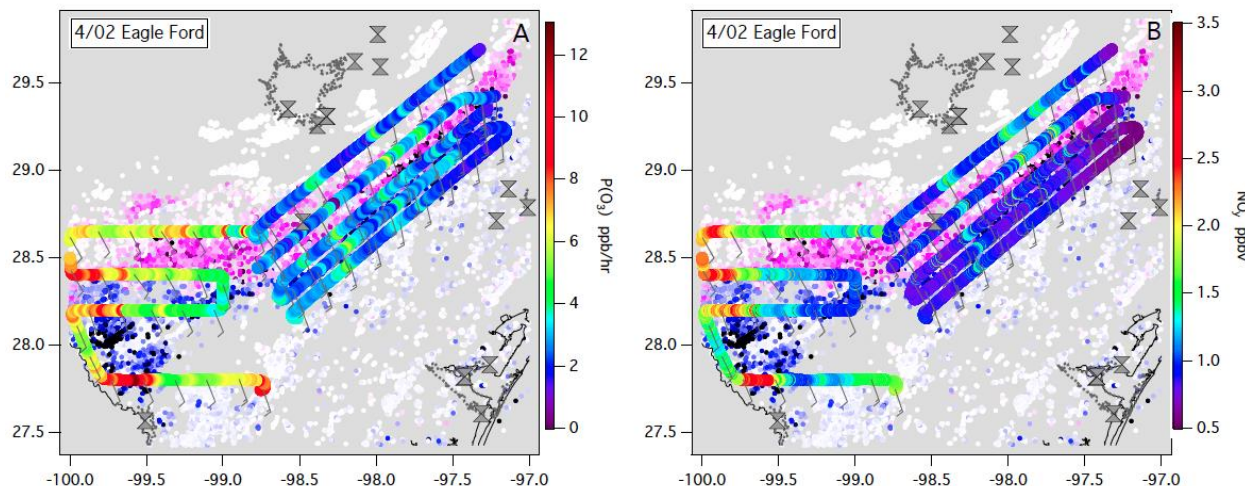


Figure 4-19. Calculated instantaneous ozone production rates and observed NO_y along the P3 flight tracks in the Eagle Ford shale region during the SONGNEX mission on April 2, 2015. Figures are in the same format as in Figure 4-17.

4.3.4 Summary and Recommendations for Further Analysis

Ambient concentrations of secondary PM result from a variety of mechanisms that convert several different precursors from two or more source sectors to PM components. Findings F1 and F2 review some surface and aircraft studies, respectively, that have identified generally small PM enhancements from the interactions of emissions from O&G emissions with other emission sectors. Findings F3, F4 and F5 present some preliminary results from analyses of data collected on flights of the NOAA WP-3D aircraft during 2013 and 2015; the focus here is on ozone production in air masses affected by VOC from O&G and NO_x from urban or point source emissions. Some evidence for synergistic ozone production is identified, but no general conclusions can yet be drawn. The NOAA WP-3D data sets provide opportunities for much more extensive and detailed analyses that can advance our full understanding of the interactions between emissions from O&G development and emissions from urban, point source and biogenic sources.

4.3.5 References

- Evanoski-Cole, A.R., Gebhart, K.A., Sive, B.C., Zhou, Y., Capps, S.L., Day, D.E., Prenni, A.J., Schurman, M.I., Sullivan, A.P., Li, Y., Hand, J.L., Schichtel, B.A., and Collett, Jr., J.L. (2017) Composition and sources of winter haze in the Bakken oil and gas extraction region. *Atmos. Environ.* 156, 77-87, doi:10.1016/j.atmosenv.2017.02.019.
- Hand, J.L., B.A. Schichtel, W.C. Malm, and M.L. Pitchford (2012), Particulate sulfate ion concentration and SO₂ emission trends in the United States from the early 1990s through 2010, *Atmos. Chem. Phys.*, 12, 10353-10365, doi:10.5194/acp-12-10353-2012.
- Lee, T., S. M. Kreidenweis and J. L. Collett, Jr. (2004), Aerosol ion characteristics during the Big Bend Regional Aerosol and Visibility Observational study, *J. Air and Waste Management Assoc.*, 54, 585-592.

- Li, Y., Schwandner, F. M., Sewell, H. J., Zivkovich, A., Tigges, M., Raja, S., Holcomb, S., Molenar, J. V., Sherman, L., Archuleta, C., Lee, T., and Collett, Jr., J. L. (2014) Observations of ammonia, nitric acid, and fine particles in a rural gas production region, *Atmos. Env.* 83, 80-89.
- Nowak, J.B., J.A. Neuman, R. Bahreini, A.M. Middlebrook, J.S. Holloway, S.A. McKeen, D.D. Parrish, T.B. Ryerson, and M. Trainer (2012), Ammonia sources in the California South Coast Air Basin and their impact on ammonium nitrate formation, *Geophys. Res. Lett.*, 39, L07804, doi:10.1029/2012GL051197.
- Pacsi, A. P., Y. Kimura, G. McGaughey, E. C. McDonald-Buller, and D. T. Allen (2015), Regional Ozone Impacts of Increased Natural Gas Use in the Texas Power Sector and Development in the Eagle Ford Shale, *Environmental science & technology*, 49(6), 3966-3973, doi:10.1021/es5055012.
- Rutter, A. P., R. J. Griffin, B. K. Cevik, K. M. Shakya, L. Gong, S. Kim, J. H. Flynn, and B. L. Lefer (2015), Sources of air pollution in a region of oil and gas exploration downwind of a large city, *Atmospheric Environment*, 120, 89-99,
[doi:http://dx.doi.org/10.1016/j.atmosenv.2015.08.073](http://dx.doi.org/10.1016/j.atmosenv.2015.08.073).

4.4 Response to Question I

Are there gaps in our understanding of chemical transformations that limit a full understanding of ozone and PM formation from O&G development emissions?

4.4.1 Working Group

David Parrish - David.D.Parrish, LLC

David Allen - University of Texas, Austin

Erin McDuffie - NOAA/ESRL/CSD

Jim Roberts - NOAA/ESRL/CSD

Greg Yarwood - Ramboll Environ

4.4.2 Background

In addition to adding to existing emissions, new or expanded O&G operations can bring the associated emissions into environments not previously significantly impacted by anthropogenic air pollutant emissions, thereby changing the local and regional atmospheric chemistry. Some gaps exist in our understanding of atmospheric transformation processes that limit our ability to accurately predict the air quality impacts specific to O&G emissions. There are also significant limits to our wider understanding of transformation processes that affect our ability to model atmospheric concentrations in all environments from urban to rural to remote. The following findings summarize some advances in our understanding of identified uncertainties that may be important.

The results [*Mao et al., 2016*] from a 2015 workshop that discussed the observations collected during the Southeast Atmosphere Studies (SAS, including SENEX, SOAS, NOMADSS and SEAC4RS) conducted during summer 2013 are a particularly informative resource. The workshop provided the opportunity for the atmospheric modeling community to evaluate, diagnose, and improve the model representation of the fundamental atmospheric processes that are essential to the formation of ozone, secondary organic aerosols (SOA) and other trace species in the troposphere over the Southeastern U.S. Findings I1 through I3 below are directly derived from the results of this workshop as described by *Mao et al. [2016]*.

Observations from field sites in Texas and Los Angeles support Findings I4-I5 and suggest a source of chlorine radicals associated with O&G emissions, whose chemistry should be incorporated into model chemical mechanisms. A model mechanism comparison of ozone production and NO_x sensitivity in an O&G basin in Colorado is used to support Finding I6. It is essential to evaluate the chemical accuracy of regional photochemical models like CAMx, as these are used to assess the influence of O&G emissions on ozone and PM production, such as in **Finding J1-J4**, which serve to inform policy relevant decisions on this topic.

4.4.3 Findings

Finding I1: In many oil and natural gas basins, isoprene plays a significant role in the atmospheric chemistry; models must include detailed isoprene oxidation mechanisms for accurate modeling of isoprene's role.

In many rural areas, VOC reactivity is dominated by isoprene, even in the presence of substantial VOC emissions from O&G activity [e.g. in the Barnett Shale region, *Rutter et al.*, 2015]. Consequently, the accuracy of photochemical modeling of the photochemical transformations of O&G emissions depends on the accurate description of isoprene oxidation chemistry. However, substantial uncertainties remain in the current reaction schemes describing this chemistry in models. Our understanding of this chemistry has been evolving rapidly in the past decade, and *Mao et al.* [2016] note the following important points:

- A major consequence of isoprene oxidation is the production of isoprene nitrates, formed from the $\text{RO}_2 + \text{NO}$ reaction in the isoprene degradation chain. Different treatments of this reaction can cause large variations of global and regional ozone budgets among different models.
- Several lines of evidence argue for a short (~ 2 hr) lifetime of total and isoprene organic nitrates. This short lifetime affects our understanding of the lifetime of NO_x, the spatial pattern of transported NO_x, and the resulting oxidation rates of many atmospheric species by OH, O₃, and NO₃.
- Recent laboratory data indicates the yield of first generation isoprene nitrates is in the range of 10% to 14%, which is much higher than 4% suggested by an earlier global model study [*Horowitz et al.*, 2007].
- The subsequent fate of these isoprene nitrates includes oxidation by OH, NO₃ and O₃. Synthesis of models and SAS observations suggests an additional important role for hydrolysis as expected based on the laboratory measurements.
- The SAS observations also identify an important role for NO₃ chemistry, especially as it contributes to oxidation of biogenic volatile organic compounds (BVOC) at night. During SAS, these reactions were a substantial sink of NO_x in addition to their role in oxidation of BVOC. To a large extent this is due to the high yield of carbonyl nitrates (65%-85%) from the isoprene + NO₃ oxidation. Models that incorporate this chemistry indicate that the isoprene+NO₃ reaction contributes more than 50% of the total isoprene nitrate production, and that the reaction is thus both a major pathway for isoprene removal and for NO_x removal.
- The reaction partners of the isoprene RO₂ radical were mostly NO and HO₂ during the day and a mix of NO₃, RO₂ and HO₂ at night.
- The role of vertical mixing in leaving BVOC in the residual layer emerged as a key issue for describing the regional scale effects of this chemistry.

Mao et al. [2016] conclude that the chemistry of isoprene should be treated in more detail than other VOCs. They recommend that photochemical modules in models include explicit

chemistry through the first and second generation of isoprene oxidation, and that no other species should be lumped with isoprene or its daughters.

Finding I2: Observations collected during the Southeast Atmosphere Study (SAS) indicate that OH concentrations are accurately predicted by models, at least if they include detailed chemistry. Previous work has reported dramatically higher OH at low NO_x concentrations than current chemistry predicts; these reports were due to measurement interferences rather than shortcomings in the model chemical mechanisms.

Over the last decade, several direct measurements have shown unexpectedly high concentrations of the hydroxyl radical (OH), without the decrease at low concentrations of NO_x that is expected from the known chemistry of the troposphere [see discussion in Rohrer *et al.*, 2014]. Some studies indicated that this phenomenon was particularly pronounced in isoprene-rich environments. On the other hand, an interference has been identified that affects some OH instruments [Mao *et al.*, 2012]. A key feature of the SAS experiments was that the NO_x concentrations encountered spanned a range that resulted in measurements where the three major fates of isoprene peroxy radicals (reaction with NO, HO₂ or isomerization) were sampled at different times and locations, which provide the opportunity to compare measured and modeled OH concentrations through all relevant conditions. These studies (Figure 4-20) showed excellent agreement between observations and model results that included the most detailed chemical mechanisms. Condensed chemical mechanisms that approximate the detailed one are expected to provide similarly good performance. These results suggest there is no need for concern regarding missing chemistry in model mechanisms yielding modeled OH concentrations that are too low at low NO_x concentrations.

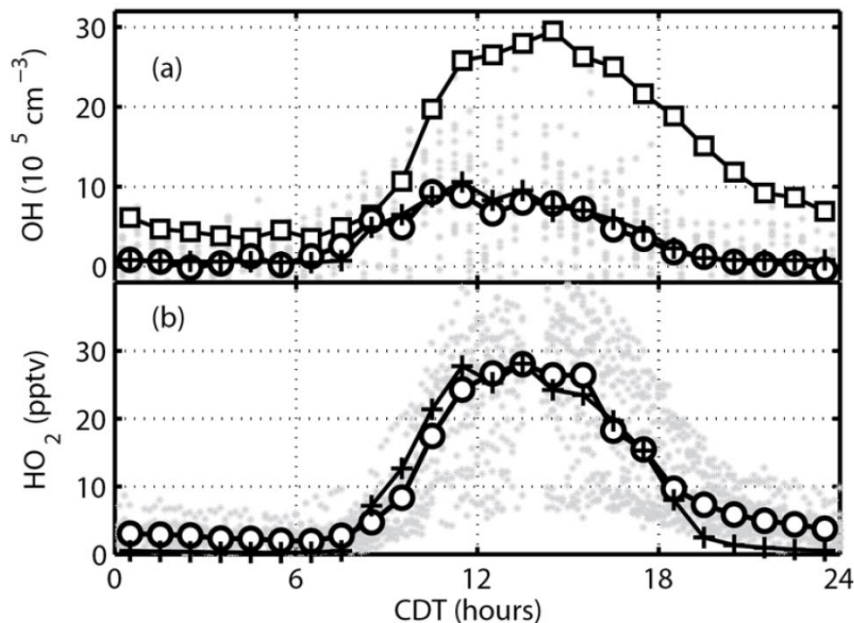


Figure 4-20. Diurnal variation of measured (gray dots are individual 10-minute average measurements) and modeled OH and HO₂ during SOAS. (a) OH measured by a traditional

laser induced fluorescence technique is shown as squares and by a new chemical scavenger method is shown as circles. The latter is considered as the “true” ambient OH. Simulated OH from a photochemical box model with Master Chemical Mechanism (MCM) v3.3.1 is shown in pluses. (b) Measured and modeled HO₂ is shown as circles and pluses, respectively. The symbols are averages over all days of measurements for 1-hour periods of the diurnal cycle. [Figure from *Mao et al.*, 2016, modified from *Feiner et al.*, 2016].

Finding I3: Fully defining the importance of SOA formation from VOC precursors emitted from O&G exploitation requires a better general characterization of SOA formation mechanisms from precursor VOCs.

Improving the representation of organic aerosol (OA) is a critical need for modeling of PM concentrations in all regions of the troposphere. Current air quality and chemistry-climate models produce a very wide range of organic aerosol mass concentrations, with predicted concentrations spread over 1-2 orders-of-magnitude [e.g., *Tsigaridis et al.*, 2014]. *Mao et al* [2016] discuss the implications of the SAS observations for understanding and accurately modeling the formation of secondary OA (SOA). This is still very much an active area of research, but *Mao et al* [2016] offer some guidance that is primarily oriented toward regions with high BVOC emissions:

- The observations reinforce the idea that NO₃ oxidation of BVOC is an important source of OA (~5-12% in SE US in summer) and raise new questions about the lifetime and products of the aerosol nitrate. Thus, NO₃ chemistry is an important element of both VOC oxidation and aerosol production.
- There is high confidence that a pathway of SOA formation from isoprene epoxydiol (IEPOX) should be included in models. However, since many of the parameters needed to predict IEPOX-SOA are uncertain, further mechanistic studies are needed to address these uncertainties.
- The importance of glyoxal (produced from isoprene, as well as from anthropogenic VOCs) as a SOA precursor remains uncertain.
- There is high confidence that models should predict SOA from urban emissions with a parameterization based on CO emissions that results in realistic concentrations. However, extending that parameterization to emissions from O&G activities is not appropriate.

Finding I4: High concentrations of a gas-phase soluble chloride species (presumably HCl) have been observed in the Barnett Shale region. The photochemical transformations that lead to the formation of this species, and any effect on photochemical ozone production, remain uncertain.

Analysis: C.B. Faxon and D.T. Allen-U. Texas at Austin; J.M. Roberts-NOAA

During the Dallas-Fort Worth (Barnett Shale) field campaign [*Griffin et al.*, 2011] measurements at the TCEQ Eagle Mountain Lake site revealed large concentrations (as high as ~2 ppb) of a soluble gas-phase chloride species (see discussion in **Finding E1**). This species is believed to be

hydrochloric acid (HCl). A strong diurnal cycle showing a mid-afternoon peak (Figure 3-32) suggests this atmospheric species has a photochemical source. This suggestion is further supported by the strong correlation of this species with nitric acid (HNO_3) shown in Figure 4-21. Note that in general a strong correlation is observed each day, but the HCl/ HNO_3 ratio varies widely between days.

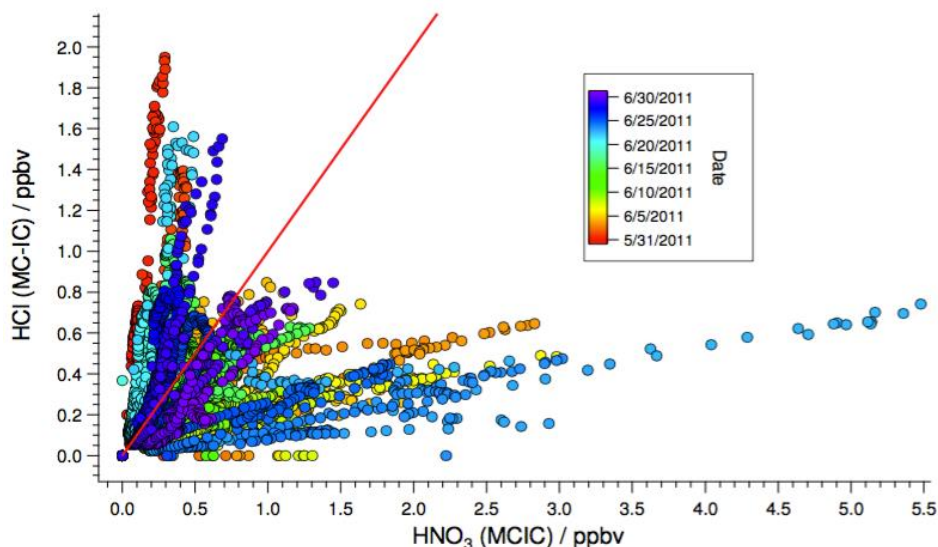


Figure 4-21. Correlation of soluble chloride and nitric acid concentrations observed during June 2011 at the TCEQ Eagle Mountain Lake measurement site [Faxon, 2014]. A 1:1 line is added for reference.

The correlations in Figure 4-21 seen in the Barnett Shale region are similar to those seen in the Los Angeles urban area during the 2010 CalNex field study (Figure 4-22), although the Los Angeles concentrations of both HCl and HNO₃ are approximately a factor of 3 greater than in the Barnett Shale region. This similarity suggests that the HCl observed at the Eagle Mountain Lake site is not solely associated with O&G development, since emissions from such development are not a significant factor in California's South Coast air basin. Indeed, such concentrations of HCl may be a general urban phenomenon, and the concentrations observed in the Barnett Shale region may reflect transport from the nearby Dallas-Fort Worth area. The emissions (see discussion in **Finding E1**), the atmospheric processes that lead to the formation of HCl, and the cause of the variability of the HCl to HNO₃ ratio are not yet clearly understood, at least in the Barnett Shale region.

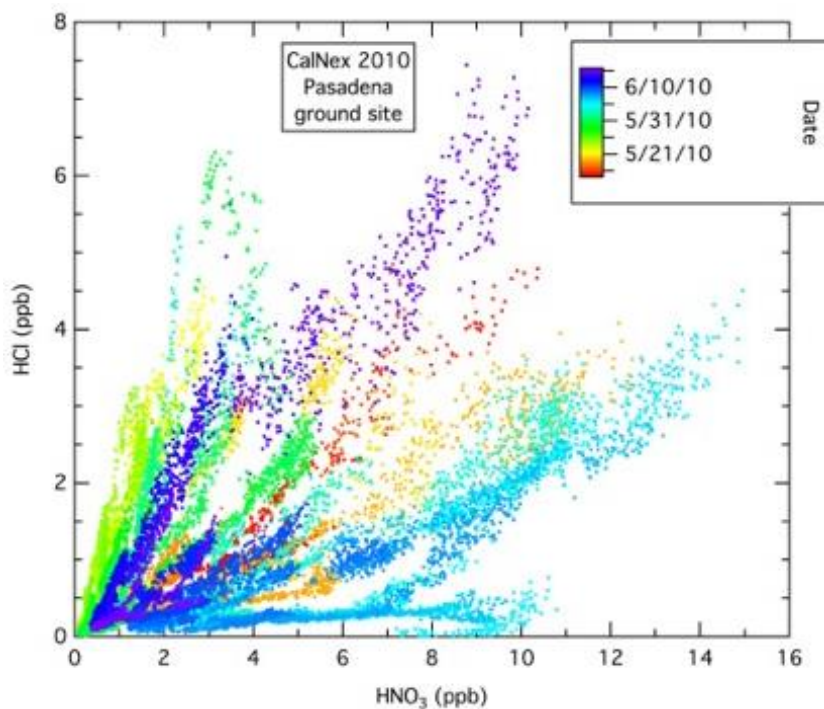


Figure 4-22. Correlation of HCl with HNO₃ colored by date for the entire CalNex 2010 Pasadena dataset.

Finding 15: Chlorine radicals do play a significant but relatively minor role in tropospheric chemistry, likely in oil and natural gas basins as well as in urban areas; accurate photochemical modeling requires inclusion of Cl reactions in the chemical mechanism.

Reviews of the role of chlorine in urban tropospheric chemistry [e.g., *Sawar et al.*, 2012; *Faxon and Allen.*, 2013] consistently identify significant roles played by chlorine. Observations also continue to report signatures of chlorine radical reactions with VOCs [e.g., *Baker et al.*, 2016], although consideration of HO_x radical propagation [*Young et al.*, 2014] suggests that such signatures should be carefully evaluated before being taken at face value.

Finding 16: Photochemical ozone formation in the Denver-Julesburg O&G Basin in Colorado was modeled with both the "lumped" CB6r3 and the explicit MCM chemical mechanisms. The total VOC OH reactivity and total ozone produced were very similar in the two calculations, and both show similar NOx dependence of the total ozone production.

Analysis: Erin McDuffie-NOAA; Greg Yarwood-Ramboll Environ

Emissions from O&G development are dominated by light alkanes (< C5) and therefore have a composition profile different from urban emissions, since Reid vapor pressure limits have largely eliminated those alkanes from gasoline. The VOC oxidation schemes generally utilized in photochemical modeling are simplified by "lumping" many VOC species together, rather than treating each species explicitly. This simplification is required due to limited computer

resources. These lumping schemes have been developed and tested to accurately model the urban photochemical environment. An open question remains whether these schemes can also accurately reproduce the photochemical environment in regions dominated by O&G emissions.

McDuffie et al. [2016] report modeling of photochemical ozone production in the Wattenberg field of the Denver-Julesburg O&G Basin. They utilized a box model with a near-explicit chemical mechanism (MCM v3.3.1), including a complete inorganic mechanism and a degradation scheme for 50 primary VOCs, with a total of 4002 species and 15,555 reactions. They ran the simulation for 24 hours (starting at 8 am local time) with the model initialized with observed temperature and concentrations of NOx and VOCs, and constrained to observed temperature and VOC concentrations every 30 minutes. Dilution, entrainment and deposition rates were selected so that the results optimally reproduced the observed concentrations of ten secondary products of the VOC photochemistry, including ozone.

To investigate the influence of the choice of chemical mechanism, the calculations of *McDuffie et al. [2016]* were repeated with the box model run in a near-identical manner, replacing the explicit MCM mechanism with the "lumped" CB6r3 mechanism. The CB6r3 mechanism included 94 species and 323 reactions (including loss through deposition). The original box model, the Dynamically Simple Model for Atmospheric Chemical Complexity (DSMACC) [*Emmerson and Evans, 2009*], was additionally updated to constrain simulations to ambient observations of pressure, and adjusted to calculate the ambient number density at every time step (10 minutes) of the 24 hour simulation. These updates allowed for more accurate calculation of chemical rate constants and 30-minute VOC mixing ratio constraints. Both MCM and CB6r3 mechanisms were run with these DSMACC model updates and comparison of the results between these calculations yields three conclusions:

- The OHR for the VOCs measured at a site adjacent to the Denver-Julesburg basin was quite similar, with the OHR for the lumped VOCs equal to 2.5 s^{-1} compared to $2.4 \pm 0.9 \text{ s}^{-1}$ calculated from explicit VOCs. The OHR from the lumped CB6r3 mechanism is within the standard deviation of the original determination from *McDuffie et al. [2016]*, indicating minimal differences in this metric between the different VOC schemes.
- Figure 8 of *McDuffie et al. [2016]* compared observed and modeled diel average ozone concentrations. Figure 4-23 reproduces that figure with adjusted MCM results from the DSMACC model updates described above, and the results from the CB6r3 mechanism. Both model mechanisms closely track the observed ozone profile during the period of photochemical production (~8am-2pm). The maximum ozone predicted is 68.8 ppb at 3 pm and 69.5 ppb at 3:30 pm with the MCM and CB6r3 mechanisms, respectively, while the maximum observed ozone is 69.0 ppb at 2 pm. Predicted ozone from both mechanisms is nearly in exact agreement, with the MCM being slightly lower than the CB6r3. Both models are also slightly late in the timing of the maximum observed ozone, but the MCM is closer to the observed than the CB6r3.

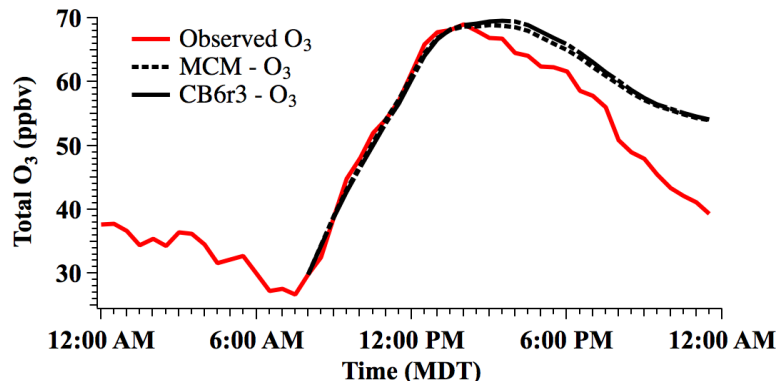


Figure 4-23. Diel average ozone observed (red line) compared to simulated with explicit (dotted black line) and lumped (dash-dot black line) VOC mechanisms.

- Figure 10 of *McDuffie et al. [2016]* compared the modeled maximum photochemical ozone produced as a function of the observed NOx concentration, scaled by a factor of 0 to 5. Figure 4-24 reproduces that figure, again with updated MCM results and the results from the CB6r3 mechanism. Results are shown for three VOCs scenarios where the O&G VOCs have been removed (blue) and doubled (green) relative to observations (black). The NOx sensitivity profiles are similar between the MCM and CB6r3 mechanisms, however, the CB6r3 mechanism predicts a more rapid increase and then decrease of ozone with increasing NOx. Both mechanisms indicate that the ozone production at the level of observed NOx (vertical solid line at NOx scaling factor =1) is NOx sensitive/VOC saturated, which was one of the main conclusions originally reached by *McDuffie et al. [2016]*. Another conclusion of that paper was that at the level of observed NOx, photochemical ozone decreased by 17.4% (17.8% in updated DSMACC simulations) when O&G VOCs were removed from the model. This result was the same (17.8%) with the CB6r3 mechanism.

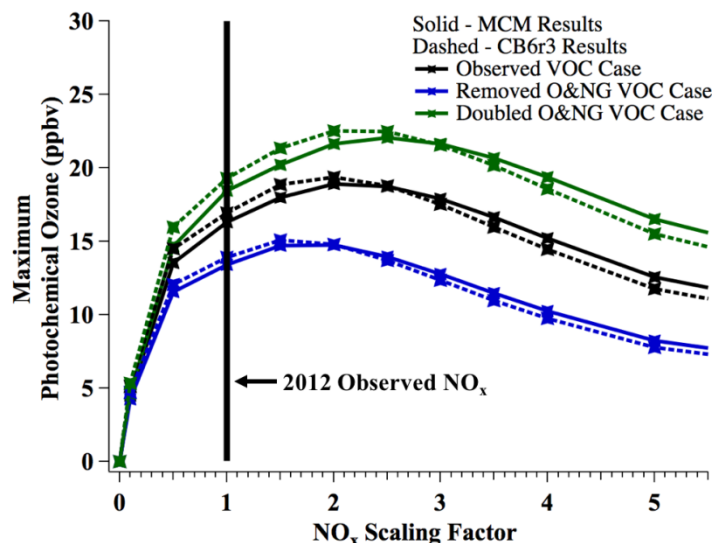


Figure 4-24. NO_x sensitivity of simulated maximum photochemical ozone mixing ratios for three VOC scenarios. Colors represent the VOC scenarios (black – observed VOCs, green – doubled O&G VOCs, blue – zero O&G VOCs). Solid lines are the updated MCM results, and the dotted lines are the CB6r3 results.

4.4.4 Summary and Recommendations for Further Analysis

Ozone and PM are formed by chemical transformations of emissions to the atmosphere. These transformation mechanisms are complex, involving hundreds of chemical reactions and physical transformations. Our understanding of these processes is certainly incomplete, but we have not identified any gaps that imply major uncertainties in our understanding of the air quality impacts of emissions from O&G development. Recent research has narrowed some perceived gaps, including the magnitude of atmospheric OH concentrations (Finding I2) and the applicability of "lumped" chemical mechanisms to O&G emissions (Finding I7), yielding reduced uncertainty in our understanding.

Finding I1 notes the importance of isoprene in some O&G basins, and some recent advances in our understanding of isoprene photochemistry. However, the fate of gas phase and particulate phase products from isoprene+NO₃ and to what extent they return NO_x remains a subject of discussion.

Findings I4, I5 and E1 discuss large measured concentrations of HCl at the TCEQ Eagle Mountain Lake site during the Dallas-Fort Worth (Barnett Shale) field campaign. The emission sources that provide the initial chlorine containing species have not been identified; one possible source that was not considered by *Faxon* [2014] is super-micron particulates containing chloride. The chemical transformations responsible for forming the HCl and the effect of those transformations on ozone formation are also not understood. For example, if HCl results from acid displacement from reaction of HNO₃ or H₂SO₄ with soil-derived particles or sea-salt, there would be little impact on ozone concentrations, but if the HCl is formed from the reaction of

chlorine atoms with VOCs, then a significant impact on the ozone budget would be expected. A clear understanding of these issues would strengthen our understanding of the atmospheric transformation processes, both in O&G basins and in urban areas.

Finding I6 discusses the excellent agreement between chemically “lumped” and explicit mechanisms in terms of the absolute amount of ozone predicted as well as ozone’s predicted sensitivity to changes in NO_x. Though promising, this result is specific to only one location at one time. Further comparisons, extending to multiple locations and over multiple time scales will be required to fully evaluate the accuracy of lumped chemically schemes, used in regional/state ozone assessments, relative to mechanism with more explicit chemistry.

4.4.5 References

- Ahmadov, R., et al. (2015), Understanding high wintertime ozone pollution events in an oil and natural gas producing region of the Western US, *Atmos. Chem. Phys.*, 15, 411-429, doi:10.5194/acp-15-411-2015.
- Baker, A.K., et al. (2016), Evidence for strong, widespread chlorine radical chemistry associated with pollution outflow from continental Asia. *Sci. Rep.* 6, 36821; doi: 10.1038/srep36821.
- Emmerson, K. M., and M. J. Evans (2009), Comparison of tropospheric gas-phase chemistry schemes for use within global models, *Atmos. Chem. Phys.*, 9(5), 1831-1845, doi:10.5194/acp-9-1831-2009.
- Faxon, C.B. (2014), *Urban atmospheric chlorine chemistry: mechanism development, evaluation and implications*, PhD thesis, U. Texas - Austin, <http://hdl.handle.net/2152/25225>.
- Faxon, C.B., and D.T. Allen, (2013), Chlorine chemistry in urban atmospheres: a review. *Environ. Chem.*, 10(3), 221. doi:10.1071/EN13026.
- Feiner, P.A., et al. (2016), Testing Atmospheric Oxidation in an Alabama Forest, *J. Atmos. Sci.*, 73, 4699-4710, DOI: 10.1175/JAS-D-16-0044.1.
- Griffin, R., Dibb, J., Lefer, B., & Steiner, A. (2011). *Final Report: Surface Measurements and One-Dimensional Modeling Related to Ozone Formation in the Suburban Dallas-Fort Worth Area* (pp.1–45), AQRP, U. Texas - Austin, http://aqrp.ceer.utexas.edu/projectinfo/10-024/10-024_Final_Report.pdf.
- Horowitz, L.W., A.M. Fiore, G.P. Milly, R.C. Cohen, A. Perring, P.J. Wooldridge, P. G. Hess, L. K. Emmons and J.F. Lamarque (2007), Observational constraints on the chemistry of isoprene nitrates over the eastern United States, *J. Geophys. Res.-Atmos.*, 112, 10.1029/2006jd007747.
- Mao, J. et al. (2012), Insights into hydroxyl measurements and atmospheric oxidation in a California forest, *Atmos. Chem. Phys.*, 12(17), 8009–8020, doi:10.5194/acp-12-8009-2012.
- Mao, J., et al. (2016), Southeast Atmosphere Studies: learning from model-observation syntheses, *Atmos. Chem. Phys. Disc.*, doi:10.5194/acp-2016-1063.

- McDuffie, E. E., et al. (2016), Influence of oil and gas emissions on summertime ozone in the Colorado Northern Front Range, *J. Geophys. Res.-Atmos.*, 121(14), 8712-8729, doi:10.1002/2016jd025265.
- Rohrer, F., et al. (2014), Maximum efficiency in the hydroxyl-radical-based self-cleansing of the troposphere, *Nature Geosci.*, 7, 559–563, doi:10.1038/ngeo2199.
- Rutter, A.P., R.J. Griffin, B.K. Cevik, K.M. Shakya, L. Gong, S. Kim, J.H. Flynn, and B.L. Lefer (2015), Sources of air pollution in a region of oil and gas exploration downwind of a large city, *Atmos. Environ.*, 120, 89–99, doi:10.1016/j.atmosenv.2015.08.073.
- Sarwar, G., H. Simon, P. Bhave, and G. Yarwood (2012), Examining the impact of heterogeneous nitryl chloride production on air quality across the United States, *Atmos. Chem. Phys.*, 12(14), 6455–6473. doi:10.5194/acp-12-6455-2012.
- Tsigaridis, K., et al. (2014), The AeroCom evaluation and intercomparison of organic aerosol in global models, *Atmos. Chem. Phys.*, 14, 10845-10895, 10.5194/acp-14-10845-2014.
- Young, C. J. et al. (2014), Chlorine as a primary radical: evaluation of methods to understand its role in initiation of oxidative cycles. *Atmos. Chem. Phys.*, 14, 3427–3440, doi: 10.5194/acp-14-3427-2014.

5.0 SYNTHESIS OF RESULTS: TRANSPORT AND METEOROLOGY

5.1 Response to Question J

What is the impact on other regions of Texas from O₃, PM and their precursors transported from oil and natural gas development areas? How does the impact from O&G development compare to impacts from other sources, e.g., upwind cities, rural power plants, and biogenic emissions?

5.1.1 Working Group

Sue Kemball-Cook - Ramboll Environ

Erin McDuffie - NOAA/ESRL/CSD

Adam Pacsi - Chevron Energy Technology Company

Greg Yarwood - Ramboll Environ

5.1.2 Background

Ozone measured at a particular location is the sum of the regional background transported into the area by the large-scale winds and ozone produced from local emissions of ozone precursors [e.g. *Berlin et al.*, 2013]. Once formed from precursors emitted near the ground, ozone can be transported downwind, either within the boundary layer or mixed upward into the overlying free troposphere. Because of its long lifetime in the free troposphere, ozone can affect distant locations if mixed back down to the surface [*Banta et al.*, 2005]. Transported ozone can affect the attainment status of downwind areas such that a region with small local emissions, may exceed the NAAQS due to the contribution of ozone from transport. It is therefore important to understand the contribution to ozone from local emissions and transport in order to understand how much of an area's ozone may be reduced by local emission control measures. In developing emission control strategies, it is also important to understand which sources of emissions are most important in producing ozone during the highest concentration days that are relevant for NAAQS compliance.

Regional photochemical grid models can be used to determine the emissions source regions and source categories that affect ozone at a particular location. The ozone impact of emissions from a particular source can be evaluated by comparing two otherwise identical photochemical model runs in which one run contains emissions from the source and the other does not. For example, *Kemball-Cook et al.* [2010] estimated the impact of O&G emissions from the Haynesville Shale by comparing the results of model runs with and without projected O&G emissions in the Haynesville region. The use of ozone source apportionment techniques allows the effects of multiple emissions source categories and source regions to be assessed within a single model run. *Pacsi et al.* [2015] used the CAMx Ozone Source Apportionment Tool (OSAT; see Appendix B) source apportionment capability in the CAMx photochemical grid model to evaluate the effect of O&G emissions in the Eagle Ford Shale. Pacsi et al. compared the magnitude of impacts from O&G emissions and other emissions sources such as power plants.

In Findings J1-J4, we evaluate the impact of transport of ozone from the Haynesville, Eagle Ford and Barnett Shale O&G development areas using a 2017 CAMx model run performed with the Anthropogenic Precursor Culpability Assessment (APCA) tool, as described in Findings F6, F7 and Appendix B. We use the CAMx APCA tool to quantify the relative magnitude of the ozone contributions from different emissions source categories in order to understand the relative importance of O&G emissions in influencing ODVs and MDA8 ozone concentrations at East Texas ozone monitors.

5.1.3 Findings

Finding J1: The ozone contribution at East Texas monitors from O&G emissions is greatest within the O&G development areas, but can extend outward beyond them. Although the contributions outside the development areas are relatively small, they can be large enough to affect ozone design values.

Analysis: Sue Kemball-Cook-Ramboll Environ

A spatial map of the contribution to 2017 ODVs from East Texas shale region O&G sources is shown in Figure 5-1. The ODV calculation method is described in Appendix B. The contribution to ODVs from O&G emissions from each shale region is greatest within that region, but ODV impacts of 1-2 ppb (gray colored cells) extend well beyond the shale basin regions.

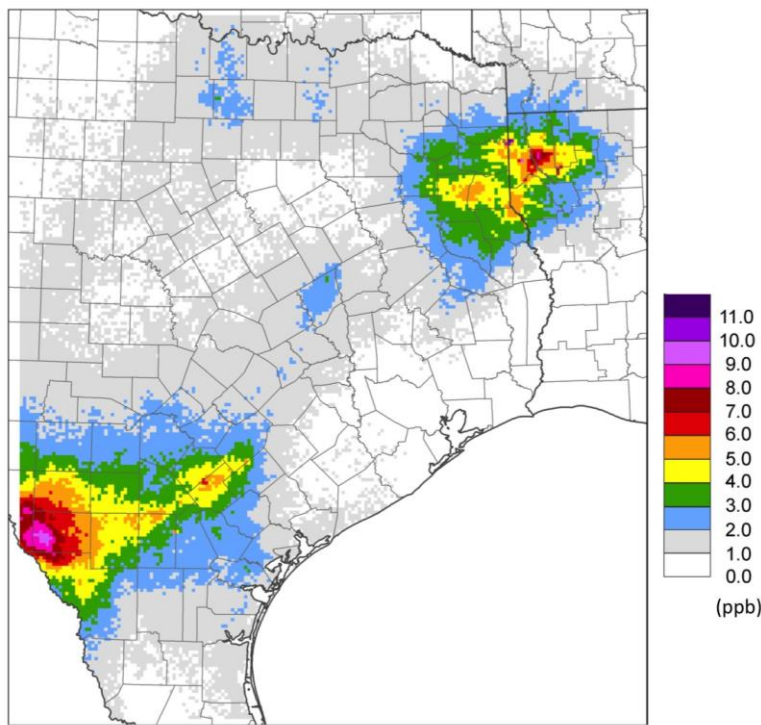


Figure 5-1. Projected contributions to 2017 ODVs from O&G emissions within the East Texas shale regions. The magnitude of the contribution to ODVs at each East Texas regulatory ozone monitor is shown in Figure 4-5.

The contribution of Barnett Shale region O&G emissions to 2017 ODVs is smaller than those of the Haynesville and Eagle Ford Shale regions. This result is broadly consistent with the results of Pacsi *et al.* [2013; 2015] and Kemball-Cook *et al.* [2010]. Barnett Shale ODV contributions range between 0-4 ppb within the Barnett Shale

region and are \leq 3 ppb outside the Barnett Shale region. At regulatory monitors in the Barnett Shale region, the Barnett O&G emission contribution to ODVs reaches a maximum of 0.8 ppb, but is \leq 0.1 ppb at monitors outside the Barnett region (Figure 4-5).

ODV impacts from Haynesville and Eagle Ford Shale area O&G emissions are larger and more widespread. ODV impacts from the Eagle Ford Shale region reach a maximum in Dimmit County, where O&G impacts on ODVs range from 4-10 ppb. Dimmit County lies within the Eagle Ford Shale and does not have regulatory monitoring. Impacts from the Eagle Ford in Texas Counties that are outside the Eagle Ford O&G development region range from 0-4 ppb. The City of San Antonio is located in Bexar County, which lies immediately north of the Eagle Ford Shale area. The State of Texas has recommended to the US EPA that Bexar County be designated as a nonattainment area under the 2015 NAAQS. Contributions to Bexar County ODVs from O&G sources range from 1-4 ppb and are 1.5-2.4 ppb at the Bexar County regulatory monitors.

In the Haynesville region, contributions from O&G emissions to Texas ODVs range from 1-9 ppb and from 2.2-4.9 ppb at Texas regulatory monitors. Haynesville O&G impacts reach a maximum of 11 ppb in northwestern Louisiana. In Texas counties outside the Hayneville region, ODV impacts range from 0-4 ppb with the maximum impacts occurring in counties adjacent to the Haynesville development area.

Overall, the contribution to ODVs from O&G emissions is largest within the O&G development regions and in areas immediately adjacent to them. Impacts in regions that are further removed are generally 2 ppb or less. Figure 5-1 shows that the influence of O&G emissions on ODVs is wide ranging in Texas, but has a relatively small impact on attainment, considering that a 2 ppb impact on the ODV represents 2.8% of a 71 ppb ODV.

Finding J2: The magnitude of the O&G contribution relative to other emissions sources varies depending on each monitor's proximity to power plants, major roadways and heavily vegetated areas.

Analysis: Sue Kemball-Cook-Ramboll Environ

The CAMx photochemical model was used to compare the magnitude of O&G emission contributions to Texas ozone with the contributions of other types of emissions. In the CAMx 2017 source apportionment modeling, all emissions sources were associated with one of the following groups: O&G, onroad mobile, electric generating units (EGUs), natural sources (biogenic emissions and wildfires), and all other sources (includes area sources, elevated shipping, non-EGU point sources, nonroad mobile sources, and offroad mobile sources). The lumping of multiple emissions source categories into one “other” category was necessary due to the large computational demands of running a seasonal model with source apportionment. The emission modeling is described in more detail in Appendix B.

The magnitude of the O&G contribution relative to the contributions of other emissions sources varied depending on each monitor's proximity to power plants, major roadways and heavily vegetated areas. Figure 5-2 shows frequency distributions for impacts on the MDA8 ozone at four East Texas monitors and illustrates the inter-monitor variation of impacts from the different emissions source categories.

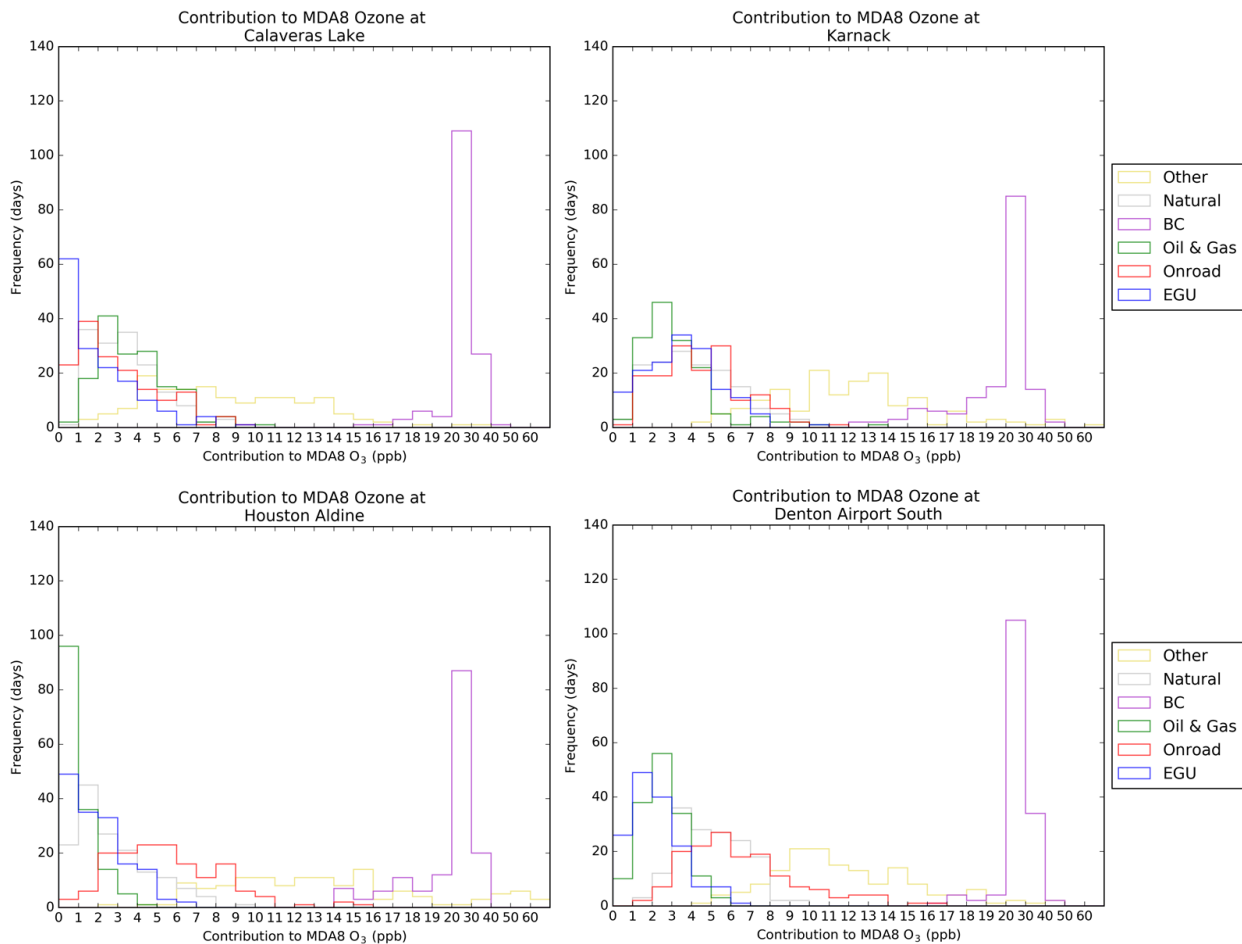


Figure 5-2. Frequency distributions of the projected contributions to 2017 MDA8 ozone concentrations from O&G emissions within the East Texas shale regions, other emissions sources and boundary conditions (BCs) at four East Texas regulatory monitors. Upper left: Calaveras Lake monitor northwest of the Eagle Ford shale. Upper right: Karnack monitor within the Haynesville Shale. Lower left: Houston Aldine monitor. Lower right: Denton Airport South monitor in Dallas-Fort Worth within the Barnett Shale region.

The Karnack, Calaveras Lake and Denton South monitors are located within the Haynesville, Eagle Ford and Barnett Shale regions, respectively, while the Houston Aldine monitor is located away from all O&G development areas. Figure 5-1 shows that the total ODV impact due to O&G emissions at all Houston monitors is < 1 ppb. The Denton South and Houston Aldine monitors were selected for analysis because they were the 2016 design value monitors for the DFW and Houston areas, respectively, and their frequency distributions are typical of monitors in their areas. The Karnack and Calaveras Lake monitors were selected for analysis because they lie within shale O&G regions and were among the East Texas monitors that had the largest ozone contributions from O&G emissions. The Karnack monitor had the highest episode average and episode maximum contribution to MDA8 ozone from Haynesville Shale O&G NO_x and O&G VOC of all Texas regulatory monitors. The Calaveras Lake monitor had the highest

episode average and episode maximum contribution to MDA8 ozone from the Eagle Ford Shale from O&G NOx and among the highest for O&G VOC. All San Antonio area monitors had very similar contributions from O&G VOC.

The O&G contribution to the MDA8 for the Houston Aldine monitor is strongly peaked in the 0-1 ppb bin. The largest contribution falls within the 4-5 ppb bin. The Calaveras Lake and Karnack monitors have their most frequent MDA8 contributions from O&G in the 2-3 ppb bin and have maximum contributions in the 10-11 ppb and 13-14 ppb ranges, respectively. This indicates that the influence of O&G sources on these two monitors is more frequent and intense than at the Houston Aldine monitor; this is consistent with Finding J1 that the largest ozone impacts from O&G emissions occur within the shale regions and that distant regions are minimally affected by transport of ozone from O&G sources. Like the Karnack and Calaveras monitors, the Denton South monitor's O&G contribution to the MDA8 has its peak in the 2-3 ppb bin, but the largest contribution falls in the 5-6 ppb range; this is consistent with Figure 5-1, which shows smaller ODV O&G impacts in the Barnett relative to those in the Haynesville and Eagle Ford regions.

At Calaveras Lake, the O&G frequency distribution has its peak at a higher value of the MDA8 than does the onroad mobile or EGU distribution; the O&G distribution also has a higher maximum value than does the EGU or onroad mobile distribution. This signifies the strength of the influence of O&G emissions at this monitor, which is located near the Eagle Ford Shale.

The two urban monitors, Denton South and Houston Aldine, have onroad mobile frequency distributions that are broader than their O&G distributions and have peaks at higher values of the MDA8. At the two urban sites, the maximum onroad mobile MDA8 ozone impacts are higher than the maximum impacts from O&G; the reverse is true for Calaveras Lake and Karnack. Calaveras Lake is located in a relatively rural area that is upwind of the San Antonio urban area under the prevailing southerly winds and has a smaller influence from onroad mobile sources than DFW and Houston urban sites. The onroad mobile frequency distribution for the Karnack monitor falls somewhere in between the urban and rural extremes, as Karnack is intermittently influenced by nearby Interstate 20 as well as the Shreveport, LA urban plume.

At nearly all monitors outside the shale regions, the maximum contribution to the MDA8 from EGUs is larger than the maximum contribution from O&G emissions. At Houston Aldine, the O&G and EGU frequency distributions are both strongly peaked in the 0-1 ppb bin, but the maximum value of the MDA8 is higher for EGUs than for O&G. Denton South and Calaveras Lake are located within shale regions, and the frequency distribution for O&G impacts peaks at a higher value of the MDA8 than that of the EGU distribution at both sites. At Karnack, on the other hand, both the EGU and O&G distributions both have broad peaks of comparable magnitude. Karnack showed the most frequent and intense EGU impacts of these four monitors due to its location near several coal-fired power plants.

At Karnack and Calaveras Lake, maximum O&G MDA8 impacts exceed those of natural emissions. For Texas monitors that are located outside the shale development areas, however, the impact of natural emissions is generally larger and more frequent than the impacts of O&G

emissions (e.g. Houston Aldine, Denton South). This is due to the abundance of highly reactive biogenic emissions in Texas. The exception to this is the Laredo Vidaurri monitor, which has a lower natural emission contribution due to the smaller biogenic emissions in this less densely wooded area of East Texas.

All four monitors show a strong peak in the 20-40 ppb range from model boundary conditions (BC), and a broad maximum from the “other” source category, into which several emissions source categories have been lumped.

The magnitude and frequency of O&G impacts differs from monitor to monitor in East Texas depending on the monitor’s proximity to O&G development. The largest O&G impacts occur within the O&G development areas, with minimal (0-2 ppb) transport of O&G ozone impacts to distant monitors. Whether O&G impacts are larger and more frequent than those of other emissions source categories depends on whether the monitor is in an urban area affected by onroad mobile emissions or is close to a power plant.

Finding J3: For all Houston-Galveston-Brazoria area monitors, the average and maximum contribution from East Texas shale O&G emissions to the MDA8 ozone was less than those of onroad mobile, natural, and EGU sources.

Analysis: Sue Kemball-Cook-Ramboll Environ

The Houston-Galveston-Brazoria (HGB) nonattainment area is located outside the Eagle Ford, Haynesville and Barnett Shale O&G development areas, and Figure 5-1 shows the effect of shale O&G emissions on HGB 2017 ODVs to be < 2 ppb. Figure 5-3 compares the impact of shale region O&G on MDA8 ozone with the impacts of other emissions sources for four monitors in the HGB area. The results from these four example monitors are typical of results at the other HGB area monitors (not shown). For all four monitors, the O&G contribution is strongly peaked in the 0-1 ppb bin. The maximum contribution to the MDA8 from O&G emissions among these four monitors is 4-5 ppb. On-road mobile sources, on the other hand, have a much larger average and maximum impact on ozone at all four monitors. The onroad mobile contributions reach a maximum of 18-19 ppb at Houston Westhollow. The influence of the dense network of roadways in Houston is apparent in the broad maxima of the onroad distributions and the maximum contributions that exceed those of the O&G emissions at all monitors. The contributions for natural and EGU emissions are not as large as those of onroad mobile, but their average and maximum ozone contributions exceed those of O&G for all four monitors shown in Figure 5-3 and for all other HGB area monitors. These results suggest that reductions in O&G emissions will be less effective in reducing ozone in the HGB area than reductions in onroad mobile and EGU emissions.

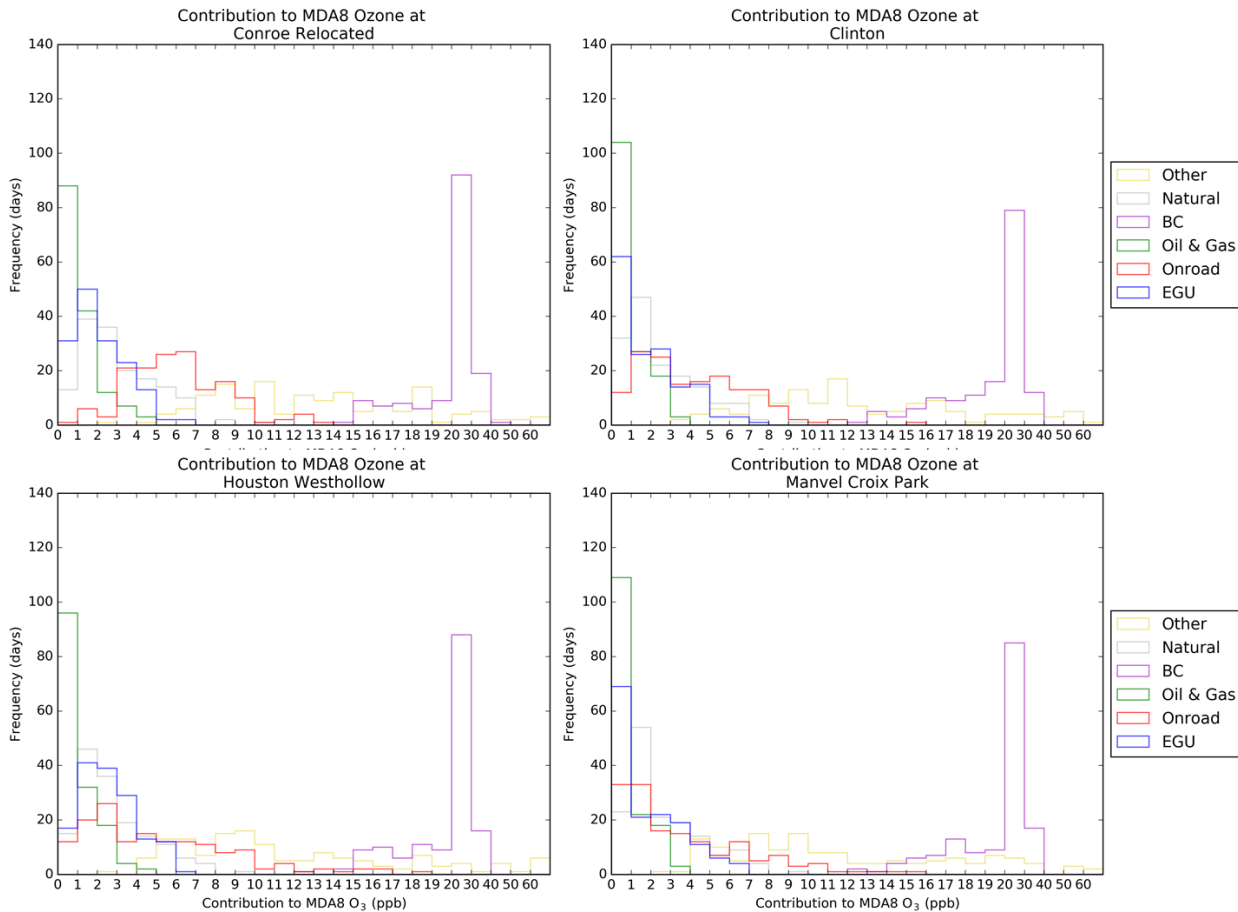


Figure 5-3. Frequency distributions of the projected contributions to 2017 MDA8 ozone concentrations from O&G emissions within the East Texas shale regions, other emissions sources and boundary conditions (BCs) at four East Texas regulatory monitors in the Houston-Galveston-Brazoria area. Upper left: Conroe Relocated monitor north of the Houston area. Upper right: Clinton monitor near the Houston Ship Channel. Lower left: Houston Westhollow monitor in the western part of the Houston urban area. Lower right: Manvel Croix in southern Houston.

Finding J4: For all Dallas-Fort Worth area monitors, the average and maximum contributions from East Texas shale O&G emissions to the MDA8 ozone were less than those of onroad mobile source emissions.

Analysis: Sue Kemball-Cook-Ramboll Environ

The Dallas-Fort Worth (DFW) nonattainment area is located within the Barnett Shale O&G development region. 2017 ODV impacts from East Texas shale gas region O&G emissions are ≤ 4 ppb at DFW regulatory monitors (figure 5-1). Figure 5-4 compares the impact of shale region O&G emissions on MDA8 ozone with the impacts of other emissions sources for four DFW area monitors. The results from these four example monitors are typical of results at the other DFW area monitors (not shown). For all DFW area monitors, the episode average and episode

maximum contributions to the MDA8 ozone from East Texas shale gas region O&G emissions were less than those of onroad mobile source emissions. This was true even for monitors such as Eagle Mountain Lake and Cleburne, which are outside the most densely populated areas of DFW and are also in close proximity to O&G development activity. For all monitors shown in Figure 5-4, the frequency distributions for onroad mobile source contributions have a peak at higher values of the MDA8 ozone than do the distributions for the O&G contributions. The maximum value of the MDA8 ozone contribution from onroad mobile sources is greater than that of the maximum O&G contribution for all monitors. These results highlight the importance of onroad mobile emissions in determining ozone concentrations in the DFW area and indicate that O&G emissions have a smaller impact. Reductions in O&G emissions are therefore expected to be less effective in reducing ozone in the DFW area than reductions in onroad mobile emissions.

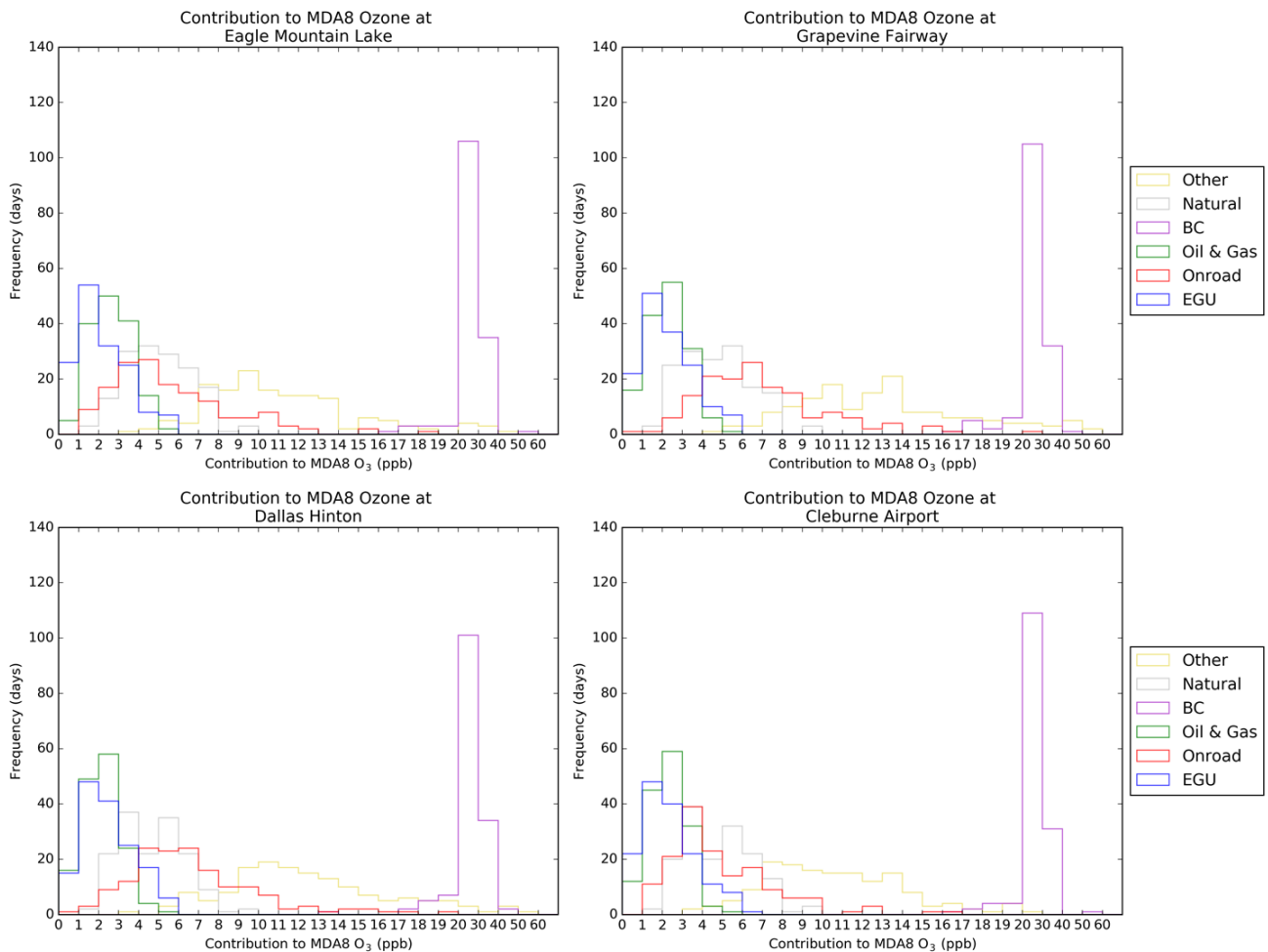


Figure 5-4. Frequency distributions of the projected contributions to 2017 daily MDA8 ozone concentrations from O&G emissions within the East Texas shale regions, other emissions sources and boundary conditions (BCs) at four East Texas regulatory monitors in the Dallas-Fort Worth Area. Upper left: Eagle Mountain Lake monitor northwest of the DFW urban area in an O&G development area. Upper right: Grapevine Fairway monitor in the northern part of the DFW urban area. Lower left: Dallas Hinton monitor in the central DFW urban area. Lower right: Cleburne Airport south of the DFW urban area in an O&G development area.

5.1.4 Summary and Recommendations for Further Analysis

Photochemical modeling of O&G emissions finds modest impacts on ozone concentrations throughout Texas. These impacts decrease with distance from the O&G basin, and in urban areas are generally smaller than the impacts of emissions from other emission source sectors. The accuracy of these model results depends on the accuracy of the underlying chemical mechanism (Finding I6) and on the accuracy of the underlying emission inventories, which has been questioned. Comparisons of bottom-up and top-down NOx emission inventories in O&G regions indicate that bottom-up inventories overestimate NOx emissions [Ahmadov *et al.*,

2015; Finding A5] and that these overestimates may introduce bias into estimates of ozone impacts from O&G development (Finding E2). Because the analysis presented here is based on bottom-up emission inventories and ozone formation is NOx-limited in the model (Finding F7), the O&G ODV impacts shown here may overestimate the actual ODV impacts. Future analysis aimed at resolving the emission inventory uncertainty could potentially improve the accuracy of the model results and would increase our confidence in them.

5.1.5 References

- Ahmadov, R., et al. (2015), Understanding high wintertime ozone pollution events in an oil- and natural gas-producing region of the western US, *Atmos. Chem. Phys.*, 15(1), 411–429, doi:10.5194/acp-15-411-2015.
- Banta, R. M., C.J. Senff, J. Nielsen-Gammon, L.S. Darby, T.B. Ryerson, R.J. Alvarez, S.P. Sandberg, E.J. Williams, and M. Trainer (2005), A Bad Air Day in Houston, *Bull. Am. Met. Soc.*, 86(5), 657–669.
- Berlin, S.R., A.O. Langford, M. Estes, M., M. Dong, and D.D. Parrish (2014), Magnitude, decadal changes, and impact of regional background ozone transported into the greater Houston, Texas, Area, *Env. Sci. & Tech.*, 47, 13985–13992 Kemball-Cook, S., A. Bar-Ilan, J. Grant, L. Parker, J. Jung, W. Santamaria, J. Matthews, and G. Yarwood (2010), Ozone impacts of natural gas development in the Haynesville Shale, *Environ. Sci. Technol.*, 44, 9357–9363, doi:10.1021/es1021137.
- Pacsi, A.P., N.S. Alhajeri, D. Zavala-Araiza, M.D. Webster, and D.T. Allen (2013), Regional air quality impacts of increased natural gas production and use in Texas, *Environ. Sci. Technol.*, 47, 3521–3527, doi:10.1021/es3044714.
- Pacsi, A.P., Y. Kimura, G. McGaughey, E.C. McDonald- Buller, and D.T. Allen (2015), Regional ozone impacts of increased natural gas use in the Texas power sector and development in the Eagle Ford shale, *Environ. Sci. Technol.*, 49, 3966–3973, doi:10.1021/es5055012.

5.2 Response to Question K

What gaps remain to accurately attribute O₃ and PM formation to emissions source sectors throughout the state?

5.2.1 Working Group

David Parrish - David.D.Parrish, LLC

Jeffrey Collett - Colorado State University

Andy Neuman - NOAA/ESRL/CSD

5.2.2 Findings

Finding K1: Uncertainty regarding the spatial and temporal distribution of gas phase NH₃ concentrations limits our ability to predict O&G contributions of NH₄NO₃ to PM_{2.5} concentrations.

Analysis: Jeffery Collette-Colorado State University

Reaction between gaseous nitric acid (HNO₃) and gaseous ammonia (NH₃) can lead to formation of semivolatile ammonium nitrate (NH₄NO₃) particles (see Finding H for related discussion). The position of the equilibrium between the precursor gases and the product NH₄NO₃ particles depends strongly on environmental conditions. Particle formation is favored when temperatures are low and humidities are high. U.S. NH₃ emissions are believed to be dominated by agriculture, including use of nitrogen-based fertilizers and animal feeding operations. Long-term measurements of ammonium ion (NH₄⁺) in wet deposition and more recent measurements of ambient, gas phase NH₃ both show a general relationship between NH₃/NH₄⁺ concentrations/deposition and proximity to regions of active agriculture. Recent analyses [Hand et al., 2012; Li et al., 2016] show decreases in atmospheric concentrations and deposition of sulfate and nitrate across much of the country, while wet deposition of ammonium has been increasing in most regions. One possible consequence of these trends is increased availability of NH₃ to react with HNO₃ to form NH₄NO₃ when environmental conditions are suitable. A tendency for co-location of O&G production with agricultural production in some regions might also favor interactions of these emissions to generate haze.

Li et al. [2014] examined the ammonia-nitrate-sulfate system in the Jonah-Pinedale gas production region of western Wyoming. Measurements in this region, which extended over a period of 7 years, provided some of the first long-term observations of NH₃ concentrations in the rural western U.S. A primary motivation for the study was to determine whether ambient NH₃ concentrations in the region were greater than or less than the 1 ppb level typically prescribed by EPA for use in assessing visibility impacts of NOx emissions.

Li et al. [2014] observed strong seasonal cycles in NH₃, HNO₃ and nitrate. Ammonia concentrations peaked in summer, a pattern also seen elsewhere in the western U.S. [e.g., Chen et al., 2014], consistent with increases in summertime NH₃ emissions during warmer

temperatures and increased long range transport. Nitrate concentrations peaked in winter, consistent with expectations for enhanced NH_4NO_3 formation at colder temperatures. Nitric acid concentrations showed a bimodal seasonal concentration profile, with peaks in summer and winter. The summer peak is typical of HNO_3 behavior in many environments: concentrations increase with increased photochemical activity and warmer temperatures that promote dissociation of NH_4NO_3 . The winter peak was unusual. Examination of Figure 5-5 below, along with knowledge from other studies of intense winter photochemistry that leads to production of ozone and HNO_3 , helps to explain this pattern. As HNO_3 is produced in winter, it reacts 1:1 with available NH_3 to form fine particle NH_4NO_3 . When the NH_3 is depleted, as illustrated in the NH_3 timeline in winter, further NH_4NO_3 formation is “shut off” and excess HNO_3 remains trapped in the gas phase. Based on these observations, *Li et al.* [2014] concluded that a lack of NH_3 strongly limited the winter formation of PM in the Jonah-Pinedale region. Ammonium nitrate formation in summer is limited by the hot, dry conditions that keep NH_3 and HNO_3 in the gas phase.

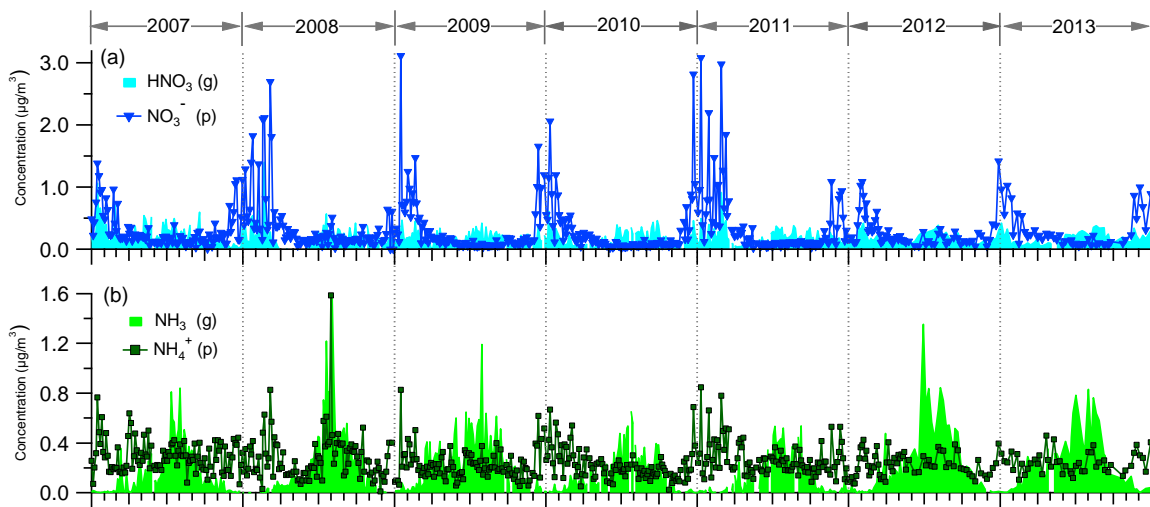


Figure 5-5. Concentrations of gaseous NH_3 , HNO_3 and $\text{PM}_{2.5}$ ammonium and nitrate measured at Boulder, Wyoming [after *Li et al.* 2014]. Note the complete depletion of NH_3 in the wintertime coupled with residual nitric acid in the gas phase. The lack of available NH_3 limits wintertime fine particle NH_4NO_3 and haze formation at this location.

Evanoski-Cole et al. [2017] examined the formation of fine particles and haze in the Bakken O&G region in western North Dakota and eastern Montana. The study (see Figure 5-6 for the study domain) was motivated by observations in the IMPROVE data network that regional concentrations of fine particle nitrate in the Bakken area were flat or increasing while concentrations across most of the country were strongly decreasing as expected based on national trends of decreasing NOx emissions. During two winters (early 2013 and 2013-14) the Bakken Air Quality Study investigated a variety of potential air quality impacts of O&G development in the region. The biggest effects observed were increases in fine particle

concentrations and haze. *Prenni et al.* [2016] looked at increased concentrations of black carbon. *Evanoski-Cole et al.* [2017] focused on NH_4NO_3 .

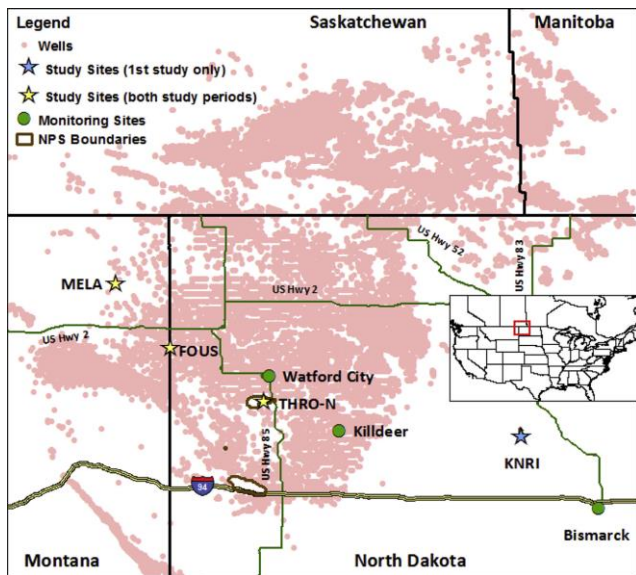


Figure 5-6. The study domain for the Bakken Air Quality Study [*Evanoski-Cole et al.*, 2017]. Study measurement sites are indicated by stars; oil wells are indicated by pink dots.

PM concentrations were higher in the first Bakken study period in early 2013, when elevated concentrations of speciated $\text{PM}_{2.5}$ components in the heart of the Bakken oil patch at Fort Union reached 48 hr average concentrations as high as $20 \mu\text{g m}^{-3}$ (Figure 5-7). During both Bakken field studies, increases in NH_4NO_3 concentrations across the study domain were tied to periods of air stagnation and/or recirculation over the Bakken region, pointing to the strong influence of local source emissions on PM concentrations. VOC composition (e.g., the i/n-pentane ratio) measured at the Bakken study field sites revealed a consistent signature associated with Bakken oil field emissions. A VOC chemical clock, making use of evolving ratios of alkyl nitrates to their parent alkanes, indicated that high PM concentrations were associated with emissions that had aged in the atmosphere for less than a day, again pointing to the important contributions of local source emissions.

A key question addressed by *Evanoski-Cole et al.* [2017] was the sensitivity of NH_4NO_3 formation to availability of precursor NH_3 to react with HNO_3 . Using the ANISORROPIA model, *Evanoski-Cole et al.* [2017] concluded that NH_4NO_3 formation was sensitive to both NH_3 and HNO_3 availability. Sensitivity to NH_3 was greatest during the coldest winter days while sensitivity to HNO_3 increased when temperatures warmed later in winter and more NH_3 was available for reaction. It is likely that the biggest impacts on NH_4NO_3 formation of any increased future NOx emissions from O&G development would be expected in early spring when NH_3 availability typically increases.

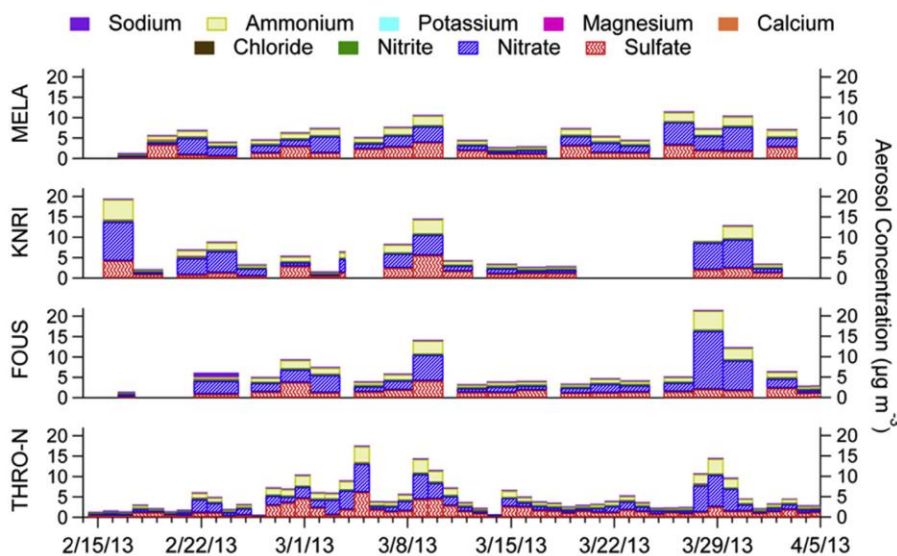


Figure 5-7. The PM_{2.5} concentrations at four Bakken area study sites as reported by Evanoski-Cole *et al.* [2017].

Prior studies of the chemistry of the ammonia-nitrate-sulfate system in rural Texas (e.g., the BRAVO study in Big Bend National Park [*Lee et al.*, 2004]) found the aerosol to usually be acidic, but this study did not look at wintertime conditions when NH₄NO₃ formation is more likely to be important and sulfate may be less abundant. Sulfate concentrations have also decreased significantly since 2000 across Texas [*Hand et al.*, 2012], presumably leaving relatively larger amounts of NH₃ to participate in NH₄NO₃ formation. Of course NH₃ concentrations in Texas are expected to be highly variable across the state. With U.S. NH₃ emissions tied primarily to agricultural activity, including animal feeding operations, regions of the state with greater agricultural and animal husbandry activity are likely to have more NH₃ available to react with HNO₃ produced from atmospheric oxidation of O&G (and other) NO_x emissions to form NH₄NO₃ particles. The Ammonia Monitoring Network (AMon), for example, finds gas phase NH₃ concentrations in the Texas panhandle that commonly exceed 4 $\mu\text{g m}^{-3}$ [<http://nadp.sws.uiuc.edu/AMoN/AMoNFactSheet.pdf>], substantially higher than measured in the BRAVO campaign in Big Bend National Park.

Even in the absence of NH₃, however, HNO₃ can enter the particle phase through reactions with soil dust or sea salt particles. The resulting coarse nitrate is supermicron, but a significant portion does fall within the PM_{2.5} mode. *Lee et al.* [2004] observed the formation of significant sodium and calcium nitrate between 1 and 2.5 μm during the Big Bend National Park BRAVO campaign.

While the chemistry of NH₄NO₃ formation is reasonably well understood, a dearth of information concerning NH₃ concentrations in the atmosphere makes it difficult to predict impacts of O&G emissions in Texas on NH₄NO₃ and haze formation. Long-term measurements of atmospheric deposition of nitrogen containing species give an indication of trends in the atmospheric abundance of NH₄NO₃. Trends in reduced and oxidized nitrogen deposition

[Schwede and Lear, 2014] based on long-term National Atmospheric Deposition Program (NADP) measurements show that reduced nitrogen over Texas O&G regions has not changed substantially between 2002 and 2010, and that oxidized nitrogen deposition has decreased over this time. This latter trend suggests that decreases in NOx emissions from other sectors may be greater than increases in NOx emissions from O&G operations, although reductions in transported oxidized nitrogen may also play a role. O&G impacts on NH₄NO₃ and haze formation are likely to be greatest where O&G activities are co-located with or downwind of important NH₃ source regions, and during the colder times of year when NH₄NO₃ formation is thermodynamically more favorable. In regions where NH₃ is abundant, improved understanding of the oxidation of emitted NOx to HNO₃ or other forms of NOy such as peroxyacetyl nitrate (PAN) will be important for ascertaining the potential for PM formation.

Because NH₃ is an unregulated pollutant, it is not commonly measured, despite its critical role in formation of fine particles including ammoniated sulfates as well as NH₄NO₃. In the past few years, the NADP has built a national NH₃ monitoring network (AMon), but sites remain sparse and coverage in the state of Texas is particularly limited (two sites are in operation, one in the Texas panhandle and one in extreme SE Texas), leaving little in the way of long-term records of ambient NH₃ concentrations. NADP wet and dry deposition sites are somewhat less sparse, and they provide a measure of fine particle ammonium. There are NADP sites in the Haynesville (Longview), Permian (Sonora) and Barnett (LBJ Grasslands) O&G regions. Generally ammonium ion concentrations over Texas O&G basins are small compared to areas heavily influenced by agriculture (e.g., http://nadp.sws.uiuc.edu/maplib/pdf/2015/NH4_conc_2015.pdf and http://nadp.sws.uiuc.edu/maplib/pdf/2015/NH4_dep_2015.pdf)

5.2.3 Summary and Recommendations for Further Analysis

Predicting O&G contributions of NH₄NO₃ to PM_{2.5} concentrations requires an accurate characterization of the spatial and temporal distribution of gas phase NH₃ concentrations, which is presently lacking. A systematic examination of the NH₃ and NH₄⁺ data sets collected at the NADP AMon and wet and dry deposition sites in Texas may provide useful information to allow characterization of the spatial and temporal distribution of gas phase NH₃ concentrations in the State.

5.2.4 References

- Chen, X., Day, D., Schichtel, B., Malm, W., Matzoll, A. K., Mojica, J., McDade, C. E., Hardison, E. D., Hardison, D. L., Walters, S., De Water, M. V., Collett, Jr., J. L. (2014) Seasonal ambient ammonia and ammonium concentrations in a pilot IMPROVE NHx monitoring network in the western United States, *Atmos. Env.*, 91, 118-126, doi:10.1016/j.atmosenv.2014.03.058.
- Evanoski-Cole, A.R., Gebhart, K.A., Sive, B.C., Zhou, Y. Capps, S.L., Day, D.E., Prenni, A.J., Schurman, M.I., Sullivan, A.P., Li, Y., Hand, J.L., Schichtel, B.A., and Collett, Jr., J.L. (2017) Composition and sources of winter haze in the Bakken oil and gas extraction region. *Atmos. Environ.* 156, 77-87, doi:10.1016/j.atmosenv.2017.02.019.

- Hand, J.L., B.A. Schichtel, W.C. Malm, and M.L. Pitchford (2012), Particulate sulfate ion concentration and SO₂ emission trends in the United States from the early 1990s through 2010, *Atmos. Chem. Phys.*, 12, 10353-10365, doi:10.5194/acp-12-10353-2012.
- Lee, T., S. M. Kreidenweis and J. L. Collett, Jr. (2004), Aerosol ion characteristics during the Big Bend Regional Aerosol and Visibility Observational study, *J. Air and Waste Management Assoc.*, 54, 585-592.
- Li, Y., Schwandner, F. M., Sewell, H. J., Zivkovich, A., Tigges, M., Raja, S., Holcomb, S., Molnar, J. V., Sherman, L., Archuleta, C., Lee, T., and Collett, Jr., J. L. (2014) Observations of ammonia, nitric acid, and fine particles in a rural gas production region, *Atmos. Env.* 83, 80-89.
- Li, Y., Schichtel, B. A., Walker, J. T., Schwede, D. B., Chen, X., Lehmann, C. M. B., Puchalski, M. A., Gay, D. A., and Collett, Jr., J.L. (2016) Increasing importance of deposition of reduced nitrogen in the United States. *PNAS*, 113 (21), 5874-5879, doi:10.1073/pnas.1525736113.
- Nowak, J.B., J.A. Neuman, R. Bahreini, A.M. Middlebrook, J.S. Holloway, S.A. McKeen, D.D. Parrish, T.B. Ryerson, and M. Trainer (2012), Ammonia sources in the California South Coast Air Basin and their impact on ammonium nitrate formation, *Geophys. Res. Lett.*, 39, L07804, doi:10.1029/2012GL051197.
- Prenni, A.J., et al. (2016), Oil and gas impacts on air quality in federal lands in the Bakken region: an overview of the Bakken Air Quality Study and first results, *Atmos. Chem. Phys.*, 16, 1401-1416, doi:10.5194/acp-16-1401-2016.
- Schwede, D.B. and G.G. Lear (2014), A novel hybrid approach for estimating total deposition in the United States, *Atmos. Env.* 92, 201-220.

APPENDIX A

Correlation Analysis of Ambient Ozone Concentrations with Oil and Gas Development Activity

Appendix A

Appendix A: Correlation Analysis of Ambient Ozone Concentrations with Oil and Gas Development Activity

Background

Finding F1 (see below) is largely based on correlation between the time series of ambient ozone concentration measurements and indicators of O&G development activities in four O&G basins, one in North Dakota and three in Texas, plus a contrasting Texas area without large O&G development. Figure 4-1 through Figure 4-5 compare these time histories and include maps showing the location of the ozone monitoring sites in relation to the O&G well locations. This Appendix presents the correlation analysis that supports Finding F1.

Finding F1: Decadal scale ozone changes in three Texas O&G basins can be quantitatively described as interannual variations about smooth, continuous declines; neither the variations nor the declines significantly correlate with O&G production or drilling activity. This lack of correlation indicates that O&G development does not have a major impact on ozone concentrations in Texas (<5 ppb on design values and median ozone season MDA8 concentrations).

This correlation analysis is based upon the interannual variations of measured ozone concentrations about the long-term trends illustrated in Figure 4-1 through Figure 4-5. The long-term trends are defined by the black curves in the figures, and the interannual variations are quantified by the differences between the curves and the measurements themselves; these differences are termed residuals. This Appendix describes the derivation of the long-term trends and discusses the correlations between the residuals and metrics of O&G production in the respective basins.

Fitting Equation 1 to the measurements from the monitors chosen to represent the ozone concentrations in each region defines the long-term trends (black lines in Figure 4-1 through Figure 4-5). Equation 1 is an exponential function with a constant positive offset that describes the time evolution of any particular measure of ozone concentration (here either the ODV or the median MDA8 ozone concentration for the selected ozone season):

$$O_3 = y_0 + A \exp\{-(\text{year}-2000)/\tau\}. \quad (1)$$

Mathematically, the first term, y_0 , is the asymptotic value toward which the regional ozone concentration is approaching, and the second term is the enhancement of the ozone concentration above y_0 . This enhancement is assumed to be decreasing exponentially with an e-folding time constant of τ years. Thus, A is the enhancement of the ozone concentration above y_0 in the year 2000. A least-squares fitting routine is used to derive the parameters of Equation 1 for any time series of ozone measurements. Equation 1 is selected because it has been shown to give an excellent representation of the ozone evolution in seven air basins in southern California [Parrish et al., 2017]. The length of the ozone measurement record in Texas

is shorter than that in California, so it is not possible to precisely define all three parameters of Equation 1 for any of the Texas data sets. In order to derive the fits utilized here, τ is set equal to 21.9 years (the value derived for southern California) in all fits shown here. There is no definitive reason to assume that the same e-folding time for the decrease in ozone enhancement should apply to both Texas and California, but the suitability of this choice can be evaluated from the ability of the black curves in Figure 4-1 through Figure 4-5 to faithfully represent the long-term trends apparent in each figure. However, these fits should be considered as a tool for evaluation of residuals rather than a definitive description of the ozone evolution in the Texas and North Dakota regions considered in this analysis.

The next step is to evaluate correlations of the derived ozone residuals with metrics that reflect O&G activity in the respective basins. Figure AppA - 1 through Figure AppA - 4 illustrated these evaluations. The selected metrics of O&G activity are drilling rig count (Bakken, Haynesville and Eagle Ford), shale oil production (Bakken), total oil production (Eagle Ford), and dry gas production (Haynesville and Barnett). The histories of these metrics were downloaded from the database maintained by the U.S. Energy Information Administration (<https://www.eia.gov>). For comparison with the residuals, these metrics were averaged over 3-year and 1-year periods to match the averaging periods of the ODVs and medians, respectively. These averages are indicated by the color-coded "dashes" in the panels (a) and (b) of the figures. The ozone residuals from the individual sites are indicated by green dots, and their averages by the black "dashes" in these same panels. Panels (c) and (d) of Figure AppA - 1 through Figure AppA - 4 are correlation plots of the residual averages with the indicated metrics of O&G production. Linear regression fits to the correlations are shown in the figures, and the slopes and correlation coefficients are annotated.

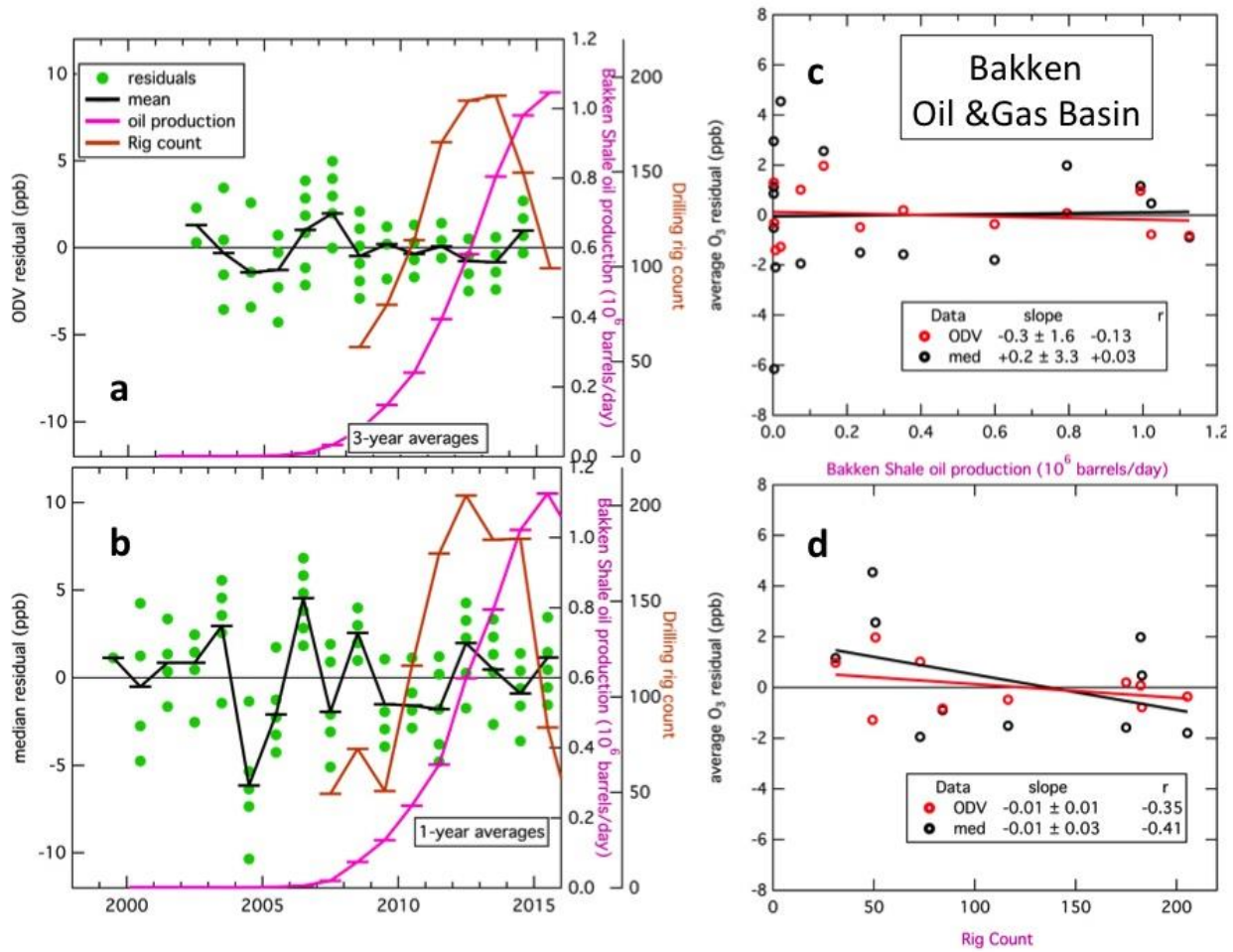


Figure AppA - 1. Time series of ODV residuals (a) and median MDA8 ozone residuals (b) in the Bakken O&G basin in North Dakota; time series of 3-year and 1-year, respectively, averages of drilling rig count and shale oil production are included for comparison. Correlations of ODV residuals (c) and median MDA8 ozone residuals (c) with the respective drilling rig count and shale oil production averages. Slopes and correlation coefficients of linear regression fits are annotated.

The correlations in these figures present a mixed picture. None of the correlations are significant in either the Bakken or the Barnett. In the Haynesville, there is a weak positive correlation ($r = 0.27$ to 0.34) of the ozone residuals with gas production, but not with drill rig count. In the Eagle Ford, there are stronger positive correlations ($r = 0.20$ to 0.91) of the ozone residuals with oil production and with drill rig count. Taken at face value, these correlations can be taken to indicate the increase in ozone concentrations that occurred when the O&G activities increased from their minima to the maxima. The largest indicated increases are about 3 ppb in the median ozone concentrations in the Haynesville and 5 ppb in the ODVs in the Eagle Ford.

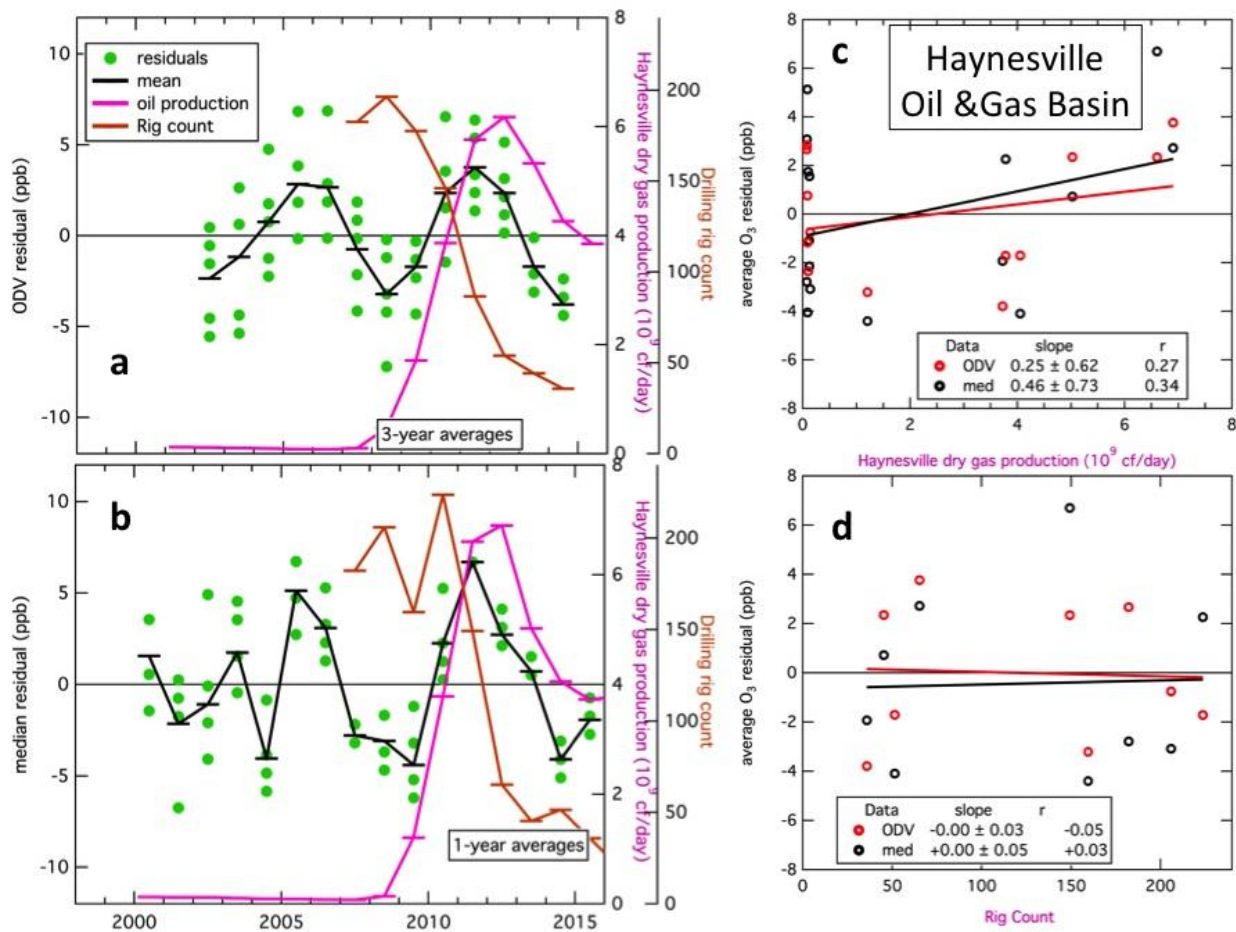


Figure AppA - 2. Same as Figure AppA - 1 for the Haynesville O&G basin, except that the production of dry gas is included.

However, it is very likely that the correlations discussed in this Appendix are largely coincidental rather than caused by increasing O&G activity. As discussed in the Response to Question F, a large fraction of the interannual variability in ozone concentrations reflect state-wide variability driven by large-scale meteorological variability, and are quite similar between the four Texas regions investigated. Notably, 2011 was a year of particularly high ozone concentrations observed throughout Texas. This year was also near the peak of gas production in the Haynesville, and the peak of drill rig count in the Eagle Ford; it is believed that this coincidence of meteorological variability and O&G activity largely accounts for the correlations discussed in this Appendix. The ultimate conclusion of this analysis is O&G in Texas enhances median ozone concentrations and ODVs by less than 5 ppb throughout the State.

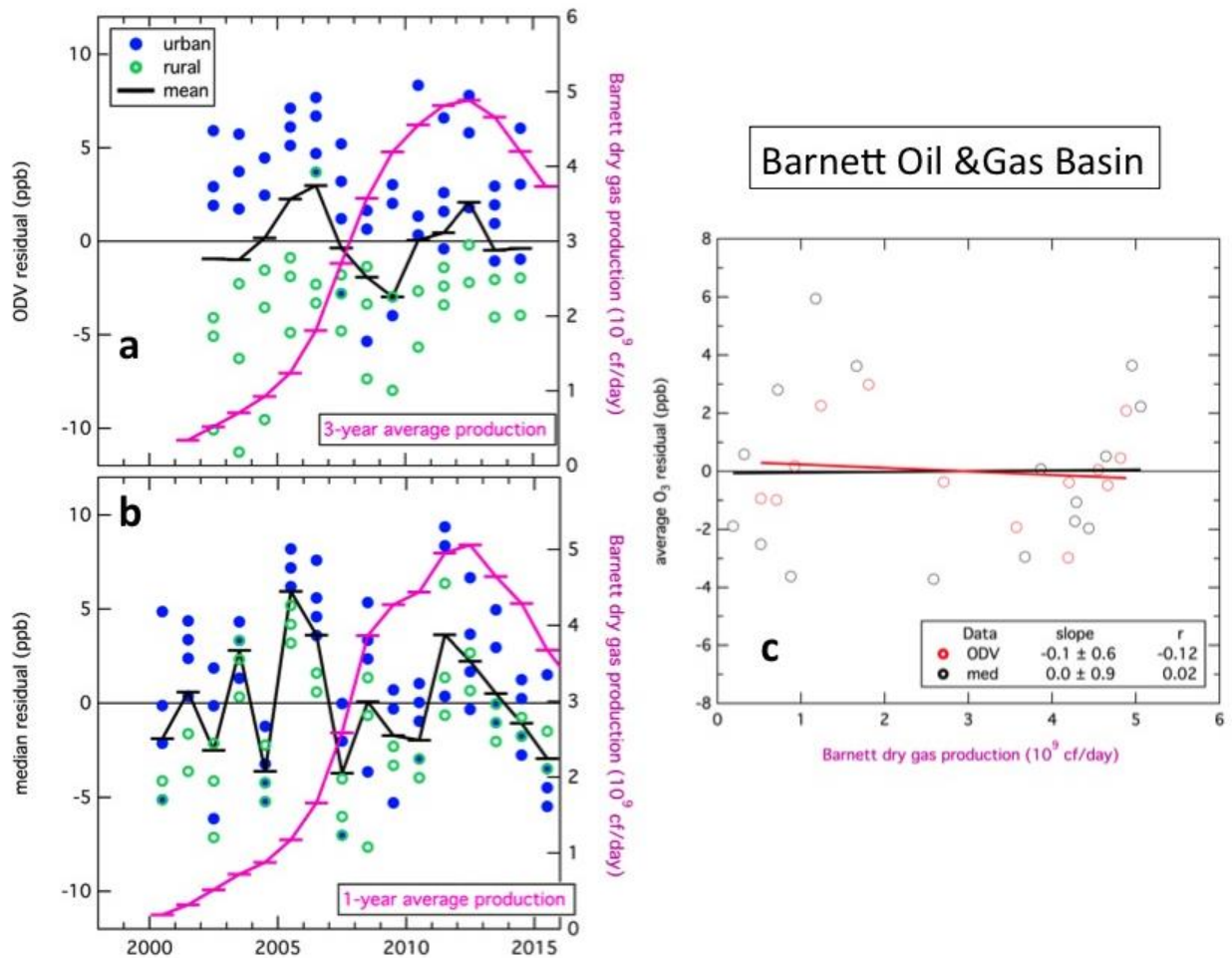


Figure AppA - 3. Same as Figure AppA - 1 for the Barnett O&G basin, except that only the dry gas production is included.

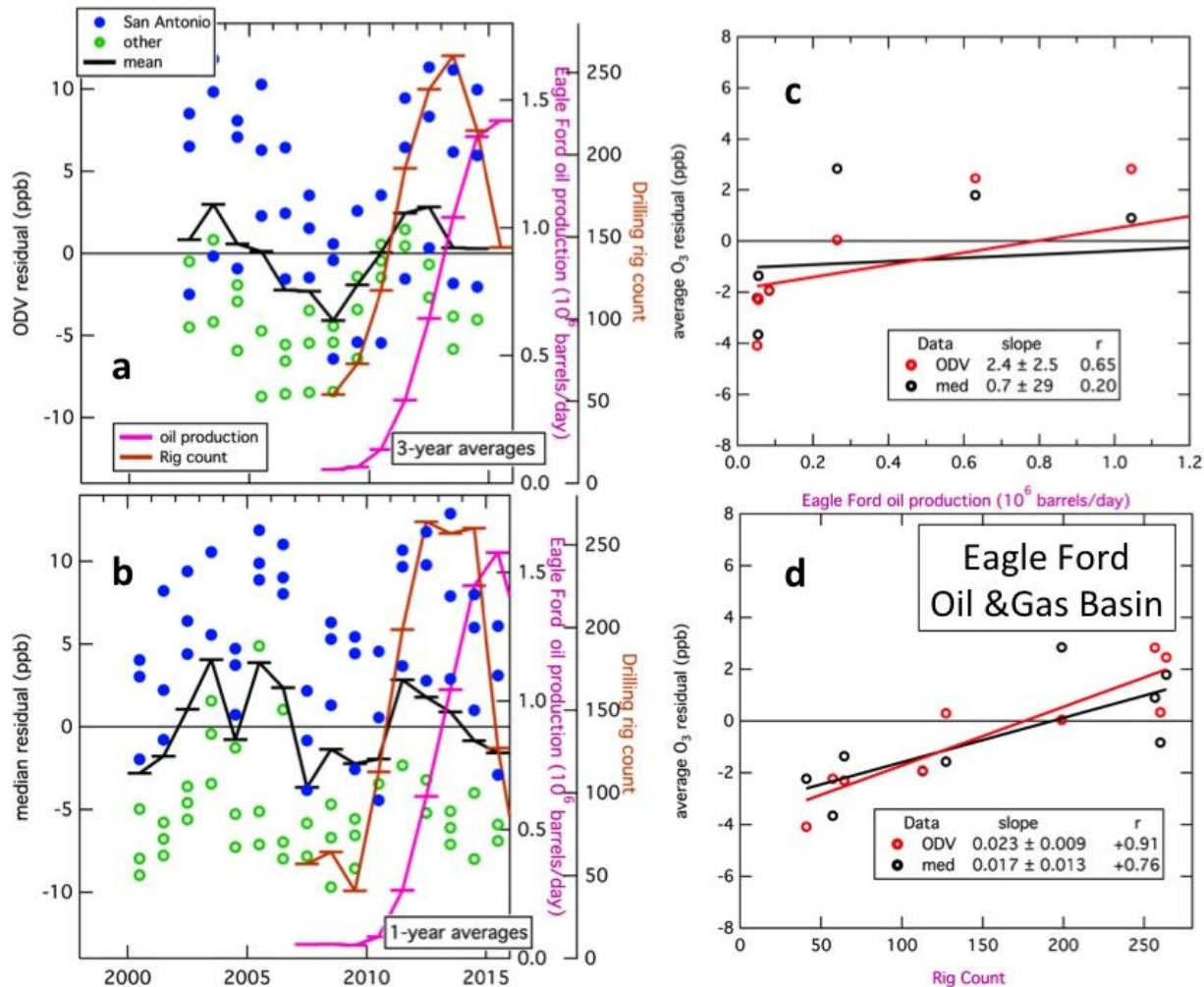


Figure AppA - 4. Same as Figure AppA - 1 for the Eagle Ford O&G basin.

References

Parrish, D.D., L.M. Young, M.H. Newman, K.C. Aikin and T.B. Ryerson (2017), Ozone design values in southern California's air basins: Temporal evolution and U.S. background contribution, *J. Geophys. Res. Atmos.*, in review.

APPENDIX B

CAMx 2017 Ozone Source Apportionment Modeling

Appendix B: CAMx 2017 Ozone Source Apportionment Modeling

Background

Findings F6, F7, J1 and J2 are based on recent ozone modeling performed by Ramboll Environ using TCEQ's 2012/2017 ozone modeling platform²¹. This Appendix provides information on the ozone modeling.

The Comprehensive Air-quality Model with extensions (CAMx) [Ramboll Environ, 2016] was used to model the United States using nested 36, 12 and 4 km resolution grids with the 4 km grid located over East Texas (Figure AppB - 1). CAMx is a three-dimensional, chemical-transport grid model used for tropospheric ozone, aerosols, air toxics and related air-pollutants and is used for air-quality planning in Texas. CAMx was used here to estimate the ozone impacts in East Texas due to O&G and other emissions in a 2017 future year emissions scenario.



Figure AppB - 1. Emissions source regions used in the CAMx ozone source apportionment modeling of 2017. The continental-scale 36 km grid is shown in black, the regional-scale 23 km grid is shown in blue and the 4 km grid focused on East Texas is light green.

The TCEQ developed a 2012 base case and 2017 future year episode for their State Implementation Plan modeling²². The seasonal base case ozone modeling episode extends from May 1-September 30, 2012. TCEQ has performed extensive model performance

²¹ <https://www.tceq.texas.gov/airquality/airmod/data/tx2012>

²² https://www.tceq.texas.gov/assets/public/implementation/air/sip/hgb/HGB_2016_AD_RFP/AD_Adoption/16016_SIP_HGB08AD_ado.pdf

evaluation of the 2012 base case modeling episode against observations [TCEQ, 2016]. The TCEQ makes publicly available their modeling inputs, including emissions, boundary conditions, and other inputs required to run the CAMx model for the seasonal episode.

The model's vertical resolution is finest near the ground (34 meter surface layer) and extends to the lower stratosphere in 29 layers. Meteorological input data for CAMx were developed using the Weather Research and Forecasting (WRF; [Skamarock *et al.*, 2008]) meteorological model. WRF provides CAMx with hourly, gridded data for wind vectors, pressure, temperature, diffusivity, humidity, clouds and rainfall. Boundary conditions for the outermost (36 km) grid were derived from a global-scale GEOS-Chem model [Yantosca *et al.*, 2013] global simulation of 2012. Large NO_x sources were treated with the CAMx plume-in-grid sub-model, and the model was run using the Wesely dry deposition algorithm [Wesely, 1989]. The TCEQ developed episode-specific 2012 biogenic emissions using the EPA's BEIS v3.61 model [Bash *et al.*, 2016] and episode-specific 2012 wildfire emissions from the Fire Inventory from the National Center for Atmospheric Research (FINN; [Wiedinmyer *et al.*, 2011]). The biogenic and fire emissions were held fixed between 2012 and 2017.

Ramboll Environ ran CAMx v6.40 with Cb6r2h chemistry [Yarwood *et al.*, 2014] for the 2012 base case and 2017 future year using the TCEQ inputs with the exception of the meteorological data, which were replaced with output from a new WRF meteorological model run performed by Ramboll Environ and aimed at improving performance for winds, clouds and precipitation over East Texas and the southeastern US. CAMx model performance for ozone and NO_x was evaluated for the modified 2012 base case and the CAMx ozone modeling performance was found to be comparable to that of the original TCEQ 2012 base case simulation [Johnson *et al.*, 2017] and adequate for the present study.

The 2017 emission inventory is described in detail in [TCEQ, 2016]. Here, we give a brief overview of TCEQ's O&G emissions inventory for 2017. TCEQ's 2017 drilling rig emission inventory for Texas was based on a 2015 survey data elicited from O&G exploration and production companies and drilling activity data from the Texas Railroad Commission. 2017 Texas O&G production emissions estimates were based on 2014 emissions developed using Texas Railroad Commission production data. For areas of the US outside Texas, TCEQ used the EPA's 2011 National Emission Inventory projected to 2017.

The TCEQ emission inventory is broken down into separate source categories suitable for source apportionment modeling. For the 2017 source apportionment run, we grouped the TCEQ 2017 inventory components into the following emissions source categories:

- Natural emissions (sum of biogenic emissions and fire emissions)
- O&G emissions
- Onroad mobile emissions (cars, trucks, busses, motorcycles, etc.)
- Electric generating unit (EGU) emissions
- Other (includes area sources, shipping sources, non-EGU point sources, nonroad mobile emissions, and offroad mobile emissions)

Nonroad mobile sources include vehicles, engines, and equipment that can change location, but do not travel on public roads. Construction and agricultural equipment are two examples of nonroad mobile sources. Offroad mobile sources include aircraft, locomotives, and commercial marine vessels. The area source inventory treats in aggregate all stationary sources that have emissions below the prescribed point source threshold. Examples of area sources include dry cleaners and residential wood heating. The use of the “Other” category, which lumps together a series of emissions source categories, represents a compromise between the need for detailed source apportionment within a number of Texas geographic source regions and the computational demands of a seasonal ozone simulation.

The modeling domain was broken down into regions (Figure AppB - 2) with each region’s emissions subdivided into the emissions source groups listed above. In selecting the O&G regions, we focused on the East Texas shale regions that have undergone extensive development during the last decade. We used the Texas Railroad Commission’s definition of the Eagle Ford, Haynesville and Barnett Shale regions, which gives a county-level geographic breakdown²³. Because of the large size of the Eagle Ford, we split it into two parts to allow quantification of impacts from the northern and southern parts of the shale region.

²³ <http://www.rrc.state.tx.us/oil-gas/major-oil-gas-formations/>

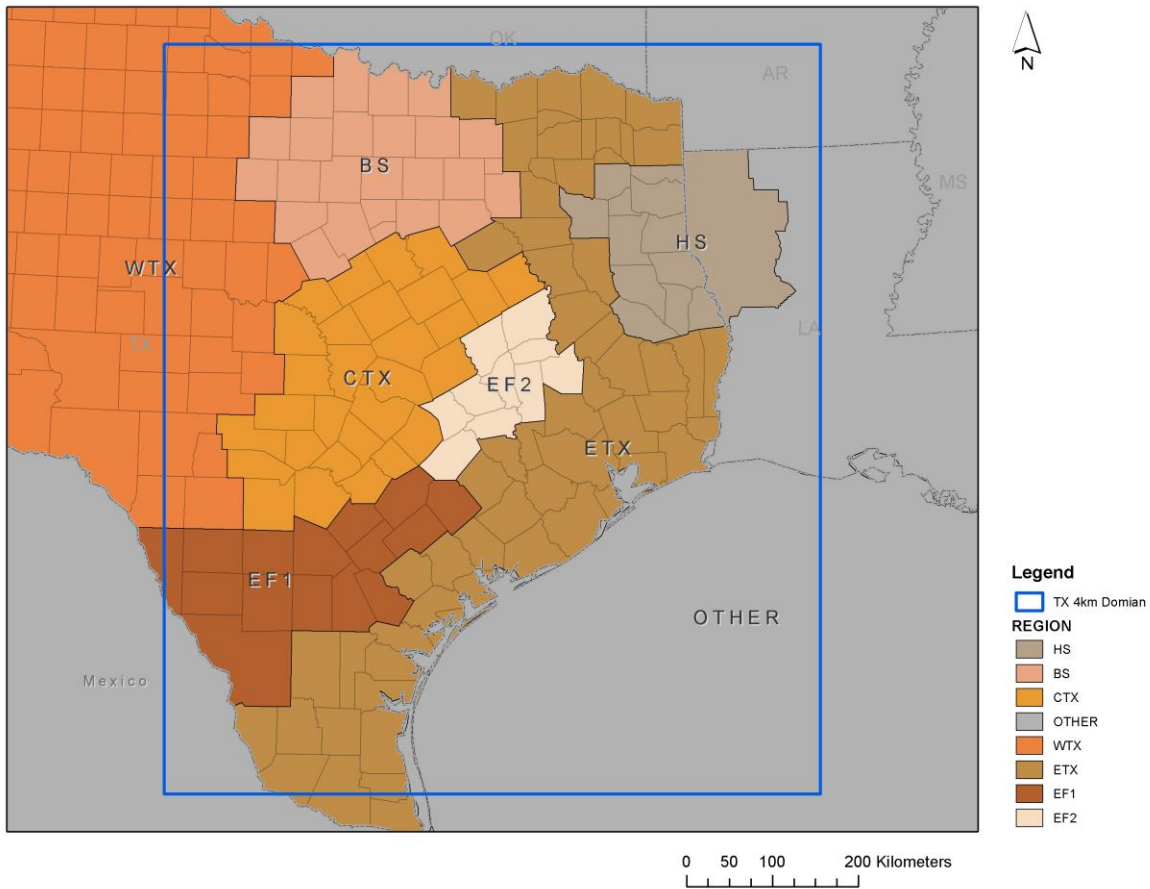


Figure AppB - 2. Emissions source regions used in the CAMx ozone source apportionment modeling of 2017. Abbreviations are BS: Barnett Shale, HS: Haynesville Shale, CTX: Central Texas, WTX: Western Texas, ETX: Eastern Texas, EF1: Eagle Ford Region 1. EF2: Eagle Ford Region 2. The blue rectangle shows the boundary of the CAMx 4 km modeling domain.

The CAMx APCA source apportionment tool uses multiple tracer species to track the fate of ozone precursor emissions and the ozone formation caused by these emissions within a simulation. The tracers operate as spectators to the normal CAMx calculations so that the underlying CAMx-predicted relationships between emission groups (sources) and ozone concentrations at specific locations (receptors) are not perturbed. APCA differs from the standard CAMx Ozone Source Apportionment Tool (OSAT) in recognizing that certain emission groups are not controllable (e.g., biogenic emissions) and that apportioning ozone production to these groups does not provide information that is relevant to development of control strategies. To address this, in situations where OSAT would attribute ozone production to non-controllable (i.e., biogenic) emissions, APCA re-allocates that ozone production to the controllable portion of precursors that participated in ozone formation with the non-controllable precursor. For example, when ozone formation is due to biogenic VOC and anthropogenic NO_x under VOC-limited conditions (a situation in which OSAT would attribute

ozone production to biogenic VOC), APCA re-directs that attribution to the anthropogenic NOx precursors present. In this study, the ozone contribution from the natural emissions source category does not provide information on the ozone contribution of biogenic VOC emissions, only on the contribution from biogenic NOx emissions. The natural emissions contribution to ozone is the sum of the contributions from biogenic NOx emissions and fire emissions.

The source apportionment analysis was aimed at understanding the impacts of O&G emissions on ODVs, by which attainment of the ozone NAAQS is reckoned. The ozone NAAQS are formulated in terms of a design value, which is calculated as the 3-year average of the fourth highest monitored daily maximum 8-hour concentration at each monitoring site. To attain the 2015 ozone standard, the ODV for a given monitor must not exceed 70 ppb. EPA's modeling guidance [EPA, 2014] for projecting future year 8-hour ODVs recommends the use of modeling results in a relative sense to scale the observed current year (2012) 8-hour ozone design value (DVC) to obtain a future year (2017) 8-hour ozone design value (DVF). The model-derived scaling factors are referred to as Relative Response Factors (RRF) and are defined as the ratio of daily maximum 8-hour ozone concentrations near a monitor averaged over several days of modeling results for the future year emissions scenario to the current year base case:

$$RRF_{monitor\ i} = \frac{\sum_{days}^{(daily\ max\ 8-hour\ ozone)}_{future\ year}}{\sum_{days}^{(daily\ max\ 8-hour\ ozone)}_{current\ year}}$$

$$DVF_{monitor\ i} = DVC_{monitor\ i} \times RRF_{monitor\ i}$$

This technique is used to minimize the effect of model uncertainty on future year ozone projections. Here, we formed the RRFs using the ratio of the 2017 and 2012 model results and calculated 2017 ODVs for the regulatory monitors in East Texas. ODVs for all East Texas monitors that are part of the EPA's Air Quality System monitoring network were calculated using EPA's Modeled Attainment Test Software (MATS; Abt, [2009]). We used MATS to perform an unmonitored area analysis [EPA, 2014] to determine 2017 ODVs for grid cells that do not contain a monitor. We ran MATS with and without the source apportionment contribution from O&G emissions to determine the contribution of O&G emissions to 2017 design values at East Texas monitors and repeated the procedure for the remaining emissions categories.

References

- Abt Associates Inc. (2009), Modeled Attainment Test Software User's Guide. Prepared for the U.S. EPA, Office of Air Quality Planning and Standards U.S. Environmental Protection Agency, Research Triangle Park, NC. March.
- EPA. (2014), Draft Modeling Guidance for Demonstrating Attainment of Air Quality Goals for Ozone, PM2.5, and Regional Haze

http://www.epa.gov/ttn/scram/guidance/guide/Draft_O3-PM-RH_Modeling_Guidance-2014.pdf. December.

Griffin, R. J., C. A. Johnson, R. W. Talbot, H. Mao, R. S. Russo, Y. Zhou, and B. C. Sive (2004), Quantification of ozone formation metrics at Thompson Farm during the New England Air Quality Study (NEAQS) 2002, *Journal of Geophysical Research: Atmospheres*, 109(D24), D24302, doi:10.1029/2004JD005344.

McDuffie, E. E., et al. (2016), Influence of oil and gas emissions on summertime ozone in the Colorado Northern Front Range, *Journal of Geophysical Research: Atmospheres*, 121(14), 8712-8729, doi:10.1002/2016jd025265.

Neuman, J. A., et al. (2009), Relationship between photochemical ozone production and NO_x oxidation in Houston, Texas, *Journal of Geophysical Research: Atmospheres*, 114(D7), D00F08, doi:10.1029/2008JD011688.

Rutter, A. P., R. J. Griffin, B. K. Cevik, K. M. Shakya, L. Gong, S. Kim, J. H. Flynn, and B. L. Lefer (2015), Sources of air pollution in a region of oil and gas exploration downwind of a large city, *Atmospheric Environment*, 120, 89-99, doi:<http://dx.doi.org/10.1016/j.atmosenv.2015.08.073>.

Skamarock, W. C., J. B. Klemp, J. Dudhia, D. O. Gill, D. M. Barker, W. Wang, and J. G. Powers, (2005), "A description of the Advanced Research WRF Version 2". NCAR Tech Notes-468+STR. http://www.mmm.ucar.edu/wrf/users/docs/arw_v2.pdf.

Trainer, M., et al. (1993), Correlation of ozone with NO_y in photochemically aged air, *Journal of Geophysical Research*, 98(D2), 2917, doi:10.1029/92jd01910.

U.S. Census Bureau Population Change for Metropolitan and Micropolitan Statistical Areas in the United States and Puerto Rico : 2000 to 2010 [Available at: <https://www.census.gov/population/www/cen2010/cph-t/CPH-T-5.pdf>].

Wiedinmyer, C., Akagi, S. K., Yokelson, R. J., Emmons, L. K., Al-Saadi, J. A., Orlando, J. J., and Soja, A. J. (2011), The Fire INventory from NCAR (FINN): a high resolution global model to estimate the emissions from open burning, *Geosci. Model Dev.*, 4, 625-641, doi:10.5194/gmd-4-625-2011.

Wesely, M. L. (1989), Parameterization of surface resistances to gaseous dry deposition in regional-scale numerical models, *Atmos. Environ.*, 23, 1293–1304.

Yantosca, B., Long, M., Payer, M., Cooper, M. (2013), GEOS-Chem v9-01-03 Online User's Guide, <http://acmg.seas.harvard.edu/geos/doc/man/>.